PHYTOCHEMICAL AND

PHARMACOLOGICAL INVESTIGATION

OF SOME MEDICINAL PLANTS

by

SOLOMON HABTEMARIAM

A THESIS PRESENTED FOR THE DEGREE OF

DOCTOR OF PHILOSOPHY IN PHARMACEUTICAL

SCIENCE OF

THE UNIVERSITY OF STRATHCLYDE

Department of Pharmaceutical Sciences

University of Strathclyde

Glasgow, U.K.

May 1992

To My Parents

ACKNOWLEDGEMENTS

ABSTRACT

This thesis describes phytochemical and biological/pharmacological studies on six medicinal plants. Plant materials were extracted by ethanol, tested for their biological activity and then subjected to "bioassay-guided fractionation" to yield active and inactive compounds. The compounds were identified by standard physico-chemical techniques including UV, IR, NMR and EIMS.

The crude ethanol extract of the leaves of *Premna shcimperi* was found to be antibacterial against gram positive bacteria (*Staphylococcus aureus* and *Bacillus subtilis*). An antibacterial bioassay-guided fractionation of the extract resulted in the isolation of the active principle, (5R,8R,9S,10R)-12-oxo-*ent*-3,13(16)-clerodien-15-oic acid (**SHM-1**). This novel compound was bactericidal against *S. aureus* and *B. subtilis* at concentrations of 25 and 50 μg ml^{-1}. Studies on the structural-activity relationship of **SHM-1** showed that the α,β-unsaturated moiety played a major role in its antibacterial activity. Investigation of the inactive fractions of *P. schimperi* extract afforded three flavonoid aglycones: luteolin, quercetin and kaempferide; three flavonoid glycosides: luteolin-4"-β-D-glucoside, quercetin-3-β-D-galactoside and quercetin-α-L-arabinopyranoside and five cinnamate and benzoate derivatives.

The ethanol extract of the leaves of *Premna oligotricha* was also found to be antibacterial against a range of gram-positive bacteria. A bioassay-directed isolation afforded three novel active principles, two diterpenes: 16-hydroxy-clerod-3,13(14)-diene-15,16-olide (**SHM-3**) and *ent*-12-oxolabda-8,13(16)-dien-15-oic acid (**SHM-5**) and a sesquiterpene, 7-α-hydroxy-2-oxo-6,11-cyclofarnes-3(15)-ene (**SHM-**

19). While the activity of **SHM-5** and **SHM-19** was marginal that of **SHM-3** was good, almost comparable with streptomycin. The antimicrobially inactive fractions of *P. oligotricha* extract yielded a novel diterpene, *ent*-8β,12α-epidioxy-12β-hydroxylabda-9(11), 13-dien-15-oic acid γ lactone and two novel flavonoids: 3,5,5'-trihydroxy-6,7,3',4'-tetramethoxyflavone and 3,5,7,5'-tetrahydroxy-6,3',4'-trimethoxyflavone.

Investigation of the leaves of *Premna recinosa* afforded six flavonoids: quercetin, luteolin, pachypodol, chrysosplenol-D, naringenin and eriodictyol and three lignans: (+)-8-hydroxy-pinoresinol, (+)-lariciresinol and (-)-*seco*-isolariciresinol.

Portulaca oleracea and *Pentas schimperiana* are used in the folk medicine as local anaesthetics. Studies on the isolated nerve and/or muscle preparations showed that extracts do block nerve conduction in these excitable tissues. A subsequent systematic bioassay-guided fractionation of crude extracts showed that excess potassioum ions in the extracts were responsible for the *in vitro* pharmacological activity of *P. oleracea* and *P. schimperiana*.

Extracts from the leaves of *Leonotis ocymifolia* var *raineriana* showed no antibacterial activity. Three novel diterpenes: *ent*-(13S)-9,13α-epoxylabda-6(19)β,16(15)-diol dilactone, (13R)-6β-acetoxy-9,13α-epoxylabda-19(20)β,16(15)-diol dilactone and 20β-acetoxy-9α,13ξ-dihydroxy-15(16)-epoxy-labd-14-en-6,19β-O-lactone together with a known compound: (13S)-20β-acetoxy-9,13α-epoxylabda-6(19)β,16(15)-diol dilactone were isolated. Investigation of the root afforded two known compounds 3-methoxy-4-hydroxy-(*trans*)-cinnamaldehyde and 3-methoxy-4-hydroxy-bezaldehyde.

Contents

II STUDIES ON THE LOCAL ANAESTHETIC AND/OR MUSCLE RELAXANT PROPERTY OF PLANT EXTRACTS 194

6 STUDIES ON THE MUSCLE RELAXANT PROPERTY OF *Portulaca oleracea* 195

III PHYTOCHEMICAL INVESTIGATION OF *LEONOTIS OCYMIFOLIA* var *RAINERIANA*   231

8 PHYTOCHEMICAL INVESTIGATION OF *LEONOTIS OCYMIFOLIA* var *RAINERIANA*   232

List of Figures

List of Tables

PREAMBLE

Many secondary metabolites in plants are designed for defence against predators (Abelson, 1990). Evolution of plants has proceeded in many directions, leading to the creation of vast arrays of substances, only some of which have been identified. The defensive chemicals interact harmfully with the biochemical apparatus of predators. While many biochemical pathways of living matter are common there are differences that can be exploited. What is one creatures poison can be innocuous to another. What is toxic to one tissue may not be toxic to the rest of the organism. Thus there is always the chance of getting useful drugs from plant defensive agents which are designed to harm predators.

The history of higher plants as drugs is as old as the history of human beings themselves. Even today, about 80% people in the world, most of them in the developing world, still rely on plants, plant extracts and other items of traditional medicine (Abebe, 1986). About 25% of all prescription drugs in industrialised countries also contain active principles that are still extracted from higher plants and this situation has persisted over the last 25 years (Farnsworth in Krogsgaard-Larsen and Christenson, 1984).

The search for useful drug molecules from plants began right after the dis-

1

covery of morphine in 1804. Since then many thousands of novel structures have been discovered from plants. In spite of this considerable research activity the number of plant-based drugs are still less than 200 (Farnsworth in Krogsgaard-Larsen and Christenson, 1984). This is partly because of the poor pharmacological/toxicological profile of many plant based drugs and also the lack of broad biological screening to go hand in hand with phytochemical studies.

There is no doubt of the continued usefulness of higher plants as a source of drugs and lead compounds thus research on bioactive compounds will continue to evolve. Considerably less than half of the total species in the world have been studied at all so far (Marderosian and Liberti, 1988). Most of the plants which have not been analysed occur in third world countries; a large fraction of them in tropical rain forests. As the forests are being destroyed due to population growth, many species are being lost that might yield useful medicine. This potential loss leads to an urgent need to search for bioactive compounds from plants.

As there are currently no scientific methods applicable for the selection of plants that can be expected to contain novel biologically active substances, the planning for plant based drug development programmes must utilize approaches that are considered to be "non scientific" by some. Historically, scientists claiming to have an interest in drug discovery from natural products have used approaches like, phytochemical screening, phytochemical work followed by bioassay and pharmacological screeings. The last and best approach however is selection based on "folklore" use. About 74% of drugs based on higher plants came to the attention of pharmaceutical house because of their use in traditional medicine (Abelson,

2

1990).

In the present study, attempts have been made to undertake a systematic phytochemical and biological/pharmacolgical study of selected medicinal plants. The biological activities were chosen based on the the folklore use of the plants. Part I includes a study on medicinal plants which have traditional uses associated with antimicrobial activity. Part II includes the study on two medicinal plants used as local anaesthesia while Part III describes the phytochemical analysis of a medicinal plant reported to be used as an anti-cancer agent and ascaricide.

Part I

PHYTOCHEMICAL AND

ANTIMICROBIAL STUDIES

ON *PREMNA* SPECIES

Chapter 1

THE GENUS *PREMNA*

1.1 The genus *Premna* and Botanical description of the Species studied

Premna is one of the 75 genera of the family Verbenaceae (Willis and Shaw, 1973). It comprises around 200 species of plants distributed in tropical and subtropical Asia and Africa. The distribution and botanical description of three Ethiopian *Premna* species examined in the present study are discussed below.

1.1.1 *Premna schimperi* Engler

Premna schimperi Engl. is a spreading shrub or a tree to 7-10 m high. The plant is widely distributed in Ethiopia between the altitudes of 1350 and 2400 m. Although not very common, the species occurs in other East African countries; Kenya, Sudan and Tanzania. Botanically the plant is described as follow (Demissew, 1988): Branches pale brown to gray, glabrous to pubescent

leaves opposite; petiole 1.5-4.5 cm long, pubescent lamina green above, green-purple to whitish below, 4.5-11.5 x 3.5-8.7 cm; broadly elliptic to ovate glabrous to tomentose on both sides, acuminate at the apex, rounded, truncate to cordate at the base, margin entire to crenate, 3-5 lateral nerves seen on both sides and dense reticulation clearer below. Inflorescence terminal, paniculate (corymbose); peduncle 1-2.5(2.7) cm; pedicle very short 0.5-1 mm. Bracts ovate, 2-3 mm long at the first branching. Flowers bisexual. Calyx campanulate ca 1.5-2 mm long, shortly 5 toothed, petals tubular. Fruit a drupe, the size of a small pea, green turning purple when mature.

1.1.2 *Premna oligotricha* Baker

Premna oligotricha (syn. *Premna somalensis*) is a spreading shrub widely distributed in Ethiopia. Compared with *P. schimperi*, this plant grows in lower altitudes (1100-1960 m). The species is also known to occur in Kenya and Somalia. Thiselton-Dyer (1959) described *P. oligotricha* as follow: an erect shrub with slender slightly pubescent branchlets. Leaves shortly petioled, suborbicular, 1-1.5 in. long, subcuneate or rounded at the base, cuspidate, distinctly crenate, membraneous, nearly glabrous above, pubescent beneath. Cymes small, terminal; pedicle as long as campanulate tube. Corolla tube rather shorter than the calyx; limb bilabrate, as long as the tube. Stamens shorter than the corolla tube.

1.1.3 *Premna recinosa* Schauer

Premna recinosa occurs at still lower altitudes (400-1800 m). It grows in areas which are often of an arid or semi-arid climate. *P. recinosa* is known to be distributed in East African countries; Kenya, Sudan, Tanzania, Uganda and also in Arabia. Botanically the species is described as follow (Demissew, 1988): a shrub up to 2(3) m high; branches white (young parts), to brown to dark (old parts), glabrous to puberulous. Leaves opposite sometimes aggregated in short shoots, concolorous, pale green on both surfaces, glabrous to puberulous; lamina elliptic to ovate, 0.6-3(4) x 0.4-2 (-2.5) cm, obtuse at the apex, cuneate at the base, margin entire to undulating crenate; 2-3 inconspicuous lateral nerves, not reticulated; oil glands clearly seen on the lower surface; petiole 2-7 mm long, pubescent. Inflorescence terminal, paniculate, 1-4 (5) cm long, pubescent; bract at the primary branching, ovate, filiform ≺ 1 mm long; peduncules 0.4 to 3 cm long; pedicels 1-2 mm long. Calyx campanulate 5-toothed, glandular, tube 1.5-2 mm long. Corolla pale yellow to cream; 4-lobed, upper lobe entire, hooded with 2-2.5 mm long tube. Ovary with 2.5-3.5 mm long style. Fruit a drupe, green turning crimson purple at maturity and brownish when dry. Fruits edible.

1.2 Previous phytochemical studies on *Premna* species

Of the 200 *Premna* species recognised only 11 have been examined for their chemical constituents. Research on the species studied during the past few

years has demonstrated that they synthesize a range of secondary metabolites. Diterpenes, sesquiterpenes, iridoids, and flavonoids are the typical constituents isolated from the genus.

1.2.1   Diterpenes of *Premna* species

Diterpenes are the chief constituents of *Premna* species. A number of pimarane type diterpenes, most of which are novel, have been recently isolated from *P. latifolia* (Table 1.1). *P. latifolia* was also shown to have abietane type diterpenoids but this class of compounds are best represented in *P. herbacea* (Table 1.2). In comparison with other types of diterpene, the abietanes have been shown to have a great deal of structural diversity. The aromatization and oxidation patterns in these unique diterpene quinones (Table 1.2) have gained considerable attention, both for their chemistry and biosynthesis (see Section 1.3.1). Diterpenes with carbon skeleton of less than 20 were recently isolated from the root bark of *P. latifolia* (Fig. 1.1). These compounds are believed to have antibiotic properties (Rao. *et al.*, 1982b).

1.2.2   Sesquiterpene and Iridoids of *Premna* species

Only a few reports exist on the sesquiterpene constituent of *Premna* species (Table 1.3). Rao *et al.* (1985) reported a novel caryophyllene sesquiterpene (**29**) from *P. integrifolia*. Another source of sesquiterpenes is *P. latifolia* from which the new compound **27** was isolated (Rao *et al.*, 1982c).

The first report on the occurence of iridoids in *Premna* species came

8

in 1981 from Rao *et al.* who isolated some novel glycosides from *P. latifolia* (Fig. 1.2). Recently, interesting iridoids which are linked with various cinnamate derivatives have been isolated from *P. odorata* (Fig. 1.3-4).

1.2.3 Other constituents of *Premna* species

Flavones were the only structural type of flavonoid which had been isolated from *Premna* species before this investigation (Table 1.4). Some of the more recently reported *Premna* flavones have been shown to have O-and C-glycosylation (Table 1.4).

β-Sitosterol and lupeol are the only triterpene-derived metabolites reported from *Premna* species. Recently, novel structures which link lupeol with fatty acids have been isolated from *P. fulva* (Table 1.5). Other miscellaneous compounds from *Premna* include the carboline derivative, trichtomine (**48**), and other unidentified alkaloids (Table 1.6) which have been shown to have some pharmacological activities (Shuichi *et al.*, 1976).
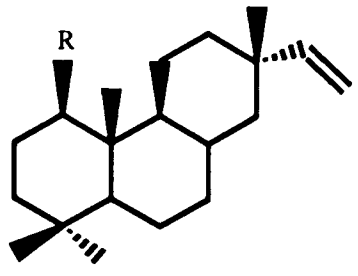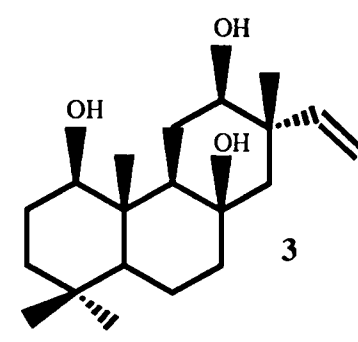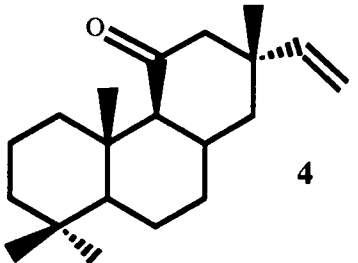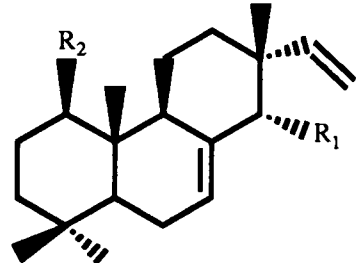
COMPOUND	PLANT NAME	PLANT PART	REFERENCES
R=H 1 R=OH 2	*P. latifolia*	ROOT	Rao *et al.*, 1982b
3	*P. latifolia*	ROOT	Rao *et al.*, 1979
4	*P. latifolia*	ROOT	Rao *et al.*, 1979
R₁=H, R₂=OH 5	*P. latifolia*	ROOT	Rao *et al.*, 1985
R₁=OH, R₂=H 6	*P. latifolia*	ROOT	Rao *et al.*, 1984

Table 1.1. Pimarane type of diterpenes from *Premna* species

Table 1.1 Contd.

7	*P. integrifolia*	ROOT BARK	Rao *et al.*, 1985
8	*P. integrifolia*	ROOT BARK	Rao *et al.*, 1985
9	*P. latifolia*	ROOT	Rao *et al.*, 1984
10	*P. integrifolia*	ROOT BARK	Rao *et al.*, 1985

11
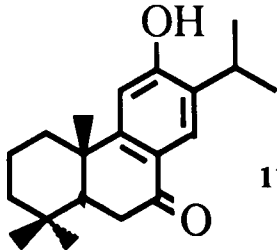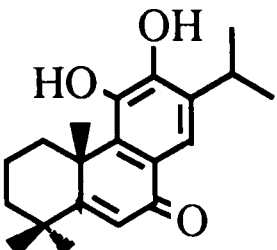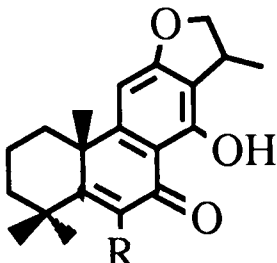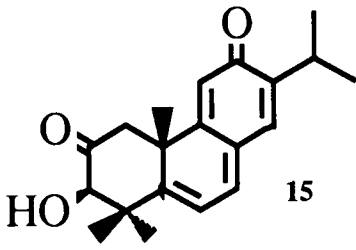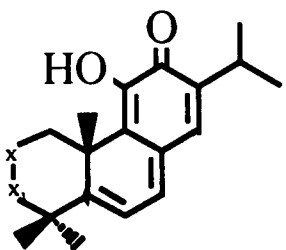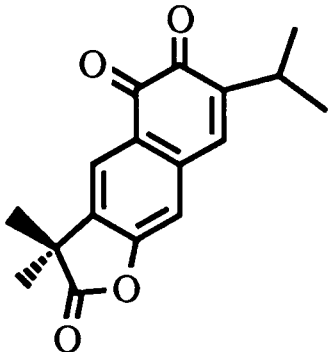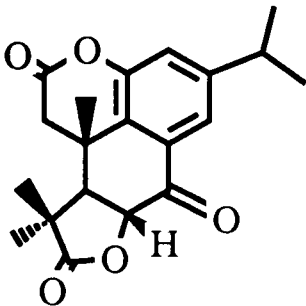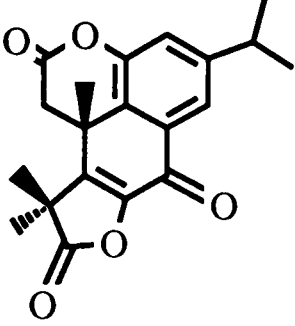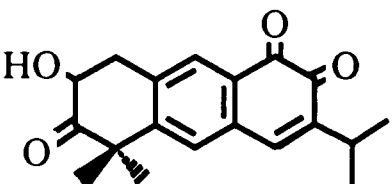
COMPOUND		PLANT NAME	PLANT PART	REFERENCES
	11	*P. herbacea*	ROOT	Meng *et al.*, 1989
	12	*P. integrifolia*	ROOT BARK	Rao *et al.*, 1987
R=H 13 R=OH 14		*P. integrifolia*	ROOT BARK	Rao *et al.*, 1987
	15	*P. herbacea*	ROOT	Sankaram *et al.*, 1989
X1=O or X=O 16 X1=CO 17		*P. herbacea*	ROOT	Sankaram and Rao., 1980

Table 1.2. Abietane and abietane derived diterpenes from
        ***Premna* species**

12

Table 1.2. cntd.

18	*P. herbacea*	ROOT	Sankaram *et al.*, 1988
19	*P. herbacea*	ROOT	Weixin *et al.*, 1989
20	*P. herbacea*	ROOT	Weixin *et al.*, 1989
21	*P. herbacea*	ROOT	Meng *et al.*, 1988
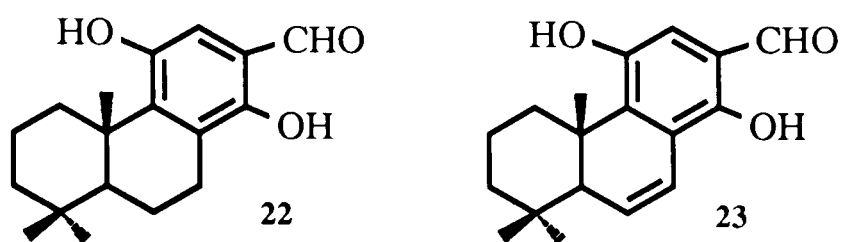
Fig. 1.1. Diterpenes of *P. latifolia* with antibiotic properties
(Rao *et al.*, 1979 and Rao *et al.*, 1982b)
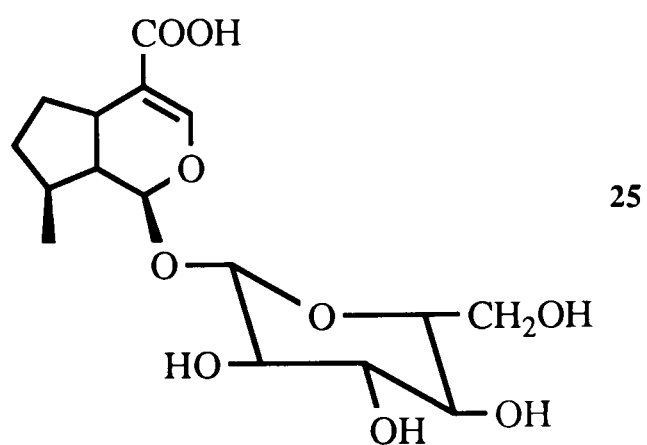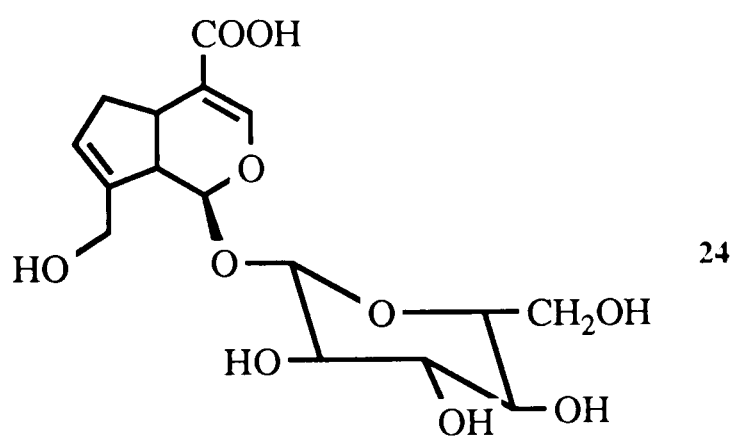
Fig. 1.2. Iridoids from the root bark of *P. latifolia*.
(Rao *et al.*, 1981)

14
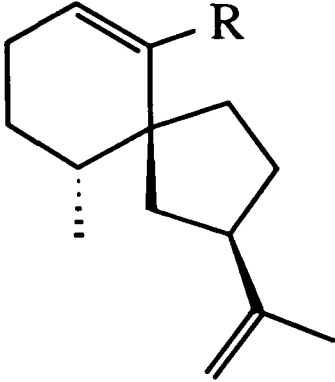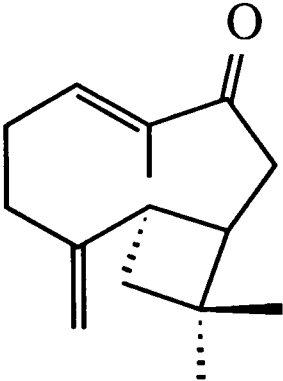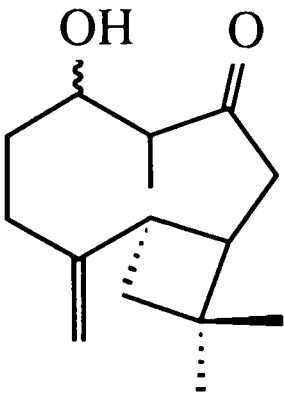
COMPOUND		PLANT NAME	PLANT PART	REFERENCES
R=CH₃	26	*P. latifolia*	ROOT BARK	Rao *et al.*, *1982c*
R=CHO	27			

R=CH$_3$ 26
R=CHO 27

	28	*P. integrifolia*	ROOT BARK	Rao *et al.*, 1985

	29	*P. integrifolia*	ROOT BARK	Rao *et al.*, *1985*

Table 1.3. Sesquiterpenes of *Premna* species

30

R₁=Caff, R₂=H   31

R₁=H, R₂=Caff   32

R,=H, R₂=H   33
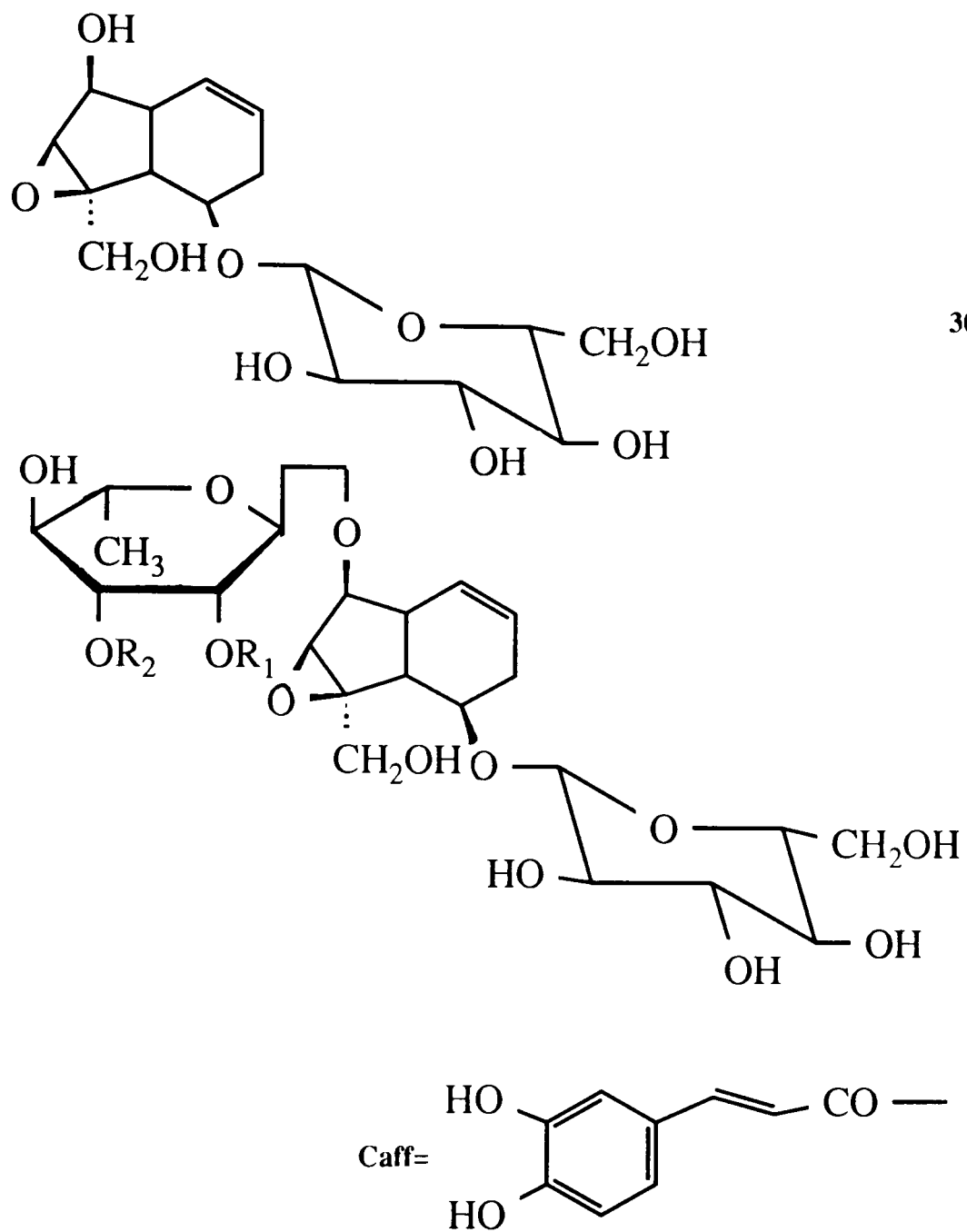
Fig. 1.3. Iridoids from the leaves of *P. odorata*

(Otusuka *et al.*, 1989a)

16

A

B

C
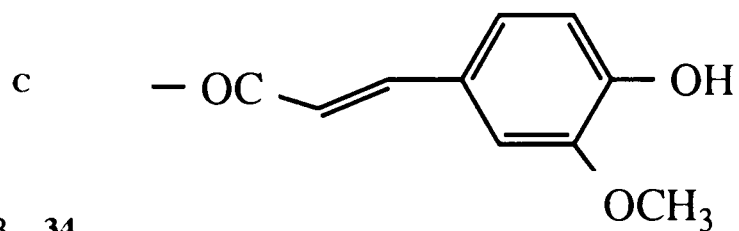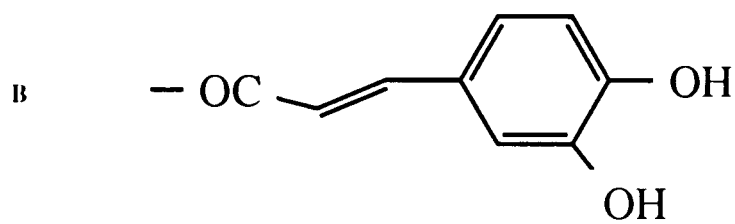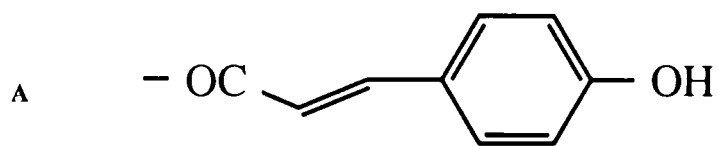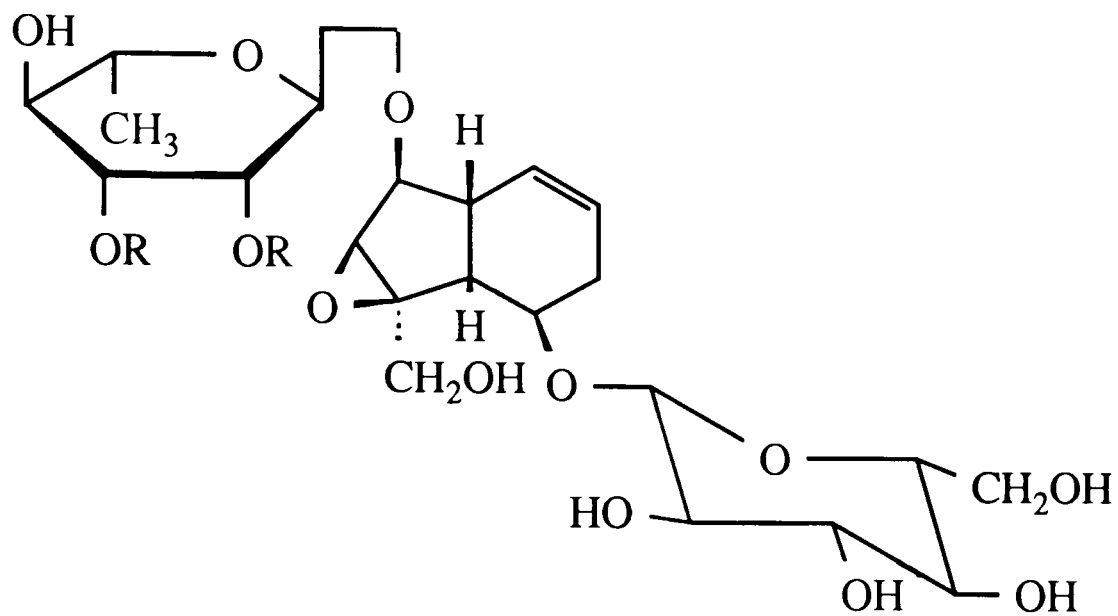
R=B, R=B   34

R=A, R=B   35

R=B, R=C   36

R=A, R=C   37

Fig. 1.4. Iridoids from the leaves of _P. odorata_

(Otsuka _et al._, 1989b)

17
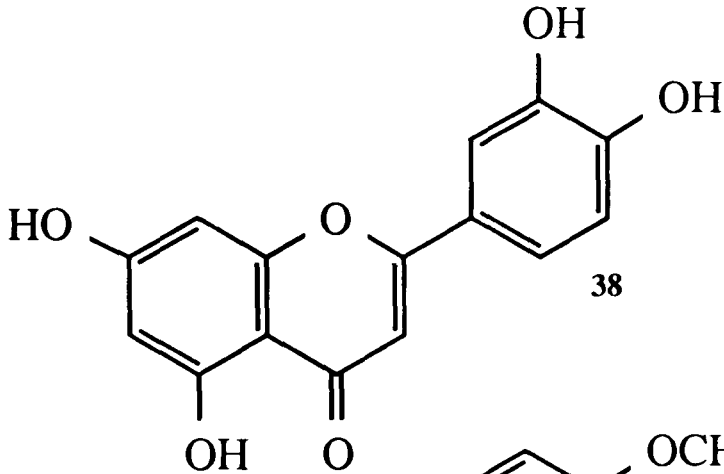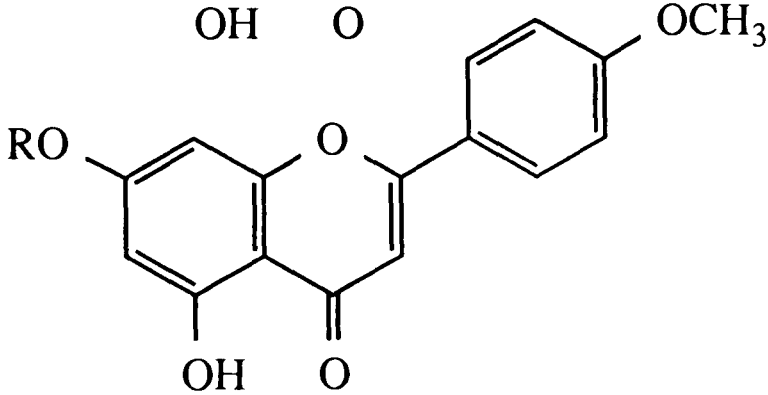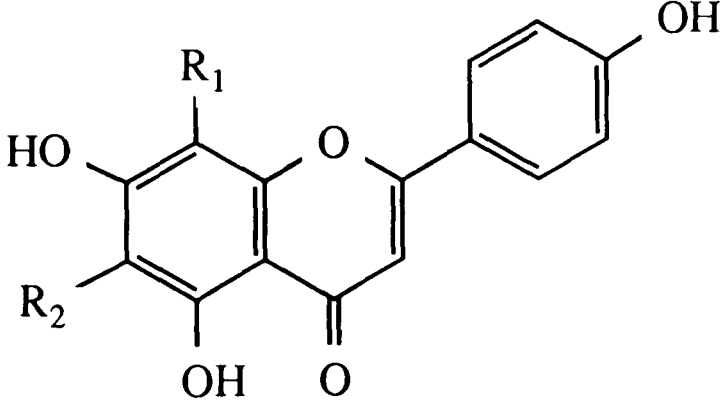
COMPOUND	PLANT NAME	PLANT PART	REFERENCES

38 *P. integrifolia* ROOT Biswanath *et al.*, 1985

| R=L-rhamnopyranosc-(1-2)-L-arabinopyranosyl | **39** | *P. latifolia* | LEAVES | Rao *et al.*, 1982a |
| R=rhamno-xylo-arabinoside | **40** | | STEM BARK | Rao *et al.*, 1981 |

| R₁=B-D-xylopyranosyl, R₂=B-D-glucopyranosyl | **41** | *P. integrifolia* | ROOT | Purushothaman and Vasanth, 1986 |

R_1=B-D-xylopyranosyl, R_2=B-D-glucopyranosyl

Table 1.4. Flavonoids of *Premna* species

18
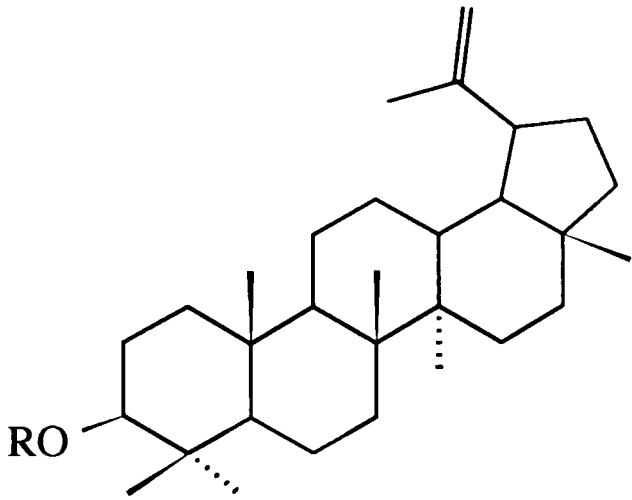
COMPOUND		PLANT NAME	PLANT PART	REFERENCES
β–Sitosterol	**42**	*P. foetida*	LEAVES	Rao *et al.*, 1984
		P. integrifolia	LEAVES	Ramaaiah *et al.*, 1978
		P. japonica	ROOT	Munehiro and Tunao, 1975
		P. latifolia	ROOT	Rao *et al.*, 1980

$R=CH_3\text{-}(CH_2)_{26}\text{-}CO$ **43**

$R=CH_3\text{-}(CH_2)_{27}\text{-}CO$ **44**		*P. fulva*	LEAVES	Song *et al.*, 1991
$R=CH_3(CH_2)_{28}\text{-}CO$ **45**				

Table 1.5. Triterpenes of *Premna* species
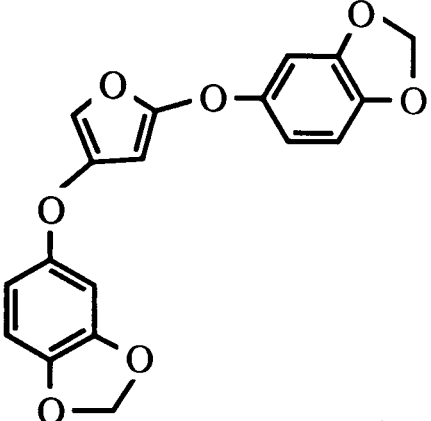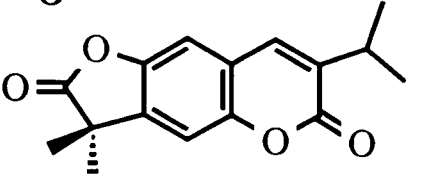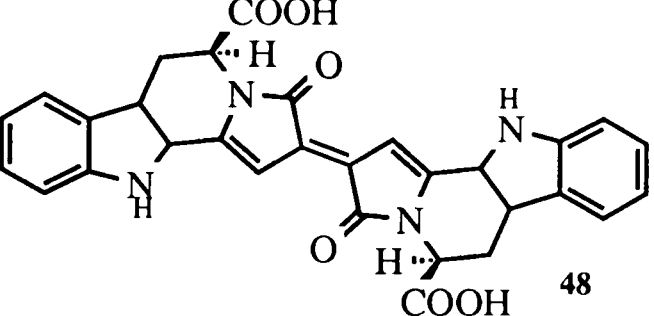
COMPOUND		PLANT NAME	PLANT PART	REFERENCES
	46	*P. latifolia*	LEAVES	Rao and Vijayakumar, 1980
	47	*P. herbacea*	ROOT	Meng *et al.*, 1987
	48	*P. microfila*	ROOT	Shuichi *et al.*, 1976
PREMNINE	49	*P. integrifolia*	ROOT	Basu and Dandiya, 1943
GANIARINE	50			
APHELADRINE	51	*P. integrifolia*	ROOT	Biswanath *et al.*, 1985

Table 1.6. Miscellaneous compounds from *Premna* species

20

1.3 BIOGENESIS OF *PREMNA* COMPOUNDS

As shown in Section 1.2. several classes of compounds; terpenes, flavonoids, cinnamate derivatives and alkaloids have been isolated from *Premna* species. In this section, the biosynthetic pathway of only major *Premna* constituents (diterpenes, cinnamate derivatives, and flavonoids) of the classes which have been isolated in the present study are discussed.

1.3.1 Biogenesis of Diterpenes

Diterpenes are compounds with a twenty carbon skeleton and occur either in acyclic or various ring forms. Like other terpenes they are a multiple of C_5 "isoprene" units linked together in head to tail fashion. The synthesis of diterpenes in living tissue has been rationalized from early isotope studies (Tavormina *et al.*, 1956). This involves three major steps: synthesis of the active isoprene units through the mevalonic acid pathway, polymerization of four isoprene units to form the parent compound of all diterpenes; geranylgeranyl pyrophosphate, and cyclization and oxidation at various centres.

The synthesis of active isoprene units starts from the most abundent primary metabolite, acetyl coenzyme A, which is continually supplied by carbohydrate metabolism or respiration. The biosynthetic pathway of mevalonate leading to active isoprene units is shown in Scheme 1.1.

Acetyl CoA condenses with acetoacetyl CoA in a branched fashion to give 3-hydroxy-3-methyl-glutaryl CoA (54) after hydrolysis. The two step reduction

O
‖
CH₃C-SCOA
52

O   O
‖   ‖
CH₃CCH₂C-SCOA
53

$-H_2O$

HO CH₃

HO   O   COSCoA

NADPH

3s-3-hydroxy-3-methyl-glutaryl COA   **54**

HO CH₃

HO   O   CH₂OH

ATP

3R-mevalonic acid   **55**

$H \overset{PO_3}{} CH_3$

H

O   C   O-H   CH₂OPP   **56**

$-CO_2$, $-HOP$

H₂C   CH₃

H H   OPP

ISOMERASE

Isopentenyl pyrophosphate (IPP)   **57**

H₃C

H₃C   OPP

Dimethylallyl pyrophosphate (DMAP)   **58**

H₃C   H₃C   OPP

H₃C

Geranyl pyrophosphate   **59**

IPP

H₃C   H₃C   H₃C   OPP

H₃C

all-trans-farnesyl pyrophosphate   **60**

IPP

OPP

trans-trans-Geranylgeranyl pyrophosphate   **61**

H⁺

20   11   OPP

2   1   15

10   16

18   H   H

62

OPP

63

Scheme 1.1. Formation of labdane skeleton through mevalonate pathway

22

with NADPH then affords mevalonic acid (55) via mevaldic acid. Phosphorylation, decarboxylation, and elimination of phosphate produces isopentenyl pyrophosphate (IPP) (57), the active isoprene unit in the polymerization stage. Isopentenyl pyrophosphate is then reversibly isomerised to dimethylallyl pyrophosphate (DMAP) (58), the starter unit of terpene biosynthesis.

DMAP and IPP are reactive alkylating agents on the strengh of phosphate being an effective leaving group with the incipient carbonium ion being stabilized by charge delocalization (Torsell, 1983). Four of these isoprene units, sequentially condensed, lead to geranylgeranyl pyrophosphate (61); a precursor of all diterpenes (Scheme 1.1).

The cyclization of geranylgeranyl pyrophosphate normally progresses direcltly to the bicyclic decalin system with the carbonium ion being subsequently discharged by addition of water or proton elimination, or *via* a series of Wagner-Meerwein shifts. A chair-chair conformation of geranylgeranyl pyrophosphate gives the labdane skeleton (62). A five step concerted Wagner-Meerwein shift with inversion at each centre, route B, leads to the clerodane skeleton (65) (Scheme 1.2). Deprotonation to form the C-8 exocyclic double bond produces labdadienol pyrophosphate (66) which is an important intermediate in the biosynthesis of tri- and tetracyclic *Premna* diterpenes. Solvolysis of labdadienyl pyrophosphate gives via the 8-pimarenyl cation (67), pimarane (68) and abietane derivatives (69), both of which are well represented in *Premna* species.

The further biosynthetic sequence to the synthesis of the abietane type of diterpenoids has recently been shown on compounds from *P. herbacea* (Sankaram
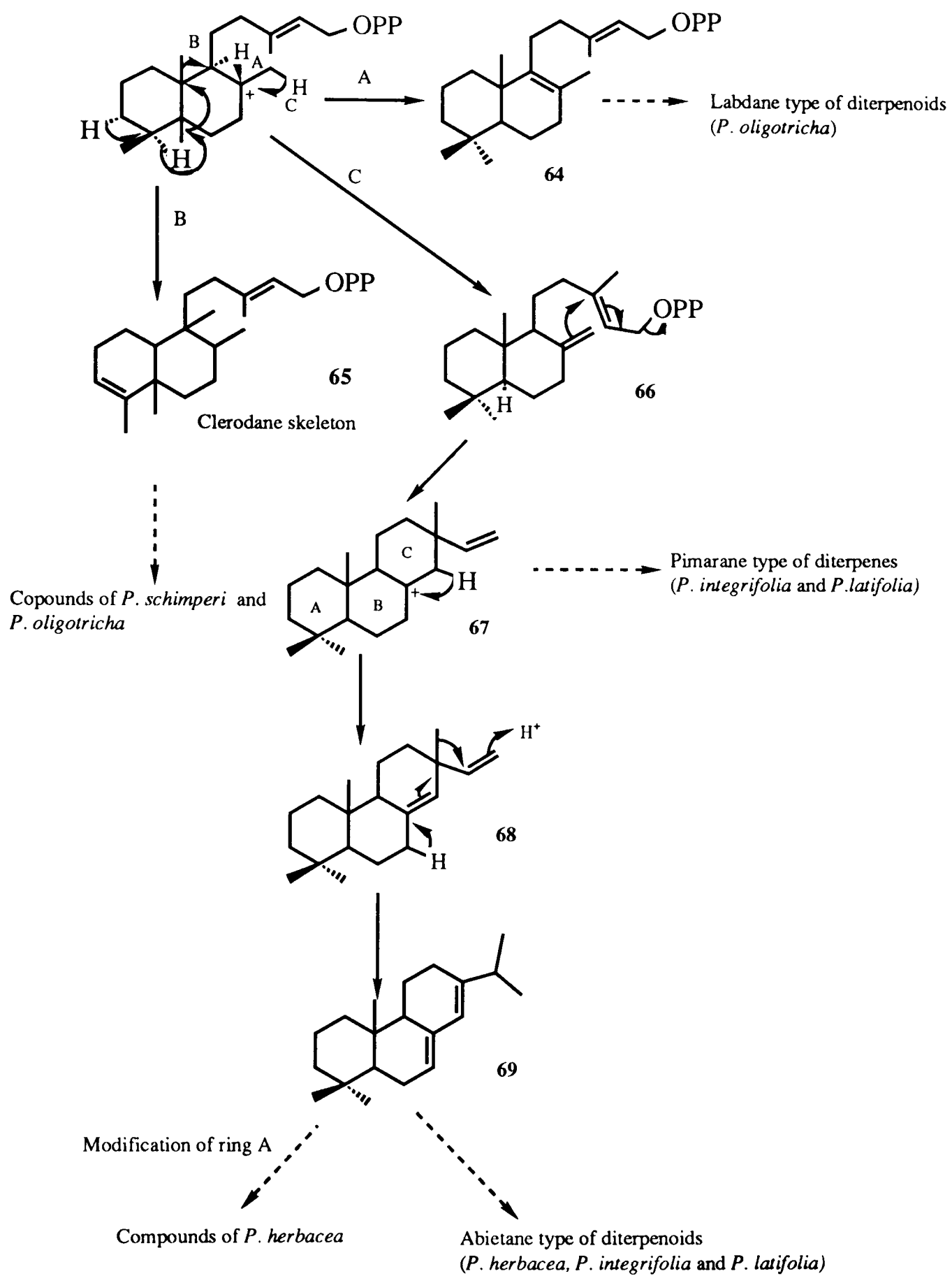
Scheme 1.2. Biosynthetic relationship between *Premna* diterpenes
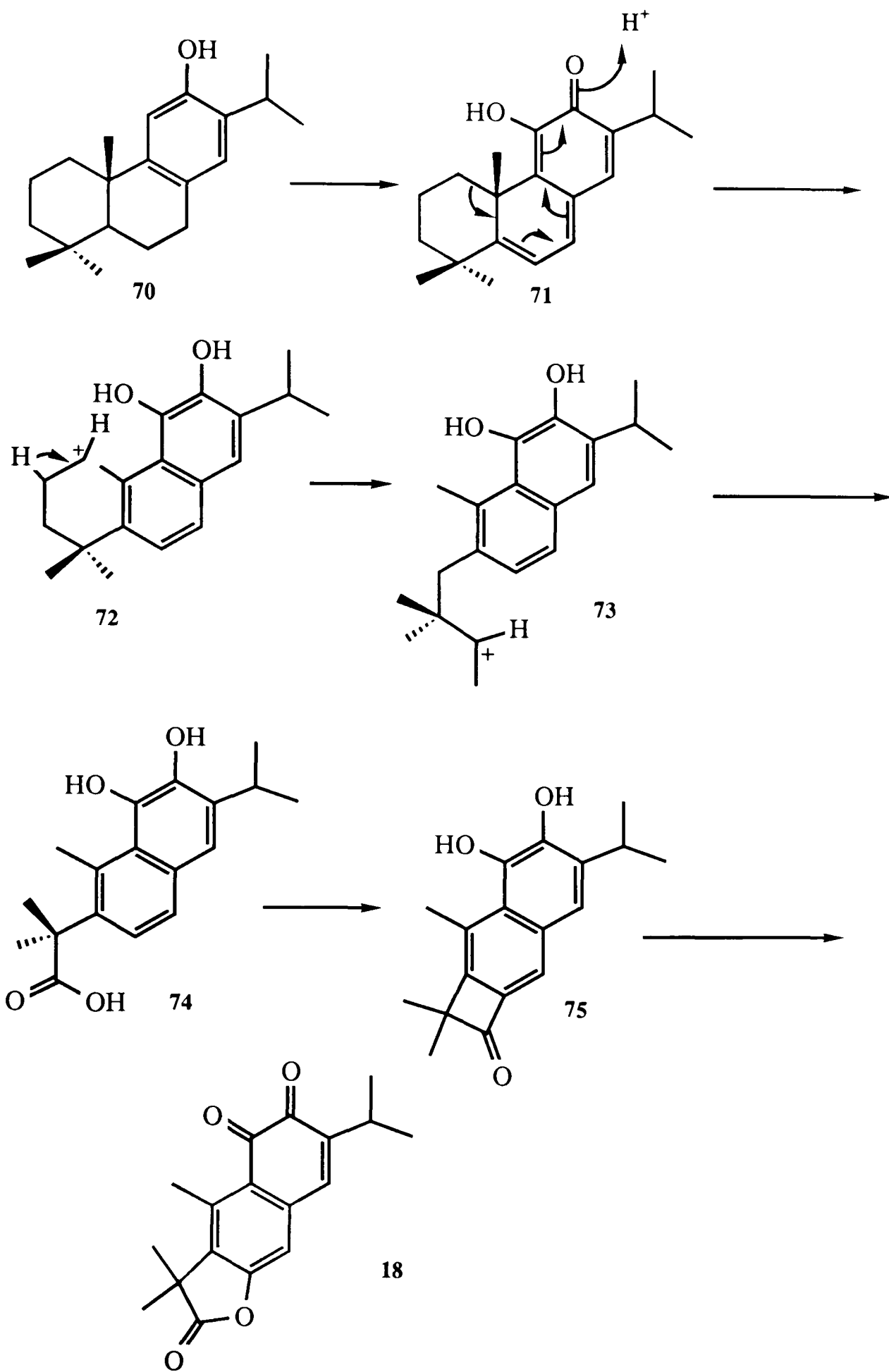
Scheme 1.3. Biogenetic route of abietane derived compounds from *P. herbacea* (Sankaram *et al.*, 1988)

25

et al., 1988). Oxidation of the A ring followed by degradation and cyclization leads to structures **18-20** (page 13). The finding of intermediates like **18** supported a biosynthetic pathway (Scheme 1.3) which started from ferrigenol (**70**) through carbonium ion rearrangement and several oxidation steps.

1.3.2 Biosynthesis of Flavonoids and other C_6-C_3 Derivatives

Flavonoids, cinnamic acids and their derivatives and lignans have common origin and exhibit a characteristic C_6-aromatic-C_3-side chain structure. The synthesis of this basic skelton is a result of one of the most important biogenetic routes in secondary metabolism; the shikimic acid pathway.

1.3.2.1 Biosynthesis of phenylalanine through shikimic acid pathway

The biosynthetic sequence leading to shikimic acid was established by ^{14}C labelling experiments (Sprinson, 1961) and is initiated by erythrose-4-phosphate (**77**) condensing with phosphoenol pyruvate (PEP) (**76**) to give a C-7 compound (**78**) which undergoes several reactions to lead to shikimic acid (**79**). The role of shikimic acid in secondary product metabolism is primarily as the source of aromatic amino acids, in the case of production of flavonoids, cinnamic acids, lignans and some alkaloids; the most important amino acid is phenylalanine. The reaction is started by regioselective phosphorylation of shikimate at C-3 and then reaction with PEP at C-5 (Scheme 1.4). This phosphorylation serves as an effecient leaving group for the subsequent elimination leading to chorismic acid

D-Erythrose-4-phosphate **77**

3-Deoxy-D-arabinoheptulosonic
acid-7-phosphate (DAHP) **78**

Shikimic acid-3-phosphate **79**

80

5-Enolpyruvylshikimic acid-3-phosphate **81**

Chorismic acid **82**

Prephenic acid **83**

Phenyl pyruvic acid **84**
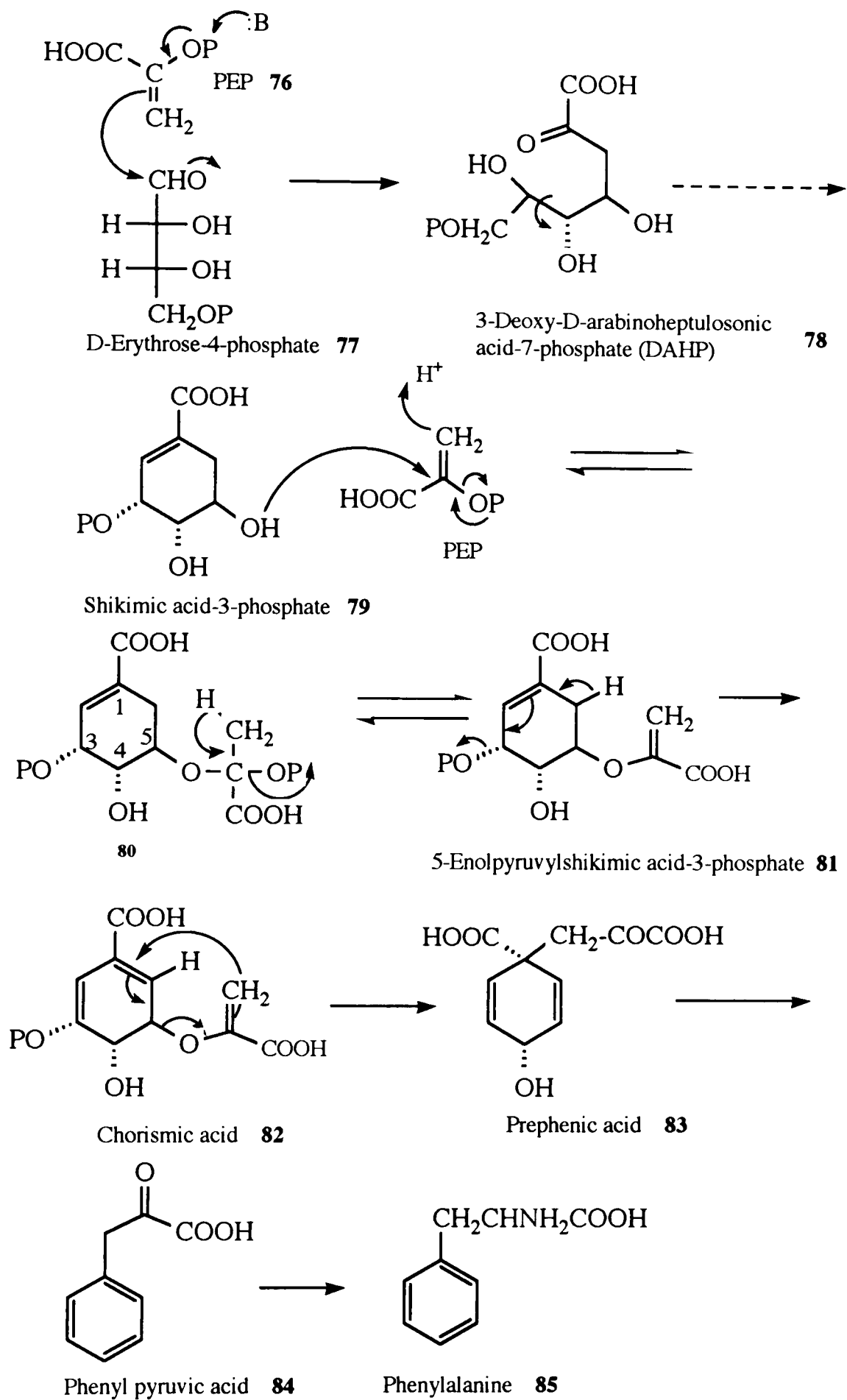
Phenylalanine **85**

Scheme 1.4. Biosynthesis of phenylalanine through shikimate

(82). Chorismic acid is an unstable intermediate, and undergoes a Claisen re-arrangement to prephenic acid (83). Decarboxylation followed by transaminase activity finally converts phenyl pyruvic acid (84) into phenylalanine (85).

1.3.2.2 Biosynthesis of cinnamic acids, benzoic acids and lignans

The widely distributed cinnamic acids arise from phenylalanine by enzymatic elimination of ammonia followed by aromatic hydroxylation and methylation (Scheme 1.5). All of these simple compounds have been isolated from plants investigated in this study either alone or incorporated with compounds derived from other biosynthetic pathways (Fig. 1.5-6).

Ferulic acid (89) undergoes phenol oxidation reactions to form 18 carbon skelton compounds, "lignans" (Scheme 1.6). Reduction of ferulic acid proceeds via the phosphate to the formation of allyl or propenyl side chains. Phenol oxidase mediated oxidation of the phenolate to phenoxy radical (97), followed by dimerization resulted in the synthesis of lignans.

1.3.2.3 Biosynthesis of flavonoids

Flavonoids are structurally characterized by having two oxygenated aromatic rings, A and B, joined by a three carbon fragment. Several structural types can be distinguished: flavanones, flavones, flavonols, isoflavonoids, aurones and anthocyanidins. Only the first three groups, which have all been isolated from *Premna* species, are discussed here. The origin of the direct flavonoid precursors 4-coumaroyl-CoA (103) and malonyl CoA and the biosynthetic relations in the flavonoid groups are reveiwed by Harborne (1988) (Scheme 1.7). Malonyl-CoA is

28

Phenylalanine

86

β-oxidation

[O]

P-OH-Cinnamic acid 87

Benzoic acid 90

[O]

P-OH-Benzoic acid 91

[O]

Caffeic acid 88

[O]

Protocatechoic acid 92

[CH₃]

[CH₃]

Ferulic acid 89

Vanillic acid 93
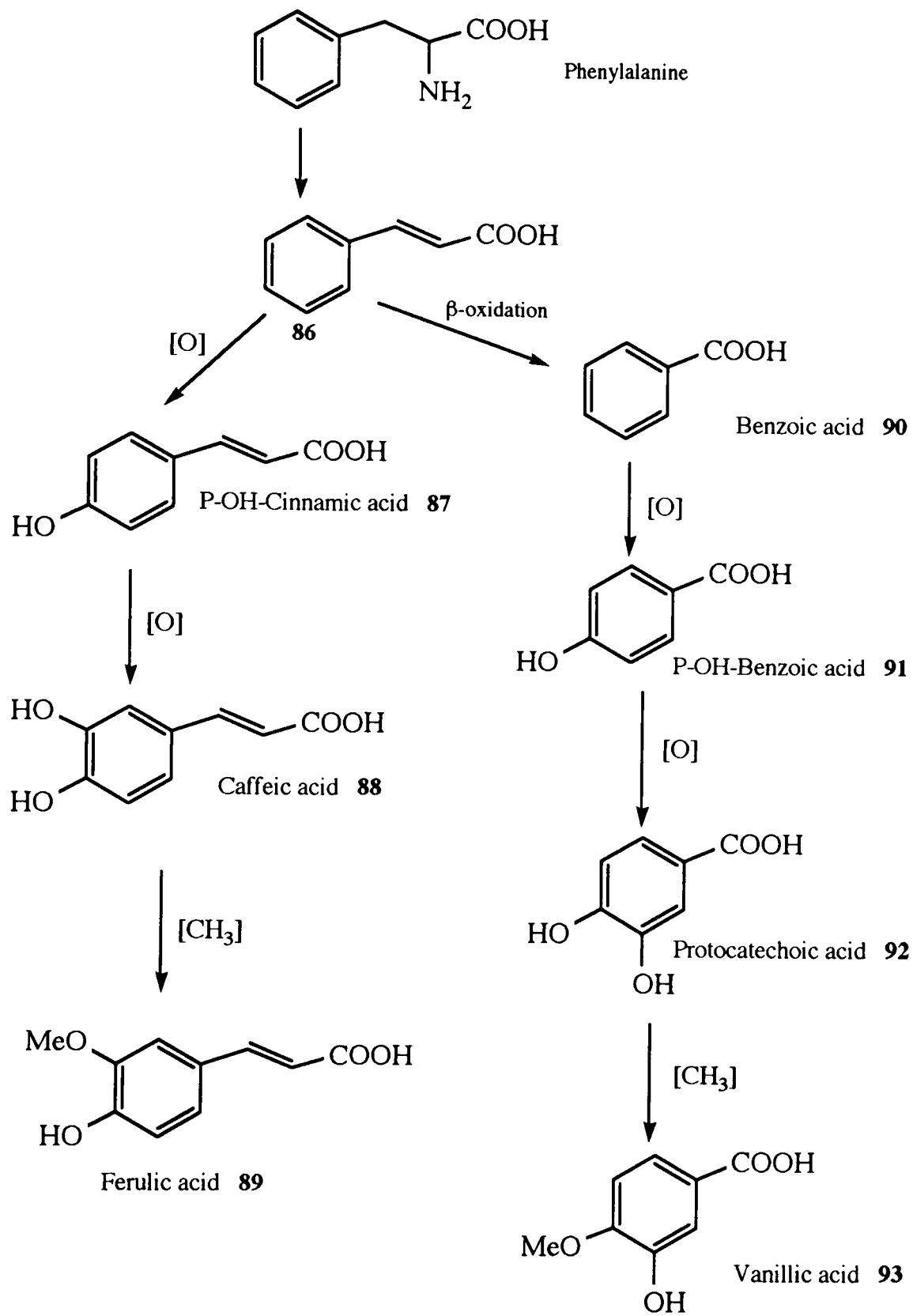
Scheme 1.5. Biosynthetic network of cinnamate and benzoic acids

29
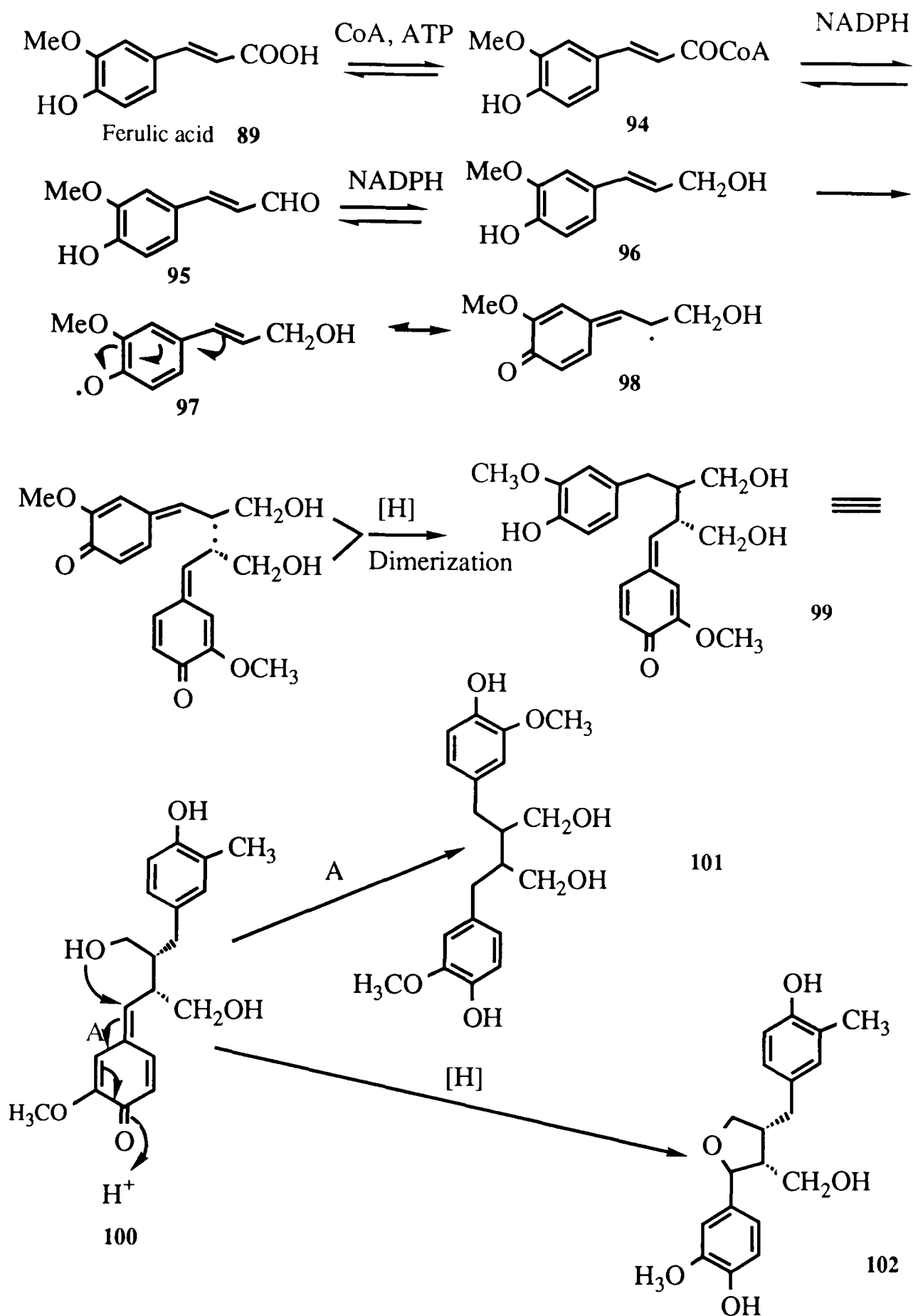
Scheme 1.6. Biosynthetic sequence to lignans
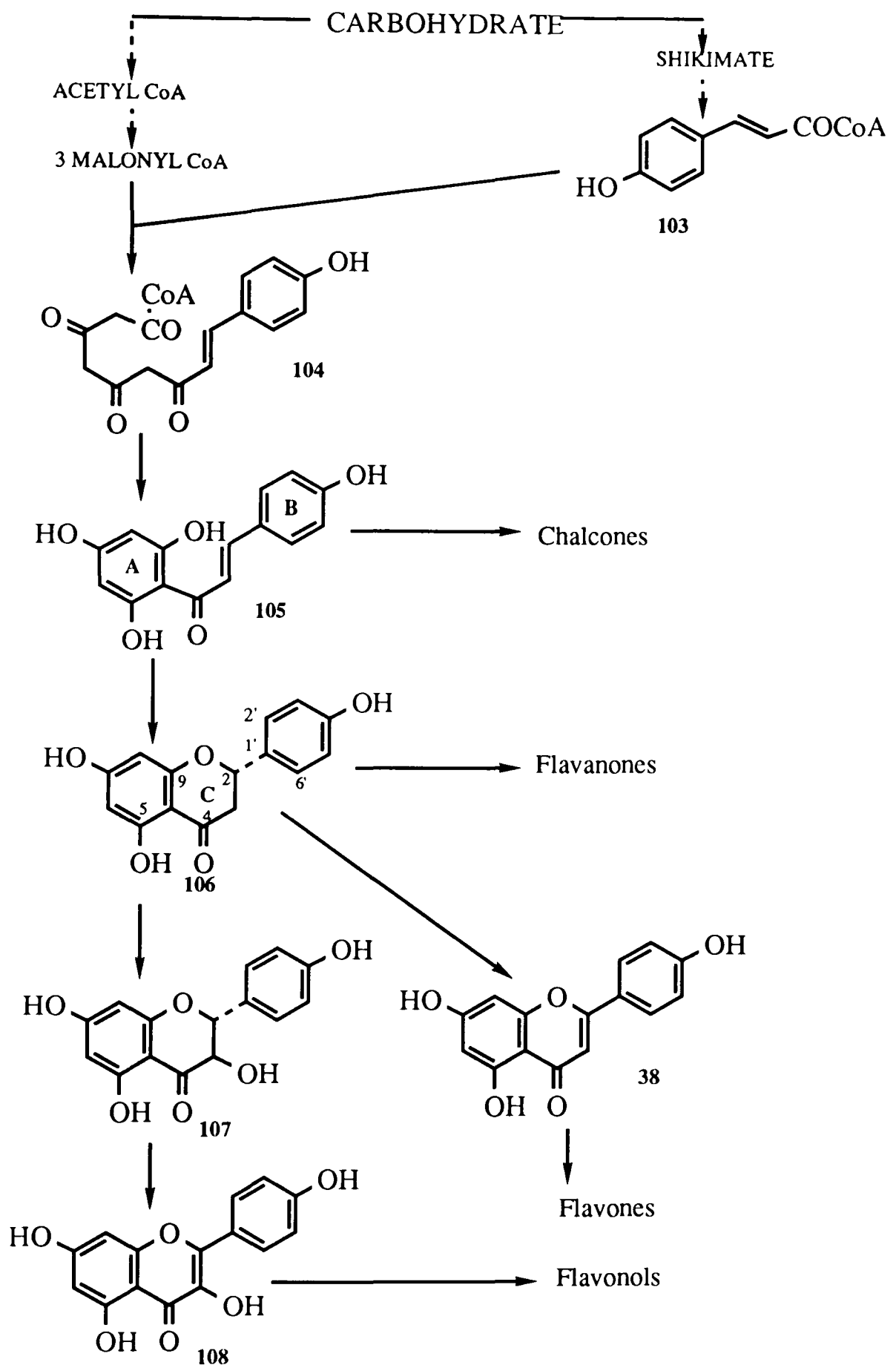
Scheme 1.7. Biosynthetic pathway of flavonoids

synthesized from the glycolysis intermediate acetyl CoA and carbon dioxide, the reaction being catalysed by acetyl-CoA carboxylase. The supply of 4-coumaroyl-CoA is discussed in Section 1.3.2.2

The central step in flavonoid biosynthesis is then the condensation of three molecules of malonyl-CoA with suitable hydroxycinnamic acid-CoA esters (ordinarily 4-coumaroyl-CoA), to give the C-15 chalcone (**105**). Transformation by stereospecific action of chalcone isomerase provides the flavanone, naringenin (**106**). Hydroxylation of naringenin at position 3 (dihydroflavonol) followed by introduction of a double bond between C-2 and C-3 leads to flavonols (**108**). The introduction of this double bond without hydroxylation at C-3 lead to flavones (**38**). B ring hydroxylation can be achieved either by incorporation of already substituted hydroxy-cinnamic acid derivatives during synthesis of the C-15 skeleton or by substitution at the C-15-stage by specific hydroxylase and methyltransferases. Incorporation of sugars at various hydroxyl sites is directed by glycosyltransferases. All these oxygenation and glycosylation patterns are shown in *Premna* flavonoids.

1.4 Medicinal Values of *Premna* species and Objective of the Present Study

1.4.1 Traditional medicnal uses of *Premna* species

Almost all of the *Premna* species which have been studied to date are known for their medicinal values.

Song *et al.* (1991) reported that *P. fulva* is one of the most important plants in Chinese folk medicine. *P. integrifolia* and *P. latifolia* are used in Philippines as a cure for stomach trouble (Quisumbing, 1978). The root of *P. integrifolia* is also regarded as medicinal in the Sankirt region of India. According to Rao *et al.* (1982), the root decoction is prescribed as a stomachic and laxative. *P. herbacea* is widely used in the Chinese folk medicine against inflammation and malaria (Meng *et al.*, 1989). In India, the juice of the root is given with the juice of ginger and warm water for asthma. The bitter root is used as a stomachic and for rheumatism and dropsy (Quisumbing, 1978).

Quisumbing (1978) reports that *P. odorata* is extensively employed in Philippines traditional medicine. A decoction of the leaves is taken as a drink to loosen phlegm and is also effective for coughs. A decoction of fresh leaves is prescribed for vaginal irritation and is claimed to be beneficial against tuberculosis. Leaves applied over the bladder facilitate urination and when similarly applied to the abdomen of a child cure tympanites. The leaves are boiled in water, the water then being used for bathing babies, and also as a treatment for beriberi. In the latter case the boiled leaves are applied to the affected part of the patient's body. A decoction of the roots, leaves, flowers and fruit is used as a sudorfic, pectoral, parasiticide, and is said to be carminative. Masticating the roots and swallowing the saliva is prescribed for cardiac trouble. In the same region, the infused leaves of *P. tomentosa* is employed as a remedy for dropsy and also as a diuretic.

There is now increasing evidence that *Premna* is an important genus

in traditional medicine of many countries. The chemical constituents of these herbal drugs have also been studied (see Section 1.2). A systematic "bioassay guided" phytochemical investigation leading to the active principles however has not been undertaken for any of these plants. Studies on the biological activities of the isolated compounds is also not well developed. Some preliminary biological studies have demostrated the antibiotic nature of compounds isolated from *P. latifolia* (Rao *et al.*, 1982b), the hypotensive property of trichtomine (**48**) from *P. integrifolia* (Shuchi *et al.*, 1976) and the sympathomimetic action of premnine from *P. integrifolia* (Basu *et al.*, 1943).

1.4.2 Traditional uses of *Premna* species examined and objective of the present study

1.4.2.1 *P. schimperi*

In the central region of Ethiopia *P. schimperi* is known as "Checho" (Amharic) and is used in the treatment of inflammation and secondary infection associated with superficial wounds. It is also employed by farmers to treat common eye infections in cattle. For both human and veterinary use the juice, or sometimes the aqueous extract, of the leaf is applied to the infected or inflamed area. The juice is prepared by simply rubbing a few leaves between the palms of the hands and the liquid released is then squeezed onto the wound. The use of *Premna schimperi* for curing wounds or local infections suggested a possible antimicrobial activity, especially against *Staphylococcus aureus*, a well known causative agent for the contamination of wounds in the rural areas of Ethiopia.

The primary objective of this project was to assess the antibacterial activity of the crude extract and to isolate and characterize the active principle(s)

1.4.2.2 *P. oligotricha*

The use *P. oligotricha* in folk medicine is not recorded but in Southern Ethiopia, where it is locally called "Tatissa" (Oromo), some traditional uses have been observed (personal observation). In this region, thin twigs of the plant are chewed until they become fibrous brush like structure and then used for tooth cleaning ("chewing stick"). Ripe fruits are edible and the smoke formed by burning the plant is used to "steralise" milk containers resulting in the milk remaining fresh for increased period of time.

To date, a number of plants used as chewing sticks are proved to have antibacterial activity (El-Said *et al.*, 1971 and Odebiyi and Sofwora, 1982). The use of *P. oligotricha* for prevention of milk souring also suggest a probable presence of some constituent which act against microorganisms responsible for milk fermentation. It was then logical to evaluate the antimicrobial activity of *P. oligotricha* and isolate the active principle(s).

1.4.2.3 *P. recinosa*

Almagboul *et al.* (1985) reported the use of *P. recinosa* in Sudan. The leaves are a source of aromatic oil and the root is employed in folk medicine for stomach pain. The authors also reported that the leaf extract exhibits antibacterial activity.

All these three species of *Premna* have traditional uses or reports asso-

ciated to antimicrobial activity. Their antimicrobial (bacteria, fungi and yeast) activity and their active and inactive constituents have been studied during this project, using a bioassay guided isolation scheme.

Chapter 2

MATERIALS AND METHODS

2.1 Plant Materials and Preparation of Extracts

2.1.1 Plant materials

The leaves of *Premna schimperi* (voucher: SHM-13) were collected in
September 1989 from the Menagesha Forest (*ca.* 2000m). Menagesha Adminis-
trative region, Shoa Province, Ethiopia; *Premna oligotricha* (voucher: SHM-12)
in September 1989 from beside the Yabellow-Mega Road at *ca.* 1600m, Sidamo
Province, Ethiopia; and *Premna recinosa* (voucher: Sebsebe 2535) in April 1990
from an *Acacia/Commiphora* woodland forest (*ca.* 870m), 2 km from Melka-
guba towards Negele, Sidamo Province, Ethiopia. Voucher specimens have been
deposited at the National Herbarium of Ethiopia, Addis Ababa University.

2.1.2   Preparation of extracts

The air dried plant materials were powdered and placed in a 10 L glass percolator. The materials were then soaked in ethanol and continually washed with fresh solvent until the solution became colourless ($\approx$ one week). Each extract was then concentrated under reduced pressure in a rotatory evaporator. In some cases plant materials were extracted to exhaustion in a Soxhlet apparatus with ethanol.

2.2   Microrganisms and Antimicrobial Assay

2.2.1   Microorganisms

The following organisms were used for the antimicrobial assay testing: gram-positive bacteria- *Bacillus pumilus* (NCTC 10327), *Bacillus subtilis* (NCTC 10452), *Lactobacillus plantarum* (Torry Research Station Aberden, 6376), *Staphylococcus aureus* (NCTC 6571), and *Streptococcus faecalis* (NCTC 775); gram-negative bacteria- *Escherichia coli* (NCTC 9001) and *Pseudomonas aeruginosa* (NCTC 6750); fungi- *Aspergillus niger* (IMI 149007) and *Penicillium notatum* (IMI 15378) and yeast- *Candida albicans* (IMI 45348). The test organisms were selected due to their fast growth in the agar media, easy in handling and their non pathogenic nature. Bacterial test organisms were maintained in nutrient agar (Oxoid No. 2) while yeast and fungal test organisms were maintained in malt agar (Oxoid no. 2). Prior to testing, bacterial and yeast test organisms were subcultured into liquid nutrient medium and kept at $37^{\circ}C$ while fungal slants

were incubated at 25°C until sporulation.

2.2.2   Antimicrobial assay

Throughout the study, two kinds of assays were performed; the agar disc diffusion assay (**DDA**) and the minimum inhibitory concentration assay (**MIC**).

2.2.2.1   The agar disc diffusion assay method (DDA)

Preliminary antimicrobial screening of various extracts was carried out using the disc diffusion assay method (Ahmad *et al.*, 1986 and Hartman, 1968). To 10 ml of molten agar (hand hot), 0.1 ml of an overnight broth of bacterial test organism or fungal spore suspension was added and then poured into a petridish. The agar was left for a few minutes at room temperature to solidify.

Discs were impregnated with various concentrations of an extract by introducing up to 10 μl of the extract solution on a 5 mm diameter filter paper (Whatman No. 1). After drying, all discs were stored at 4°C until used. Discs were then placed on top of the test plate and incubated at 37°C for 18 hours. For each organism, the experiment was carried out in triplicate and discs of a standard antibiotic (chloramphenicol) were used for positive control.

As it was designed for simplicity, and not particularly for a high degree of accuracy (Borchardet and Andrews, 1952), the disc diffusion assay method is not quantitative and probably permits only a distinction between active and inactive substances *in vitro*. The method, however, is very efficient for the screening of numerous fractions and crude extracts and serves as a good guide for following

the active principle. In this assay, inhibition of microbial growth by extracts and known antibiotics could be detected as clear zone around discs impregnated with the extract (Fig.2.1)

Figure 2.1: **Agar plates showing inhibitory zones in the DDA**

Staphylococcus aureus   *Bacillus subtilis*
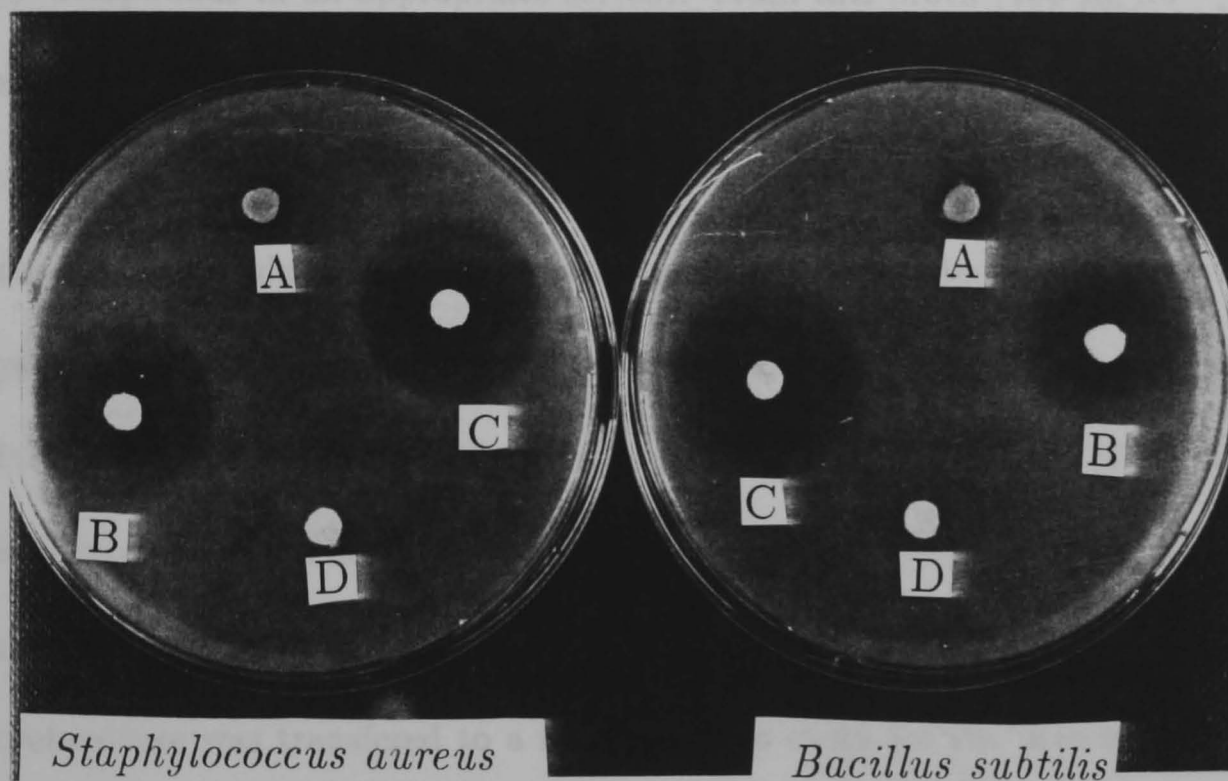
A = crude extract (200 μg per disc of ethanol extract of *Premna schimperi*)[1]

B = Active fraction (100 μg per disc of chloroform fraction of the ethanol extract)[1]

C = Active compound (100 μg per disc of SHM-1)[1]

D = Inactive fraction

[1]See Scheme 3.1, page 54

2.2.2.2 Minimum inhibitory concentration (MIC) assay

Once the active compounds are isolated, a tedious but more quantitative and reproducable experiment which requires less sample, was used. The method described by Schwarz and Brown (1954) was adopted.

To 2 ml of nutrient broth was added 20 μl of 1% w/v solution of the test compounds in an appropriate solvent. From this broth (100 μg ml^{-1}, two-fold serial dilutions in nutrient broth were prepared (down to 0.5 μg ml $^{-1}$). A bacterial suspension (10^7 ml^{-1}) of each bacterial test organism was prepared and 0.1 ml inoculated into each broth to give a final bacterial concentration of approximately 10^6 ml^{-1}. Control experiments using streptomycin and solvent blank were also prepared. All tubes were incubated at 37°C for 16 h and the lowest concentration at which no growth was observed was taken as the minimum inhibitory concentration of the compound. In the tubes where growth was absent, a subculture was transfered to a fresh broth to check for the presence of viable bacteria.

In some cases the bactericidal activity of compounds with time was studied. 25 and 50 μg ml^{-1} solutions of the active compounds were prepared in 10 ml of sodium chloride solution (0.9% w/v). After inoculation of bacteria to a final concentration of 10^6 ml^{-1}, 1 ml samples were counted at various intervals for viable bacteria (surface plate technique) after sutable dilution in sodium chloride (0.9% w/v). For comparative purposes, a preservative, nipagin M (methyl p-hydroxybenzoate), was also assayed at a concentration of 2 mg ml^{-1}.

2.3 Separation Techniques Employed

2.3.1 Chromatographic techniques

2.3.1.1 Vacuum liquid chromatography (VLC)

Throughout this study VLC (Pelletier *et al.*, 1986) was the first chromatographic technique used to fractionate crude extracts. Silica gel (Merck 7749) was packed into a sintered funnel under applied vacuum to give a column of about 5 cm in diameter and 5 cm in hight. Plant extracts were dissolved in methanol, mixed with silica gel (1:1 w/w) and taken to dryness under reduced pressure. The powdered sample was then placed on top of the column and eluted with solvents of increasing polarity; in most cases starting from petrol and progressing through chloroform then ethyl acetate and, finally methanol. VLC eluents were collected and fractions analysed by TLC for their constituents.

Polyamide (MN Sc 6) VLC was also employed in the same way as described for silica gel VLC. However, elution was carried out starting with water and subsequently incorporation of methanol in the water.

2.3.1.2 Column chromatography

2.3.1.2.1 Sephadex

Sephadex LH 20 columns were used extensively to remove chlorophyll and for the separation of flavonoids. Columns of different sizes were prepared by mixing the Sephadex with a chloroform and methanol mixture (1:1) and pouring the slurry into a glass column half filled with solvent. This was allowed to stand

for a few hours before the commencement of the experiments.

In all cases the samples were dissolved in a few drops of solvent (chloroform:methanol, 1:1) and the solution pipetted onto the top of the column. Elutions were carried out using a single solvent system (chloroform:methanol, 1:1) and eluents were treated in the same way as described for VLC.

2.3.1.2.2 Silica columns

Silica gel 60 (Merck) columns were packed in the same way as described for Sephadex columns. Non-polar solvents, usually petroleum ether, were used to pack the column. The samples were applied in a powder (adsorbed in silica, 1:1 w/w) or in solution and eluted with solvents[1] of increasing polarity. Depending upon the column size, 10-50 ml of fractions were collected and their contents analysed by TLC.

2.3.1.3 Preparative thin layer chromatography (PTLC)

Cleaned 20 x 20 cm glass plates were used to prepare preparative TLC plates. 40 gm of silica gel 60-PF_{254} (Merck) was mixed with 80 ml of distilled water and the slurry was spread into five plates to give a layer of 0.5 mm thickness. The plates were air dried and activated in an oven at 105°C for at least 2 hours.

Samples dissolved in an appropriate solvent were applied at the base of the plates, dried and developed using an appropriate solvent system[1]. Multiple development was performed for some samples to get good separation of compounds which had close R_f values. The developed plates were visualised by

---

[1] Details of the solvent systems are described in the text under a particular experiment

UV light and spray reagents and bands scraped into a sintered glass filter funnel. The compounds were then washed off with polar solvents and concentrated under reduced pressure.

2.3.1.4 High performance liquid chromatography (HPLC)

HPLC was used to isolate polar compounds which could not be separated by other chromatographic techniques. A Gilson HPLC pump (model 302), a manometric module (model 802 C), an analytical reverse phase silica gel column (ODS TES-800, 250 mm x 4.6 mm) or a preparative reverse phase silica column (ODS TES 800, 25 cm x 10 mm) and a UV detector (Shimadzu, model SPD-6AV) attached to a recorder were used. The samples were introduced *via* a Rheodyne injection valve fitted with a 20 μl sample loop for the analytical column and a 2 ml loop for the preparative column. Fractions[2] were collected based on the retention time established from the analytical scale studies and the purity checked by reinjecting the samples in the analytical column.

2.3.2 Detection/visualization of compounds

Pre-coated TLC (silica gel 60 PF-254) plastic sheets were used to detect compounds. Samples were applied to a TLC plate and developed using an appropriate solvent. After drying, the developed plates were viewed under UV light (254/366 nm). Compounds were further visualised by spraying the chromatoplates with vanillin (1%) in concentrated sulphuric acid followed by heating

---

[2]Details of solvent systems are discussed in the text under particular experiment

at 100°C for a few minutes.

2.3.3 Acetylation of compounds

Compounds were acetylated by dissolving about 10 mg of each sample in 1 ml of pyridine and 2 ml of acetic anhydride. The reaction mixtures were then allowed to stand at room temperature for 12 hours to yield peracetate derivatives.

2.4 Spectroscopic Identification Techniques

2.4.1 Instrumentation

Melting points were determined on a Reichart sub-stage microscope and are uncorrected. Ultra-violet spectra (UV) were obtained using a Perkin-Elmer 552 UV/visible spectrophotometer with either ethanol or methanol as solvent. Infra-red (IR) spectra were recorded as KBr discs using a Perkin-Elmer 781 infrared spectrophotometer. Specific rotations $[\alpha]_D$ were determined at the sodium-D line using a Perkin-Elmer 241 polarimeter. Mass spectra were recorded on either a AEI MS 902 double focussing spectrophotometer (direct probe insert, 70 eV) or a VG ZAB-E (FAB-MS). ^{1}H and ^{13}C NMR spectra were recorded on either Brucker WH-250, Brucker AC300 or Brucker AMX-400 instruments. All the spectra were referenced using the residual solvent peaks: δ 7.26 for ^{1}H and δ_C 77.2 for ^{13}C NMR for CDCl$_3$; δ 7.19 for ^{1}H and δ_C 123.5 for ^{13}C NMR for pyridine-d$_5$; δ 2.04 for ^{1}H and δ_C 29.8 for ^{13}C NMR for acetone-d$_6$ and δ 3.35 for ^{1}H NMR for deutereomethanol.

2.4.2 Recording the UV spectra of flavonoids

UV spectroscopy was used extensively for the identification of flavonoids. Flavones and flavonols in general give two bands in the region 240-400 nm. Since band I (300-400 nm) is considered to be due to the B-ring cinnamoyl system and band II (240-285 nm) to absorption involving the A-ring benzoyl system (Mabry *et al.*, 1970), the substitution pattern of flavonoids can be determined by means of several shift reagents which specifically interact with various hydroxyl sites. The following shift reagents were used to study the substitution pattern of flavonoids:

Sodium methoxide (NaOMe). Freshly cut metallic sodium (2.5 gm) was added in small portions to dry methanol (100 ml).

Aluminum chloride (AlCl$_3$). Five gram of fresh anhydrous reagent grade AlCl$_3$ were added to methanol (100 ml).

Hydrochloric acid (HCl). Concentrated reagent grade HCl (50 ml) was mixed with distilled water (100 ml).

Sodium acetate (NaOAc). Anhydrous powdered reagent grade NaOAc was used.

Boric acid (H$_3$BO$_3$). Anhydrous powdered reagent grade or methanol (100 ml) saturated with anhydrous reagent grade H$_3$BO$_3$ was used.

The spectra were recorded according to a standard procedure (Mabry *et al.*, 1970). A stock solution of the flavonoid was prepared by dissolving a small amount of the compound (about 1 mg) in about 100 ml of dried methanol. The concentration was then adjusted so that the optical density (OD) was reading in the region 0.6 to 0.8. The UV spectrum of this methanol solution was mea-

sured using 3 ml of the solution and re-run after addition of three drops of the NaOMe stock solution. The $AlCl_3$ spectrum was similarly recorded after adding six drops of $AlCl_3$ stock solution and the $AlCl_3/HCl$ spectrum obtained by addition of three drops of stock HCl solution to the cuvette containing the $AlCl_3$. The NaOAc spectrum was determined by adding powdered NaOAc with shaking. About a 2 mm layer of NaOAc remained on the bottom of the cuvette. Finally the $NaOAc/H_3BO_3$ spectrum was recorded by adding either sufficient H_3BO_3 to saturate the solution or 2-3 drops of stock solution into the cuvette containing NaOAc.

2.4.3   NMR techniques

The structural determinations of compounds isolated in the present study were based largely on a number of NMR experiments. While one dimentional ^1H and/or ^{13}C NMR were sufficient for simple and known compounds, unambiguous assignment of complex and new compounds required the use of recently evolved NMR techniques. In this section, a *J*-modulated ^{13}C NMR and correlation spectroscopy are described.

2.4.3.1   *J*-modulated ^{13}C NMR spectroscopy

J-modulated ^{13}C NMR spectroscopy was one of the techniques used to determine ^{13}C multiplicities. With this procedure non-protonated (quaternary) and methylene (CH_2) carbons give rise to positive signals in contrast to methine (CH) and methyl (CH_3) carbons which give negative or inverted signals.

A *J*-modulated spectrum can be obtained by using either the GASPE sequence techniques described by Cookson and Smith (1981) or the APT sequences (Patt and Shoolery, 1982).

This procedure suffers from the disadvantage that confusion may arise in distingushing CH_2 from quaternary carbon signals and CH_3 from CH signals. Recently, this problem has been overcome by using a series of delay time which vary the intensity of C signals from CH_2 and CH from CH_3 (Sadler, 1988). Thus, a delay time of 5-6 ms showed signals from CH_3 and saturated CH_2 with marked lower intensities than those from CH and quaternary carbons. A delay time of 8 ms was used for unsaturated aromatic systems.

2.4.3.2   Correlation spectroscopy

The assignment of chemical shifts and coupling constants in complex systems has traditionally been simplified by obtaining NMR spectra, generally either ^1H or ^{13}C; at higher magnetic fields. However, the complexity of the NMR spectra of many structures can still not be sufficiently simplified by this technique, and overlapping of multiplets remains a problem. This problem is partly overcomed by using correlation or 2-D NMR spectroscopy.

As originally proposed by Jenner *et al.* (1979), 2-D NMR spectroscopy is based on the concept of plotting NMR spectral data obtained in one time domain against data obtained in another. The data obtained through a 2-D experiment can then be displayed in a number of different ways, all of which generate a correlation map. The map may show either interactions among nuclei of the

48

same species as in ^{1}H-^{1}H COSY and NOESY or between two different nuclides in a molecule as in HMBC and HMQC.

2.4.3.2.1 ^{1}H-^{1}H correlation spectroscopy (COSY)

^{1}H-^{1}H COSY spectra correlate chemical shifts through homonuclear scalar couplings. These couplings appear in the spectrum as cross peaks in a square pattern which allows connectivity to be mapped directly.

Like any other 2-D NMR experiments a ^{1}H-^{1}H COSY involves evolution, mixing and detection time intervals (Haasnoot, 1984). During the evolution period (t_1), between two 90° pulses, the various magnetization components are labelled with their characteristic precision frequences. The second 90° or "mixing" pulse induces transfer of coherence between scalar coupled spines. The free induction delay is then recorded immediately after the second pulse and after 2-D Fourier transformation the coherence transfer process will show up as cross peaks in the final 2-D spectrum. In the present study, most of the COSY experiments were carried out using a pulse sequence of 45° (COSY-45) on a Brucker AMX 400 spectrometer.

2.4.3.2.2 ^{1}H-^{1}H NOESY (Nuclear overhauser enhancement spectroscopy)

The normal nOe is caused by cross relaxation between species of interacting nuclei (Paudler, 1987). Such interaction is noticable over short distances (2-4 Å) and rapidly falls as the distance between the nuclei increases. The nOe thus gives valuable information on the stereochemical relationship of various protons

49

in the molecule. The measurment of this effect has recently been approached by 2-D NMR spectroscopy, "NOESY" (Derome, 1989).

The NOESY spectrum has similar appearance to the COSY except that cross peaks correlate resonances that are in close spacial proximity rather than through bonds. As shown by Derome (1989), a NOESY experiment at one time setting represents one point in the nOe build up curve. For this reason one NOESY experiment may not give all the information required. In the present study, two to three NOESY experiments were performed for each compound using different mixing time.

2.4.3.2.3 ^{1}H-^{13}C correlation spectroscopy (HMBC, HMQC)

One of the of the most important advances in the evolution of 2-D Fourier transform NMR spectroscopy is techniques for correlating chemical shifts based on spin-spin coupling in the spectra of two different nuclei. This includes the HMQC (heteronuclear multiple quantum coherence) technique, which showes direct C-H couplings (Bax and Subramaniam, 1986), and HMBC (heteronuclear multiple bond connectivity) which plays an important role in determining long-range (two or three bonds) ^{1}H-^{13}C connectivity (Bax and Summers, 1986).

During the past few years several pulse sequence programmes to measure δ_C/δ_H correlations have evolved (Ngadjui $et\ al.$, 1991). In this study, HMQC spectra were run with the BIRD9 Brucker programme. ^{13}C decoupling was performed during acquisition with the GASP sequence using a BFX5 amplifier. Recovery delays were optimised to null ^{13}C-H and found to equal 0.3 seconds. HMBC spectra were run using the INV4DR2LP programme. No ^{13}C decoupling was performed

50

during acquisition and evolution delay was set at 70 ms ($1/2\ J$), corresponding to approximately 7 Hz C-H coupling (^2J or ^3J).

Chapter 3

PHYTOCHEMICAL AND ANTIMICROBIAL STUDIES ON *PREMNA SCHIMPERI*

3.1 Bioassay Guided Isolation of the Antibacterial Principle

3.1.1 Bioevaluation of the crude ethanol extract

The antimicrobial activity of *Premna schimperi* was tested on two gram-positive (*Staphylococcus aureus* and *Bacillus subtilis*) and two gram-negative bacteria (*Escherichia coli* and *Pseudomonas aeruginosa*), two fungal (*Aspergillus niger* and *Penicillium notatum*) and one yeast (*Candida albicans*) species.

The crude ethanol extract of leaves of *Premna schimperi* was found to

be antibacterial when tested by the disc diffusion assay (DDA) against a range of micro-organisms. 300 μg of this extract could produce an inhibitory zone measuring 8 and 9 mm in diameter against *Bacillus subtilis* and *Staphylococcus aureus* respectively. Since the crude extract contains several compounds and the concentration of the active principle(s) was not known, comparison of the crude extracts activity with known antibiotics was not made at this time. No activity was observed against gram-negative test organisms (*Escherichia coli* and *Pseudomonas aeruginosa*) and even against gram-positive bacteria at a concentration of 100 μg per disc. The same concentration of the extract did not also show antifungal (*Aspergillus niger* and *Penicillium notatum*) and yeasticidal (*Candida albicans*) activity.

3.1.2   Isolation of the active principle(s)

The general isolation methodology is outlined in Scheme 3.1 (page 54). The concentrated ethanol extract of *Premna schimperi* was fractionated by vacuum liquid chromatography (VLC) over silica gel eluting with solvents of increasing polarity. Bioassay of these fractions (DDA) showed that the hexane:chloroform (1:1) and chloroform fractions contained the active principle(s). In comparison with the crude extract there was greater activity; 10 and 12 mm diameter inhibitory zones were observed against *Bacillus subtilis* and *Staphylococcus aureus* using the same concentration of extract. Inhibitions were also observed at lower concentrations. The active fractions were subsequently treated by column chromatography over silica gel   eluting with hexane   containing   increasing

CRUDE EXTRACT

|

VACUUM LIQUID CHROMATOGRAPHY

Hexane   Hexane:CHCl₃   CHCl₃   CHCl₃:EtOAc   EtOAc   Acetone   MeOH
                1:1   1:1

INACTIVE

ACTIVE

INACTIVE

COLUMN CHROMATOGRAPHY (Silica gel)

Petroleum ether ------> CHCl₃ ------------> EtOAc

INACTIVE   **INACTIVE**

PURIFICATION, Silica gel column
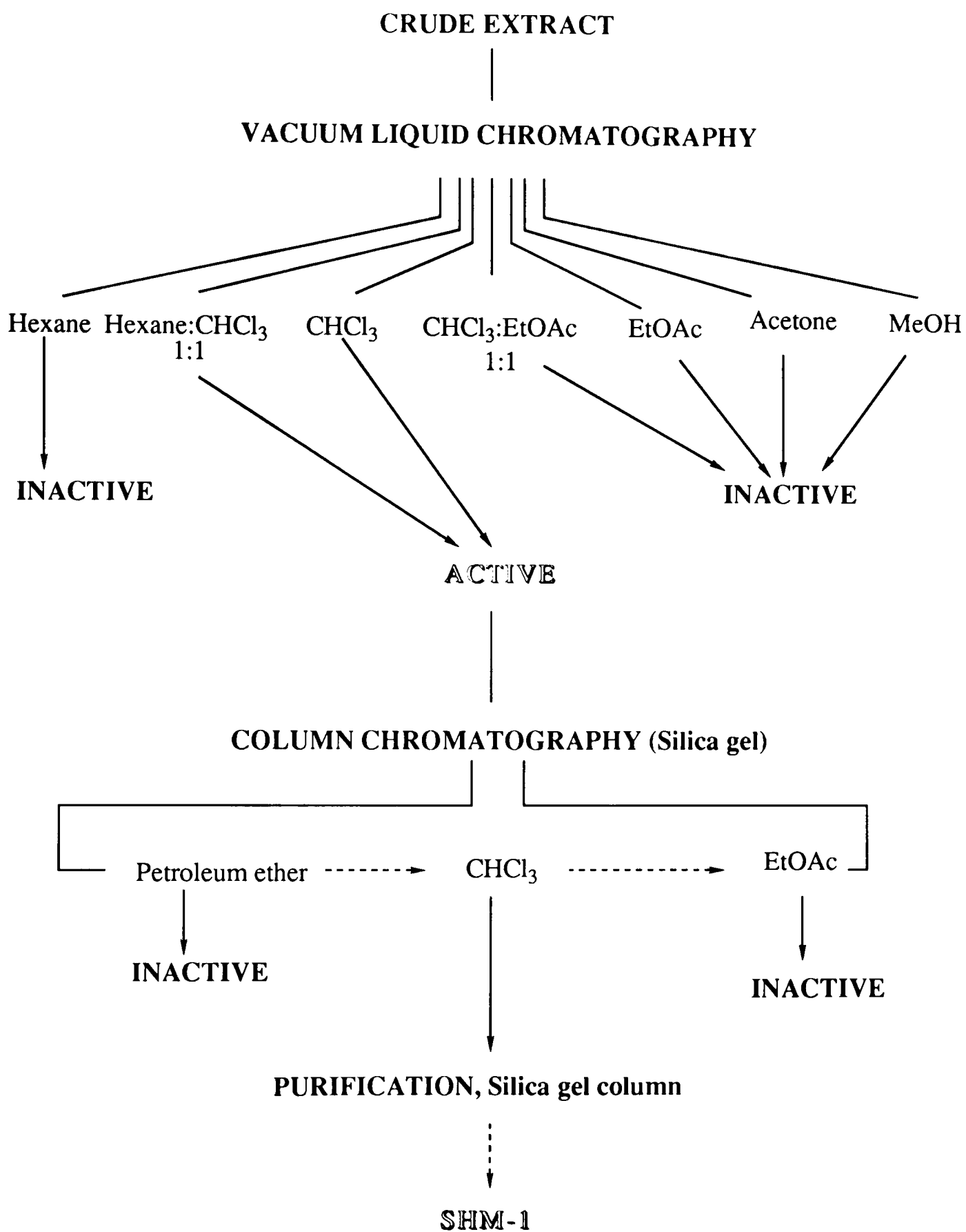
SHM-1

Scheme 3.1. Bioassy guided isolation of SHM-1

54

amounts of ethyl acetate. Further purification was associated with an increase in the antibacterial activity (Fig. 3.1) and finally led to a single compound (SHM-1) which gave a pink colour with vanillin-sulphuric acid spray reagent. Fractions containing this compound were bulked and concentrated to give an oil which was recrystallysed from benzene as prisms.

3.1.3 Identification of SHM-1 as (5R,8R,9S,10R)-12-oxo-*ent*-3,13(16)-clerodien-15-oic acid (111)

SHM-1 was obtained in a yield of 0.1% and had UV absorption at 230 nm and optical rotation of -74°. In the IR spectrum, absorption bands at 1728 and 1670 cm^{-1} were indicative of carbonyl systems, the latter being conjugated with a double bond (α, β-unsaturated ketone) (William and Fleming, 1989). High resolution EIMS revealed a molecular ion at m/z 318 for $C_{20}H_{30}O_3$. The EIMS further revealed fragments at m/z 190 $[C_{14}H_{22}]^+$ and 113 $[C_5H_5O_3]^+$ (Scheme 3.2) indicating a diterpene with a side chain bearing three oxygens.

The ^{1}H NMR spectrum (Fig. 3.2) showed resonance for four methyls: two quaternaries at δ 0.96 (Me-19) and 0.78 (Me-20); one secondary at 0.83 (J=6.7 Hz, Me-17) and one olefinic at 1.53 (Me-18). The ^{1}H NMR further revealed a multiplet at δ 5.11 (H-3) which was decoupled to a triplet by irradiating at the olefinic methyl signal at δ 1.53. This establishes a partial structure **109** (Fig. 3.3). All these data, together with a 1H double-doublet at δ 1.68, for an axial H-10 proton suggested a clerodane nucleus substituted with a double bond between C-3 and C-4. This hypothesis was substantiated by the fragment $m/z = 190$ in
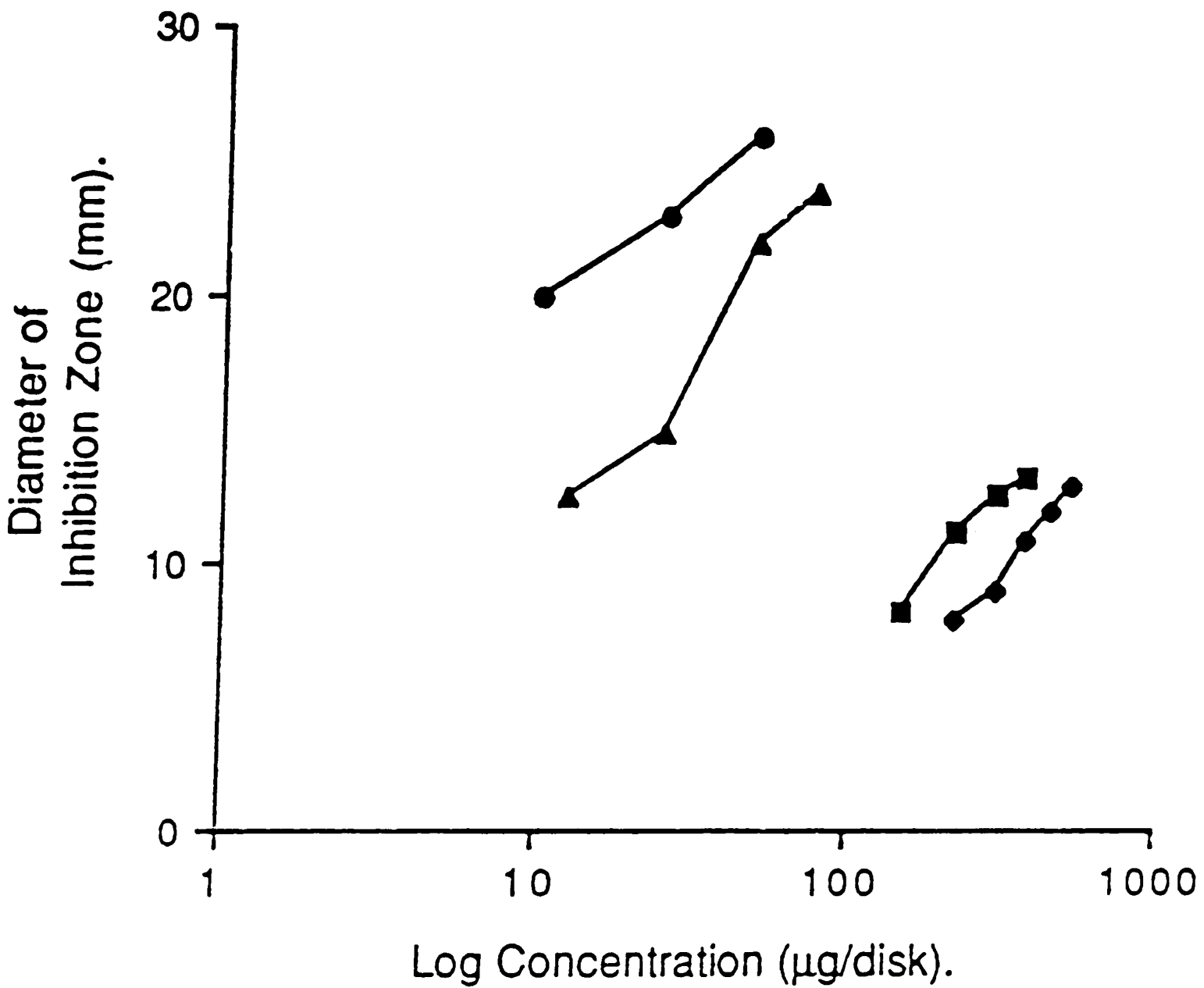
Figure 3.1: Antibacterial activity of chloramphenicol (●),
SHM-1 (▲), chloroform fraction from VLC (■), and crude
ethanol extract (◆) in the DDA against *Staphylococcus
aureus*.

Figure 3.2: ^{1}H NMR (250 MHz, CDCl$_3$) spectrum of SHM-1
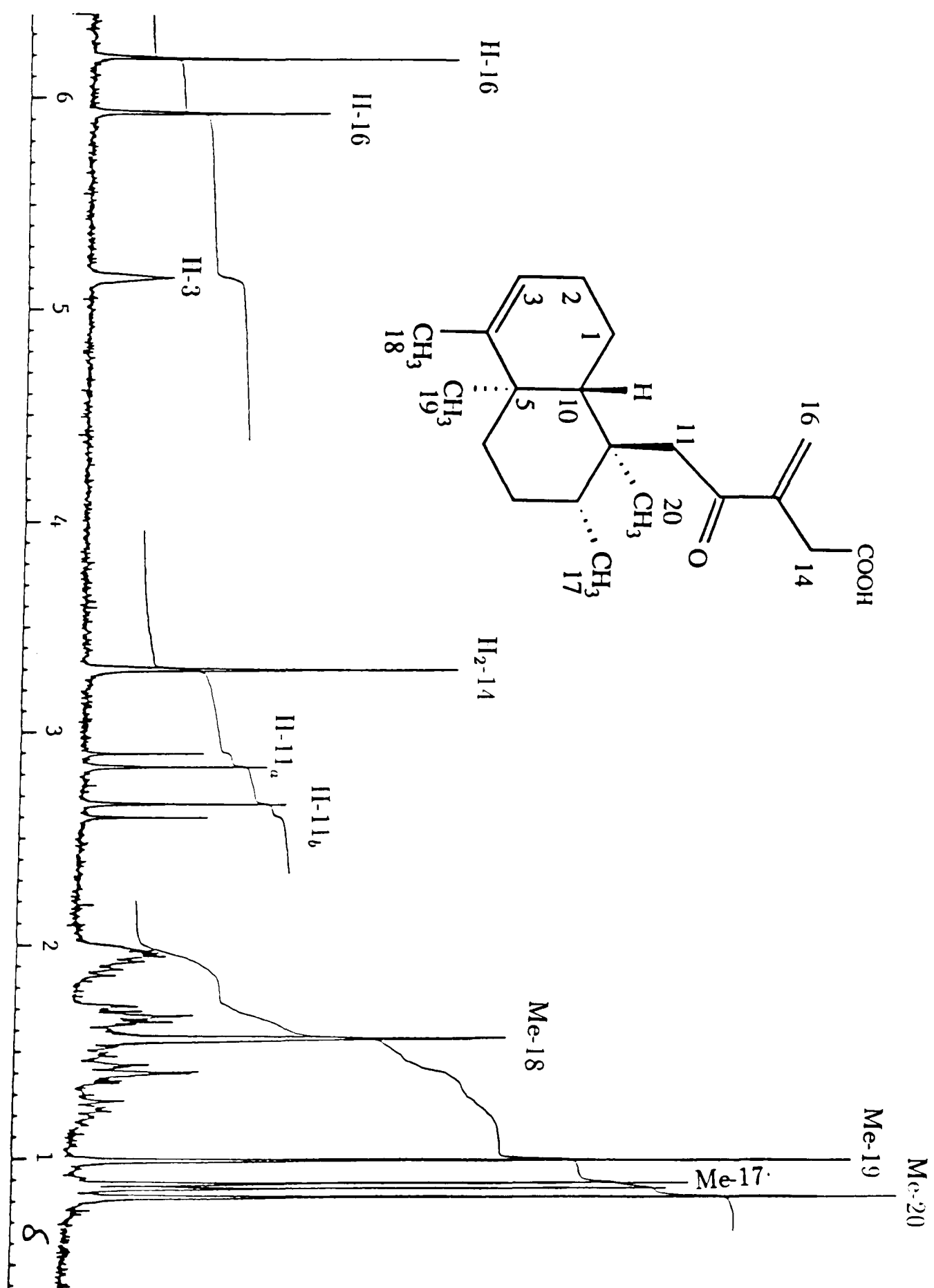
the EIMS (Scheme 3.2) and the close agreement of the ^{13}C NMR data (Table 3.2) with a related structure (**113**, Fig. 3.4). Other features of the ^{1}H NMR spectrum were a broad singlet at δ 10.45 ppm for an acid proton. By methylation using methanolic KOH, this was converted to a methyl ester (singlet = 3.95 ppm).

In addition to the previously mentioned carbons of the clerodane skeleton, the broad band decoupled ^{13}C NMR spectrum showed six carbons; two carbonyls at 201.2 (C-12) and 176.1 (C-15), one quaternary at 143.4 (C-13) and three carbons which were shown as methylenes (37.3, C-11; 43.4, C-14 and 120.6, C-16) by the off resonance decoupled ^{13}C NMR spectrum. These data together with the ^{1}H NMR spectrum which showed three isolated methylene moietes at δ = 5.87, 6.14 (H-16) a singlet at 3.27 (H-14) and an AB quartet centered at 2.82, 2.59 (J=15.5 Hz, H-11) establish a partial structure **110** (Fig. 3.3). This partial structure was also substantiated by the ion m/z=113 which could occur where fission occurs α to the carbonyl (Scheme 3.2). On the basis of these data SHM-1 was assigned to a novel structure **111** (Fig. 3.4) in which the A/B ring is trans fused.

The relative stereochemistry was determined by a series of nuclear Overhauser experiments (NOE) (Table 3.2) which confirmed the stereochemical relationship between the methyl substituents and also suggested the preferred conformation of the side chain (Fig. 3.5). Key features of this study were enhancement between 17-Me and 19-Me, 20-Me and *vice versa*. This requires the placement of these methyl groups to the same face of the molecule (Fig. 3.5). The negative optical rotation ($[\alpha]_D$ -74°) was indicative of the absolute stereochemistry

depicted in **114.**

109

110
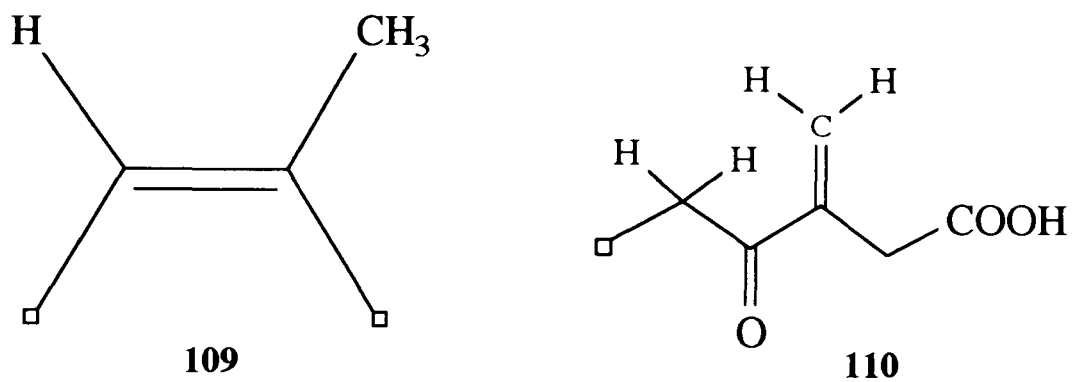
Fig. 3.3. Partial structures of SHM-1

R=H=SHM-1   **111**   Lopes *et al.*, 1987   **113**

R=CH₃   **112**
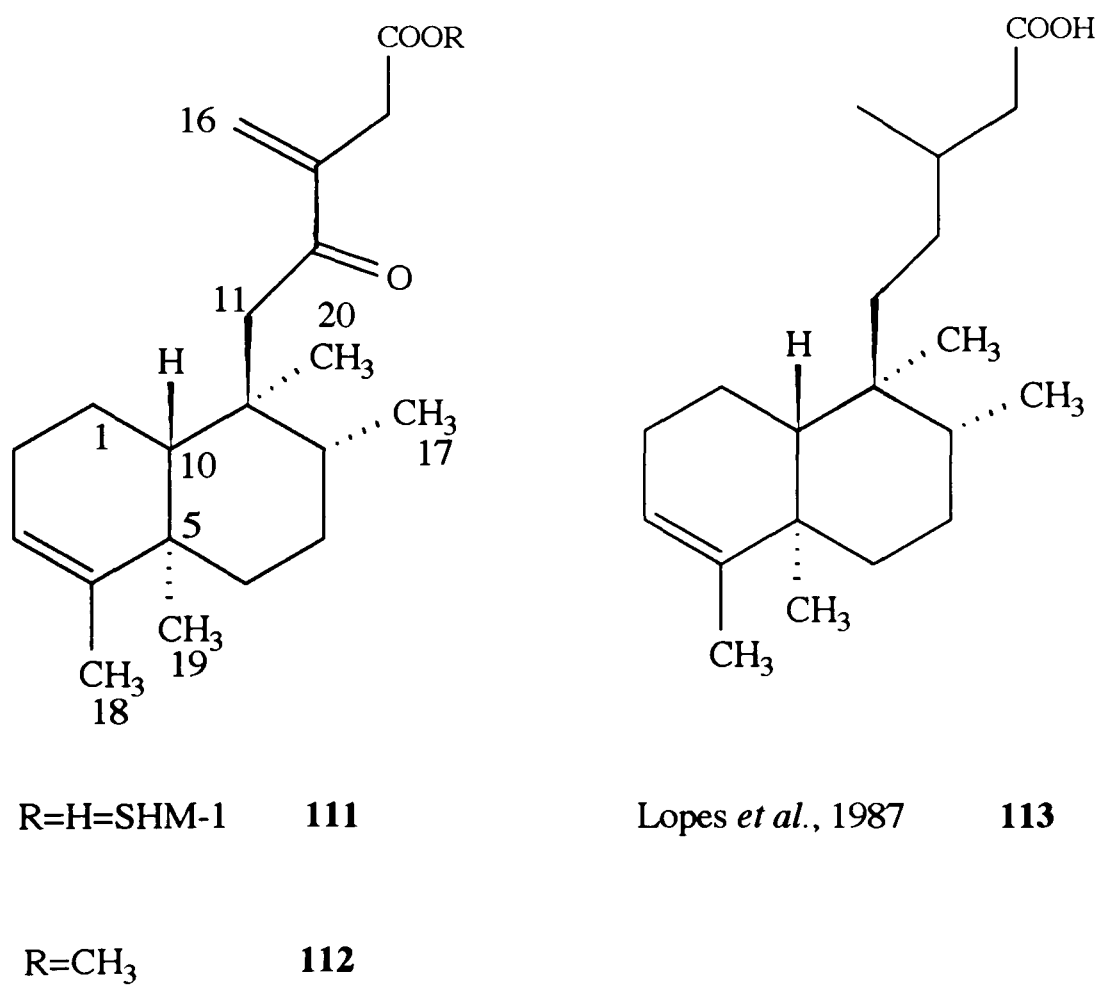
**Fig. 3.4. Structure of SHM-1 and a related
clerodane diterpene**

C	113	SHM-1	C mult. of SHM-1[a]
1	17.4	19.3	t
2	27.6	27.6	t
3	120.6	120.6	d
4	144.4	143.8	s
5	38.3	38.5	s
6	36.5	36.3	t
7	27.0	26.6	t
8	36.3	37.0	d
9	38.7	42.3	s
10	46.6	46.8	d
11	35.1	37.3	t
12	35.6	201.2	s
13	31.0	143.0	s
14	41.7	43.5	t
15	179.8	176.1	s
16	19.9	126.6	t
17	16.1	16.6	q
18	18.4	18.0	q
19	20.0	20.9	q
20	18.1	17.6	q

Table 3.1: ^{13}C NMR assignment of SHM-1 (62.9 MHz, CDCl$_3$) and 113 (Lopes *et. al.*, 1987).

[a] ^{13}C NMR multiplicities were determined from the ^{1}H-coupled ^{13}C experiment

and designated by the symbols: s=singlet, d=doublet, t=triplet and q=quartet.

319, $C_{20}H_{30}O_3$ (10.9%)

190, $C_{14}H_{22}$ (89.8%)

175, $C_{13}H_{19}$ (100%)

113, $C_5H_5O_3$ (3.6%)

85, $C_4H_5O_2$ (42.1%)
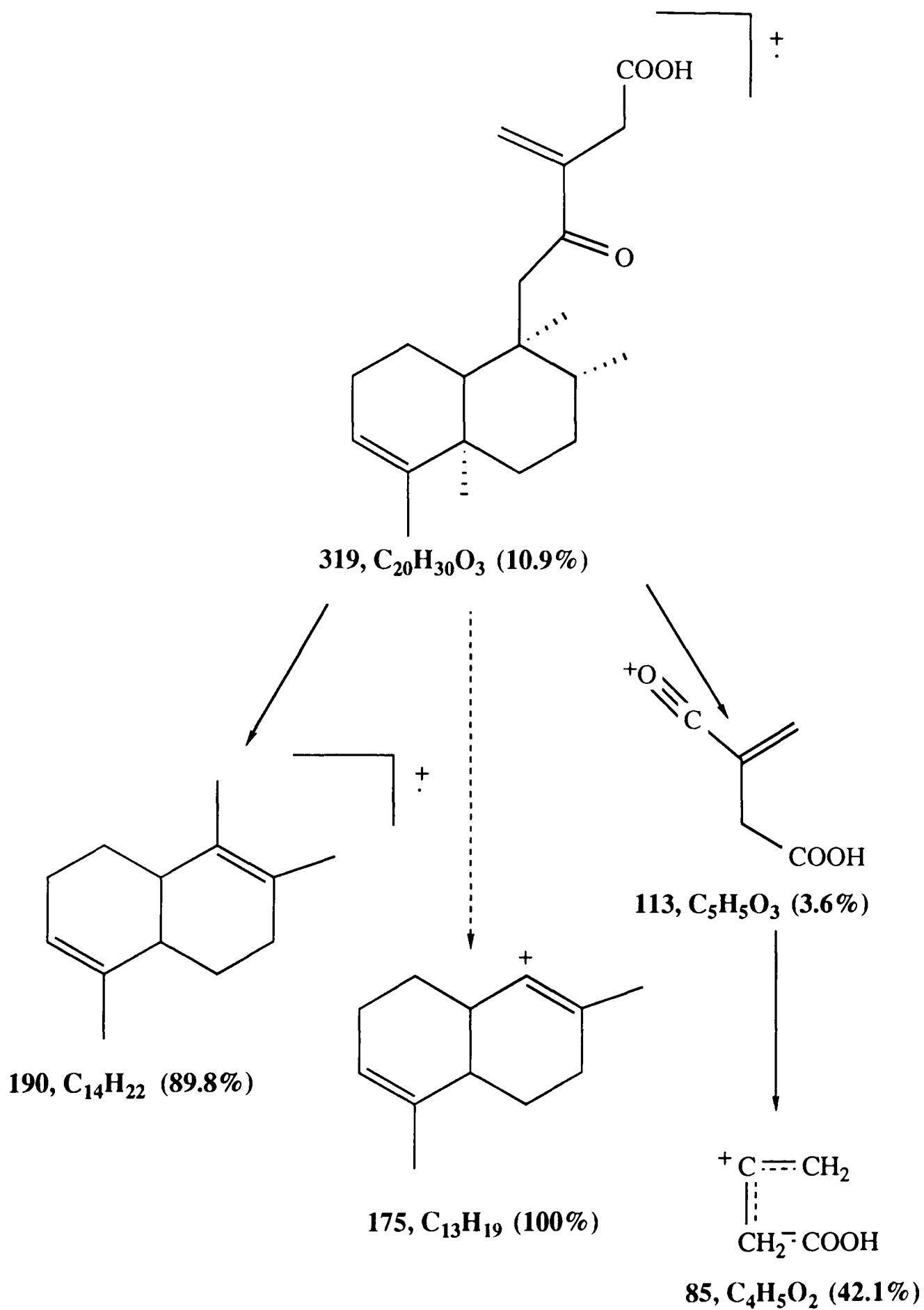
Sheme 3.2. Possible mass fragmentation pattern of SHM-1
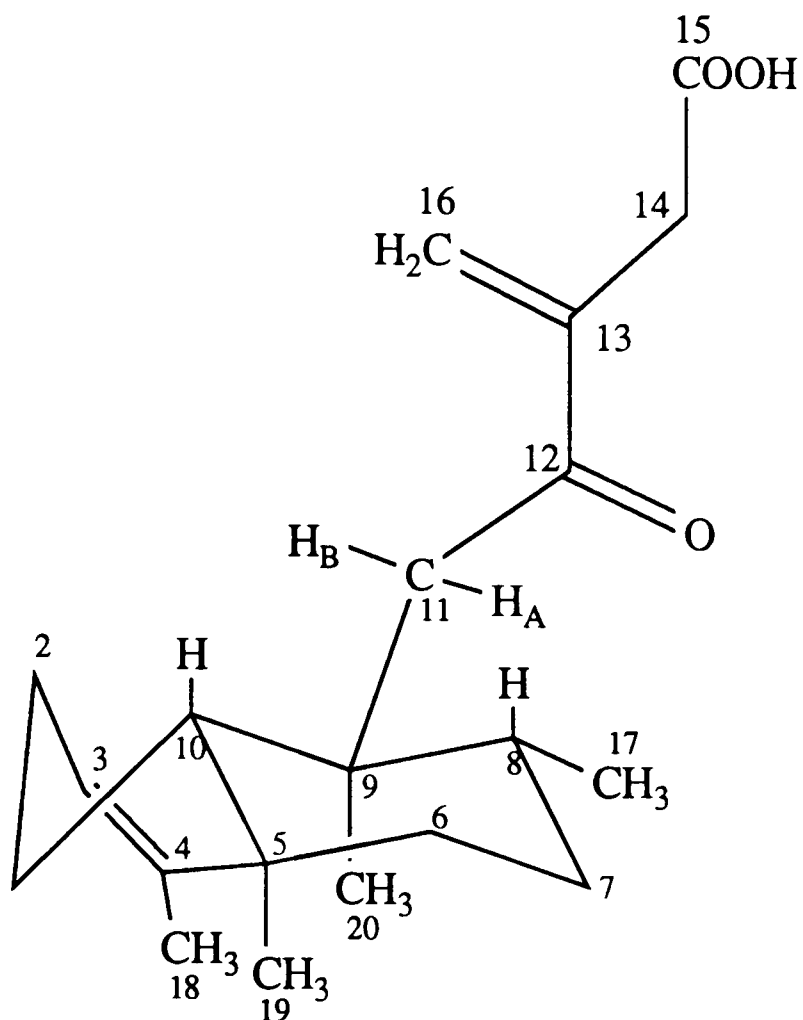
Figure 3.5: **Stereochemistry of SHM-1 based on nOe studies**

Proton irradiated	Proton(s) enhanced (%)
Me-20 (δ=0.78)	H-11 (a)* (3.5)
	H-11 (b)* (2.5)
	Me-17 (2)
	Me-19 (2)
Me-17 (δ=0.83)	H-11 (a)* (1)
	H-8 (1)
Me-19 (δ=0.96)	Me-18 (1)
	Me-20 (2)

Table 3.2: **Enhancements from nuclear overhauser experiments on SHM-1.**

* For distinction between H-11 (a) and H-11 (b), see Fig. 3.5

3.1.4 Antibacterial activity of SHM-1

The results for the DDA method, with the crude extract, the chloroform eluate from VLC, pure **111** and chloramphenicol (as standard), against *S. aureus* are presented in Fig. 3.1. There is clearly increasing activity with increasing purification of the active compound, culminating with pure **111**, and the similarity of the slopes of the plots suggests that **111** is largely responsible for the activity in each fraction. SHM-1 was proved to be active (MIC) below 25 μg/ml against the gram-positive bacterial test organisms (Table 3.3) but was inactive against gram-negative organisms, even at concentrations of 100 μg/ml. Most antibiotics in clinical use exhibit activity below the level of 10 μg/ml but compounds with activity only at the level of 100 μg/ml can be used routinely, provided they are non-toxic (Korolkovas and Burckhalter, 1976). It remains to be seen whether **111** will be too toxic for general use but, meantime, the employment of extracts of *P. schimperi* to treat infections caused by *S. aureus*, a common cause of eye and skin infection in rural Ethiopia, has been validated.

Most chemical antibacterial agents possess both bactericidal and bacteriostatic properties, the action depending largely on the concentration of the agent employed. In a few case, for example the acridines, the effect is acknowledged to be mainly bacteriostatic and only slowly bactericidal whereas in others, for example the chlorine releasing compounds, the activity is exclusively bactericidal. The action of the antibacterial compound (SHM-1) from *P. schimperi* was studied in order to ascertain whether its activity was bacteriostatic, bactericidal or both. No viable organisms could be recovered on subculture of test broths

above the measured MIC indicating that the compound has a bactericidal action. Further studies on viable bacteria counts after different time of exposure with the drug demonstrated that 111 was rapidly bactericidal against *S. aureus* at concentrations of 25 and 50 μg/ml (Fig. 3.6). The progressive decline of viable bacteria was observed throughout the experiment leading to no viable count after the exposure of the test organisms to the compound for 2.5 hours. The same trend was observed for *B. subtilis*, but counting colonies of this organism was not possible due to the spreading growth on the test plate. The mechanism of bactericidal/lethal process may be protein denaturation, enzyme inactivation, blocking of an essential metabolic pathway, damage to the membrane or other biological macromolecules, none of which have, as yet been studied for this compound.

Drug	*S. aureus*	*B. subtilis*
SHM-1 (111)*	20	25
SHM-1-methyl ester (112)	25	25
SHM-12 (116)	100	100
SHM-12-methyl ester (117)	200	150
Streptomycin sulphate	6	12

Table 3.3: Minimum inhibitory concentration (μg ml^{-1}) of SHM-1 and its derivatives

* Inactive upto 100 μg ml^{-1}, against *P. aeruginosa* and *E. coli*

Figure 3.6: **Bacterial growth** (*S. aureus*) **after exposure to SHM-1 and Nipagin M**
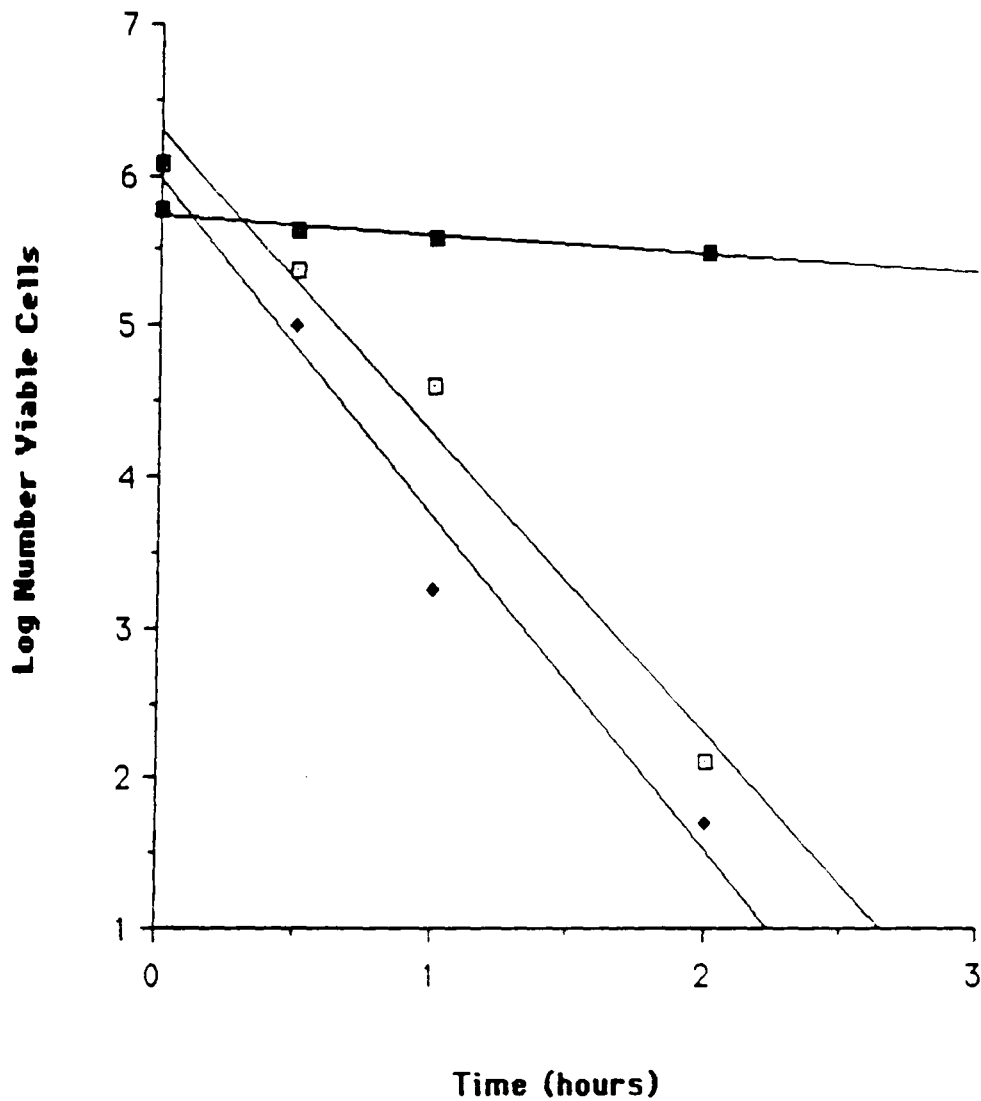
▫	25 μg/ml of SHM-1	Y = 6.302 - 2.0049X R=0.99
◆	50 μg/ml of SHM-1	Y = 5.9654 - 2.2319X R=0.99
■	0.2% of Nipagin-M	Y = 5.7402 - 0.1211X R=0.97

3.1.5 Study on the mode of action of SHM-1

Many reports on the antimicrobial and cytotoxic activities of diterpenes are now appearing. However, little work has been done on the mechanisms of action of these compounds although there exists a general agreement that most of them act like the sesquiterpene lactones. During the past few years, several sesquiterpene lactones possessing an α, β-unsaturated moiety have been studied for their mechanism of action (Groutas *et al.*, 1984). These compounds have general alkylating properties and their cytotoxic activity mainly derives from a Michaelis-type interaction of the α, β-unsaturated group with nucleophile cellular components (Stang and Trepton, 1981). Unfortunately this kind of indiscriminate reaction with nucleophilic cellular components inhibits the use of these compounds as pharmacological agents due to their toxicity.

Since SHM-1 has shown to have antibacterial and cytotoxic (LD_{50}=1.9 $\mu g/ml$, KB cells)[1] properties and also has the α, β-unsaturated moiety in question, it seemed worthwhile to examine the involvement of this structural group to the observed biological activity. This and the possible effect of the carboxylic acid functional group was studied by making several derivatives of SHM-1 followed by the biological assay test.

3.1.5.1 Derivatization of SHM-1

Sodium borohydride normally reduces aldehydes and ketones to alcohols but olefinic bonds conjugated to carbonyls (α, β-unsaturation) are expected to

---

[1]Tested by Dr C. MacDonald, Dept. of Immunology

66

be reduced first (Norman, 1978). Treatment of SHM-1 with this reagent gave SHM-12 (**116**, 12-oxo-*ent*-3-clerodene-15-oic acid) (Scheme 3.3) in the yield of 12%.

High resolution EIMS established the molecular formula of SHM-12 as $C_{20}H_{32}O_3$, 2MU more than SHM-1. As compared with SHM-1, the ^{1}H NMR spectrum of SHM-12 (Fig. 3.7) lack the olefinic methylene signals and the isolated methylene singlet in SHM-1 (δ H-14) is replaced by a complicated multiplet (δ 2.7-2.9). A second methyl doublet (δ 1.12, J=7.2 Hz) was also observed in the ^{1}H NMR spectrum of SHM-12. These data all indicated that the C-16 methylene group in SHM-1 was reduced to a methyl group in SHM-12. The coupling pattern of signals in the ^{1}H NMR spectrum (Fig. 3.7) of the latter compound indicated that it was a C-13 epimeric mixture. Treatment of SHM-12 with diazomethane gave methyl-12-oxo-*ent*-3-cerodene-15-oic acid (**117**). This methylated product was identified from the ^{1}H NMR spectrum which showed a methyl singlet at δ 3.60.

3.1.5.2 Biological activity of SHM-1 derivatives

The minimum inhibitory concentraions (μg ml^{-1}) of SHM-1 and its derivatives against *S. aureus* and *B. subtilis* are shown in Table 3.3. The methyl ester of SHM-1 had a comparable activity with that of SHM-1 indicating that the carboxylic acid group in SHM-1 did not play a major role for the observed biological acticity. Removal of the α,β-unsaturated moiety however had a significant effect as SHM-12 was about   five times weaker   in its antibacterial activity

15C̲OOH

16

13

11

20CH₃

17CH₃

O

H

1

2

10

5

9

CH₃ **19**

CH₃

18

111

C̲OOH

CH₃

CH₃

O⁻

H

CH₃

CH₃

115

15

C̲OOR

16

11

20CH₃

17CH₃

O

H

1

2

10

5

9

CH₃ **19**

CH₃

18

Na⁺

H

H—B—H

H ⊖

H⁺

SHM-12 R=H **116**

R=CH₃ **117**
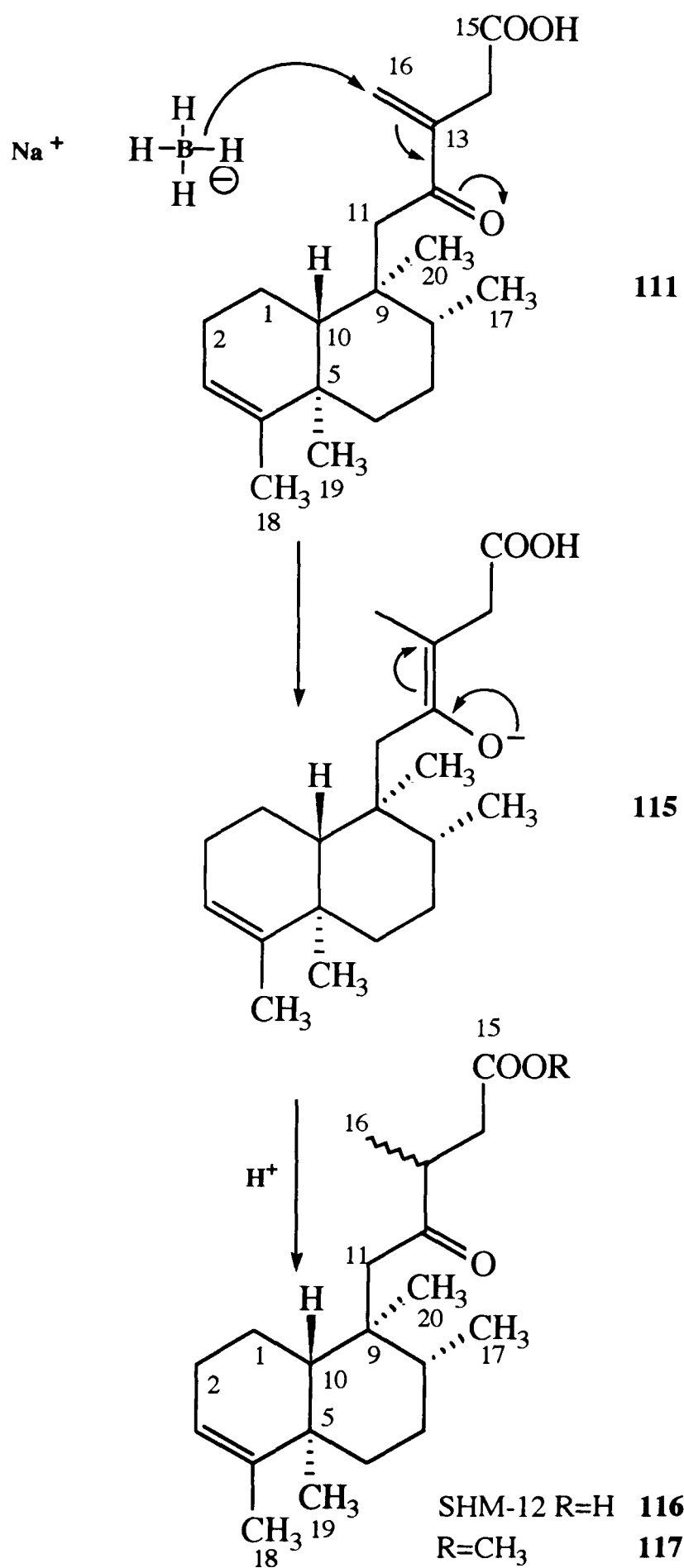
Scheme 3.3. Reduction of SHM-1

68

Figure 3.7: ^{1}H NMR (250 MHz, CDCl$_3$) of SHM-12
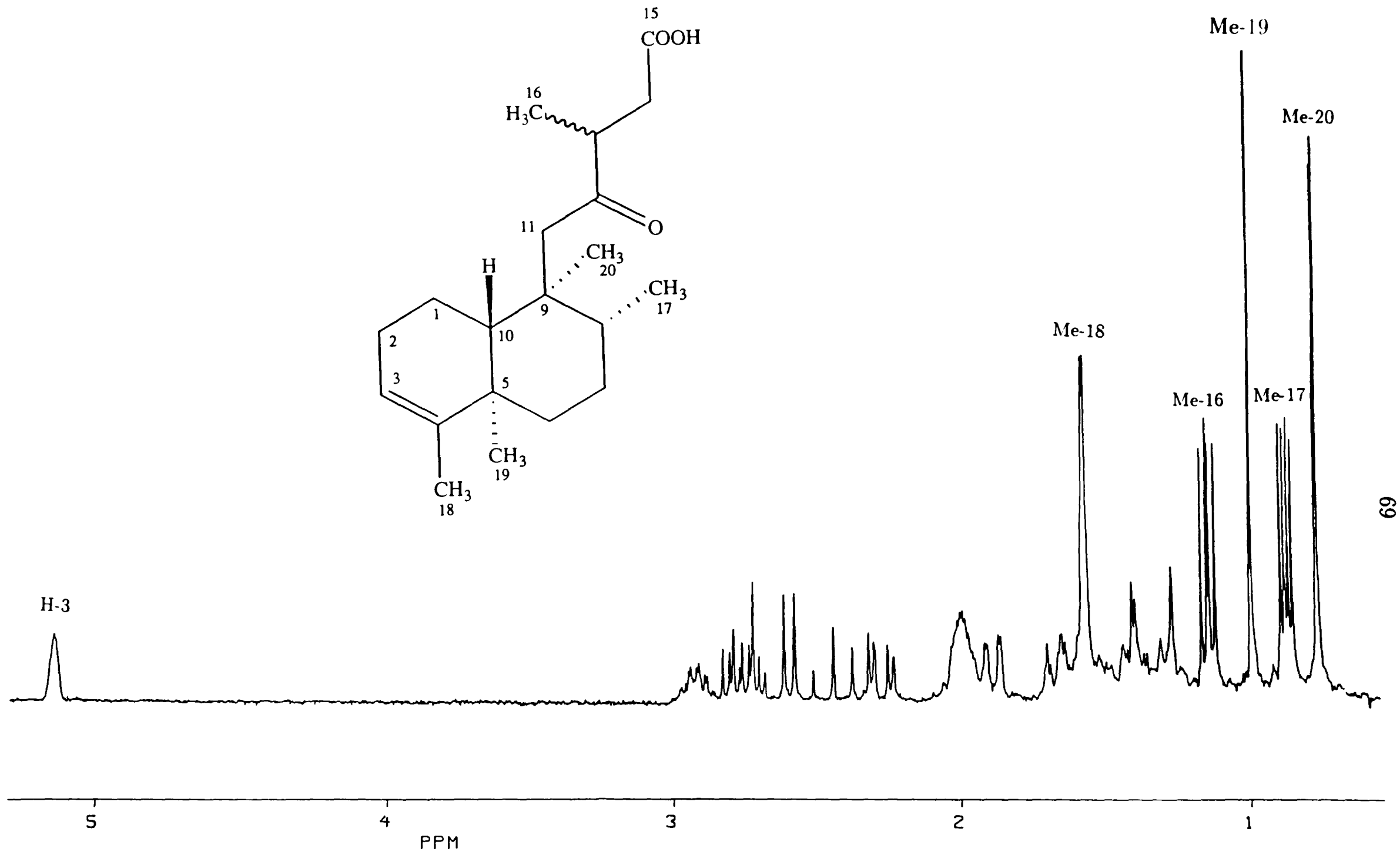
than SHM-1. This weak antibacterial activity observed for SHM-12 could, however, be partly due to the carboxylic acid moiety, as methylation of SHM-12 further reduced its activity two fold.

This study showed that the α,β-unsaturated moiety in the structure of SHM-1 played a major role for the observed biological activity. It is thus possible to invisage that SHM-1, like many sesquiterpenes and diterpenes, acts primarily by alkylating biological nucleophiles.

3.2 Phytochemical Examination of the 80% Ethanol Extract of *Premna schimperi*

Analysis of the 80% ethanol extract of the leaves of *Premna schimperi* resulted in the isolation of three flavonoid aglycones, three flavonoid glycosides, and five cinnamate and benzoate derivatives (Scheme 3.4).

3.2.1 Examination of the 90% methanol-soluble fraction of the 80% ethanol extract

A combination of Sephadex and column chromatography of the 90% methanol soluble fraction of the 80% ethanol extract afforded three known flavonoids, quercetin, luteolin and kaempferide (Fig. 3.8).

3.2.1.1 Identification of SHM-35 as quercetin (108)

High resolution EIMS of the major constituent (yield 0.02%) of the 90% methanol soluble fraction showed a molecular ion at m/z 302 (100%) that analysed for $C_{15}H_{10}O_7$. A major fragment at m/z 153 and a minor fragment at m/z 179 $[C_9H_7O_4]^+$ were indicative of a flavonol with dihydroxy substitution in the B ring. This was confirmed by the ^{1}H NMR spectrum (Table 3.4) which revealed three B ring proton signals; two doublets at δ 8.62 (J=2.2 Hz) and 7.38 (J=8.3 Hz) and one doublet doublet at δ 8.11 (J=8.3, 2.2 Hz). This was indicative of the 3',4'-dihdyroxyl substitution pattern of a flavonoid (Harborne, 1975). The ^{1}H NMR also revealed two *meta*-coupled proton signals for the A ring (Table 3.4)

POWDERED LEAVES OF *PREMNA SCHIMPERI*

| 80% ethanol percolation, solvent removal

CRUDE ETHANOL EXTRACT

CHCl$_3$/water partitioning

WATER FRACTION

CHLOROFORM SOLUBLE

hexane/90% MeOH partitioning

EtOAc extraction

HEXANE SOLUBLE

ETHYL ACETATE SOLUBLE

SHM-36A
SHM-36B

90% METHANOL SOLUBLE

WATER FRACTION

n-butanol extraction

WATER SOLUBLE

SHM-1
SHM-35
SHM-36-4
SHM-37A

BUTANOL SOLUBLE

SHM-42A
SHM-42B
SHM-43C
SHM-42D
SHM-42F
SHM-42G

Scheme 3.4. Extraction and fractionation of the ethanolic extract residue of *P. schimperi*

SHM-36-4 **38**

SHM-35 **108**

SHM-37A **118**
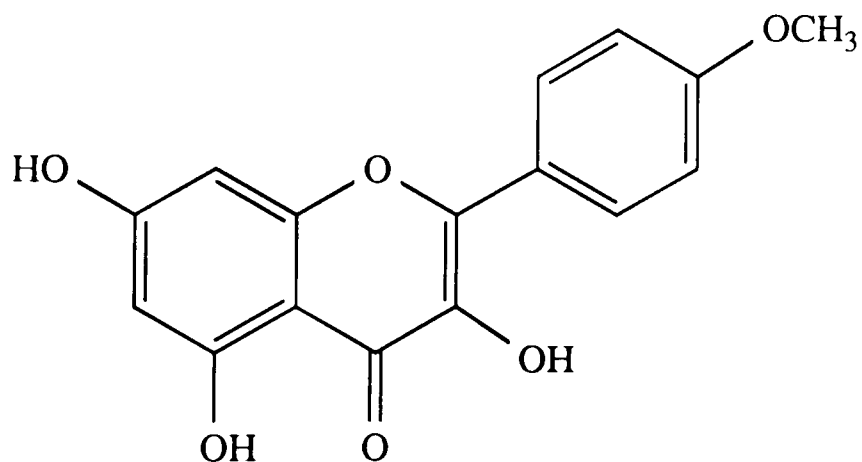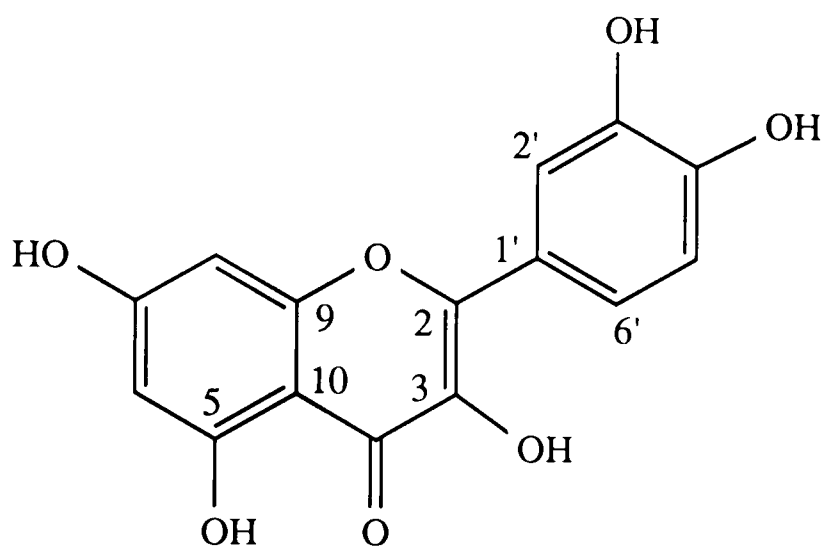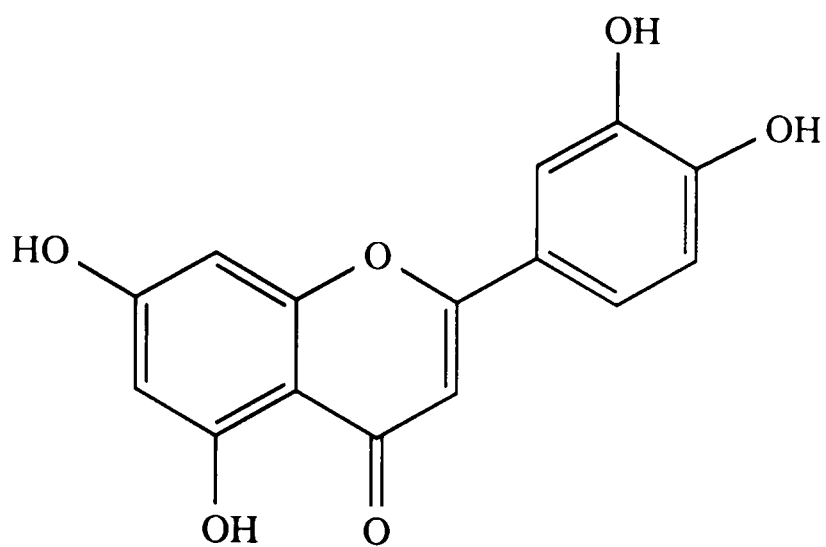
Fig. 3.8. Flavonoid aglycones isolated from the 90% methanol soluble fractioon of the 80% ethanol extract

73

and hence supported 5,7-dihydroxyl substitution. On the basis of these data SHM-35 was identified as 3,5,7,3',4'-pentahydroxyflavone (quercetin, **108** , Fig. **3.8**).

3.2.1.2 Identification of SHM-36-4 as luteolin (38)

The yellow needles of SHM-36-4 were obtained in a yield of 0.0017% and gave a yellow colour on spraying with vanillin in conc. sulphuric acid. The high resolution EIMS showed a molecular ion at m/z 286 (100%) and analysed for $C_{15}H_{10}O_6$. The ^1H NMR spectrum (Table 3.4) showed signals indicative of the 3',4'-dihydroxylated B ring and 5,7 dihydroxylated A ring of a flavonoid as described for SHM-35 (quercetin). In addition, the ^1H NMR spectrum of SHM-36-4 showed a 1H singlet at δ 6.93 assignable to H-3 of the C-ring. On the basis of these data, SHM-36-4 was identified as 5,7,3',4'-tetrahydroxyflavone (**38**, luteolin) (Fig. 3.8).

3.2.1.3 Identification of SHM-37A as kaempferide (118)

The high resolution EIMS of SHM-37A (yield 0.002%) showed a molecular ion at m/z 300 (100%) ($C_{16}H_{12}O_6$) for a flavonoid having one methoxyl functional group. A minor fragment at m/z 153 and major fragment at m/z 135 (Scheme 3.5) was indicative of a flavonol with the methoxyl functional group on the B ring. This substitution pattern was supported by ^1H NMR data which showed two *ortho*-coupled aromatic proton signals each integrating for two protons (Table 3.4). The ^1H NMR spectrum further revealed signals for the A ring protons as expected and also a methoxyl singlet at δ 3.70 (Table 3.4). Finally

HO

OCH₃

M^+, 300 (100%)

-H → 299 (21.3)

-CH₃ → 285 (26.1)

OH

OH

OH

$C=OH$

[A + H]⁺, 153 (6.2%)

OCH₃

B_2^+, 135 (22.7%)
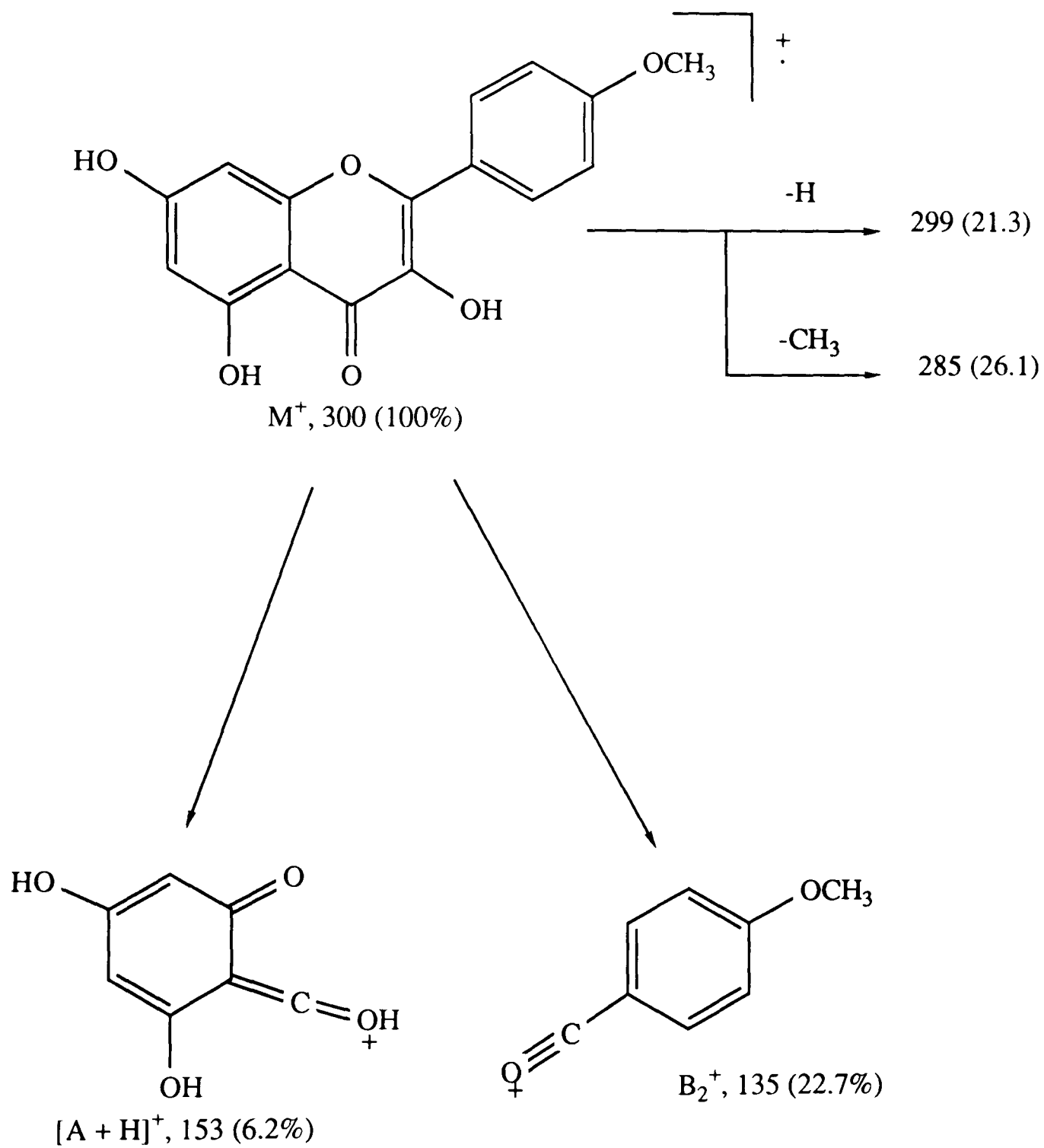
Scheme 3.5. Possible mass fragmentation pattern of SHM-37A

75

the assignment of the methoxyl position at C-4' was confirmed by a NOESY NMR study. This revealed interaction between the methoxyl proton signal at δ 3.70 and the shielded doublet signals of the B ring protons (H-3' and H-5') indicating a 4'-methoxyl position. On the basis of these data and comparison with that reported (Bohlmann et al., 1985), SHM-37A was identified as 3,5,7-trihydroxy-4'-methoxyflavone (kaempferide, 118, Fig. 3.8)

H	SHM-35	SHM-37A	SHM-36-4
3			6.93 s
6	6.71 d (2.2)	6.74 d (2.0)	6.73 brs
8	6.75 d (2.2)	6.82 d (2.0)	6.73 br s
2'	8.62 d (2.2)	8.51 d (9.1)	7.91 d (2.2)
3'		7.11 d (9.1)	
5'	7.38 d (8.3)	7.11 d (9.1)	7.28 d (8.3)
6'	8.11 dd (8.3, 2.2)	8.51 d (9.1)	7.54 dd (8.3, 2.2)
5-OH	13.83 s		13.79 br s
4'-OMe		3.70 s	

Table 3.4: ^{1}H NMR (250 MHz, in pyridine-d$_5$) data of flavonoid aglycones isolated from the 90% methanol soluble fraction of the ethanol extract

^{1}H multiplicities are shown by the symbols: s=singlet, d=doublet, dd=double doublet and br=broad. Figures in brackets represent coupling constants (J) in Hz.

3.2.2 Examination of the butanol soluble fraction of the 80% ethanol extract

Treatment of the butanol fraction on Sephadex and silica gel columns failed to afford any pure compounds. Visualization of compounds using silica gel coated TLC plates was also unproductive due to the tailing of compounds on silica gel TLC plates. The compounds isolated from this fraction were eventually obtained by fractionation over polyamide VLC with solvents containing increasing amount of methanol in water. HPLC chromatograms of the 10, 20, and 50% methanol VLC fractions are shown in Fig. 3.9. The major constituents shown in this chromatogram were isolated using reverse phase silica HPLC.

3.2.2.1 Identification of SHM-42A as caffeic acid (88)

The mass spectrum of SHM-42A (yield 0.028%) showed a molecular ion at m/z 180 (100%) and analysed for $C_9H_8O_4$. The ^1H NMR data (Table 3.5) showed, in the aromatic region, signals for three protons; one *meta*-coupled (J=2.0 Hz) and two *ortho*-coupled (8.2 Hz) one of which showed further *meta*-coupling (2.0 Hz) and appeared as a double doublet. This was characteristic for an 1,3,4-trisubstituted aromatic ring system. The ^1H NMR spectrum (Table 3.5) further revealed two signals at δ 6.22 and 7.51 which exhibited a typical *trans* coupling pattern of a double bond. The chemical shift of these protons was also indicative of an α,β-unsaturated system. Additional evidence for the latter assumption came from the IR data which showed a band at 1690 cm^{-1} (carbonyl of the α,β unsaturated system) and a broad band at 3320-2320 cm^{-1} for the

77
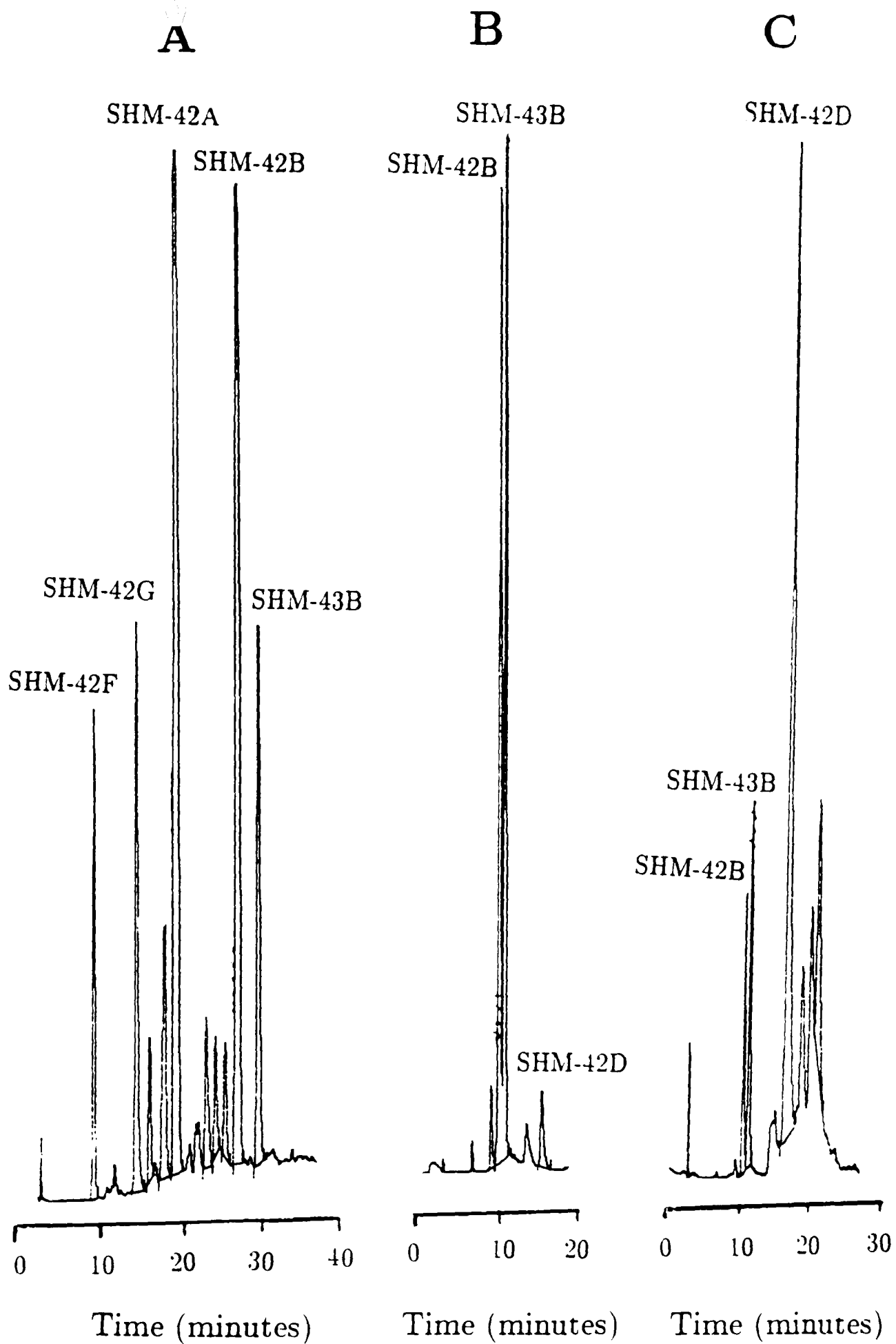
Fig. 3.9: HPLC chromatograms of the 10% (**A.** solvent system B)[1] 20% (**B.** solvent system A)[1] and 50% (**C.** solvent system A)[1] methanol VLC (polyamide) fractons.

[1] Details of solvent systems and retention times are described in Section 3.3.3, page 101
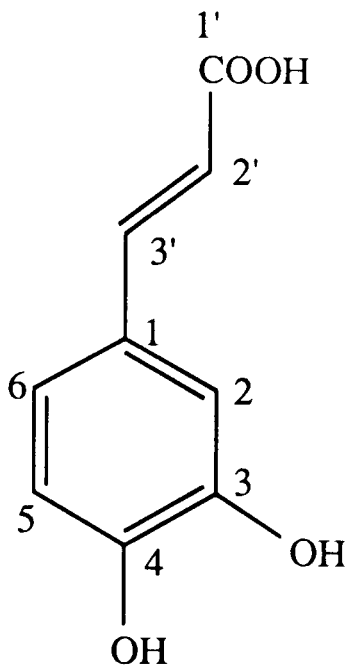
SHM-42A   **88**
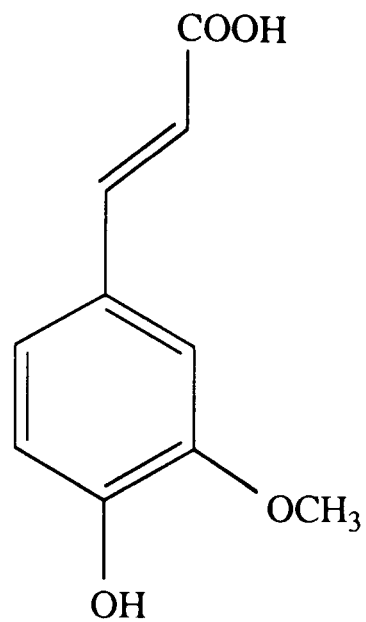
SHM-42B   **89**
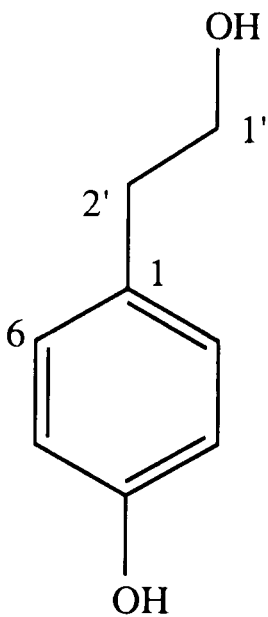
SHM-43B   **119**
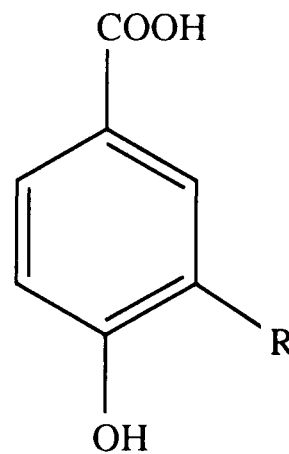
R=H=SHM-42G   **91**

R=OH=SHM-42F   **92**

Fig. 3.10. Cinnamate and benzoate derivatives from the butanol soluble fraction of 80% ethanol extract

carboxylic acid functonal group. On the basis of these data, SHM-42A was identified as caffeic acid (88, Fig. 3.10).

3.2.2.2 Identification of SHM-42B as ferulic acid (89)

High resolution EIMS of SHM-42B (yield 0.0026%) showed a molecular ion at m/z 194 that analysed for $C_{10}H_{10}O_4$. The ^1H NMR spectrum (Table 3.5) revealed aromatic proton signals showing *ortho-* and *ortho, meta*-coupling patterns indicative of the 1,3,4-trisubstituted aromatic ring system as described for SHM-42A (caffeic acid). The *trans*-coupled (J=15.8 Hz) olefinic proton signals, together with the IR data which revealed characteristic bands (1690 and 3100-2000 cm^{-1}) for the α,β unsaturated carboxylic acid moiety, were also indicative of the cinnamate side chain. The ^1H NMR spectrum further revealed a 3H singlet resonance at δ 3.93 assignable to an aromatic methoxyl group. This methoxyl group must be placed at C-3 as the NOESY revealed interaction between a methoxyl signal and a *meta*-coupled proton signal at δ 7.17 (H-2). On the basis of these data, SHM-42B was identified as ferulic acid (89, Fig. 3.10).

3.2.2.3 Identification of SHM-43B as 2(4-hydroxyphenyl)-ethanol (119)

High resolution EIMS of SHM-43B (yield 0.00096%) showed a molecular ion at m/z 138 (70.5%) and analysed for $C_8H_{10}O_2$. The ^1H NMR spectrum in the aromatic region (Table 3.5) revealed two signals at δ 6.69 and 7.02 each integrating for two protons and showing *ortho*-coupling (J=8.7 Hz). This was indicative of a 1,4-disubstituted aromatic ring system. The ^1H NMR spectrum further revealed a triplet at δ 2.73 for benzylic methylene, next to the carbinol methylene, which

appeared as a triplet at δ 3.67. These data, together with the IR data showing a hydroxyl functional group (3390 cm^{-1}), supported the identification of SHM-43B as a C_6-C_2 compound, 2(4-hydroxyphenyl)-ethanol (**119**, Fig. 3.10).

3.2.2.4 Identification of SHM-42G as *para*-hydroxy benzoic acid (91)

The high resolution EIMS of SHM-42G (yield 0.0014%) showed a molecular ion at m/z 138 (70.5%) which analysed for $C_7H_6O_4$. The IR spectrum revealed bands for hydroxyl (3390 cm^{-1}) and carboxylic acid (3110-2400 cm^{-1}) functional groups. The ^{1}H NMR spectrum (Table 3.5) showed signals for a 1,4,- disubstituted aromatic ring, as described for SHM-43B. On the basis of these data, the compound was identified as *p*-hydroxy benzoic acid (**91**, Fig.3.10).

3.2.2.5 Identification of SHM-42F as protocatechuic acid (92)

The high resolution EIMS of SHM-42F (yield 0.0009%) showed a molecular ion at m/z 154 (81%) which analysed for $C_7H_6O_4$. The IR spectrum showed a broad band at 3600-2000 cm^{-1} for a carboxylic acid and/or hydroxyl functional groups. The ^{1}H NMR spectrum (Table 3.5) revealed three signals in the aromatic region typical for the 1,3,4-trisubstituted aromatic ring as described for SHM-42A. On the basis of these data, the compound was identified as protocatechuic acid (**92**, Fig. 3.10).

H	SHM-42A	SHM-42B	SHM-43B	SHM-42G	SHM-42F
2	7.03	7.17	7.02	7.85	7.43
	d (2.0)	d (1.8)	d (8.7)	d (9.0)	br s
3			6.69	6.78	
			d (8.7)	d (9.0)	
5	6.77	6.81	6.69	6.78	7.41
	d (8.2)	d (8.2)	d (8.7)	d (9.0)	br d (8.7)
6	6.93	7.06	7.02	7.85	
	dd (8.2, 2.0)	br d (8.2)	d (8.7)	d (9.0)	d (8.7)
1'			2.73		
			t (7.3)		
2'	7.51	7.59	3.67		
	d (15.9)	d (15.8)	t (7.3)		
3'	6.22	6.35			
	d (15.9)	br d (15.8)			
OMe-3		4.93			
		s			

Table 3.5: ^{1}H NMR (250 MHz, in pyridine-d_5) data of cinnamate and benzoate derivatives isolated from the butanol soluble fraction of the 80% ethanol extract

^{1}H multiplicities are shown by the symbols: s=singlet, d=doublet, dd=double doublet, t=triplet and br=broad. Figures in brackets represent coupling constants (J) in Hz.

3.2.2.6 Identification of SHM-42D as quercetin-3-β-D-galactopyrano-side (120)

The yellow powder of SHM-42D was obtained in a yield of 0.007%. The ^{1}H NMR spectrum showed, in the aromatic region (Table 3.6), signals typical of the 3',4'-, and 5,7-dioxygenated B and A rings of a flavonoid respectively, as described for quercetin (page 71). The ^{1}H NMR spectrum further revealed signals for seven protons between δ 4.1 and 6.0 suggesting a hexose carbon sugar.

The position of attachment of the sugar to the flavonoid skeleton was established from a number of experiments. The downfield signal at δ 13.10 in the ^{1}H NMR spectrum was indicative of a hydrogen bonded 5-hydroxyl group. Addition of sodium acetate in the methanolic solution of SHM-42D caused a bathochromic shift in the band II region of the UV spectrum by 10 nm suggesting a free 7-hydroxyl group. A free 4'-hydroxyl group was supported by a sodium methoxide induced bathochromic shift of band I region by 42 nm with *increase in intensity*. Finally, a shift of the band I region by sodium acetate in the presence of boric acid (+24 nm) establish free 3',4'-dihydroxy functional groups and hence leaves the C-3 position as the only site for the sugar attachment.

The identification of the sugar and its attachment site were unambiguously established from long range heteronuclear multiple bond correlation (HMBC), NOESY and ^{1}H-^{1}H COSY studies. The major ^{1}H-^{13}C couplings in the HMBC studies are shown on Table 3.7. Except for the H-6' proton (which resonates together with a pyridine signal), all the expected long range ^{1}H-^{13}C couplings were observed for the A and B ring protons. This supported the assignment of

all carbon signals of the quercetin skeleton (Table 3.6). Probably the most important information obtained from the HMBC NMR studies was, however, from the ^3J coupling of the anomeric sugar proton signal (δ 6.04) with carbon signal at δ 135.6. This supported the assignment of the sugar attachment site at C-3 of the quercetin skeleton.

The anomeric configuration of pyranose sugar can often be established from the ^{1}H-^{1}H coupling constant for the anomeric position (H-1"-H-2"). This value (7.8 Hz) supports an axial rather than equatorial orientation for H-1". In the COSY spectrum (Fig. 3.11) the anomeric proton (δ 6.04) was coupled to a triplet at δ 4.79 (H-2") which also has a coupling pattern (triplet J=7.9 Hz) indicative of the H-3"s axial orientation. This latter proton (H-3") appeared as a broad doublet due to the equatorial orientation of H-4" which appeared as a broad singlet and also showed connectivity with both H-3" and H-5" in the COSY spectrum (Fig. 3.12). The 6-carbon sugar could therefore be identified as galactose rather than glucose, in which all protons have an axial orientation. Finally, the NOESY studies showed interaction between one of the H-6" sugar proton (δ 4.41, H-6"a) and H-5' of the flavonoid skeleton and thus support the structure **120** as shown in Fig. 3.12. Quercetin-3-galactoside was first isolated from *Hypericum perforatum* (Jerzmanowska, in Harborne, 1975).

Figure 3.11: COSY spectrum (400 MHz, CDCl₃) of SHM-42D (sugar region)
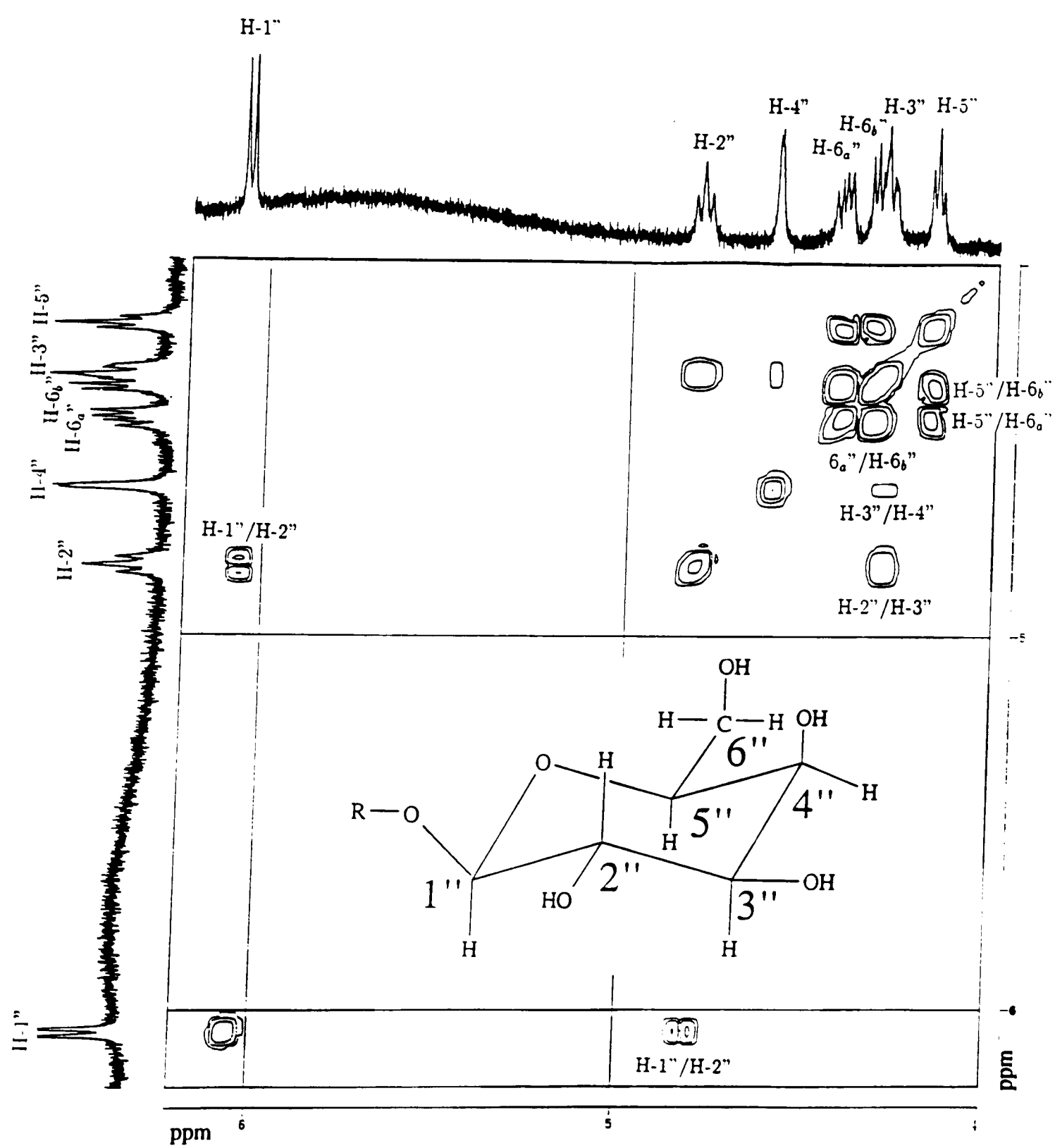
C	δ C	C mult.[b]	δ H	H pattern[c]	J (Hz)
2	158.1	s			
3	135.6	s			
4	179.3	s			
5	158.3	s			
6	100.4	d	6.61	d	2.0
7	168.6	s			
8	95.1	d	6.67	d	2.0
9	163.2	s			
10	105.6	s			
1'	122.8	s			
2'	118.4	d	8.41	d	2.2
3'	143.2	s			
4'	151.3	s			
5'	116.8	d	7.23	d	8.5
6'	123.2	d	8.11	dd	8.5, 2.2
1"	106.0	d	6.04	d	7.8
2"	73.9	d	4.79	t	7.9
3"	75.9	d	4.31	br d	5.2
4"	70.3	d	4.58	s	
5"	78.1	d	4.15	br d	5.9
6"$_a$	62.4	t	4.41	m	
6"$_b$			4.34	m	
5-OH			13.10	br s	

Table 3.6: ^{1}H and ^{13}C NMR assignments of SHM-42D (120)[a]

[a] ^{1}H and ^{13}C NMR spectra were taken at 400 and 100 MHz NMR respectively in pyridine-d$_5$

[b] ^{13}C NMR multiplicities were obtained from the J-mod. ^{13}C data and designated by the symbols: s=singlet, d=doublet, and t=triplet.

[c] Patterns are designated by the symbols: s=singlet, d=doublet, m=multiplet and br=broad.

H	δ C
	^2J and ^3J Correlations
H-6	105.6, 158.1, 168.6
H-8	105.6, 163.2, 168.6
H-2'	123.2, 151.3
H-6'	118.4, 151.3, 158.1
H-1"	135.6
H-2"	106.0
H-3"	70.3, 78.1
H-5"	62.4, 106.0

Table 3.7: **HMBC correlations for SHM-42D (120)**
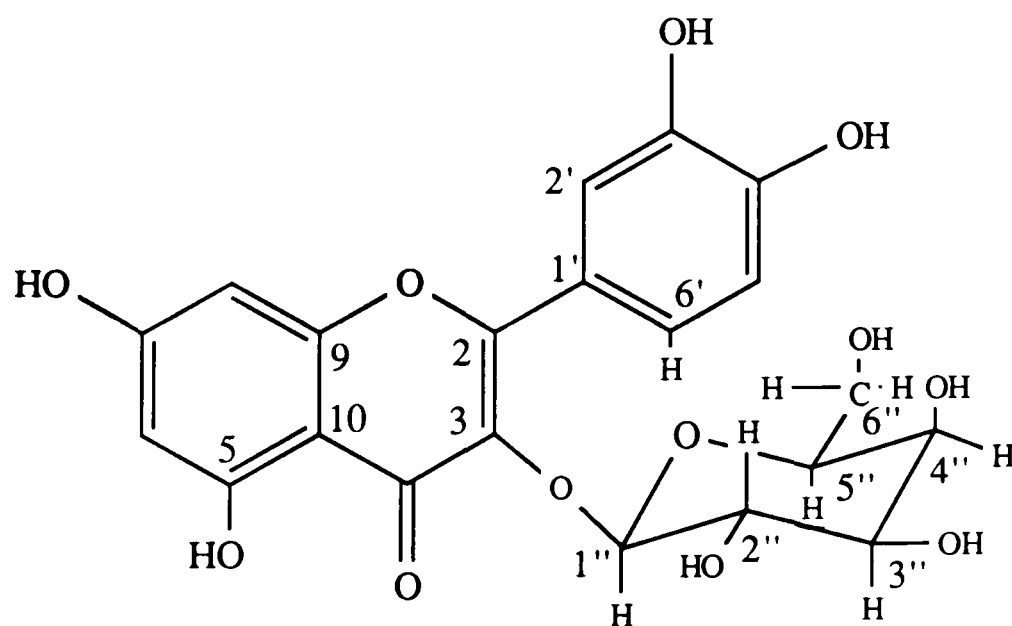
Fig. 3.12. Structure of SHM-42D

3.2.3 Examination of the ethyl acetate soluble fraction of the 80% ethanol extract

HPLC chromatography of the ethyl acetate soluble fraction (Fig. 3.13) showed two major constituents which had very close retention times. These compounds were isolated by HPLC using reverse phase silica columns.

Figure 3.13: **HPLC chromatogram of the ethyl acetate solouble fraction**

SHM-36A

SHM-36B

Solvent system A[1]

[1] Details of the solvent system and retention times are described in Section 3.3.3, page 101

0   20   40

Time (minutes)
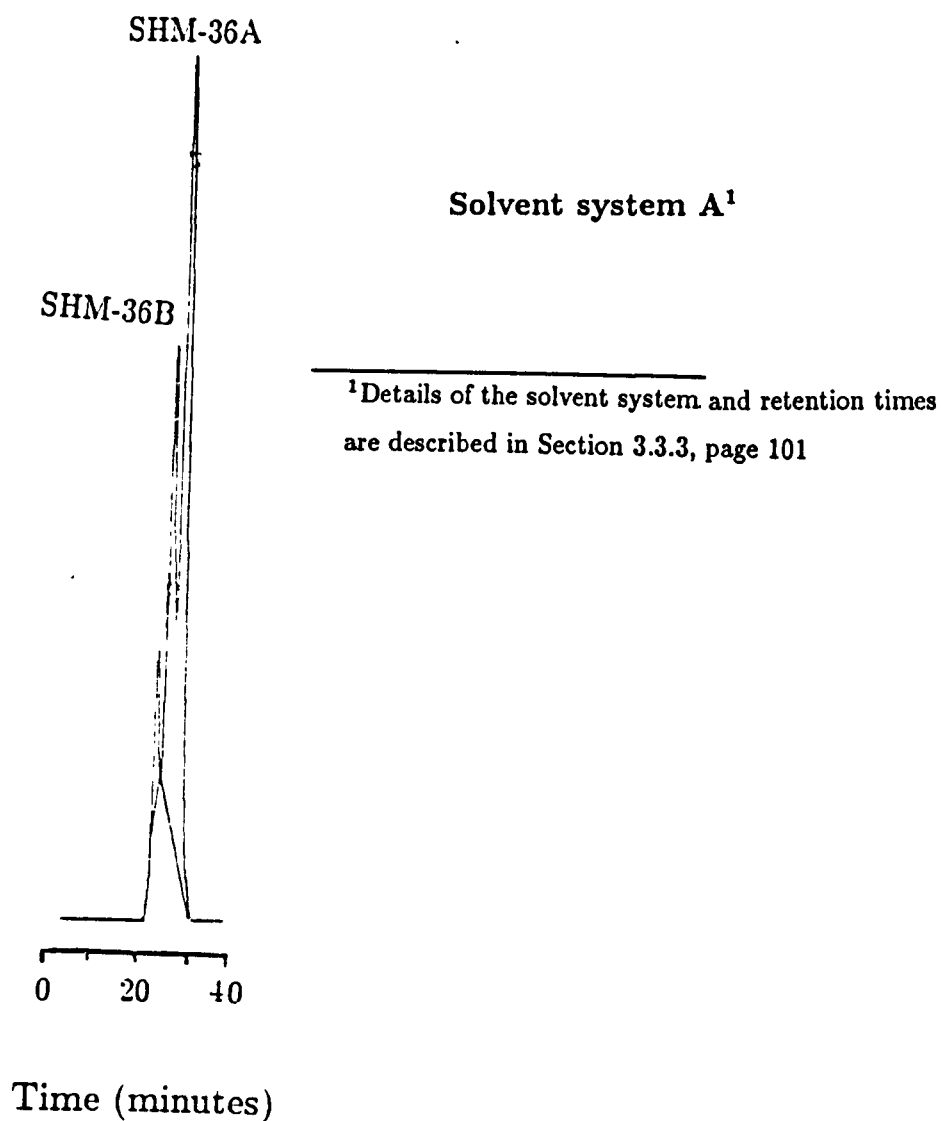
3.2.3.1 Identification of SHM-36A as luteolin-4'-β-D-glucopyranoside (121)

SHM-36A was a yellow powder obtained in a yield of 0.0007%. The aglycone moiety of the molecule could be identified as luteolin from ^{1}H NMR spectral data (Table 3.8) as described for SHM-36-4 (see Section 3.2.1.2).

^{1}H and ^{13}C signals assigned to C-1" through C-6" of the sugar moiety fall within the range corresponding to α-D/L-glucopyranoside. As described for SHM-42D (page 84), a coupling constant of 7.9 Hz between the anomeric proton signal and the H-2" pattern was indicative of axial-axial coupling. The coupling constants observed for all of these sugar protons (Table 3.8) were also typical of axial-axial coupling, as in glucopyranoside. Assignment of the sugar proton resonances were based on ^{1}H-^{1}H COSY NMR studies (Fig. 3.14).

As with SHM-42D, HMBC studies were employed to assist the assignment of ^{13}C signals and identify the attachment site of the sugar. In these studies (Fig. 3.15), all the three B ring protons and the anomeric proton signals were coupled to a carbon signal at δ 149.9. This identifies the C-4' position which can have ^2J coupling with H-5' and ^3J couplings with H-2', H-6' and the anomeric proton (H-1"). Additional evidence on the sugar attachment site came from the NOESY studies which showed interaction between the anomeric proton signal and H-5'. On the basis of these data SHM-36A was identified as luteolin-4'-β-D-glucopyranoside (121, Fig. 3.12). 121 was first isolated from *Turgenia latifolia* (Harborne and Williams, 1972).

89

Figure 3.14: **COSY spectrum of (400 MHz, CDCl₃) SHM-36A** (sugar region)
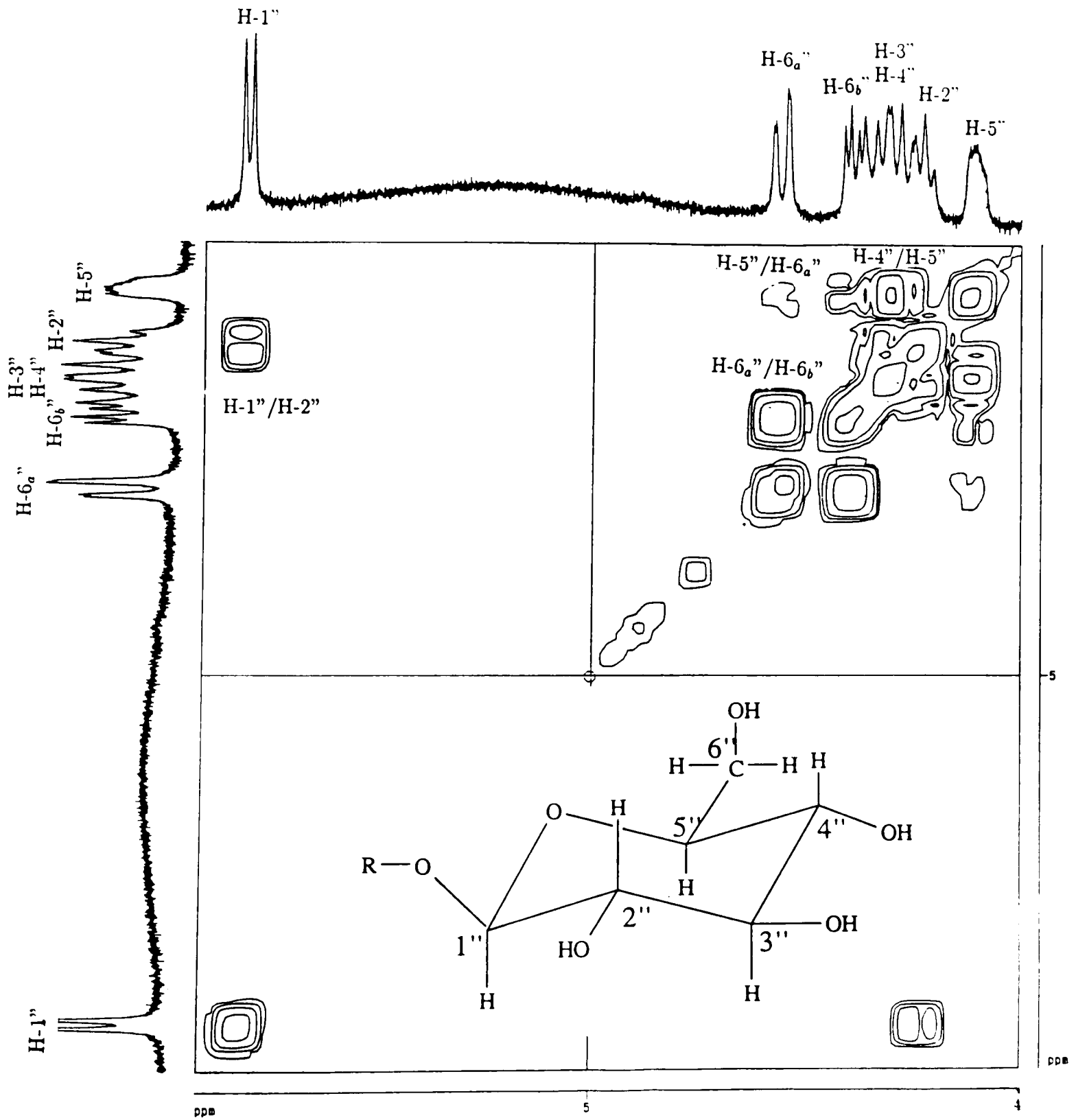
Figure 3.15: HMBC spectrum (400 MHz, pyridine-d$_5$) of SHM-36A
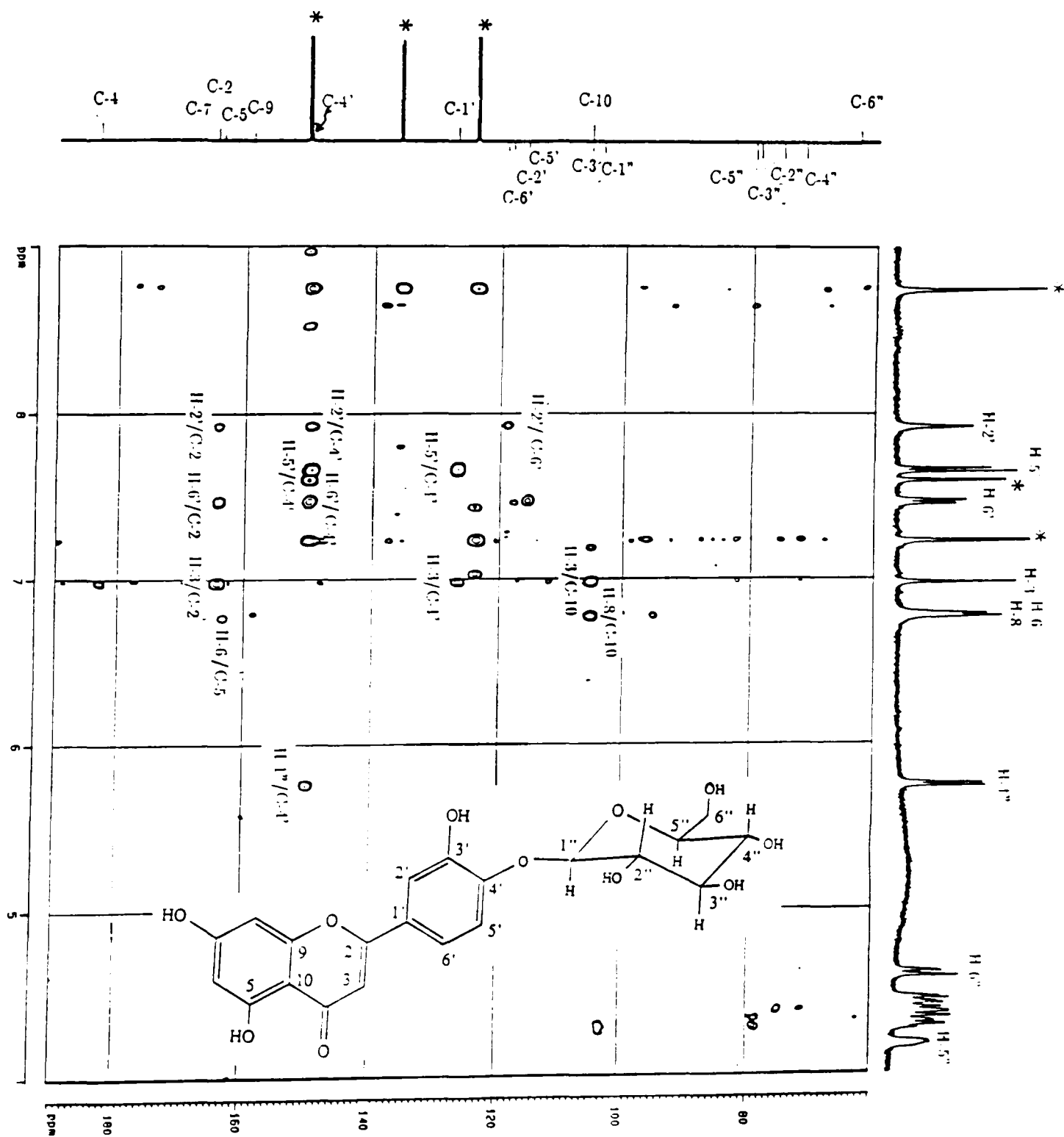
C	δ C	C mult.[b]	δ H	H pattern	J (Hz)
2	164.6	2			
3	105.6	d	7.22	s	
4	183.2	s			
5	163.6				
6	NOT SEEN	d	6.08	br s	
7	166.6	s			
8	95.0	d	6.77	br s	
9	159.0	s			
10	105.5	s			
1'	127.1	s			
2'	118.3	d	7.92	br s	
3'	NOT SEEN				
4'	149.9	s			
5'	115.8	d	7.68	d	8.8
6'	119.2	d	7.44	br d	8.8
1"	103.6	d	5.74	d	7.9
2"	75.3	d	4.28	t	8.5
3"	78.9	d	4.33	t	8.7
4"	71.7	d	4.36	m	
5"	79.7	d	4.17	m	
6"$_a$	62.8	t	4.59	dd	10.5, 5.2
6"$_b$			4.53	br d	10.5
5-OH			13.66	br s	

Table 3.8: ^{1}H and ^{13}C NMR assignments of SHM-36A (121)[a]

[a] ^{1}H and ^{13}C NMR spectra were taken at 400 and 100 MHz NMR respectively in

pyridine-d

[b] ^{13}C NMR multiplicities were obtained from the J-mod. [13]C data and designated

by the symbols: s=singlet, d=doublet, and t=triplet.

[c] Patterns are designated by the symbols: s=singlet, d=doublet, m=multiplet

and br=broad.

121
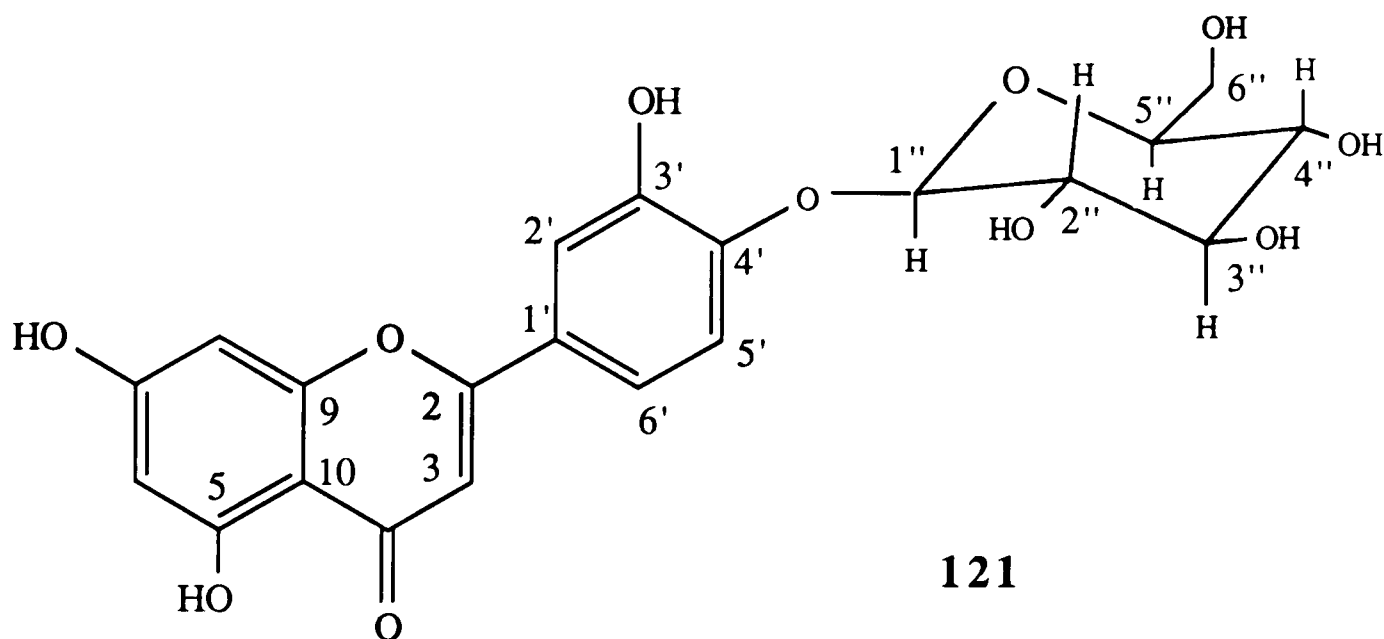
Fig. 3.16. Structure of SHM-36A

3.2.3.2 Identification of SHM-36B as quercetin-α-L-arabinopyranoside (122)

The yellow amorphous solid of SHM-36B was obtained in a yield of only 0.00044%. The ^{1}H and ^{13}C NMR spectra (Table 3.9) of the peracetate showed signals in the aromatic region typical of the quercetin skeleton (see Section 3.2.1.1). The ^{1}H and ^{13}C NMR signals (Table 3.9) assigned to C-1" through C-5" of the sugar fell within the range corresponding to α-L-arabinopyranose. As described for SHM-42D on page 83, a large coupling constant (6.8 Hz) between the anomeric

proton (H-1", δ 5.56) and H-2" (δ 5.40) is indicative of axial-axial coupling. Further analysis of couplings and assignment of ^{1}H signals were substantiated by the COSY NMR. In this study (Fig. 3.17), the H-2" doublet of doublets at δ 5.40 was connected to a doublet of doublets at δ 5.14 (H-3") which exhibited a coupling pattern indicative of axial (9.2 Hz) H-2" and equatorial (3.6 Hz) H-4" orientations. H-4" appeared as broad singlet (δ 5.15) due to its equatorial position and coupled (from the COSY spectrum) with both H-3" and H_2-5". The latter methylene protons (H-5) appeared as two doublet of doublets at δ 3.80 and 3.52. While the HMBC spectrum (Table 3.10) supported the assignment of ^{13}C signals in the aromatic region, it failed to show a ^3J coupling between the anomeric proton and carbon at the quercetin skeleton. This problem could not be solved by the NOESY and UV shift reagent studies. In the latter studies no bathochromic shift was observed for sodium methoxide and band I appeared at unusually long wavelengh (416.5 nm). The possibility of inorganic salts substituted at various hydroxyl sites could not be discounted. From the data obtained, the structure of SHM-36B could be identified as either the 3, 7, 3' or 4'-β-L-arabinopyranoside of quercetin (**122**, Fig. 3.18). As **122** lacked bioactivity it was not further investigated.

Figure 3.17: COSY spectrum (400 MHz, CDCl$_3^*$) of SHM-36B acetate (123)
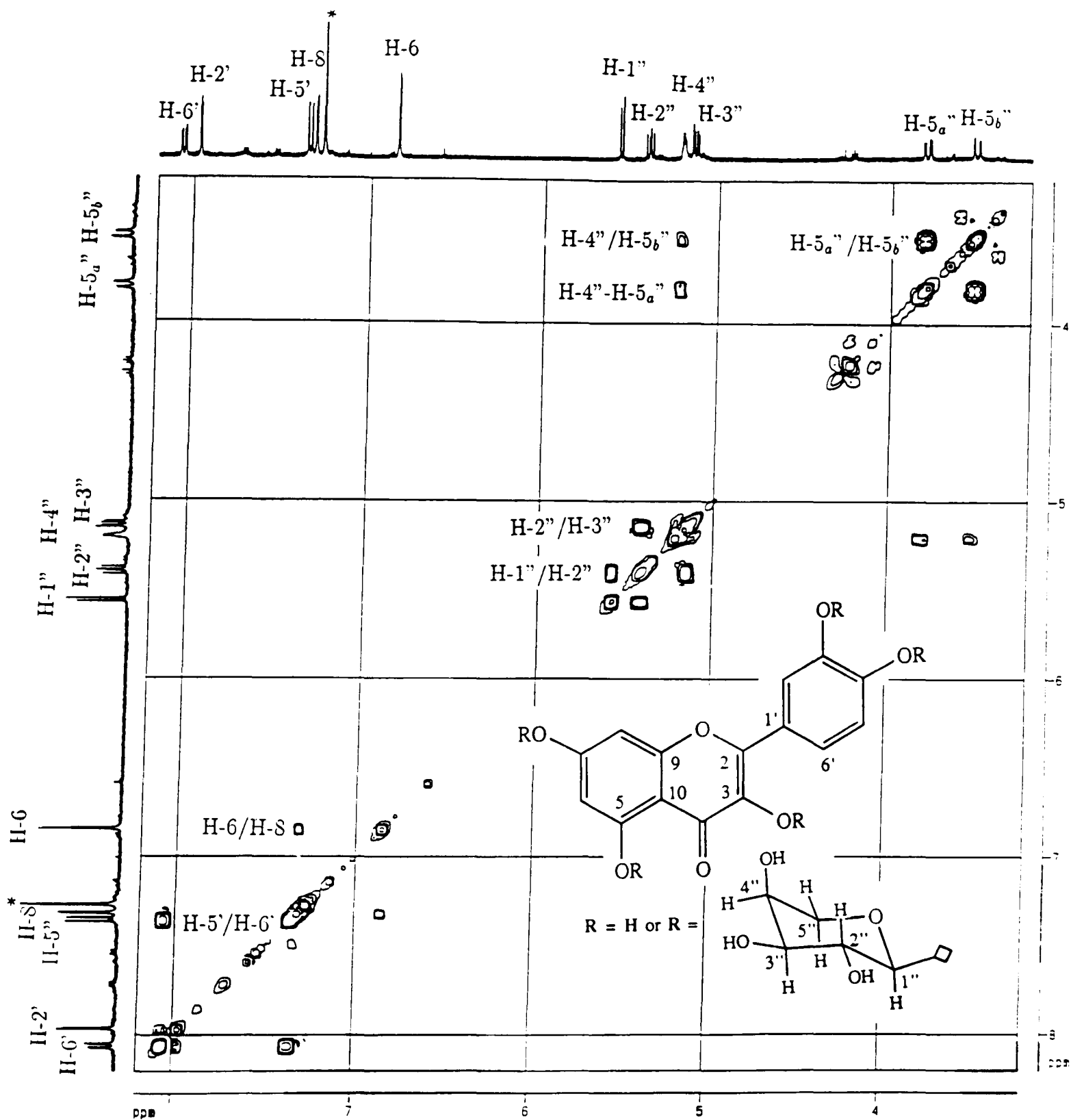
C	δ C	C mult.[b]	δ H	H pattern	J (Hz)
2	154.0	s			
3	137.3	s			
4	172.4	s			
5	150.4	s			
6	113.7	d	6.84	d	
7	156.7	s			
8	109.1	d	7.32	d	
9	154.2	s			
10	115.2	s			
1'	128.9	s			
2'	124.6	d	7.96	d	
3'	142.2	s			
4'	144.5	s			
5'	123.5	d	7.35	d	
6'	127.7	d	8.05	dd	
1"	99.4	d	5.56	d	6.8
2"	70.1	d	5.40	dd	9.2, 6.8
3"	69.6	d	5.14	dd	9.2, 3.6
4"	67.6	d	5.15	br s	
5"$_a$	63.7	t	3.80	dd	11.2, 3.4
5"$_b$			3.52	br d	11.2

Methyls of Acetate	δ_C	20.8, 20.8, 20.9, 21.0, 21.1, 21.3, 21.4
	δ_H	2.05, 2.08, 2.13, 2.33, 2.34, 2.35, 2.45
Carbonyl of acetate	δ_C	168.0, 168.1, 168.2, 169.5, 170.0, 170.2, 170.6

Table 3.9: ^{1}H and ^{13}C NMR assignments of SHM-36B acetate (123)[a]

[a] ^{1}H and ^{13}C NMR spectra were taken at 400 and 100 MHz NMR respectively in CDCl$_3$.

[b] ^{13}C NMR multiplicities were obtained from the J-Mod. ^{13}C data and designated by the symbols: s=singlet, d=doublet, and t=triplet.

[c] Patterns are designated by the symbols: s=singlet, d=doublet, m=multiplet and br=broad.

| H | δ C |
	^2J and ^3J Correlations
H-6	115.2, 150.4
H-8	113.7, 115.2, 154.2, 156.7
H-2'	123.6, 142.2, 144.5, 154.0
H-5'	128.9, 142.2
H-6'	144.5
H-5"	67.6, 99.4

Table 3.10: HMBC correlations for SHM-36B acetate (123).

SHM-36B R = H or R =

SHM-36B acetate   123

122
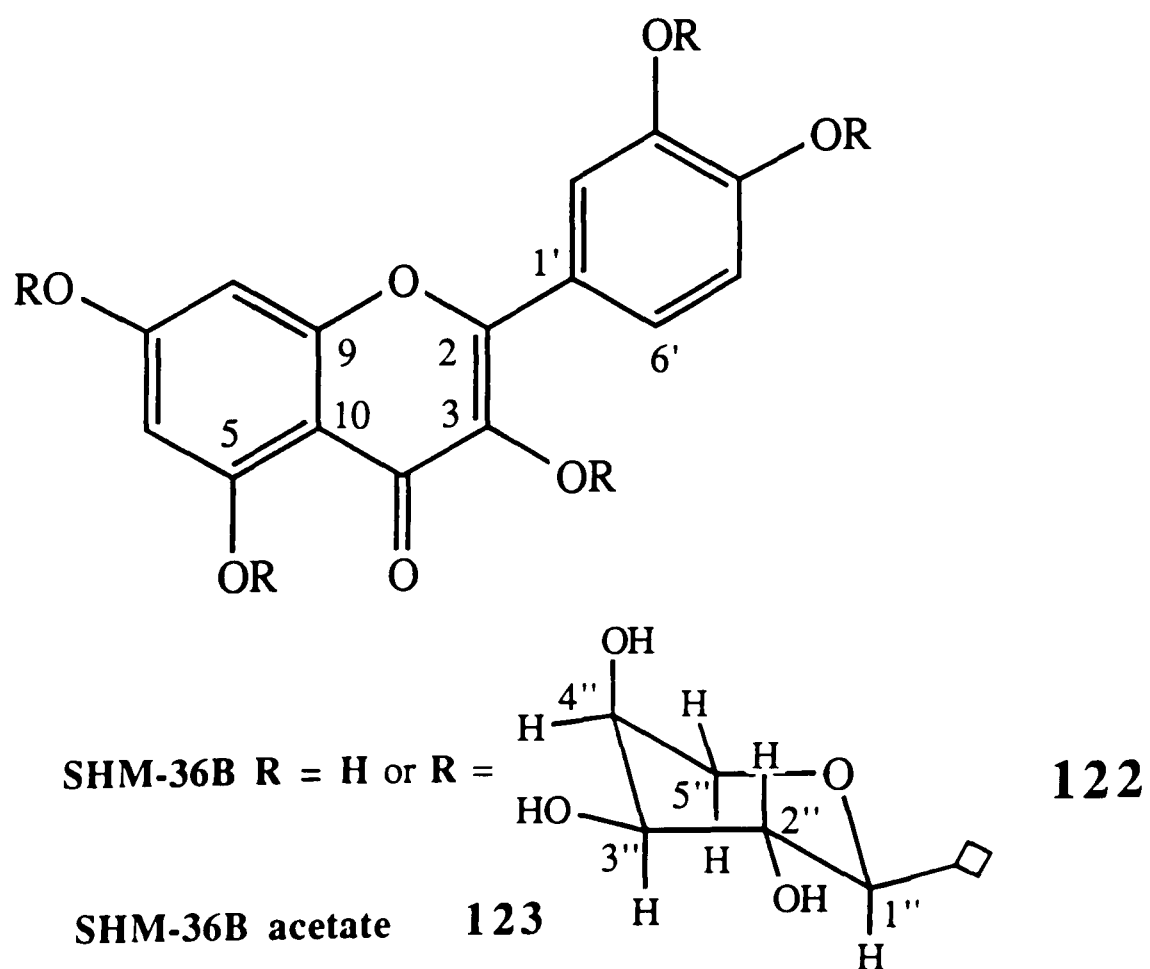
Fig. 3.18. Structure of SHM-36B

3.3 Experimental

3.3.1 Isolation of the antibacterial principle from *Premna schimperi*

3.3.1.1 Extraction and isolation

The dried leaves (900 gm) of *P. schimperi* were extracted in a Soxhlet with ethanol and the solvent removed under vacuum to yield a crude extract (190 gm). This extract was tested for antibacterial activity by the DDA method (300 μg/disc). The extract was then fractionated by VLC over silica gel G (Merck 7749) eluting with solvents of increasing polarity (Scheme 3.1); i.e., hexane, hexane:chloroform, chloroform, chloroform:ethyl acetate, ethyl acetate, acetone and finally methanol. Fractions were concentrated and tested using the DDA method and the hexane:chloroform (1:1) and chloroform fractions found to be active. These fractions were bulked and subjected to column chromatography over silica gel G eluting with hexane containing increasing amounts of ethyl acetate. Antibacterial activity (DDA) was identified with a single compound [R_f, 0.48 on silica gel G (Merck Art. 5735), solvent chloroform:methanol 5:1] which gave a pink colour on heating after spraying with 1% vanillin in concentrated H_2SO_4. Fractions containg this spot were bulked and the resulting oil was recrystallysed from benzene at 4°C to give SHM-1 (927 mg).

3.3.1.2 Properties of SHM-1 ((5R,8R,9S,10R)-12-oxo-*ent*-3,13(16)-clero-dien-15-oic acid) (111)

Prisms from benzene, mp 96-98°C; $[\alpha]_D$ -74° (c. 0.1, $CHCl_3$). Found 318.2200, $C_{20}H_{30}O_3$, requires 318.2195; UV λ_{max}^{EtOH} nm = 230; IR ν_{max}^{KBr} cm^{-1} = 3380, 3190, 2960, 2900, 1730, 1620, 1210, 1170, 1055, 965 nm; ^{1}H NMR (360 MHz, CDCl$_3$) δ = 0.78 (3H, s, Me-20), 0.83 (3H, d, J=6.7 Hz, Me-17), 0.96 (3H, s, Me-19), 1.53 (3H, s, Me-18), 1.68 (1H, dd, J=12.1, 1.7 Hz, H-10), 1.88 (1H, m, H-8), 1.92 (2H, m, CH$_2$-2), 2.59, 2.82 (2H, ABq, J=15.5 Hz, CH$_2$-11), 3.27 (2H, s, CH$_2$-14), 5.11 (1H, m, H-3), 5.87 (1H, br s, H-16), 6.14 (1H, s, H-16), 10.45 (1H, br s COOH); ^{13}C NMR-see Table 3.1; EIMS m/z (rel. int.) = 318 (10.9) 190 (89.8), 188 (14.8), 175 (100), 147 (17.4), 122 (10.0), 113 (3.6), 93 (11.0),85 (31.2), 55 (42.1).

3.3.1.3 Methylation of SHM-1

25 mg of SHM-1 was dissolved in a few drops of methanol in a separating funnel, mixed with 2 ml of 5% (w/w) KOH in methanol and allowed to stand for 30 minutes. After adding an equal amount of distilled water, the methylated product was extracted into chloroform and washed with distilled water (2x). The sample was then dried using anhydrous Na$_2$SO$_4$ and concentrated under reduced pressure. ^{1}H NMR (250 MHz, CDCl$_3$) δ = 0.72 (3H, s, Me-20), 0.79 (3H, d, J=7.0 Hz, Me-17), 0.90 (3H, s, Me-19), 1.49 (3H, br s, Me-18), 2.65 (2H, t, J=12.0 Hz, CH$_2$-11), 2.90 (2H, s, CH$_2$-14), 3.95 (3H, s, OMe), 5.09 (1H, br s, H-3), 5.70 (1H, br s, H-16) and 5.92 (1H, br s, H-16).

3.3.2 Reduction of SHM-1

100 mg of SHM-1 was dissolved in ethanol and refluxed (for 10 hours) and 100 mg of sodium borohydride added in lots of 25 mg every two hours. The whole mass was acidified and filtered. The filtrate was extracted with chloroform and the major spot detected by TLC was isolated using prep. TLC (petrol:CHCl₃:EtOAc, 4:6:4) to give 12 mg of SHM-12 (**116**).

3.3.2.1 Properties of SHM-12 (12-oxo-*ent*-3-cleodene-15-oic acid) (**116**)

Yellow gum. Found 320.2369, $C_{20}H_{32}O_3$, requires 320.2351; ^{1}H NMR (250 MHz, CDCl₃) δ = 0.75 (3H, s, Me-20), 0.85 (3H, d, *J*=6.8 Hz, Me-17), 0.97 (3H, s, Me-19), 1.12 (3H, d, *J*=7.2 Hz, Me-16), 1.56 (3H, br s, Me-18), 2.2-2.6 (2H, m, CH₂-11), 2.7–2.9 (2H, m, CH₂-14), 5.14 (1H, br s, H-3); EIMS *m/z* (rel. int.) = 320 (4.7), 204 (43.1), 190 (39.0), 189 (40.5), 175 (100), 173 (37.3), 123 (18.4) 122 (10.9), 121 (27.3), 119 (21.0), 115 (10.3), 105 (29.9), 95 (40.8), 87 (7.2).

3.3.2.2 Methylation of SHM-12

Diazomethane was prepared by adding a cold solution of diazald (1g) in Et₂O (20 ml) from a dropping funnel to an ethanolic solution of potassium hydroxide (5%) in a mini-diazald apparatus maintained at 65°C. The ethereal distillate of diazomethane (CH₂N₂) was collected in an ice cold receiver. When the dropping funnel was empty, more ether (20 ml) was added slowly and the distillation continued until the distilling ether was colourless. SHM-12 in ether was then treated with the freshly made diazomethane and the mixture left overnight.

The methyl ester of SHM-12 (**117**) was obtained in quantitative yield. SHM-12-methyl ester=^{1}H NMR (250 MHz, CDCl$_3$) δ = 0.74 (3H, s, Me-20), 0.85 (3H, d, J=7.0 Hz, Me-17), 0.95 (3H, s, Me-19), 1.11 (3H, d, J=7.2 Hz, Me-16), 1.60 (3H, br s, Me-18), 3.60 (s, OMe) and 5.15 (1H, br s, H-3).

3.3.3 Analysis of the 80% ethanol extract of leaves of *Premna schimperi*

3.3.3.1 HPLC solvent systems used

A solvent gradient was used by mixing solvent I (double distilled water containing 0.5% (v/v) formic acid) and solvent II (75% methanol). The two solvent gradients (Solvent system A and B) used for the separation and detection of compounds are shown in the table below.

Solvent system	Time	% Solvent II
A	0	50
	1	50
	25	75
	30	100
	45	100
B	0	20
	1	20
	50	75
	60	100

3.3.3.2 Separation of compounds

Powdered leaves of *Premna schimperi* (700 g) were placed in a glass percolator and continually extracted with 80% ethanol. Removal of solvent under reduced pressure yielded 96 g of extract residue which was subsequently partitioned into CHCl$_3$ and water (see Scheme 3.4). The chloroform fraction was defatted by further partitioning into hexane and 90% methanol. Column chromatography (Sephadex LH-20) of the latter fraction (90% methanol) (10 g) gave impure SHM-37A from the last fraction. This was recrystalised from MeOH to yield **118** (6mg). PTLC (silica gel, CHCl$_3$:MeOH 7:3) of the first column fraction afforded SHM-35 (150 mg) and SHM-36-4 (12 mg).

The water fraction (chloroform/water partitioning) was further partitioned into ethyl acetate and water and the former was subjected to HPLC (reverse phase silica, 250mm x 10mm column, solvent A) to yield 5 mg of SHM-36A and 4 mg of SHM-36B. The water fraction left in the above partitioning was further partitioned (n-butanol and water) to give 20 gm of the butanol soluble residue which was subsequently subjected to vacuum liquid chromatography (Plyamide MN Sc 6) eluting with water containing an increasing amount of methanol. A repetitive HPLC separation (reverse phase silica, 250 mm x 10 mm column, solvent B) of compounds from the 10% methanol fraction afforded 6.4 mg of SHM-42F and 10 mg of SHM-42G. Similar treatment of the 25% methanol VLC eluent afforded 20 mg of SHM-42A, 18.3 mg of SHM-42B and 6.7 mg of SHM-43B. The 50% methanol VLC eluent finally afforded 50 mg of SHM-42D. The retention times of compounds isolated using reverse phase silica HPLC are

shown in the table below.

Compound	Retention Time (minutes)
SHM-36A	24.8
SHM-36B	22.4
SHM-42A	7.2
SHM-42B	11.1
SHM-42D	15.5
SHM-42F	4.4
SHM-42G	6.5
SHM-43B	12.7

Retention times of compounds (solvent system A, ODS TES 800, 25 cm x 4.6 mm column)

3.3.4 Properties of compounds

3.3.4.1 Properties of SHM-36-4 (5,7,3',4'-tetrahydroxyflavone) (Luteolin, 38)

Yellow needles, mp 326-328°C. Found 286.0494, $C_{15}H_{10}O_6$, requires 286.0477; UV λ_{max}^{MeOH} nm=250, 256 sh, 345; IR ν_{max}^{KBr} cm^{-1} = 3300br, 2920, 1650, 1600, 1500, 1445, 1355, 1160; ^{1}H NMR δ = see Table 3.4; EIMS m/z (rel. int.) = 286 [M]$^+$ (100), 153 (37.0), 137 (6.8).

3.3.4.2 Properties of SHM-35 (3,5,7,3',4'-pentahydroxyflavone) (Quercetin, 108)

Yellow needles, mp 310°C. Found 302.0454, $C_{15}H_{10}O_7$, requires 302.0427: UV λ_{max}^{MeOH} nm = 256, 375, 428sh; IR ν_{max}^{KCl} cm^{-1} = 3300br, 2910, 1650, 1600, 1500, 1310, 1170; ^{1}H NMR δ = see Table 3.4; EIMS m/z (rel. int.) = 302 [M]$^+$ (100), 166 (21.3), 153 (51.6), 136 (16.1).

3.3.4.3 Properties of SHM-37A, (3,5,7-trihydroxy-4'-methoxyflavone) (Kaempferide, 118)

Yellow needles, mp 229-231°C. Found 300.0634, $C_{16}H_{12}O_6$, requires 300.0634; UV λ_{max}^{MeOH} nm = 267, 321 sh, 323; IR ν_{max}^{KCl} cm^{-1} = 3505, 3290, 2920, 1655, 1625, 1560, 1510, 1375, 1170; ^{1}H NMR δ = see Table 3.4; EIMS m/z (rel. int.) = 300 [M]$^+$ (100), 199 (21.3), 285 (26.1), 271 (10.1), 257 (21.7), 229 (20.6), 150 (21.8), 135 (22.7), 77 (15.4).

3.3.4.4 Properties of SHM-42A (Caffeic acid, 88)

White powder. Found 180.0422, $C_9H_8O_4$, requires 180.0422, UV λ_{max}^{MeOH} nm = 237, 294 sh, 321; IR ν_{max}^{KCl} cm^{-1} = 3420, 3300-2300, 1690, 1620, 1600, 1510, 1430, 1270, 1200, 1030, 850, 800; ^{1}H NMR δ = see Table 3.5; EIMS m/z (rel. int.) = 180 (100), 179 (12.6), 163 (27.9), 136 (33.4), 135 (17.7), 134 (37.4), 89 (23.8), 77 (10.9).

3.3.4.5 Properties of SHM-42B (Ferulic acid, 89)

White powder. Found 194.0543 $C_{10}H_{10}O_4$, requires 194.0579; UV λ_{max}^{MeOH} nm = 232, 297 sh, 321; IR ν_{max}^{KCl} cm^{-1} = 3455, 3100-2000, 1690, 1665, 1620, 1600, 1510, 1465, 1430, 1275, 1200, 1175, 1035, 850, 800. ^{1}H NMR δ = see Table 3.5; EIMS m/z (rel. int.) = 194 (2.5), 164 (100), 163 (26.1), 147 (40.2), 119 (25.6), 118 (15.5), 91 (17.2), 77 (4.0).

3.3.4.6 Properties of SHM-43B (2(4-hydroxyphenyl)-ethanol, 119)

Yellow gum. Found 138.0663, $C_8H_{10}O_2$, requires 138.0681; UV λ_{max}^{MeOH} nm = 243, 329; IR ν_{max}^{KCl} cm^{-1} = 3390, 2910, 1610, 1595, 1510, 1450, 1350, 1240, 1050, 800; ^{1}H NMR δ = see Table 3.5; EIMS m/z (rel. int.) = 138 (70.5), 106 (2.4), 78 (12.6), 77 (38.7).

3.3.4.7 Properties of SHM-42F (Protocathechuic acid 92)

White powder. Found 154.0272, $C_8H_{10}O_2$, requires 154.0266; UV λ_{max}^{MeOH} nm = 256, 292; IR ν_{max}^{KCl} cm^{-1} = 3600-2000, 1670, 1600, 1510, 1290; ^{1}H NMR δ = see Table 3.5; EIMS m/z (rel. int.) = 154 (81), 137 (100), 109 (25.7), 81 (14.0).

3.3.4.8 Properties of SHM-42G (p-hydroxybenzoic acid, 91)

Brown needles. Found 138.0328, $C_7H_6O_3$, requires 138.0317; UV λ_{max}^{MeOH} nm = 263, 321 sh; IR ν_{max}^{KCl} cm^{-1} = 3390, 3100-2400, 1670, 1605, 1590, 1460, 1420, 1315, 1290, 1240, 1170, 850,750; ^{1}H NMR δ = see Table 3.5; EIMS m/z (rel. int.) = 138 (72.5), 121 (100), 93 (25).

3.3.4.9 Properties of SHM-42D (Quercetin-3-β-D-galactopyranoside (120)

Yellow powder, $[\alpha]_D$ +28° (c, MeOH). UV λ_{max}^{MeOH} nm = 270, 369; (NaOMe) 271, 411; (AlCl$_3$) 274, 434 (AlCl$_3$ + HCl) 270, 370 sh, 430; (NaOAc) 275.84, 386.73; (NaOAc + H$_3$BO$_3$) 261.54, 380.77; IR ν_{max}^{KBr} cm^{-1} = 3500-2500, 1650, 1600, 1500, 1440, 1360, 1300, 1200, 1070; ^{1}H and ^{13}C NMR = δ see Table 3.6.

3.3.4.10 Properties of SHM-36A (Luteolin-4'-β-D-glucopyranoside, 121)

Yellow powder. $[\alpha]_D$ -88° (c, MeOH). UV λ_{max}^{MeOH} nm = 268, 345; (NaOMe) 268, 381; (AlCl$_3$) 268, 351, 381; (AlCl$_3$ + HCl) 265, 351, 381; (NaOAc) 268, 369; (NaOAc + H$_3$BO$_3$) 267.5, 345; IR ν_{max}^{KBr} cm^{-1} = 3400 br, 1650, 1600, 1375, 1290, 1200, 1060; ^{1}H and ^{13}C NMR δ = see Table 3.8.

3.3.4.11 Propreties of SHM-36B (Quercetin-α-L-arabinopyranoside, 122)

Yellow powder. $[\alpha]_D$ -72° (c, MeOH). UV λ_{max}^{MeOH} nm = 279, 327 sh, 417; (NaOMe) 279, 327 sh, 417; (AlCl$_3$) 279, 327 sh, 357 sh, 417; (AlCl$_3$ + HCl) 273, 327 sh, 357 sh, 405; (NaOAc) 279, 339 sh, 417; (NaOAc + H$_3$BO$_3$) 279, 327 sh, 417; IR ν_{max}^{KBr} cm^{-1} = 3400 br 2910, 1650, 1600, 1360, 1300, 1200, 1075; ^{1}H and ^{13}C NMR of peracetate (123) δ = see Table 3.9.

Chapter 4

PHYTOCHEMICAL AND ANTIMICROBIAL STUDIES ON *PREMNA OLIGOTRICHA*

4.1 Bioassay Guided Isolation of the Active Principles

4.1.1 Bioevaluation of the crude extract

The crude ethanol extract of *P. oligotricha* was tested for its antimicrobial activity using the DDA method as described previously for *P. schimperi* (see Section 3.1.1). The extract exhibited activity against gram-positive bacteria (*S. aureus* and *B. subtilis*) at concentrations higher than 100 μg per disc. Like the *P. schimperi* extract, no activity was observed against gram-negative bacteria (*E.*

coli and *P. aeruginosa*), fungi (*A. niger* and *P. notatum*) and yeast (*C. albicans*) at concentrations up to 500 μg per disc.

4.1.2   Isolation of the antibacterial principle(s)

A bioassay guided fractionations were carried out (Scheme 4.1) to isolate the active principle(s). Fractionation of the ethanolic extract over VLC (silica gel) followed by bioassay, revealed two active fractions (Scheme 4.1): activity being greatest in the petrol:ethyl acetate (7:3) fraction. Further purification by silica gel column and prep. TLC led to fractions with stronger antibacterial activity and finally to the isolation of three active principles (Fig. 4.1).

4.1.3   Identification of the active principles

4.1.3.1   Identification of SHM-3 as 16-hydroxy-clerod-3,13(14)-diene-15,16-olide (124)

The most active constituent of *P. oligotricha* was a yellow gum (yield 0.01%) which had optical rotation of -21° and UV absorption at 230 nm. A broad band in the IR spectrum at 3350 cm^{-1} was indicative of a hydroxy functional group while bands at 1750 and 1640 cm^{-1} suggested a β-substituted butenoloid moiety (William and Fleming, 1989). The high resolution EIMS showed a molecular ion at *m/z* 318, $C_{20}H_{30}O_3$.

The ^{1}H NMR spectrum (Table 4.1) revealed three tertiary and one secondary methyl groups one of which was vinylic (δ 1.58) and exhibited log-range coupling (1.2 Hz) with an olefinic proton at δ 5.19 (d, *J*=1.2 Hz). This, together

108

Crude Extract

VLC

Petrol → **Petrol:Ethyl acetate** → **Ethyl acetate** → **Methanol**
95:5--8:2--7:3--1:1--2:7

INACTIVE   ACTIVE   INACTIVE

Gel Filtration (sephadex)

Column Chromatography (silica gel)

Column Chromatography (silica gel)
Petrol ---95:5---9:1--8:2------- Ethyl acetate

Chlorophyll

SHM-15B   SHM-15C

Crystallization

Prep TLC

SHM-4

INACTIVE

SHM-19   SHM-3   SHM-5
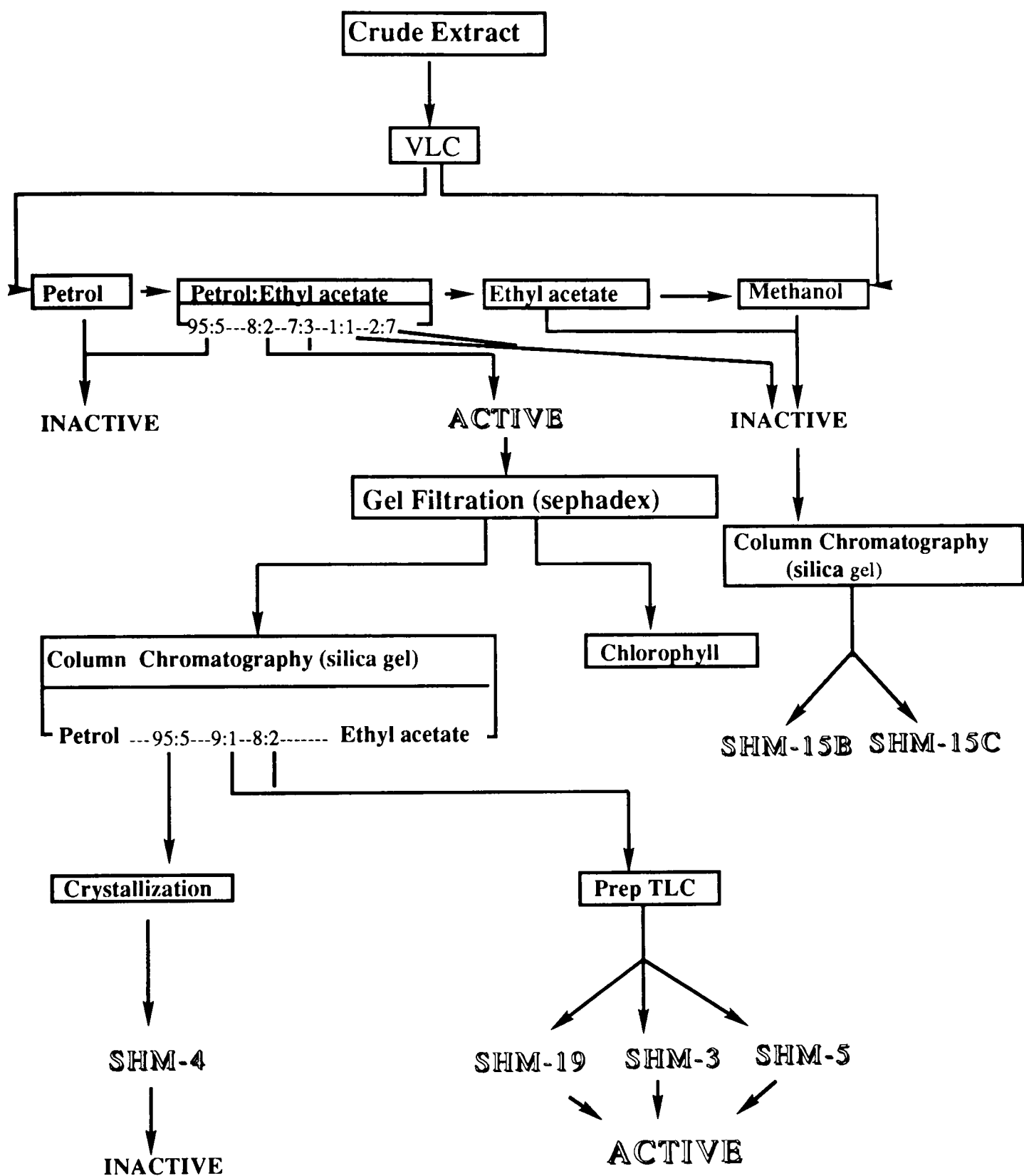
ACTIVE

Scheme 4.1. Bioassay guided isolation of the active principles

SHM-3 124
β OH 125
α OH 126

SHM-5 127

SHM-19 128
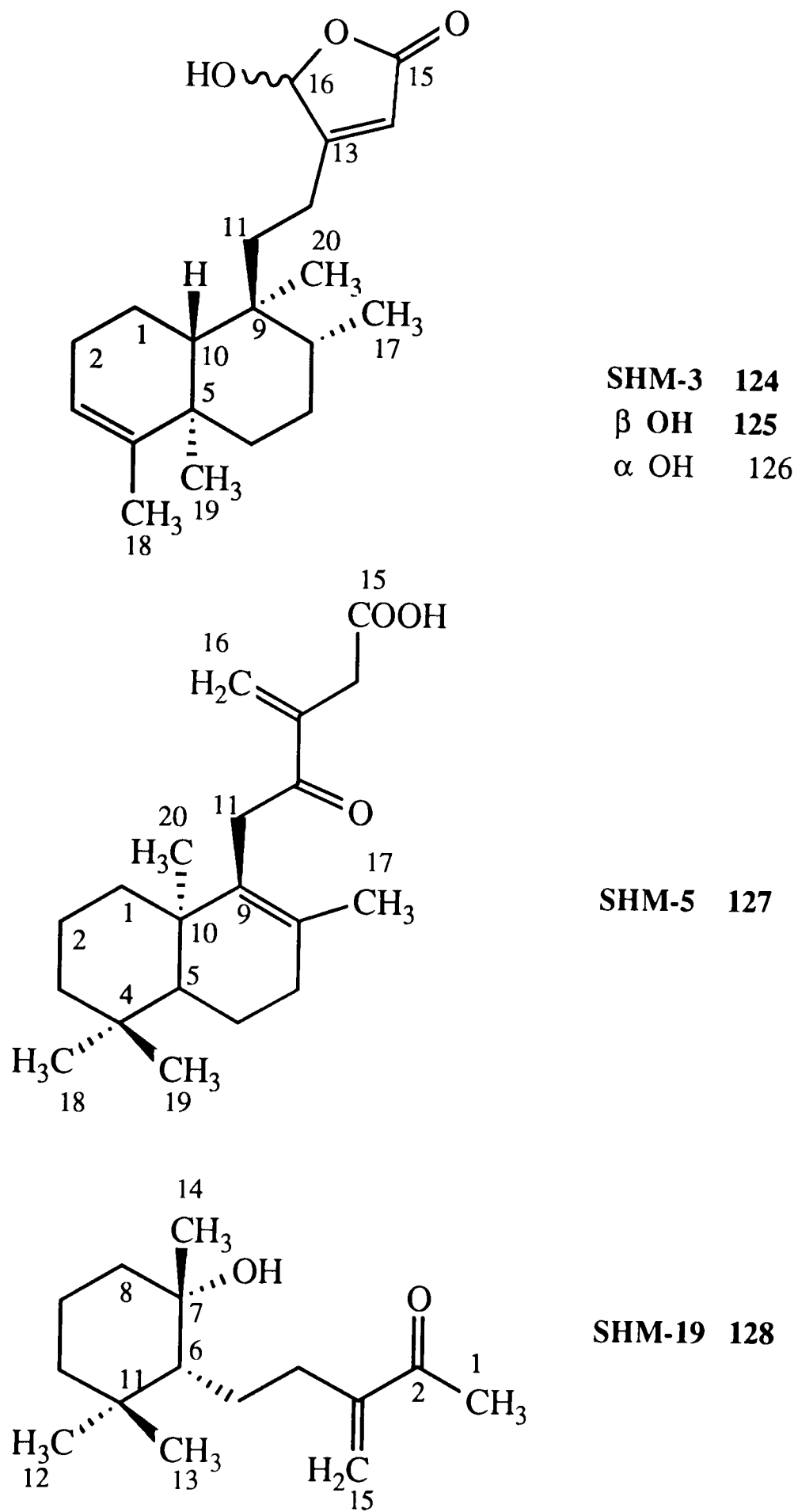
Fig. 4.1. Antibacterial constituents of *P. oligotricha*

with the major fragment (EIMS) at m/z 190, $[C_{14}H_{22}]^+$ and minor fragment at m/z 127, $[C_6H_7O_3]^+$ (Scheme 4.2), suggested a clerodane skeleton with all oxygens located at the six-carbon side-chain. The ^{13}C NMR data (Table 4.1) was also in agreement with a clerodane skeleton as described previously for SHM-1 (see Section 3.1.3).

A β-substituted butenoloide moiety in the six carbon-side chain was indicated by ^1H NMR signals at δ 5.85 (d, J=0.9 Hz) and 6.00 (d, J=0.9 Hz) which were assignable to H-14 and H-16 respectively; and the fragment in the EIMS at m/z 114 (6.9) (Scheme 4.2). This hydroxy bearing lactone ring was substantiated by characteristic signals in the ^{13}C NMR spectrum (Table 4.1). In this spectrum, resonances for the carbonyl carbon at δ 170.8 (C-15), olefinic carbons at δ 171.8 (C-13) and 116.9 (C-14), and a methine carbon bearing two oxygens at δ 99.2 supported the structure of SHM-3 as **124** (Fig. 4.1).

The relative stereochemistry of SHM-3 was established from a series of nuclear Overhauser experiments. Like SHM-1, irradiation of Me-19 caused an enhancement of the Me-20 signal by 2% and *vice versa*, thereby requiring both to be placed on the same side of the molecule. All the data were in agreement with that reported previously (Phadnis *et al.*, 1988) for a clerodane (**126**) isolated from *Polyalthia longifolia* (Annonaceae). As shown by the ^1H NMR spectrum, SHM-3 was a C-16 epimeric mixture (**125** and **126**) in the ratio of 7:3.
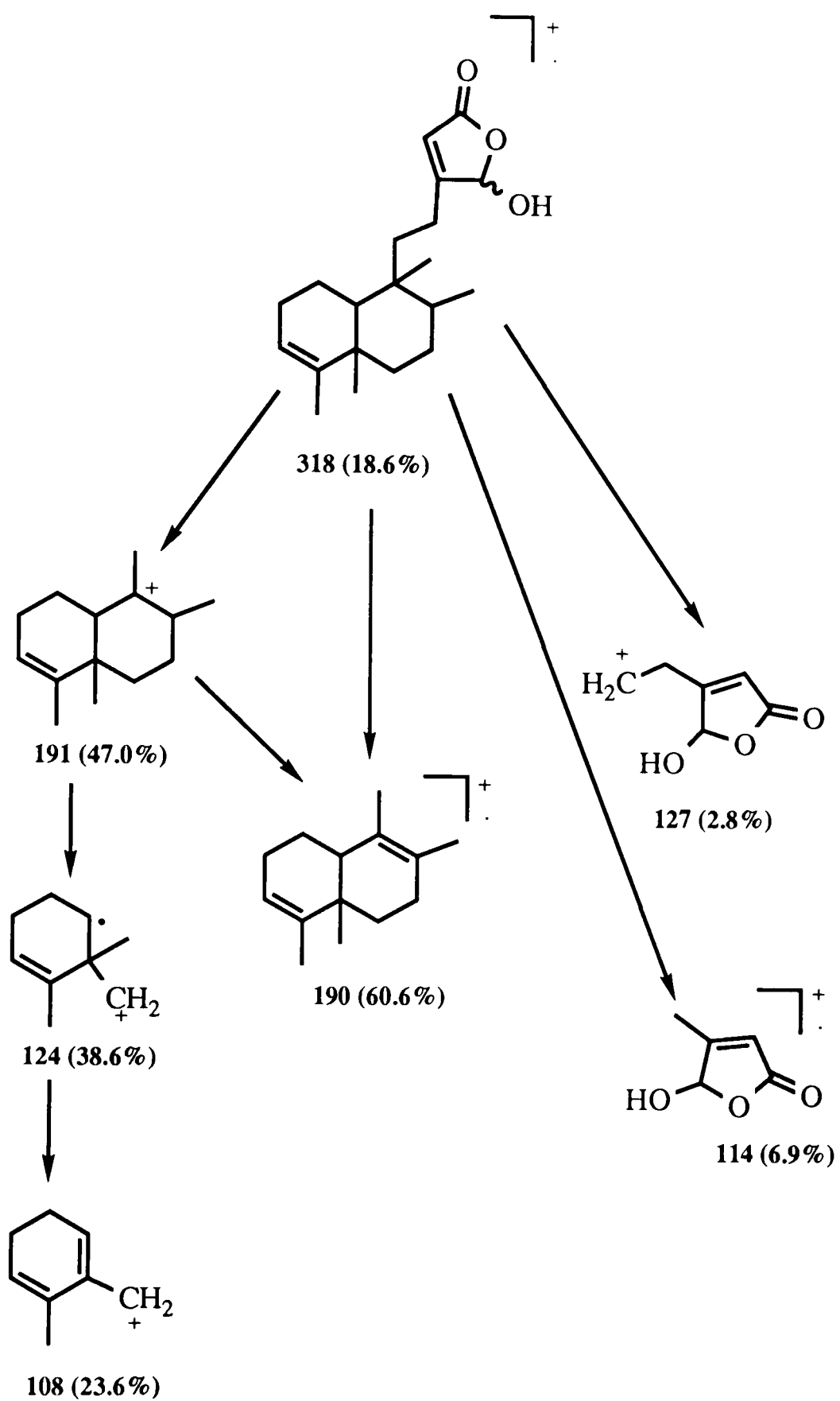
Scheme 4.2. Possible mass fragmentation pattern of SHM-3

112

C	δ C	C mult.[b]	δ H	H pattern[c]	J (Hz)
1	18.3	t			
2	27.4	t			
3	120.3	d	5.19	d	1.2
4	144.3	s			
5	38.2	s			
6	36.7	t			
7	26.8	t			
8	38.3	d			
9	38.7	s			
10	46.5	d			
11	34.8	t			
12	21.4	t			
13	171.8	s			
14	116.9	d	5.85	d	0.9
15	190.8	s			
16	99.2	d	6.00	d	0.9
17	16.0	q	0.82	d	8.0
18	18.2	q	1.58	d	1.2
19	19.7	q	1.00	s	
20	18.0	q	0.77	s	
16-OH			4.90	s	

Table 4.1: **^{1}H and ^{13}C NMR assignments for SHM-3 (124)**[a]

[a] ^{1}H and ^{13}C NMR spectra were taken at 300 and 75.5 MHz NMR respectively in CDCl$_3$.

[b] ^{13}C NMR multiplicities were obtained from the J-Mod. ^{13}C data and designated by the symbols: s=singlet, d=doublet, t=triplet and q=quartet.

[c] Patterns are designated by the symbols: s=singlet, d=doublet, and br=broad.

4.1.3.2 Identification of SHM-5 as *ent*-12-oxolabda-8,13(16)-dien-15-oic acid (127)

The second antibacterial compound was a yellow gum obtained in the yield of 0.025%. A single maximum in the UV spectrum at 230 nm together with IR absorption bands at 3700-2000 and 1682 cm^{-1} were characteristic of an α, β-unsaturated carboxylate moiety (see Section 3.1.3). The high resolution EIMS exhibited a molecular ion at m/z 318 $[C_{20}H_{30}O_3]^+$ indicating an oxygenated diterpene.

The EIMS fragmentation pattern of this compound (Scheme 4.3) exhibited similarities with that of SHM-1 (page 61). Major fragments at m/z 191 $[C_{14}H_{23}]^+$, 190 $[C_{14}H_{22}]^+$ and 113 $[C_5H_5O_3]^+$ indicated that all the three oxygens are located at the six carbon side-chain. This six-carbon side-chain was identical with that of SHM-1 (111) as the ^{1}H NMR spectrum (Table 4.2) revealed isolated methylene resonance for 11-H$_2$, 14-H$_2$ and 16-H$_2$. However, unlike SHM-1 the ^{1}H NMR resonance of the decalin system showed four methyl singlets (one vinylic).

Further structure elucidation of **127** (Fig. 4.1) and unambiguous ^{1}H and ^{13}C NMR chemical shift assignments (Table 4.2) are based on HMBC NMR studies. Key observations are shown in Table 4.3. A ^3J interaction between two methyls (δ_H 0.92, 0.89; δ_C 33.1, 21.6) permits them to be placed as the *geminal* C-4 substituents. A ^2J interaction from these two methyl protons to a singlet at δ_C 33.2 identifies C-4, and ^3J methyl coupling to a methylene (δ_C 41.4) and methine (δ_C 51.2) similarly identify C-3 and C-5, respectively. A further ^3J coupling to C-5 from another methyl resonance (δ_H 0.92, δ_C 19.8) allows assignment of the C-20

114

methyl group, which also shows a ^2J coupling to identify C-10 and ^3J couplings to C-1 (methylene) and C-9 (quaternary olefinic). Thus the double bond in the decalin system must be placed at C-8/C-9 and this was confirmed by interactions for the vinylic 8-methyl (δ_H 1.43, δ_C 20.0) which shows ^3J interaction to C-9 and the C-7 methylene, and a ^2J coupling to C-8.

This analysis of connectivities from the HMBC can readily be extended into the side-chain. The 11-H_2 methylene protons reveal four interactions, ^3J to C-8 and C-10 and ^2J to C-9 and C-12. The C-12 carbonyl carbon is further linked to 14-H_2 and 16-H_2 by ^3J interactions, while ^2J couplings are observed for 16-H_2 to C-14, 14-H_2 and 16-H_2 to C-13 and 14-H_2 to the carboxylic acid carbon C-15. Thus, only C-2 and C-6 methylenes have not been directly assigned through this process.

SHM-5 was assumed to be an *ent*-labdane in the light of its negative specific rotation (- 71°). A persual of the literature (Buckingham, 1982-87) revealed that *ent*-labdanes are laevorotary while labdanes are dextrorotary. Caputo *et al.* (1974) also reported that the specific rotation of a number of labd-8-ene derivatives are dextrorotary. On the basis of these data, SHM-5 was assigned structure **127** (Fig. 4.1), which appears to be novel.

113 (42.7%)

85 (38.1%)

205 (12.4%)

318 (48.7%)

135 (23.3%)

190 (100%)

123 (22.3%)

303 (21.8%)

109 (40.9%)

121 (32.3%)
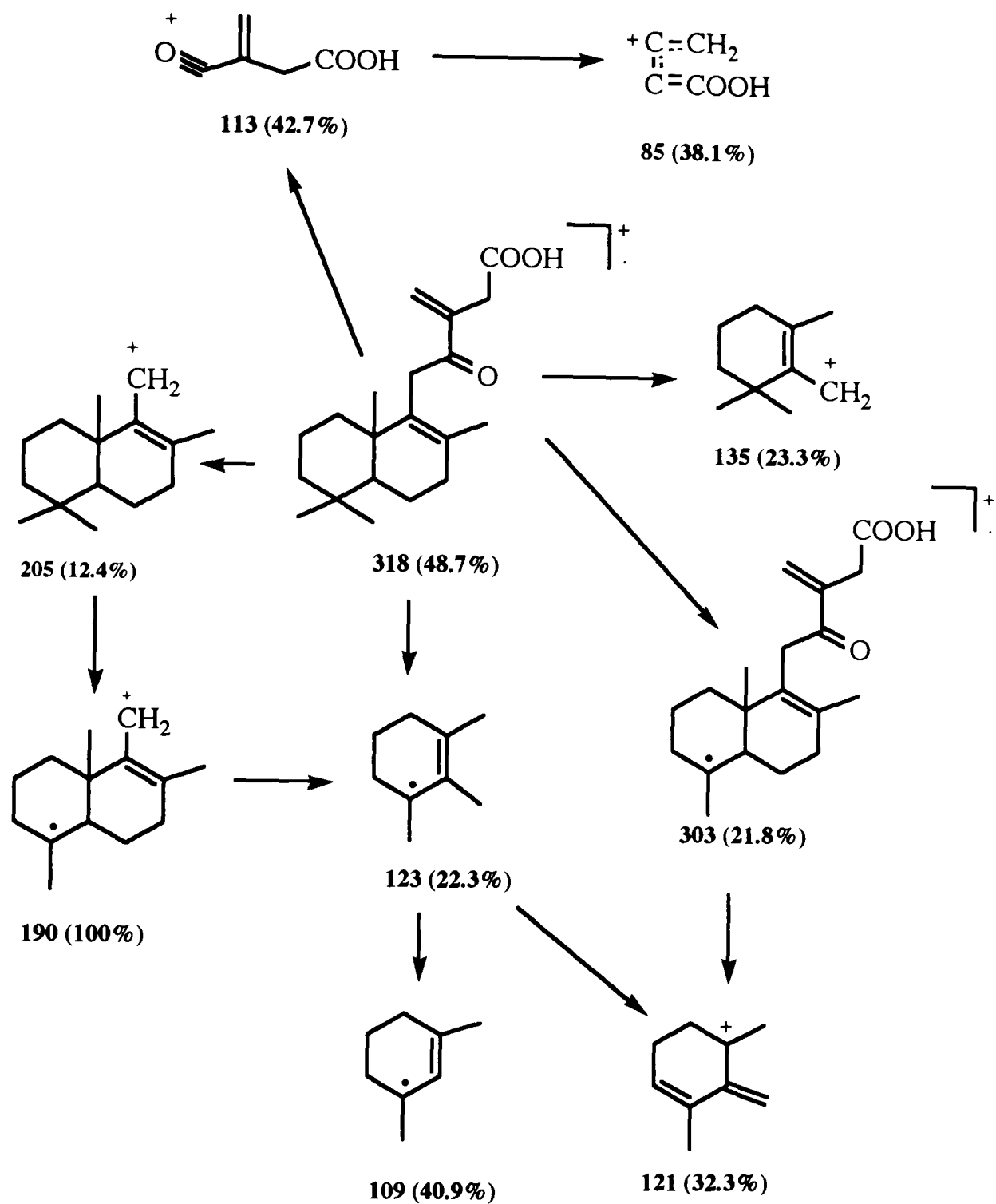
Scheme 4.3. Possible mass fragmentation pattern of SHM-5

116

C	δ C	C mult.[b]	H[c]	δ H	H pattern[d]	J (Hz)
1	36.1	t	1a	1.43	m	
			1b	1.03	ddd	
2	18.9	t	2	1.43	m	
3	41.4	t	3a	1.38	m	
			3b	1.18	ddd	
4	33.2	t				
5	51.2	d	5	1.22	dd	
6	18.9	t	6	1.47	m	
7	33.5	t	7	2.17	m	
8	130.1	s				
9	133.7	s				
10	38.2	t				
11	36.1	t	11a	3.55	ABq	18.0
			11b	3.42	ABq	18.0
12	198.8	s				
13	141.7	s				
14	37.5	t	14	3.35	s	
15	176.5	s				
16	126.4	t	16a	6.25	s	
			16b	5.93	s	
17	20.0	q	17	1.43	s	
18	33.1	q	18	0.89	s	
19	21.6	q	19	0.82	s	
20	19.8	q	20	0.92	s	

Table 4.2: ^{1}H and ^{13}C NMR assignments for SHM-5 (127)[a]

[a] ^{1}H and ^{13}C NMR spectra were taken at 300 and 75 MHz NMR respectively in CDCl$_3$.

[b] ^{13}C NMR multiplicities were obtained from the J-Mod. ^{13}C data and designated by the symbols: s=singlet, d=doublet, t=triplet and q=quartet.

[c] a and b denote magnetically unequivalent geminal protons where a appeared downfield to b.

[d] Patterns are designated by the symbols: s=singlet, d=doublet, dd=double doublets, ddd=doublet of double doublets, ABq= AB quartets and m=multiplet.

^{1}H	^{13}C	
	^3J	^2J
18-H$_3$	21.6, 41.4, 51.2	33.2
19-H$_3$	33.1, 41.4, 51.2	33.2
20-H$_3$	36.1, 51.2, 133.3	38.2
17-H$_3$	33.5, 133.7	130.1
11-H$_2$	38.2, 130.1	133.7, 198.8
16-H$_2$	37.5, 198.8	141.7
14-H$_2$	198.8	141.7, 176.5

Table 4.3: **HMBC correlations for SHM-5 (127)**

4.1.3.3 Identification of SHM-19 as 7-α-hydroxy-2-oxo-6,11-cyclofarnes-3(15)-ene (128)

The last active constituent of *P. oligotricha* was a minor constituent

obtained in a yield of only 0.00075%. The single maximum in the UV spectrum

at 230 nm and an IR band at 1670 cm^{-1} was again typical of an α, β-unsaturated

carbonyl functional group (William and Fleming, 1989). A tertiary hydroxy

functional group which could not be acetylated was evident by a band in the IR

spectrum at 3490 cm^{-1}. High resolution EIMS established the molecular formula

as $C_{15}H_{26}O_2$ as required for **128** (Fig. 4.1)

Further evidence supporting the presence of an α, β-unsaturated carbonyl

system came from the ^{13}C NMR spectrum (Table 4.4) which showed signals for a carbonyl carbon (δ 200.5) and two olefinic carbons as an exocyclic methylene at δ 150.0 and 125.5 ppm. In the ^{1}H NMR spectrum (Table 4.4) the exocyclic methylene protons appeared as broad singlets at δ 6.00 and 5.82. The ^{1}H and ^{13}C NMR spectra further revealed a strongly deshielded methyl singlet (δ 2.34, δ_C 26.1, Me-1) and methylene protons (δ 2.45 and 2.35; δ_C 34.4, H$_2$-4), allowing placement of a terminal methyl and the methylene next to the exocyclic double bond. This data, together with the EIMS (Scheme 4.4) which showed a fragment at m/z 85 (61%) [C$_5$H$_7$O]$^+$, established a partial structure **129** (Fig. 4.2).

In addition to the previously mentioned resonances, the ^{13}C NMR spectrum (Table 4.4) showed signals for a quaternary carbinol, one methine, three tertiary methyls, four saturated methylene and a saturated quaternary carbon. Based on these data and the already established molecular composition which require three double-bond equivalent, one ring system was necessary in the strucure of SHM-19. Further assignment of a novel structure **128** and unambiguous ^{1}H and ^{13}C NMR chemical-shift values were based on the HMBC, COSY and NOESY NMR studies.

The major ^2J and ^3J ^{1}H-^{13}C connectivities in the HMBC studies are shown in Table 4.5. A ^3J interaction between two methyls (δ_H 0.78, δ_C 21.4; δ_H 0.95, δ_C 32.9) allowed them to be placed as geminal C-11 substituents. A ^2J interaction between these two methyl protons and a quaternary carbon (δ 35.6) and ^3J interaction with a methylene (δ 41.7) and methine carbon (δ 37.1) identified the C-11, C-10 and C-6 positions respectively. A ^3J coupling of the

129

130
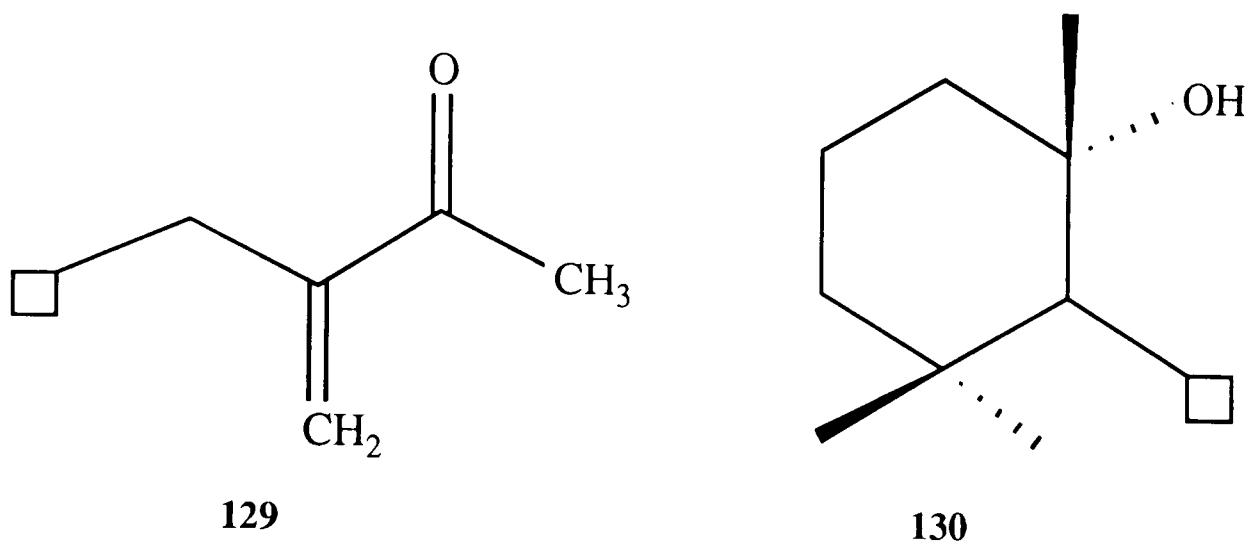
Fig. 4.2. Partial strucures of SHM-19

131
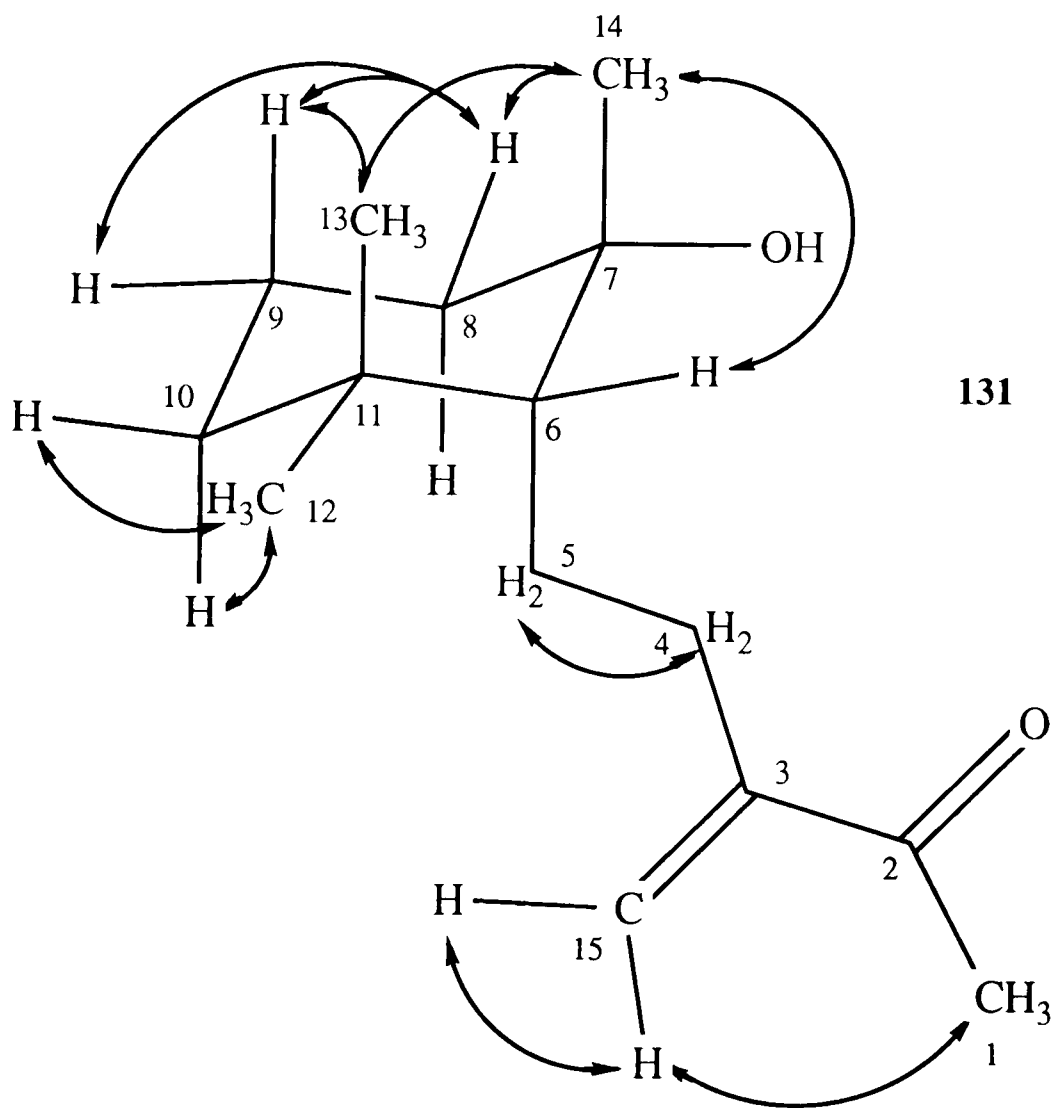
Fig. 4.3. Stereochemistry of SHM-19 based on NOESY interactions
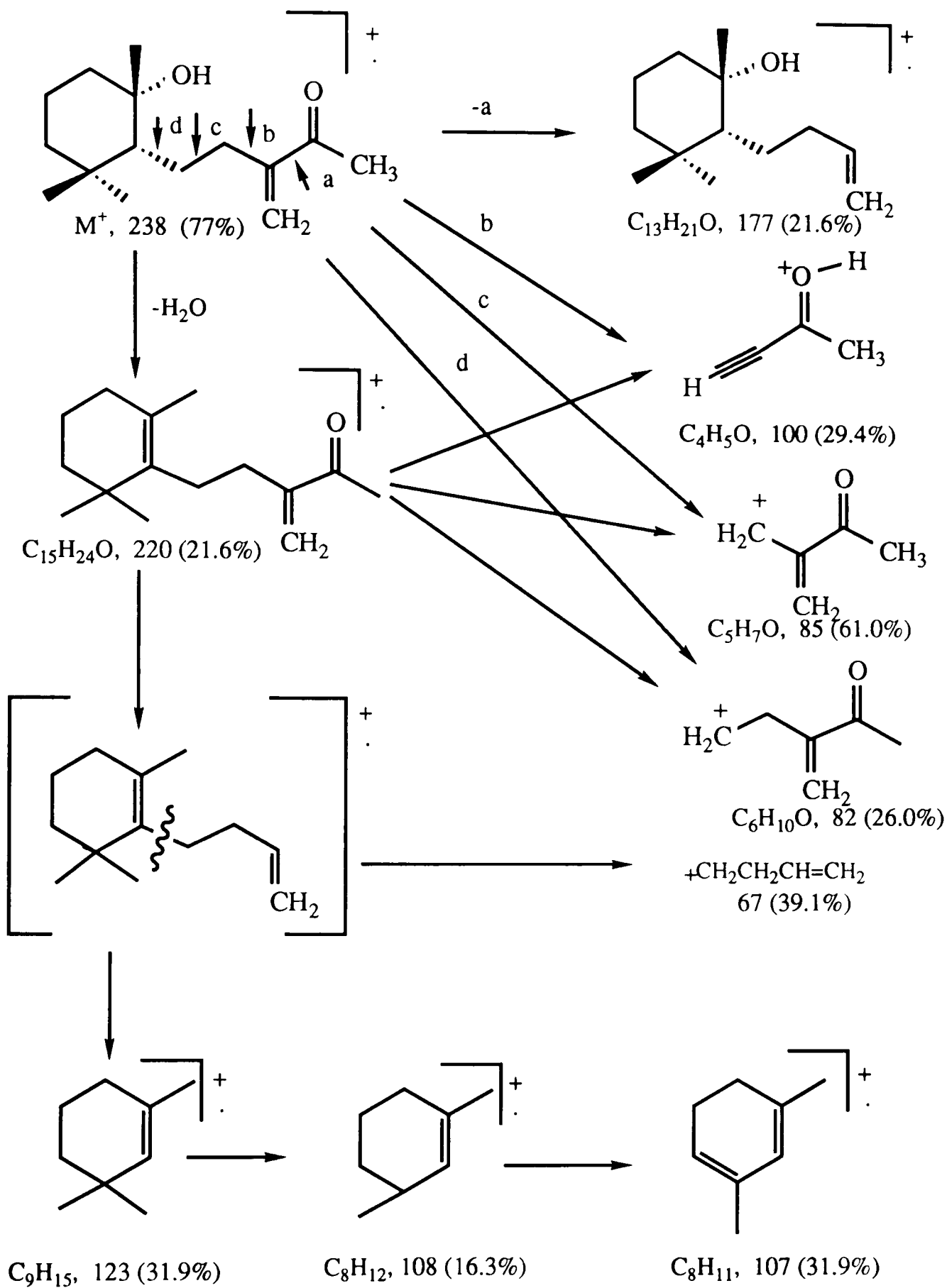
Scheme 4.4. Possible mass fragmentation pattern of SHM-19

C-6 carbon with a methyl ^{1}H resonance (δ 1.17), which in turn showed ^2J and ^3J couplings with the carbinol (δ 74.7) and methylene (δ 43.2) carbons similarly identified the C-7 position. This required that the compound has a partial structure **130** (Fig. 4.2).

This analysis of connectivities also confirmed the partial structure **129** in the six-carbon side-chain. The carbonyl carbon (δ 200.5, C-2) showed ^2J coupling with the deshielded methyl protons (δ 2.34) and ^3J interaction with the olefinic methylene protons (H-15) and aliphatic methylene protons (δ 2.35, 2.45, H-4) which are assigned at H$_2$-4. The latter protons (H$_2$-4) showed further ^2J interactions with C-5 (δ 25.8) and C-3 (δ 150.0) and ^3J couplings with the olefinic methylene carbon (δ 125.5, C-15) and methine carbon of the cyclohexane skeleton (C-6). All the expected connectivities for the C-5 methylene protons were also observed (Table 4.5). Thus except C-9 all carbons could be assigned through this process.

The relative stereochemistry (Fig. 4.3, page 120) and assignment of all ^{1}H resonances were supported by the COSY and NOESY NMR studies. In the NOESY studies (Fig. 4.3), interactions between Me-13 (δ 0.78) and Me-14 (δ 1.17) and H-6 (δ 1.40) were observed. This requires them to be placed on the same face of the molecule (**131**) and also supports the stereochemistry at C-6 and C-7 as shown in Fig. 4.3 (page 120). In the COSY studies an isolated 1H ^{1}H resonance at δ 1.72 (H-8eq) showed strong interactions with multiplets at δ 1.52 and 1.32. This identifies the axial H-8 and H-9 protons respectively. The NOESY study further revealed interaction between the H-8eq resonance and a multiplet

at δ 1.36 thereby identifying H-9 *eq*. H-10 protons were similarly identified as they showed strong interaction with Me-12 in the NOESY study.

C	δ C	C mult.[b]	H[c]	δ H	H pattern[d]
1	26.1	q	1	2.34	s
2	200.5	s			
3	150.0	s			
4	34.4	t	4a	2.45	dddd
			4b	2.35	dddd
5	25.8	t	5a	1.49	m
			5b	1.39	m
6	57.1	d	6	1.40	m
7	74.8	s			
8	43.2	t	8*ax*	1.52	m
			8*eq*	1.72	m
9	20.6	t	9*ax*	1.32	m
			9*eq*	1.36	m
10	41.7	t	10*ax*	1.22	ddd
			10*eq*	1.35	ddd
11	35.6	s			
12	32.9	q	12	0.95	s
13	21.4	q	13	0.78	s
14	23.6	q	14	1.17	s
15	125.5	t	15a	6.00	s
			15b	5.82	s

Table 4.4: ^{1}H and ^{13}C NMR assignments for SHM-19 (128)[a]

[a] ^{1}H and ^{13}C NMR spectra were taken at 400 and 100 MHz NMR respectively in CDCl$_3$.

[b] ^{13}C NMR multiplicities were obtained from the *J*-Mod. ^{13}C data and designated by the symbols: s=singlet, d=doublet, t=triplet and q=quartet.

[c] *ax* and *eq* denote geminal protons where axial (*ax*) is perpendicular to the plane and equatorial (*eq*) on the plane of chair conformation of cyclohexane. a and b denote magnetically unequivalent protons where a appeared downfield to b.

[d] Patterns are designated by the symbols: s=singlet, d=doublet, dd=double doublets, ddd=doublet of double doublets, dddd=doublet of doublets of double doublets and m=multiplet.

123

^{1}H	^{13}C	
	^3J	^2J
1-H$_3$		200.5
12-H$_3$	21.4, 41.69, 57.1	35.6
13-H$_3$	32.9, 41.69, 57.1	35.6
14-H$_3$	43.2, 57.1	74.8
4-H$_2$	57.1, 125.5	25.8, 150.0
5-H$_2$	74.8, 150.0	34.4, 57.1
16-H$_2$	34.4, 200.5	150.0

Table 4.5: **HMBC correlations for SHM-19 (128)**

4.1.3.3.1 Biosynthesis of SHM-19

The possible biosynthetic pathway of SHM-19 starting from the parent compound of all sesquiterpenes "farnesyl pyrophosphate" (**60**) is shown in Scheme 4.5. As described for diterpenes (page 21) cyclization initiated by electrophilic attack at C-10 can lead to the unstable carbocation (**132**) which can be readily attacked by a hydroxy radical to give **133**. A subsequent loss of pyrophosphate followed by double bond rearrangement gives structure **135**. Further oxidation at the terminal double bond, probably through epoxidation, finally leads to SHM-19 (**128**).
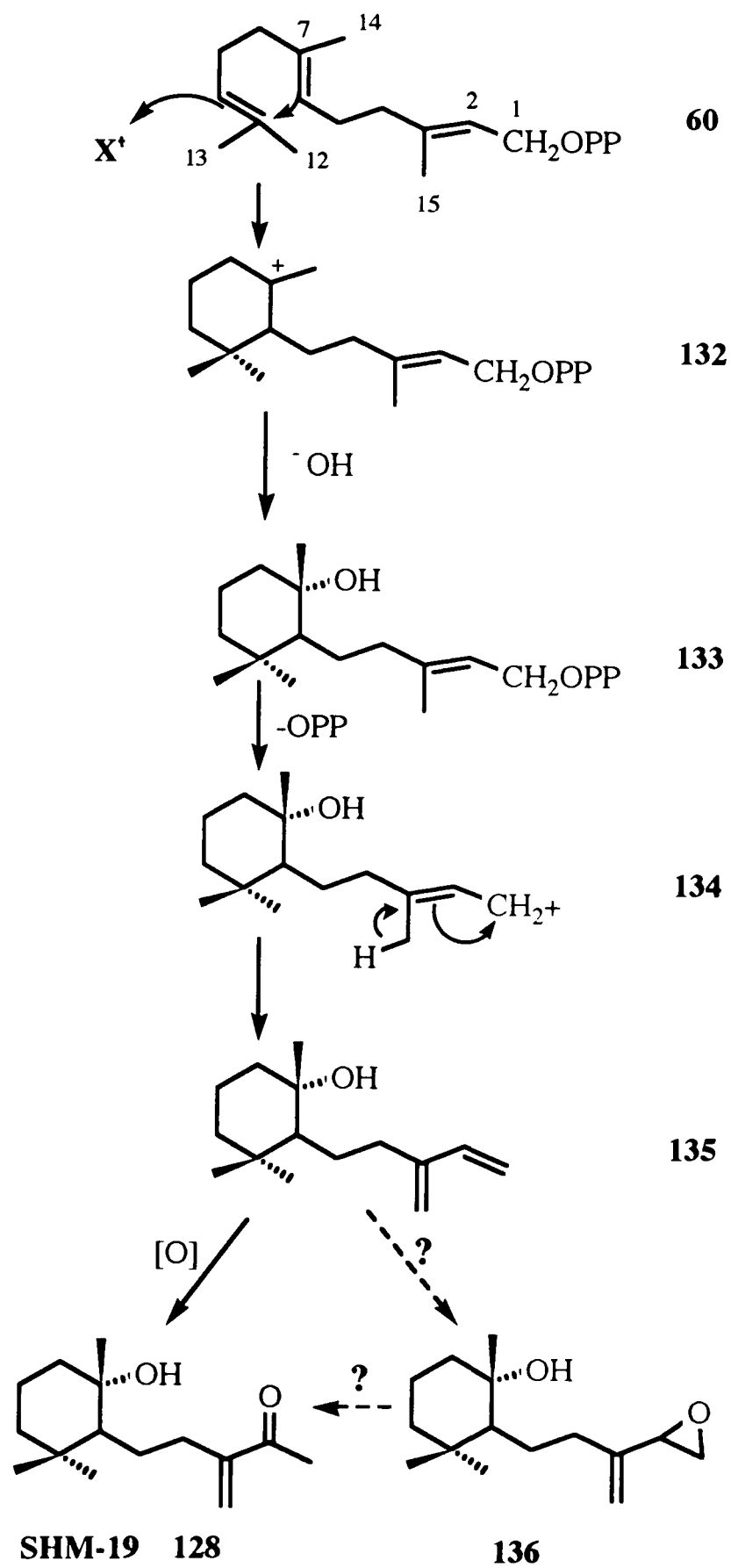
Scheme 4.5. Possible biosynthetic pathway of SHM-19

125

4.1.4 Bioevalution of the active principles

The three active constituents of *P. oligotricha* showed activity against a number of gram-positive bacteria (Table 4.6). While the activity of SHM-5 and SHM-19 were marginal that of SHM-3 was good, almost comparable with streptomycin and significantly better than the other two active compounds. No viable organisms could be recovered on subculturing broths containing these compounds greater than the MIC, suggesting that their activity was bactericidal. Neither the crude extract nor the isolated compounds showed any activity against gram-negative bacteria.

A number of gram-positive bacteria, particularly *Streptococcus* species have been implicated in causing dental caries and related disorders (Menaker, 1980). The use of *P. oligotricha* as a chewing stick could therefore provide some chemical defence against the build up of harmful gram-positive bacteria. Among bacteria involved in the spontaneous fermentation of milk gram-positive *Lactobacillus* species are very important and this group of acid forming bacteria are also liable to cause dental problems (Menaker, 1980). Because of the slow growth of *Lactobacillus* species observation of growth in the presence of these active compounds could not be measured with sufficient accuracy. However, concentrations of 25 μg ml^{-1} of SHM-3 completely inhibit growth of *Lactobacillus plantarum* using the MIC assay. It is at present unclear as to whether by burning *P. oligotricha* an antibacterial smoke can be produced but the value of using this species as a chew stick has been validated. The mechanism of action of these compounds has not been studied but all of them, like SHM-1, have an α, β-unsaturated moiety

(Fig. 4.1) which may be involved in alkylating biological nucleophile.

Test organisms	SHM-3	SHM-5	SHM-19	Streptomycin sulphate
Bacillus pumilus	3.75	50	50	0.94
Bacillus subtilis	7.50	50	100	3.75
Staphylococcus aureus	7.50	50	50	3.75
Streptococcus faecalis	30	100	150	15

Table 4.6: **Minimum inhibitory concentration (MIC μg ml^{-1}) of SHM-3, SHM-5 and SHM-19**

SHM-3, SHM-5 and SHM-19 were inactive against *Escherichia coli* and *Pseu-domonas aeruginosa* at the level of 100 μg ml^{-1}.

4.2 Antimicrobially Inactive Constituents of *Premna oligotricha*

4.2.1 Diterpenes of *Premna oligotricha*

4.2.1.1 Identification of SHM-4 as *ent*-8β,12α-epidioxy-12β-hydroxylabda-9(11),13-dien-15-oic acid γ-lactone (139)

Column chromatography (silica gel) of the 7:3 eluent of the VLC fraction (Scheme 4.1) gave SHM-4 as a major constituent in the yield of 0.025 %. It was a solid which crystallized from methanol and gives a deep blue colour with vanillin spray. High resolution EIMS of this compound was ambiguous, giving a weak ion

at m/z 332 $[C_{20}H_{28}O_4]^+$ and a stronger ion at m/z 300 $[C_{20}H_{28}O_2]^+$. The validity of the 332 MU ion was confirmed by fast-atom bombardment MS, which revealed MH^+ at m/z 333. This suggested the presence of a peroxide, for which M^+-32 is a common fragment in the EIMS (Scheme 4.6).

The ^1H NMR spectrum (Table 4.7) showed the presence of five methyl singlets, of which one was vinylic and showed long-range coupling to an olefinic proton at δ 5.98. A second olefinic proton appeared as a sharp singlet at δ 5.23. All remaining signals occured between δ 1.90 and 1.45, except for two ddds (1H each) at δ 1.22 and 1.26 for axial methylene protons. The ^{13}C NMR spectrum revealed the presence of five methylenes, three methines and seven quaternary carbons (Table 4.7). ^1H and ^{13}C resonances (direct coupling) were correlated using the Heteronuclear Multiple Quantum Coherance technique (HMQC).

As with SHM-5 and SHM-19 ^1H-^{13}C connectivities were established through an HMBC experiment (Table 4.8). Assignments around C-18 and C-19 methyl groups followed exactly the same arguments as for SHM-5 (**127**). For 20-H_3 and 17-H_3 ^3J correlations revealed that C-9 was again an olefinic carbon but in this case the ^2J coupling from 17-H_3 revealed that C-8 was an oxygen-bearing sp^3 carbon. This suggested that SHM-4 has a partial structure **137** (Fig. 4.4).

The isolated olefinic proton had to be placed at C-11 as it showed ^3J interactions with C-8 and C-10, while a ^2J coupling linked it to a singlet resonating at δ_C 107.1. This carbon must be assigned to C-12, which was confirmed by ^3J interactions with the second olefinic proton (14-H) and the vinylic methyl (16-H_3). The only other interaction of significance was a ^2J coupling linking 14-H

128
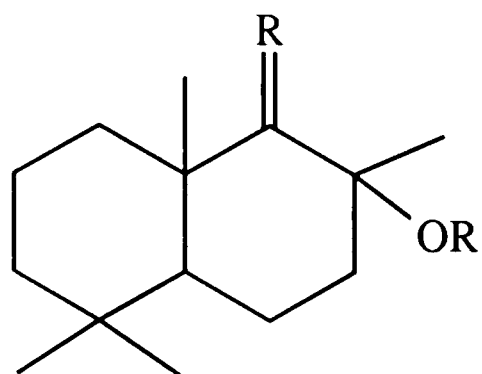
137
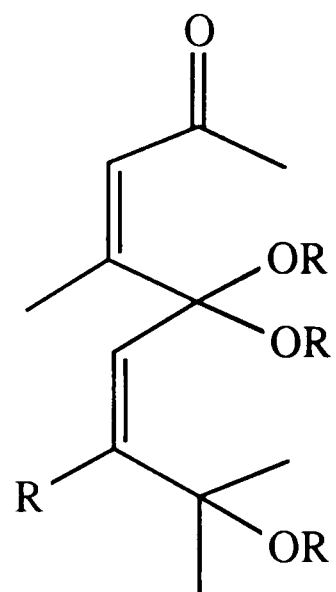
138

Fig. 4.4. Partial structures of SHM-4
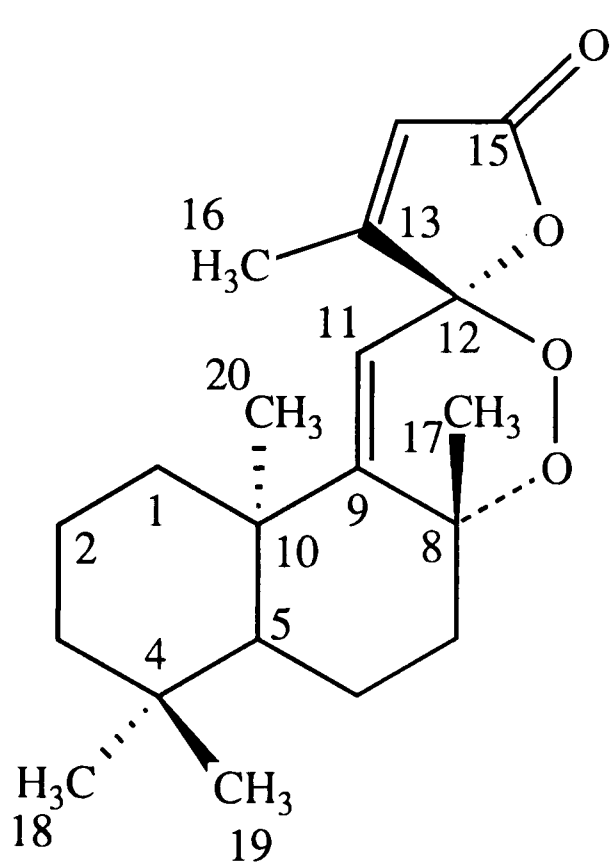
SHM-4 139
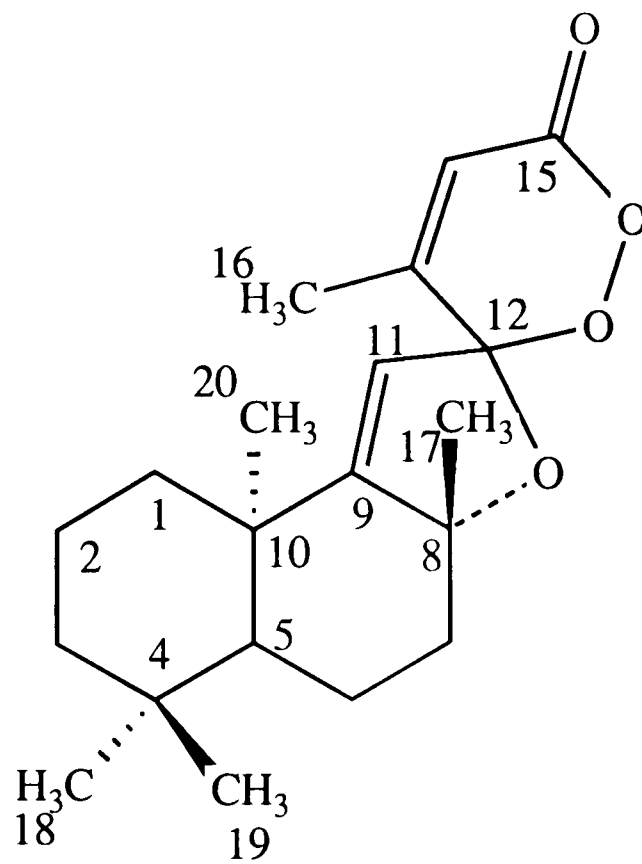
140

Fig. 4.5 Structure of SHM-4

to a carbonyl (C-15), which must form part of a lactone sytem (ν_{max} 1770 cm^{-1}).

In this diterpene only three carbons exist to which oxygen is bonded. C-8, C-12 and C-15. The strongly deshielded nature of C-12 (δ 107.1) suggests it to be bonded to two oxygen atoms (partial structure **138** Fig. 4.4). Given that the compound contains four oxygens this requires that a peroxide be present. In theory this peroxide could be placed between C-8 and C-12 (structure **139**, Fig. 4.5) or between C-12 and C-15 (structure **140**, Fig. 4.5). None of the NMR experiments performed allowed for differentiation between these possibilities. The identity of the new compound as **139** (Fig. 4.5) was finally confirmed by means of X-ray diffraction studies (see Appendix). This revealed that the A-ring is in a normal chair conformation but ring B is severely distorted due, primarily, to the 9(11) double bond (Fig 4.6). The peroxide ring is almost planar between C(9)-C(11)-C(12)-O(12), while O(8) is displaced below the plane of the ring. The absolute stereochemistry of SHM-4 has not been unambiguously assigned but it seems probable that, like SHM-5, it is based on the *ent*-labdane skeleton.

Figure 4.6: **X-ray molecular structure of SHM-4**
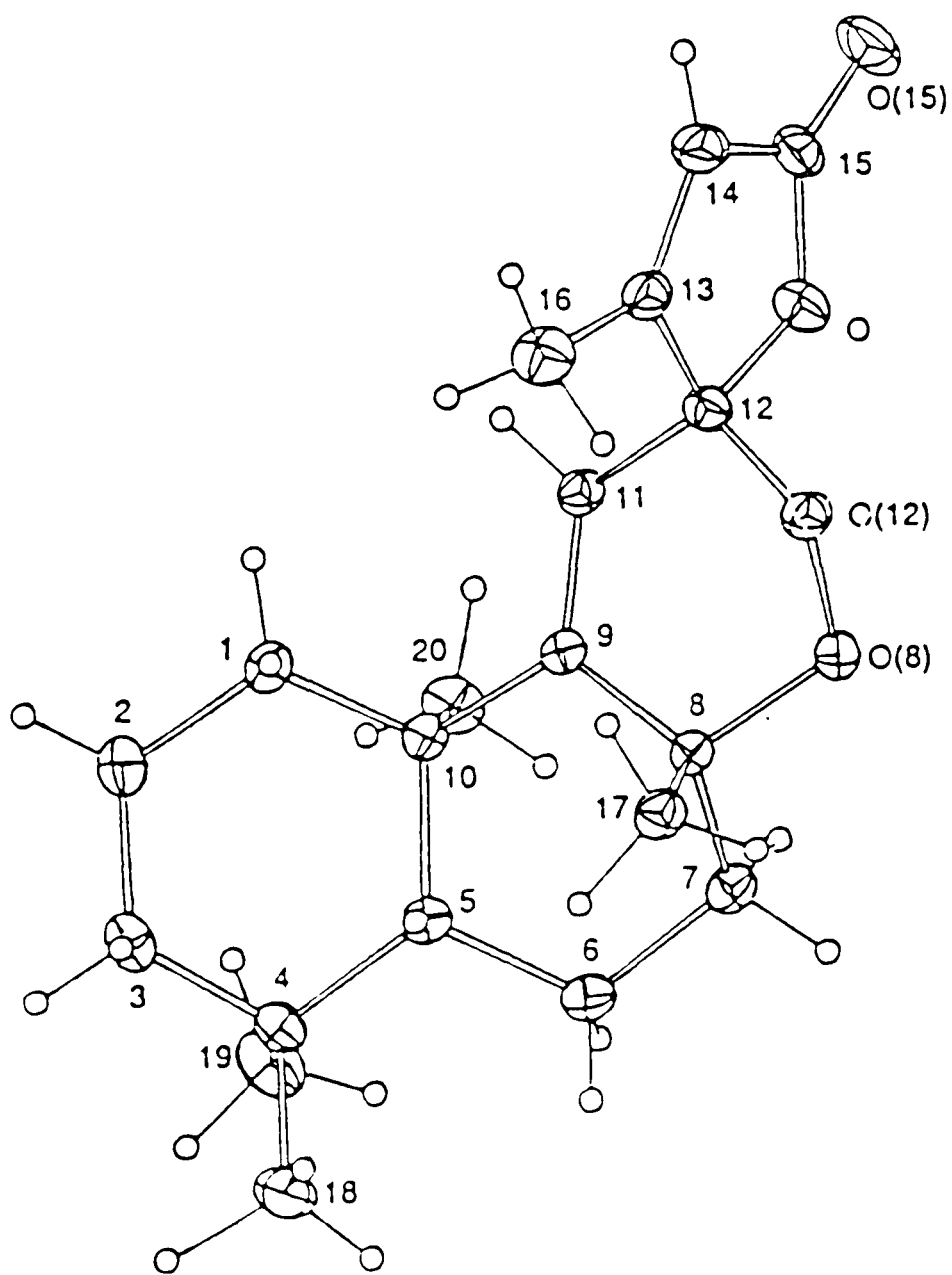
141
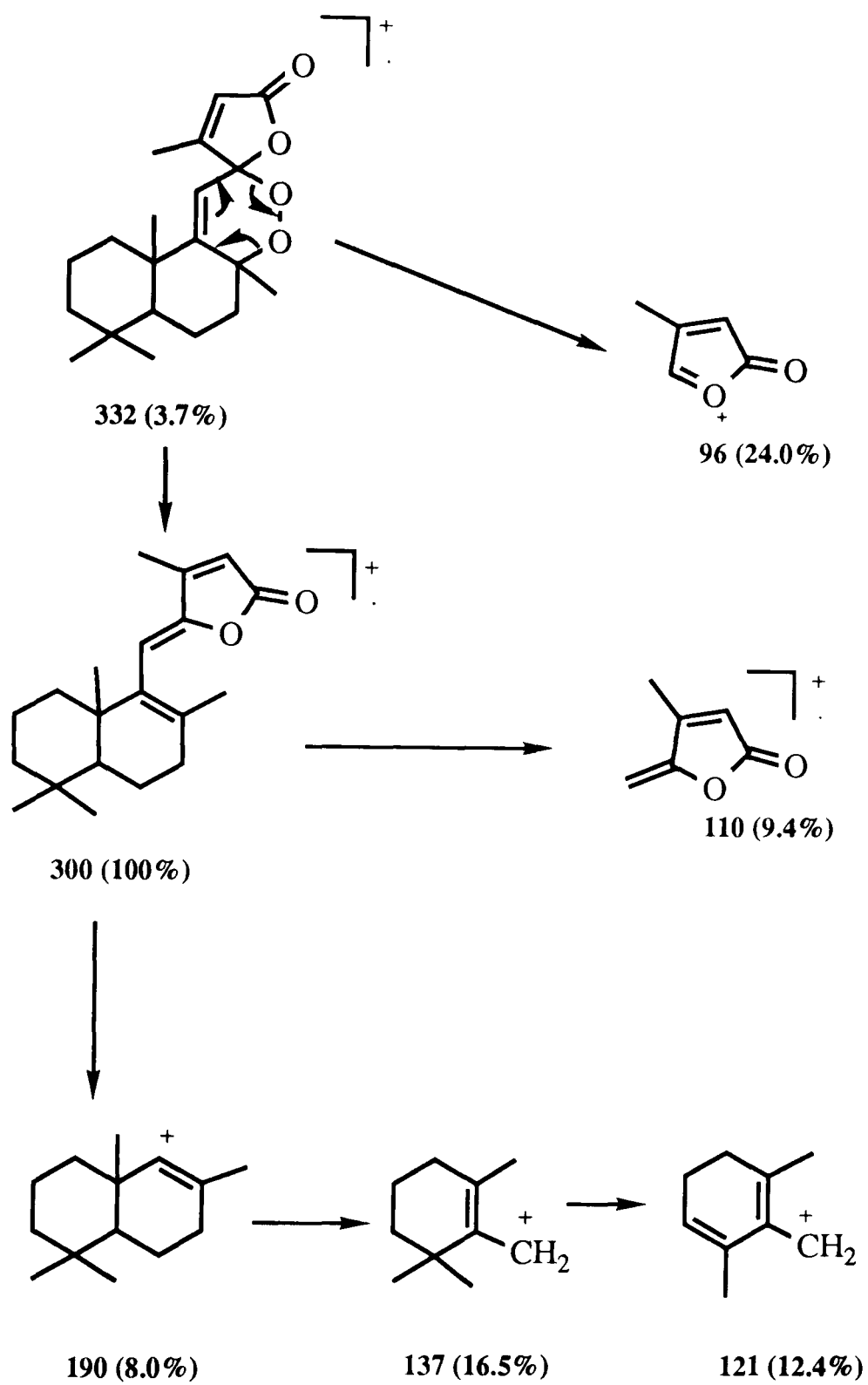
Scheme 4.6. Possible mass fragmentation pattern of SHM-4

132

C	δ C	C mult.[b]	H[c]	δ H	H pattern[d]	J (Hz)
1	40.3	t	1a	1.85	m	
			1b	1.26	ddd	
2	19.0	t	2	1.50-1.60	m	
3	41.8	t	3a	1.50	m	
			3b	1.22	ddd	
4	33.5	s				
5	43.6	d	5	1.57	m	
6	16.5	t	6	1.50-1.60	m	
7	26.3 7	t	7	1.65	m	
8	78.1	s				
9	163.1	s				
10	38.4	s				
11	111.2	d	11	5.23	s	
12	107.1	s				
13	162.4	s				
14	121.0	d	14	5.98	q	2.0
15	169.5	s				
16	13.0	q	16	2.01	d	2.0
17	25.3	q	17	1.70	s	
18	32.9	q	18	0.91	s	
19	21.2	q	19	0.94	s	
20	25.6	q	20	1.23	s	

Table 4.7: ^{1}H and ^{13}C NMR assignments for SHM-4 (139)[a]

[a] ^{1}H and ^{13}C NMR spectra were taken at 300 and 75 MHz NMR respectively in $CDCl_3$.

[b] ^{13}C NMR multiplicities were obtained from the J-Mod. [13]C data and HMQC studies and designated by the symbols: s=singlet, d=doublet, t=triplet and q=quartet.

[c] a and b denote magnetically unequivalent geminal protons where a appeared downfield to b.

[d] Patterns are designated by the symbols: s=singlet, d=doublet, dd=double doublets, ddd=doublet of double doublets, q=quartets and m=multiplet.

^{1}H	^{13}C	
	^3J	^2J
18-H$_3$	21.2, 41.8, 43.6	33.5
19-H$_3$	32.9, 41.8, 43.6	33.5
20-H$_3$	40.3, 43.6, 163.1	38.4
17-H$_3$	26.3, 163.1	78.1
11-H$_2$	38.4, 78.1	107.1
16-H$_2$	107.1, 121.0	162.4
14-H$_2$	107.1	169.5

Table 4.8: **HMBC correlations for SHM-4 (139)**

4.2.2 Photooxygenation of SHM-5

It is possible to envisage the formation of SHM-4 from SHM-5 and to speculate that SHM-4 is an artifact. While not ruling out this possibility exposure of SHM-5 at room temperture for months and even bubbling of oxygen through a solution of it failed to lead to the production of detectable amount of SHM-4. SHM-4 could also be detected ten minutes after commencing maceration of the powdered leaves of *P. oligotricha* in the dark, suggesting that it is a genuine natural product.

There is now an increasing evidence showing that the first intermediate in the biosynthesis of various aliphatic hydroxyls and ethers is a peroxide (Torssell,

1983). One can then speculate on the role of compounds like SHM-4 in the biosynthesis of levantenolide type of diterpenes (Fig. 4.7) which have an oxygen bridge between C-8 and C-12. It has also been suggested that oxygen activated to the singlet state is responsible for the synthesis of peroxides in living cells (Markel and Kearns, 1972). Patai (1983) showed that the reaction of this singlet oxygen in living tissue and *in vitro* follows the ene reaction with olefins and add in a Diels-Alder-type reaction to 1,3 dienes (Scheme 4.7). One of the simplest experimental methods to investigate such a reaction is photooxygenating dienes by visible light with a dye as a sensitizer (Frimer *et al.*, 1977).

In order to examine the biosynthetic relationship between SHM-4 and SHM-5, the latter was photooxygenated using eosin as a sensitizer. This gave a product SHM-20 (**149**) (Scheme 4.8) in a yield of 1.8%. SHM-20 (**156**) was identical in all respect to SHM-4 except the coupling patterns of signals in the ^{1}H NMR spectrum suggesting that it was epimeric at either C-8 and/or C-13. It is still not clear how the 13/16 double bond in SHM-5 (**127**) rearranges to give the 13(14) double bond in SHM-20 (**149**) but the study clearly showed that SHM-5 could be the precursor in the biosynthesis of SHM-4. Such kind of reaction may also play a role in the synthesis of levantenolide diterpenes reported by Aasen *et al.* (1975), Gonzalez *et al.* (1976) and Kato *et al.* (1971) (Fig. 4.7).

4.2.2.1 Bioevaluation of SHM-4

The main feature of a peroxide bond is that it is weak with a homopolar dissociation energy of only 51 Kcal mole^{-1} (Weeks and Rabani, 1966). As a result

135
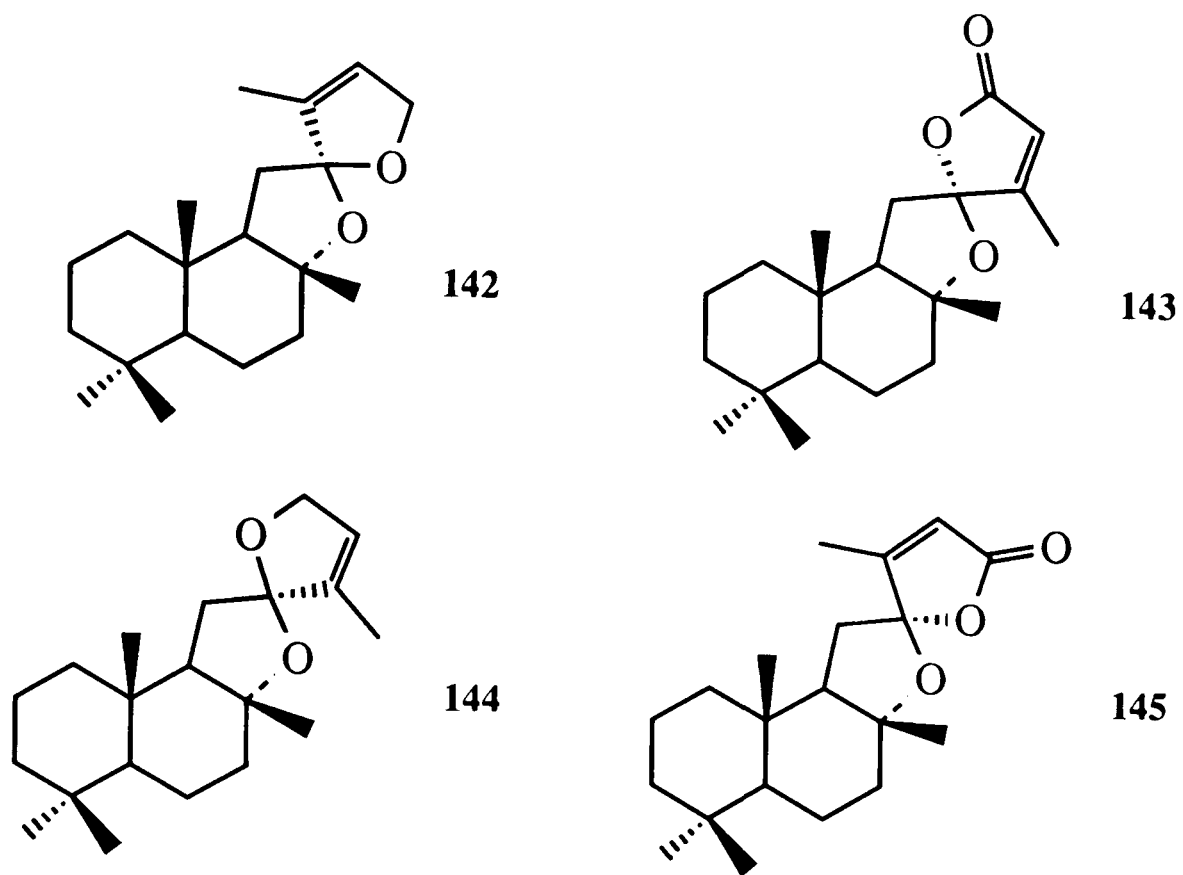
Fig. 4.7 Levantenolide diterpenes of Tobacco
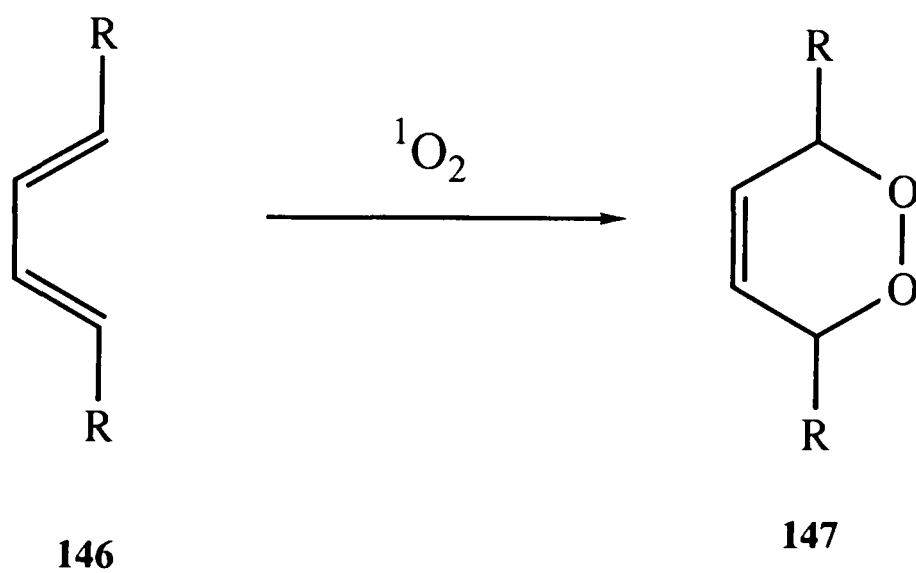
Scheme 4.7. Singlet oxygen ($^1O_2$) Diels-Alder reaction

SHM-5   **127**

148

SHM-20   **149**
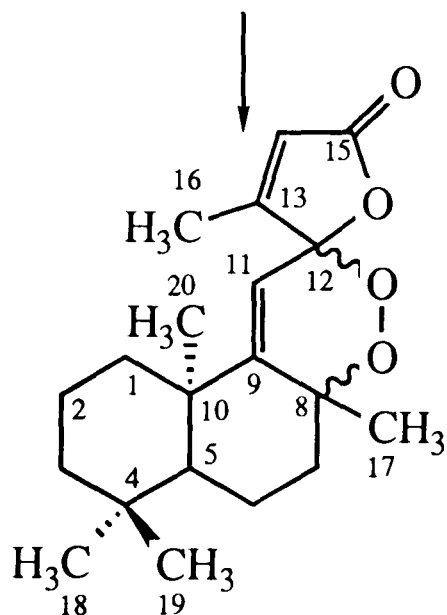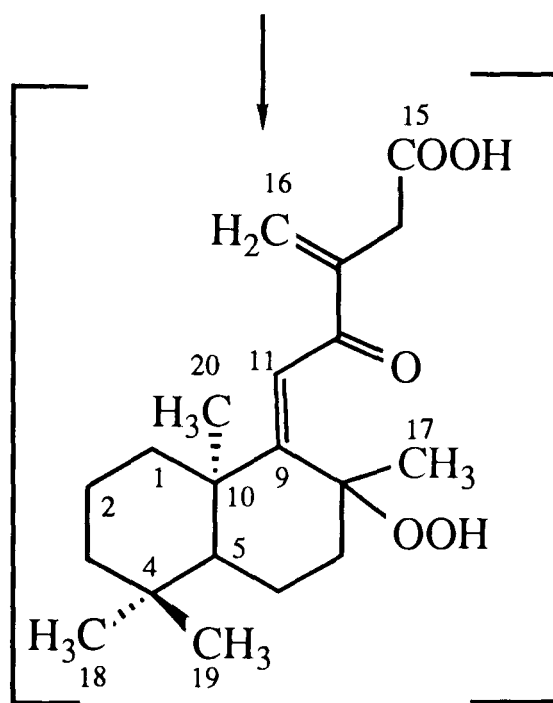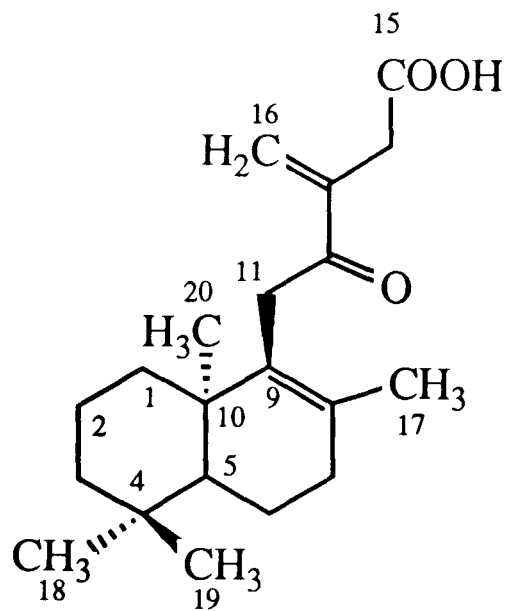
Scheme 4.8. Photooxygenation of SHM-5

of this, it can be cleaved by addition of an electron and the very reactive hydroxyl can be formed. It is also a strong oxidant with weak acidic properties and hence compounds with this structural group are often reactive and biologically active.

To date a number of natural peroxides with biological activities are known (Fig. 4.8). Askaridol (150) was the first ever natural peroxide known in this regard (Szmant and Halpern, 1949). Simple compounds like 151-153 are known for their antimicrobial activity (Higgs and Faulkner, 1978; Stierle 1979) and the prostaglandin PGH_2 (154) has been shown to have inflammatory activity 100-450 times greater than similar compounds without the peroxide moiety (Hamber and Samuelsson, 1973). Recently a number of antimalarial endoperoxides have been isolated. However, by far the most interesing peroxide is artemisinine (155). It has been shown that artemisinine is the most active antimalarial agent found to date (Liang, 1983). With such evidence on the biological activity of peroxides it seemed worthwhile to screen SHM-4 for various biological activities.

Despite the structural similarity of SHM-4 with artemisinine, its antimalarial activity was not encouraging. The IC_{50} value[1] against *Plasmodium falciparum* (K-1) *in vitro* was 1.66 μg ml^{-1} while that of chloroquine disulphate and artemisinine were 0.2 and 0.002 μg ml^{-1}. SHM-4 did not also have any anti-inflammatory activity when tested using the acute inflammatory model. Up to 200 mg kg^{-1} of the compound could not reduce the carageenin induced oedema of the rat paw. Although the structure of SHM-4 has an α, β-unsaturated moiety,

---

[1]Tested by Prof. J.D. Phillipson, Dept. of Pharmacognosy, School of Pharmacy, University of London

138
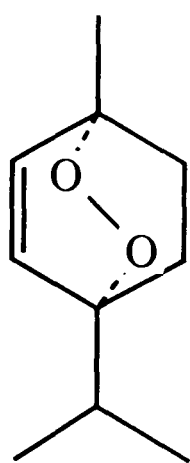
150
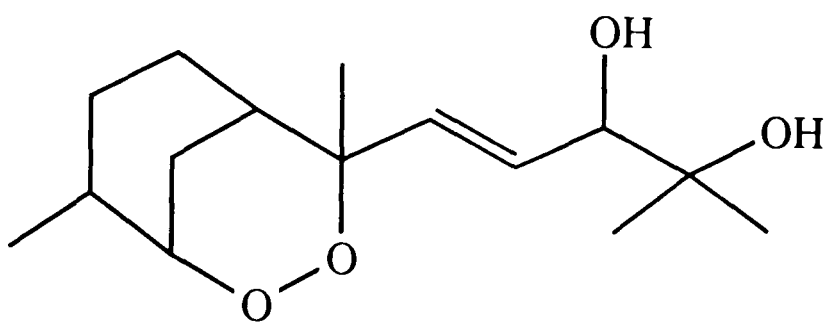
151
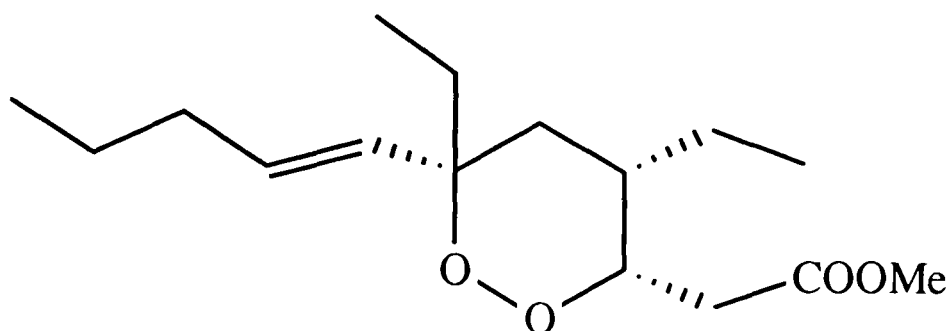
152
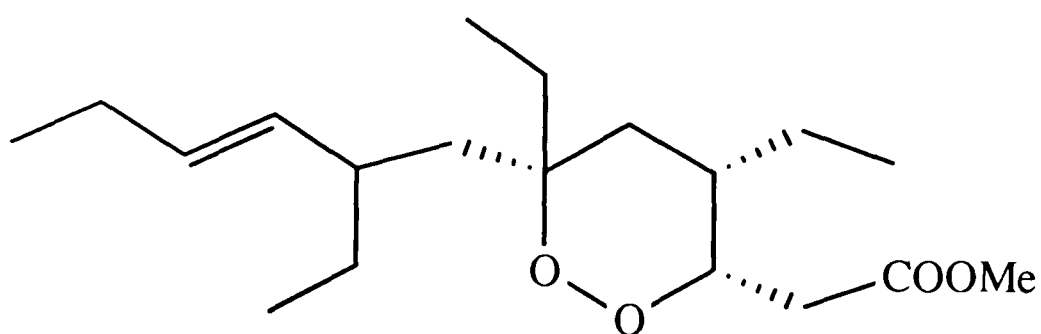
153
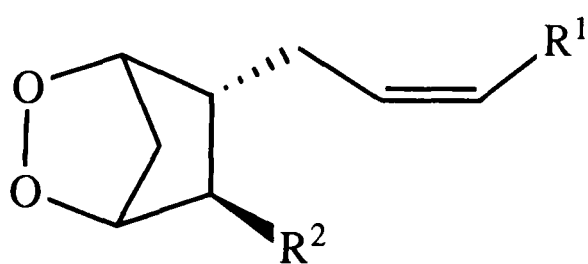
154
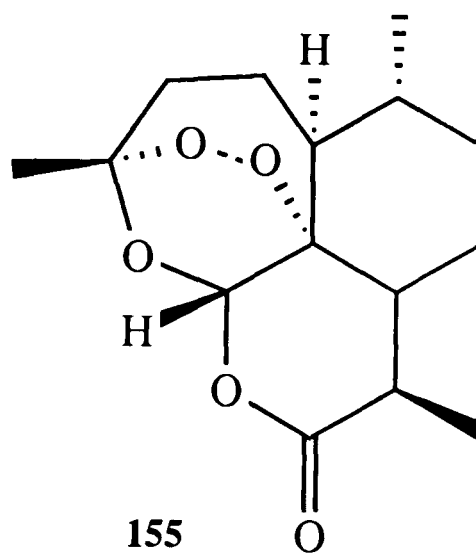
155

Fig. 4.8. Some bioactive natural endoperoxides

like the active antibacterial agents described previously, and also possesses the peroxy bridge, it did not show any antimicrobial and cytotoxic (KB cells) activity. Despite the structural similarity of this compound with levantenolide diterpenes (Fig 4.8) which have been shown to inhibit seed germination, SHM-4 failed (up to 5 mg ml^{-1}) to do so when tested on cress seeds. No insecticidal (and antifeedant) and antitripanasomal[2] activity was also observed for this compound.

The surprisingly inert nature of SHM-4 could be explained by its extreme structural stability. Unlike most peroxides, SHM-4 was stable at room temperature and even under basic solvents like pyridine and methanol, failed to reduce to a diol with thiourea, failed to be converted to a diepoxide by thermolysis and was resistant to further oxidation by singlet oxygen. As a result of this structural stability, SHM-4 does not seems to have pharmacological activity.

4.2.3   Flavonoids of *P. oligotricha*

Column chromatography of the ethyl acetate VLC fraction (see Scheme 4.1), which was devoid of antimicrobial activity afforded two flavonoids.

4.2.3.1   Identification of SHM-15C as 3,5,5'-trihydroxy-6,7,3'-4'-tetra-methoxyflavone (158)

SHM-15C was obtained in a yield of 0.005%. The high resolution EIMS established a flavonoid with four methoxyl and three hydroxyl groups: [M]$^+$ at m/z 390 (100%) corresponding to $C_{19}H_{18}O_9$. The ^1H NMR spectrum (Fig. 4.9)

---

[2]Experiment was carried out in the Veterinary School, Glasgow University

Figure 4.9: ^{1}H NMR (250 MHz, pyridine-d_5^*) of SHM-15C
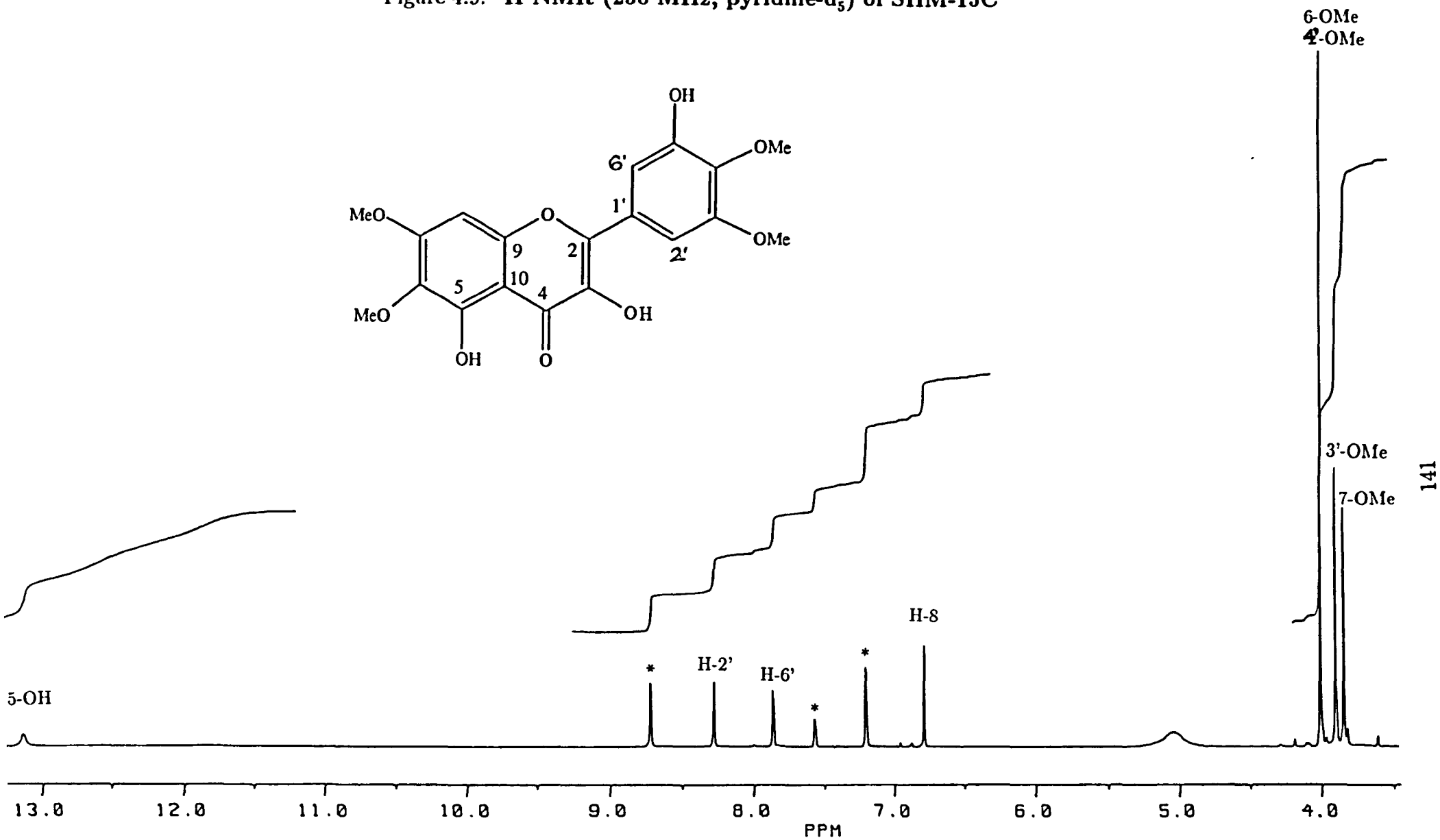
of the aromatic region showed two *meta*-coupled proton signals at δ 7.82 and 8.21 (2.0 Hz), typical for the B ring carrying three oxygen functions and assymetrically substituted (Harborne *et al.*, 1975). The ^1H NMR spectrum (Fig. 4.9) also showed another aromatic proton, four methoxyl resonances and a deshielded H-bonded hydroxyl resonance at δ 13.12, typical of the 5-OH of a flavonoid.

The data suggested that the compound was a partially methylated flavonol carrying oxygenation at C-5, C-7, C-3', C-4', C-5' and two other positions (from C-3, C-6, C-8). An extensive NMR study of the peracetate derivative aided assignment of the methoxyl groups on the A and B rings. The ^{13}C NMR spectrum of this peracetate (Table 4.9) revealed two methoxyl carbons resonating at *ca.* 56 ppm and two at *ca.* 61 ppm. The former methoxyl must have at least one *ortho* position unsubstituted while the latter must have them both substituted (Panichpol and Waterman, 1978). A NOESY study further revealed enhancement between one methoxyl and a *meta*-coupled (B ring) proton and between a second methoxyl and the aromatic singlet. Therefore one methoxyl must be placed at C-7 (adjacent to an isolated H-6 or H-8 proton) and the other at C-3' adjacent to the *meta*-coupled H-2' proton. Therefore C-3 must be oxygenated and C-5 and C-5' must carry hydroxyls, in the latter case this being established by the absence of any enhancement of H-6' in the NOESY spectrum. The remaining two methoxyls must therefore be at C-3, C-6/C-8 or C-4'.

Placement of one methoxyl at C-4' followed from the EIMS (Scheme 4.9) which revealed a fragment at *m/z* 181, $[B_2]^+$ which requires two methoxyl groups in ring-B. The 8- (**158**) and 6-methoxyl (**160**) positions could also be distingushed
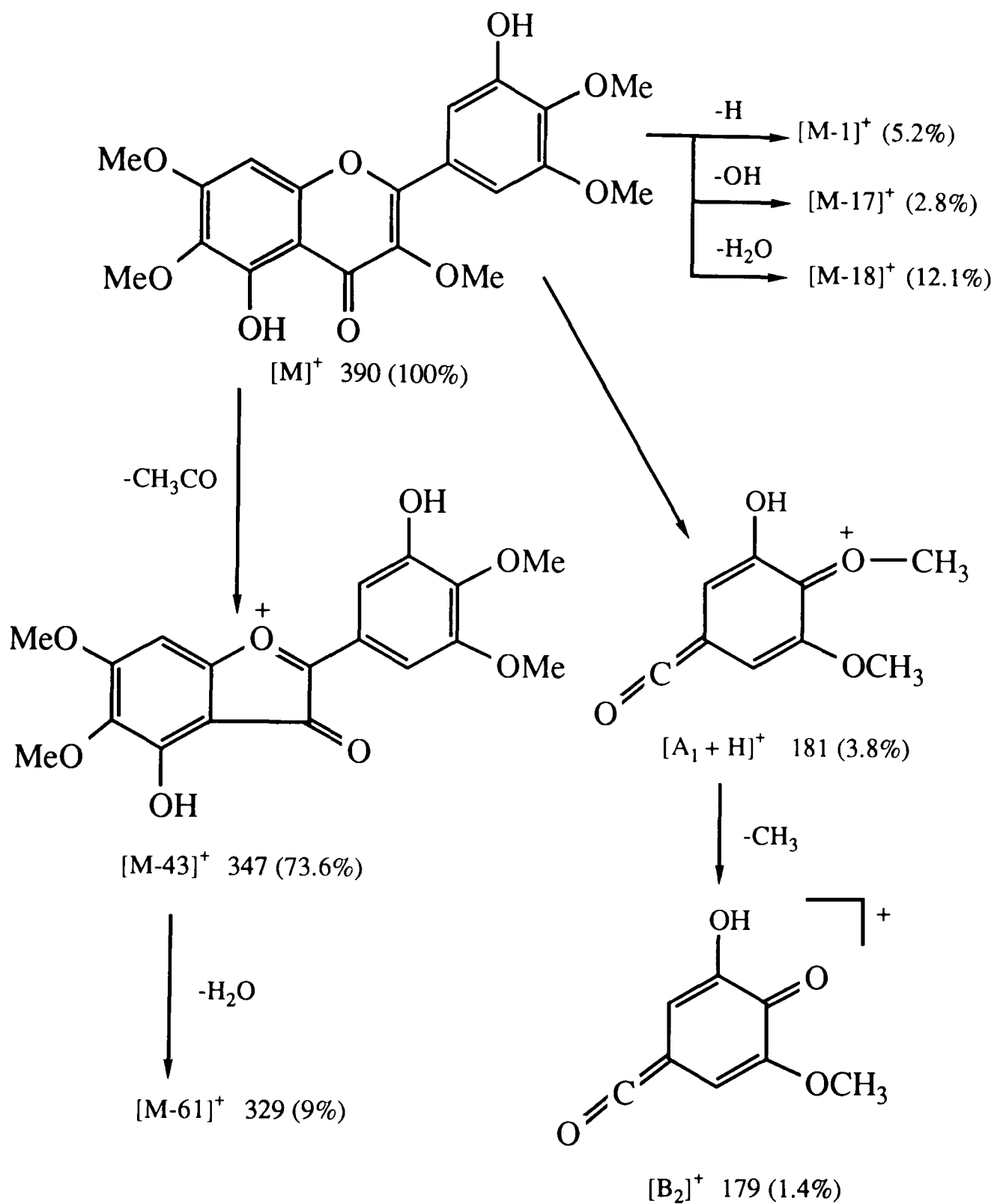
Scheme 4.9. Possible mass fragmentation pattern of SHM-15C

143

from the EIMS data. One of the distinctive feature of 8-methoxyl flavonols from that of 6-methoxyl flavonoids is the appearance of [M-15]$^+$ as a base peak (Roitman and James, 1985). Alternatively, the occurence of the molecular ion as base peak and an [M-18]$^+$ fragment at greater than 10% are characteristic for a 6- rather than 8-methoxyl substituent (Roitman and James, 1985 and Goudard *et al.*, 1978). This latter situation was observed in the EIMS of SHM-15C (Scheme 4.9). The free 3-hydroxyl position was also evident as the compound appeared as a dull yellow fluorescent spot on paper in UV light with and without ammonia, which indicates the presence of 3-and 5-hydroxyl groups (Mabry *et al.*, 1970).

The assignment of the methoxyl to C-6 was finally established from a long range ^{1}H-^{13}C coupling study on the peracetate using the HMBC technique. The results of this are outlined in Table 4.10. The key features of this experiment were the ^2J and ^3J coupling of H-8 (δ 6.88) to the carbons at 158.1 and 139.8 ppm; these two carbons also show ^3J coupling to the protons of two of the methoxyl resonances (δ_H 3.99, δ_C 56.5 and δ_H 3.89, δ_C, 61.5 respectively). This can occur only if the methoxyls are placed at C-7 and C-6 and not at C-7 and C-3. The HMBC studies also supported the assignment of two methoxyl functions in the B ring as the two remaining methoxyl signals (δ_H 3.92 and 3.91) showed ^3J coupling to the two oxygen bearing carbons at δ 153.5 (C-3') and 143.5(C-143.5). On the basis of these data the flavonoid was characterized as 3,5,5'-trihydroxy-6,7,3',4'-tetramethoxyflavone (**158**, Fig. 4.10), which appears to be novel.
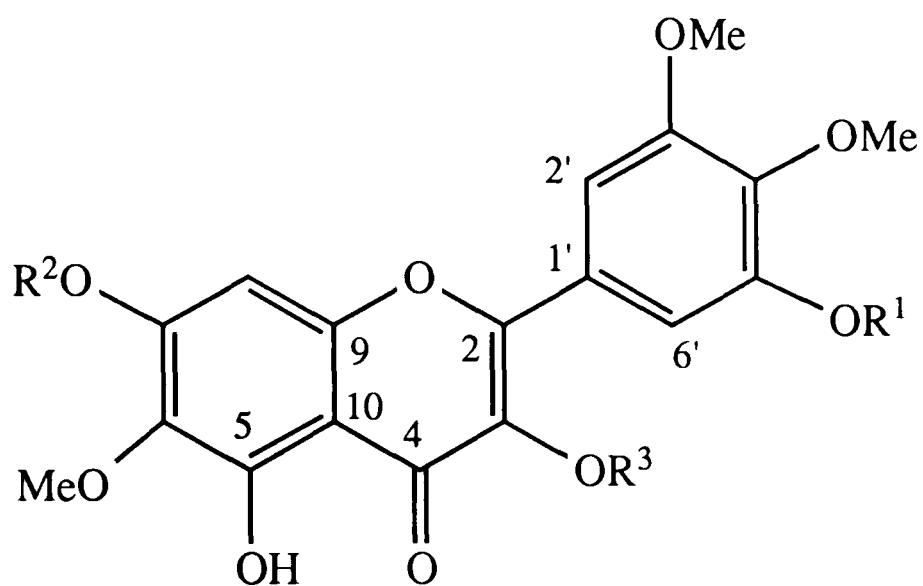
SHM-15B $R^1=R^2=R^3=H$ **156**
SHM-15B acetate $R^1=R^2=R^3=Ac$ **157**
SHM-15C $R^1=R^3=H$, $R^2=Me$ **158**
SHM-15C acetate $R^1=R^3=Ac$, $R^2=Me$ **159**

160
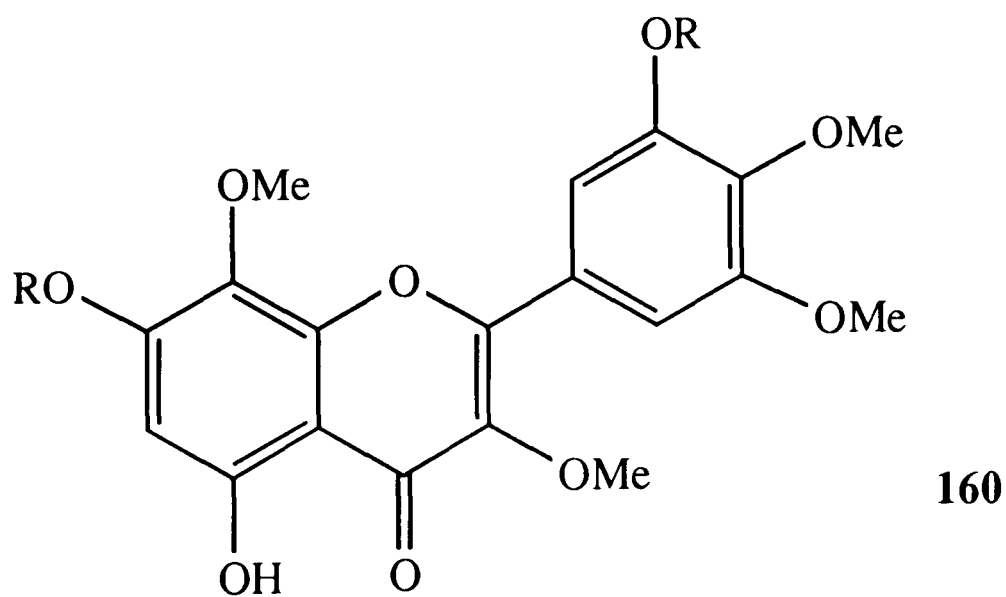
Fig. 4.10. Flavonoids of *P. oligotricha*

145

C	δ C	C mult.[b]	δ H	H pattern[c]	J (Hz)
2	153.7	s			
3	133.8	s			
4	170.1	s			
5	142.0	s			
6	139.8	s			
7	158.1	s			
8	98.1	d	6.88	s	
9	153.4	s			
10	111.2	s			
1'	124.6	s			
2'	110.0	d	7.24	d	2.0
3'	153.5	s			
4'	143.5	s			
5'	143.9	s			
6'	115.7	d	7.15	d	2.0
6-OMe	61.5	q	3.89	s	
7-OMe	56.7	q	3.99	s	
3'-OMe	56.2	q	3.92	s	
4'-OMe	60.9	q	3.91	s	
Ac	168.0, 168.8, 169.7	s			
	20.5, 20.7, 20.9	q	2.32, 2.36, 2.37	s	

Table 4.9: ^{1}H and ^{13}C NMR assignments for SHM-15C acetate (159)[a]

[a] ^{1}H and ^{13}C NMR spectra were recorded at 400 and 100 MHz NMR respectively in CDCl$_3$.

[b] ^{13}C NMR multiplicities were obtained from the J-Mod. ^{13}C data and designated by the symbols: s=singlet, d=doublet and q=quartet.

[c] Patterns are designated by the symbols: s=singlet and d=doublet.

^{1}H	^{13}C		
	^3J	^2J	^1J
H-8	139.8, 111.2	158.1, 153.4	98.1
H-2'	143.5		110.0
H-6'	143.5	153.5, 124.6	115.7
OMe-6	139.8		61.5
OMe-7	158.1		56.5
OMe-3'	153.5		56.2
OMe-4'	143.5		60.9

Table 4.10: **HMBC correlations for SHM-15C acetate (159)**

4.2.3.2 Identification of SHM-15B as 3,5,7,5'-tetrahydroxy-6,3',4'-tri-methoxyflavone (156)

The second flavonoid was a yellow powder which was obtained in a yield of 0.002%. The high resolution EIMS established the molecular formula $C_{18}H_{16}O_9$ in accord with a flavonoid containing four hydroxyl and three methoxyl groups. The ^{1}H NMR spectrum, in the aromatic region (Fig. 4.11), revealed a similar pattern to that of SHM-15C, indicating identical substitution. The ^{1}H NMR spectrum of this compound differed from that of SHM-15C by loss of one methoxyl resonances.

Acetylation of this compound led to the resonance for H-8/C-8 being

147

Figure 4.11: ^{1}H NMR (250 MHz, pyridine-d$_5^*$) of SHM-15B
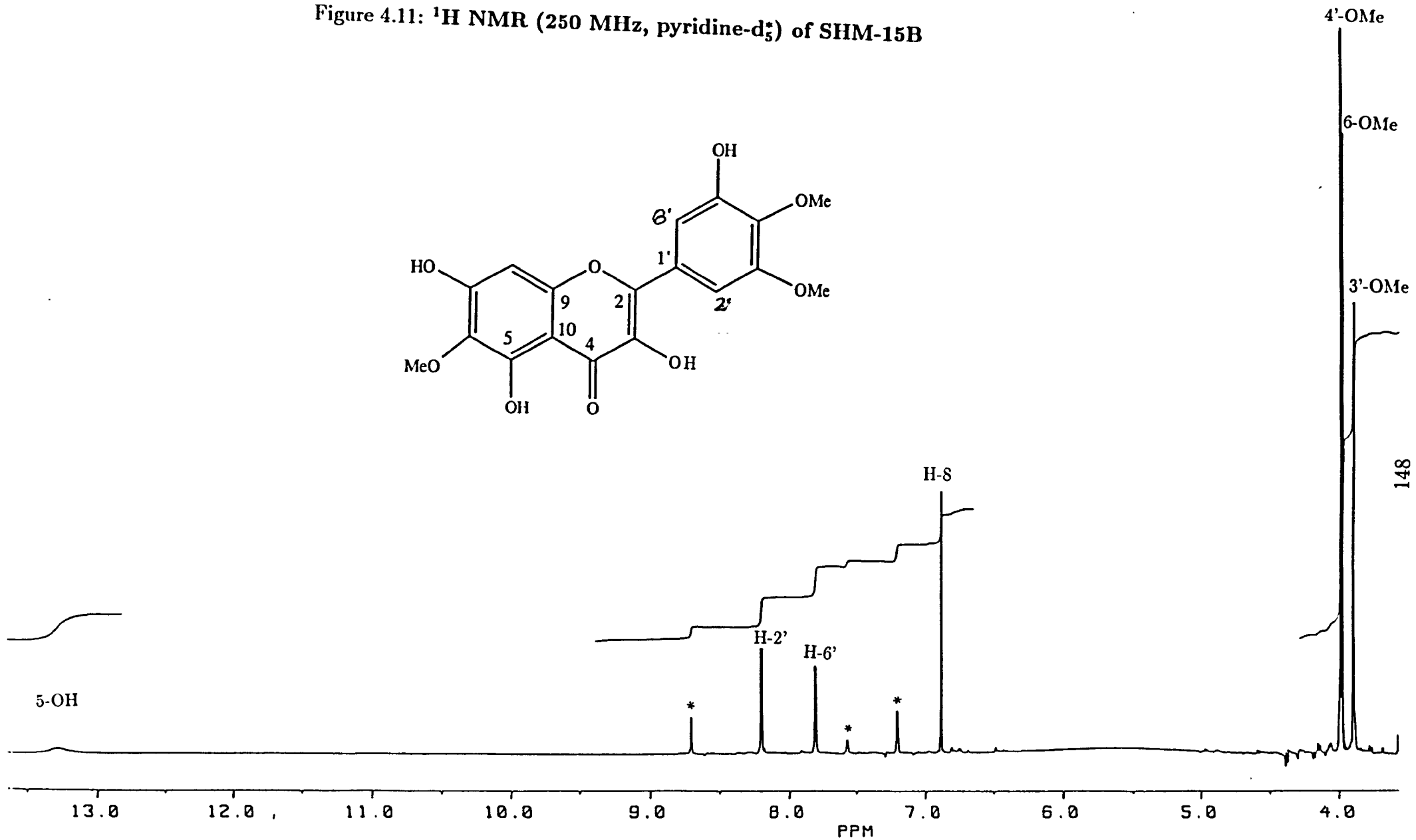
C	δ C	C mult.[b]	δ H	H pattern[c]	J (Hz)
2	153.4	s			
3	133.2	s			
4	170.1	s			
5	142.4	s			
6	142.4	s			
7	151.7	s			
8	110.2	d	7.25	s	
9	148.6	s			
10	115.7	s			
1'	124.2	s			
2'	109.8	d	7.24	d	2.0
3'	153.5	s			
4'	143.7	s			
5'	143.8	s			
6'	115.9	d	7.16	d	2.0
6-OMe	60.8	q	3.86	s	
3'-OMe	56.2	q	3.88	s	
4'-OMe	61.8	q	3.91	s	
AC	168.9, 168.7	s			
	167.8, 167.6	s			
	20.6, 20.6	q	2.32, 2.35	s	
	20.6, 20.9	q	2.37, 2.48	s	

Table 4.11: ¹H and ¹³C NMR assignments for SHM-15B acetate (157) [a]

[a] ¹H and ¹³C NMR spectra were recorded at 400 and 100 M Hz NMR respectively in CDCl₃.

[b] ¹³C NMR multiplicities were obtained from the J-Mod. ¹³C data and designated by the symbols: s=singlet, d=doublet and q=quartet.

[c] Patterns are designated by the symbols: s=singlet and d=doublet.

shifted downfield in the ^{1}H and ^{13}C NMR spectra (Table 4.11) and addition of sodium acetate in the methanolic solution of SHM-15B led to a small bathochromic shift in the band II region of the UV spectrum; all features suggesting a free hydroxyl at C-7. This was confirmed by the HMBC analysis of the peracetate (Table 4.12) which still showed ${}^3J$ coupling between H-8 and a carbon carrying a methoxyl (δ 142.4) but not the comparable ${}^2J$ coupling. In this study the two B ring methoxyl proton resonances showed ${}^3J$ coupling to two oxygen bearing carbons (C-3' and C-4') as in SHM-15C. This flavonoid must therefore be 3,5,7,5'-tetrahydroxy-6,3',4'-trimethoxyflavone (**156**, Fig 4.10), which also appears to be novel.

^{1}H	^{13}C		
	${}^3J$	${}^2J$	${}^1J$
H-8	142.4	148.6, 151.7	110.2
H-2'	143.7	124.2, 153.5	109.8
H-6'	109.8	124.2, 143.8	115.9
OMe-6	142.4		60.8
OMe-3'	153.5		56.2
OMe-4'	143.7		61.8

Table 4.12: **HMBC correlations for SHM-15B acetate (157)**

4.3 Experimental

4.3.1 Isolation of the antibacterial principles from *Premna oligotricha*

4.3.1.1 Extraction and isolation

Ground aerial parts (1 kg) were extracted with cold ethanol as described for *P. schimperi* (page 102). Concentration of the solvent yielded a gum (190 gm) which was tested for antibacterial activity by the disc diffusion method and found to be active. The gum was then subjected to vacuum liquid chromatography over silica gel (Merck 7749) eluting with solvents of increasing polarity (Scheme 4.1). The petrol:EtOAc (7:3) fraction which was proved to contain most of the activity was passed through a small Sephadex LH 20 column to remove chlorophyll and then fractionated by column chromatography over silica gel, eluting with petrol:EtOAc mixtures. The 8:2 fraction proved to contain the antibacterial activity and on repetitive prep. TLC (silica gel; solvent hexane:CHCl$_3$:EtOAc, 6:6:1) gave a minor constiuent SHM-19 (15 mg). Preparative TLC of the same fraction with a polar solvent (petrol:EtOAc, 2:3) afforded SHM-3 (100 mg) and SHM-5 (250 mg)

4.3.1.2 Properties of SHM-3 (16-hydroxy-15-oxoclero-3,13-diene-15,16-olide, 124)

Gum, $[\alpha]_D$ -21° (c. 0.1, CHCl$_3$). Found 318.2190, C$_{20}$H$_{30}$O$_3$, requires 318.2195; UV λ_{max}^{EtOH} nm = 230; IR ν_{max}^{KBr} cm^{-1} = 3350, 3190, 1750, 1640, 1450,

1380, 125, 1130, 950, 755; ^{1}H and ^{13}C NMR δ = see Table 4.1; EIMS m/z (rel. int.) = 318 (18.6), 301 (1.9), 191 (47.0), 190 (60.6), 189 (100), 177 (23.1), 175 (15.4), 135 (35.3), 133 (21.3), 127 (2.8), 124 (38.6), 123 (88.0), 121 (59.7), 119 (39.6).

4.3.1.3 Properties of SHM-5 (*ent*-12-oxolabda-8,13(16)-dien-15-oic acid, 127)

Gum, $[\alpha]_D$ -71° (c. 0.1, CHCl$_3$). Found 318.2186, C$_{20}$H$_{30}$O$_3$, requires 318.2195; UV λ_{max}^{EtOH} nm = 230; IR ν_{max}^{KBr} cm^{-1} = 3500, 1701, 1680; ^{1}H and ^{13}C NMR δ = see Table 4.2; EIMS m/z (rel. int.) = 318 (48.8), 303 (21.8), 285 (15.5), 205 (12.4), 191 (47.3), 190 (100), 189 (11.6), 181 (12.6), 180 (11.50, 176 (10.2), 175 (71.2), 163 (31.4), 149 (18.5), 135 (23.3), 121 (32.3), 119 (24.9), 113 (42.7), 109 (40.9), 107 (21.9), 105 (35.2), 95 (38.8), 93 (22.9), 91 (18.7) 85 (38.1).

4.3.1.4 Properties of SHM-19 (7-α-hydroxy-2-oxo-6,11-cyclofarnes-3(15)-ene, 128)

Yellow gum, $[\alpha]_D$ -17° (c. 0.1, CHCl$_3$). Found 238.1926, C$_{15}$H$_{26}$O$_2$, requires 238.1933; UV λ_{max}^{EtOH} nm = 230; IR ν_{max}^{KBr} cm^{-1} = 3490 br, 2910, 1670, 1460, 1360, 1100; ^{1}H and ^{13}C NMR δ = see Table 4.4; EIMS m/z (rel. int.) = 238 (77), 223 (10.5), 220 (21.6), 181 (19.0), 180 (12.0), 177 (21.6), 163 (13.0), 138 (11.3), 137 (24.7), 136 (52.8), 135 (22.4), 127 (15.5), 125 (43.6), 124 (12.7), 123 (31.9), 121 (27.2), 119 (14.4), 111 (84.4), 110 (14.0), 109 (88.8), 108 (16.3), 107 (31.9), 105 (13.1), 99 (13.1), 97 (2.6), 96 (63.6), 95 (61.7), 94 (23.5), 93 (31.8), 91 (21.3), 85 (61.0), 84 (28.2), 82 (26.0), 71 (91.8), 69 (100), 67 (39.1), 56 (14.2),

55 (75.2).

4.3.2 Analysis of the antibacterially inactive fraction of the ethanol extract

The 95:5 petrol:EtOAc eluent of the silica column (see Section 4.3.1.1) afforded 250 mg of SHM-4 as a white solid. The EtOAc VLC fraction (see Scheme 4.1), which was devoid of the antibacterial activity, was further subjected to column chromatography over silica gel eluting with CHCl$_3$:MeOH mixtures of increasing polarity. The fraction eluted with 80% CHCl$_3$ afforded SHM-15B (**163**, 20 mg) while the 40-60% CHCl$_3$ eluents gave impure **158** which was recrystallised from MeOH to give SHM-15C (50 mg).

4.3.2.1 Properties of SHM-4 (ent-8β,12α-epidioxy-12β-hydroxylabda-9(11),13-dien-15-oic acid γ-lactone (139)

Needles, mp 216°C; $[\alpha]_D$ -128° (c. 0.1, CHCl$_3$). Found 332.1985, C$_{20}$H$_{28}$O$_4$, requires 332.1988; UV λ_{max}^{EtOH} nm = 227; IR ν_{max}^{KBr} cm^{-1} = 3500, 2950, 1770, 1658, 1455, 1435, 1370, 1240, 1190, 950, 920; ^{1}H and ^{13}C NMR δ = see Table 4.7; EIMS m/z (rel. int.) = 332 (3.7), 301 (43.2), 300 (100), 189 (17.5), 179 (9.0), 177 (14.7), 137 (16.5), 123 (14.6), 121 (12.4), 119 (10.9), 112 (2.7), 111 (12.2), 110 (9.4), 109 (14.3), 96 (24.0), 85 (2.0).

153

4.3.3 Photooxygenation of SHM-5

The condition described by Bladon and Sleigh (1965) was adopted.
SHM-5 (500 mg) was dissolved in toluene (325 ml) and ethanol (275 ml). Eosin
(a filtered solution of 1 gm of the dye in 100 ml of ethanol) and pyridine (5 ml)
were added, and the solution was placed in a vertical Pyrex glass tube sealed at
the lower end. Oxygen was passed through, while the tube was illuminated by a
22 inch 20 W "warm white" fluorescent tube placed vertically and parallel to the
reaction tube. The reaction was allowed to proceed for 16 hours and the solution
taken to dryness to give a deep red gum which was dissolved as far as possible
in chloroform. This chloroform solution was filtered and subjected to prep. TLC
(6:6:2) to give 9 mg of SHM-20 (**149**).

4.3.3.1 Properties of SHM-20 (149)

^{1}H NMR (250 MHz, CDCl$_3$) δ = 0.90 (3H, s, 18-Me), 0.92 (3H, s, 19-
Me), 1.22 (3H, s, 20-Me), 1.68 (3H, s, 17-Me), 1.99 (3H, d, J=1.5 Hz), 5.24 (1H, s,
H-11) and 5.98 (1H, d, J=1.5 Hz, H-14); UV, IR, EIMS and TLC characteristics
were found to be identical with that described for SHM-4 (**139**).

4.3.3.2 Properties of SHM-15C (3,5,5'-trihydroxy-6,7,3',4'-tetramethoxy-
flavone, 158)

Yellow needles, 211°C. Found 390.0927, $C_{19}H_{18}O_9$, requires 390.0951:
UV λ_{max}^{MeOH} nm (log ε) = 260 (4.15), 356 (4.39), 422 (3 .61); (AlCl$_3$) 266, 416:
(NaOMe) 260, 410; (NaOAc) 260, 338 sh, 368, 416 sh; (NaOAc + H$_3$BO$_3$) 260,

356. IR ν_{max}, cm^{-1} = 3450, 3300, 2950, 1650, 1590, 1490, 1210. ^{1}H NMR (400 MHz, pyridine-d$_5$) δ = 3.82 (3H, s, OMe-7), 3.88 (3H, s, OMe-3'), 3.99 (6H, s, OMe-6, OMe-4'), 6.80 (1H, s, H-8), 7.85 (1H, d, J=2, H-6'), 8.26 (1H, d, J=2 Hz, H-2'), 13.12 (1H, br s, OH-5); ^{1}H and ^{13}C NMR of peracetate (159) δ = see Table 4.9.; EIMS m/z (rel.int.) = 390 (100) 347 (74), 329 (9), 181(3).

4.3.3.3 Properties of SHM-15B (3,5,7,5'-tetrahydroxy-6,3',4'-trimethoxy-flavone, 156)

Amorphous solid, 253°C. M$^+$ not seen in the EIMS but M$^+$ of peracetate found 544.1249 C$_{26}$H$_{24}$O$_{13}$ (4.3); UV λ_{max}^{MeOH}, nm (log ε) = 245 (4.22), 266 (4.25), 362 (4.35) ; (AlCl$_3$) 270, 362, 418; (NaOMe) 270, 398; (NaOAc) 272, 380; (NaOAc + H$_3$BO$_3$) 254, 166, 362. IR ν_{max}, cm^{-1} = 3380, 3310, 2950, 1655, 1630, 1600, 1550, 1490, 1400, 1210, 800. ^{1}H NMR (400 MHz, pyridine-d$_5$) δ = 3.88 (3H, s, OMe-3'), 3.95 (3H, s, OMe-6), 3.97 (3H, s, OMe-4), 6.89 (1H, s, H-8), 7.82 (1H, d, J=2, H-6'), 8.21 (1H, d, J=2, H-2'), 13.30 (1H, br s, OH-5); ^{1}H and ^{13}C NMR of peracetate (157) δ = see Table 4.11.

Chapter 5

PHYTOCHEMICAL AND ANTIMICROBIAL STUDIES ON *PREMNA RECINOSA*

5.1 Antimicrobial Evaluation of *Premna* recinosa

The crude ethanol extract of *Premna recinosa* was tested for its antimicrobial activity as described for *Premna schimperi* (Section 3.1). No antibacterial activity was observed when tested up to 500 μg per disc. A weak antifungal (*Penicillium notatum* and *Aspergillus niger*) activity was observed at concentrations higher than 1000 μg per disc. As described in Section 1.4.2.3, antibacterial activity of the leaves of *P. recinosa* was reported (Almagboul *et al.*, 1985). The concentration used by these authers (200 mg per well) however is very high and is

156

not considered active in our experimental protocol. For this reason. a systematic bioassay guided search of active principle(s) was not carried out for this plant.

5.2 Phytochemical Examination of *Premna recinosa*

Vacuum liquid chromatography followed by preparative TLC of the cold ethanol extract of *P. recinosa* resulted in the isolation of six flavonoids and three lignans.

5.2.1 Flavonoids of *P. recinosa*

5.2.1.1 Flavone

5.2.1.1.1 Identification of SHM-12 as 5,7,3',4'-tetrahydroxyflavone (38, Luteolin)

SHM-12 was the only flavone isolated from *P. recinosa*. It was obtained as yellow needles in a yield of 0.0012% and identified as luteolin (**38**, Fig. 5.1) from the spectral data (EIMS, IR, UV and NMR) as described for SHM-36-4 (page 74).

5.2.1.2 Flavonols

5.2.1.2.1 Identification of SHM-10 as 3,5,7,3',4'-pentahydroxyflavone (108, Quercetin)

SHM-10 was obtained as yellow needles in a yield of 0.0014%. It was

SHM-12 R=H   **38**
SHM-10 R=OH   **108**

SHM-8A   **161**

SHM-11   **162**
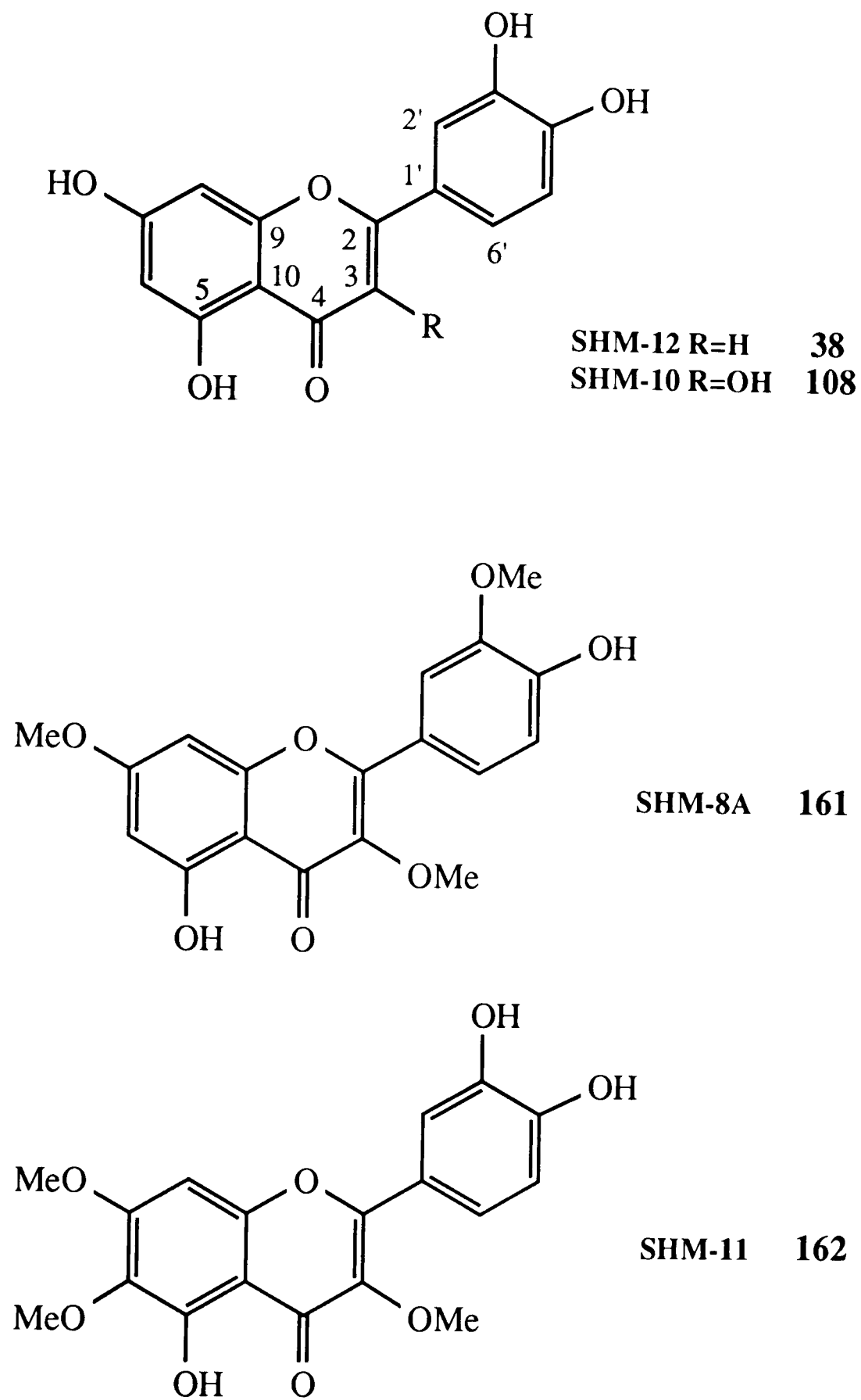
Fig. 5.1. Flavone and Flavonols of *P. recinosa*

158

identified as quercetin (**108**, Fig. 5.1) from the spectral data (EIMS, IR, UV and NMR) as described for SHM-35 (page 71).

5.2.1.2.2   Identification of SHM-8A as 5,4'-dihydroxy-3,7,3'-trimethoxy-flavone (161, Pachypodol)

SHM-8A was obtained as needles in a yield of 0.0032%. The high resolution EIMS exhibited a molecular ion M^+ at 344 (100%), ($C_{18}H_{16}O_7$) for a flavonoid containing three methoxy and two hydroxy groups. The ^1H NMR spectrum of this compound (Fig 5.2) showed two doublets at δ 7.80 (J=2.0 Hz) and 7.10 (J=8.3 Hz) and a doublet of doublets at δ 7.70 (J=8.3, 2.0 Hz); characteristic for the 3',4'-dioxygenated B ring of a flavonoid. The ^1H NMR spectrum further revealed two *meta*-coupled A ring protons of a flavonoid (δ 6.50 d, J=2.2; H-8 and δ 6.40 d, J=2.2 Hz; H-6) and three methoxyl resonances (δ 3.95, 3.84 and 3.82).

Assignment of one methoxyl group in the B ring was supported by the EIMS which showed $[A_1+H]^+$ and B_2 fragments (Scheme 5.1). The methoxyl group in the B ring has to be placed at C-3' as the free 4'-hydroxyl group was supported by the UV data (Table 5.1), in which addition of sodium methoxide to a methanolic solution of SHM-8A caused a bathochromic shift of 60 nm with an *increase in intensity*. A free 5-hydoxyl group was also evident in the structure of SHM-8A as the ^1H NMR spectrum (Fig 5.2) showed a hydrogen-bonded proton signal at δ 12.61. Given that the compound has three methoxyl groups and the C-4' and C-5 positions are not methoxylated, the remaining two methoxyl groups must be assigned at C-3 and C-7.

159

Figure 5.2: ^{1}H NMR (250 MHz, CDCl$_3$) spectrum of SHM-8A

[M-61]$^+$, 283 (5.1%)

[M-43]$^+$, 301 (62.8%)

- CH$_3$.CO

- H → [M-1]$^+$, 343 (76.9%)

- H$_2$O → [M-18]$^+$, 326 (9.9%)

- OMe → [M-31]$^+$, 313 (22%)

344 [M]$^+$, C$_{18}$H$_{16}$O$_7$

[B$_2$]$^+$, 151 (7.3%)

[A$_1$ + H]$^+$, 167 (9.5%)
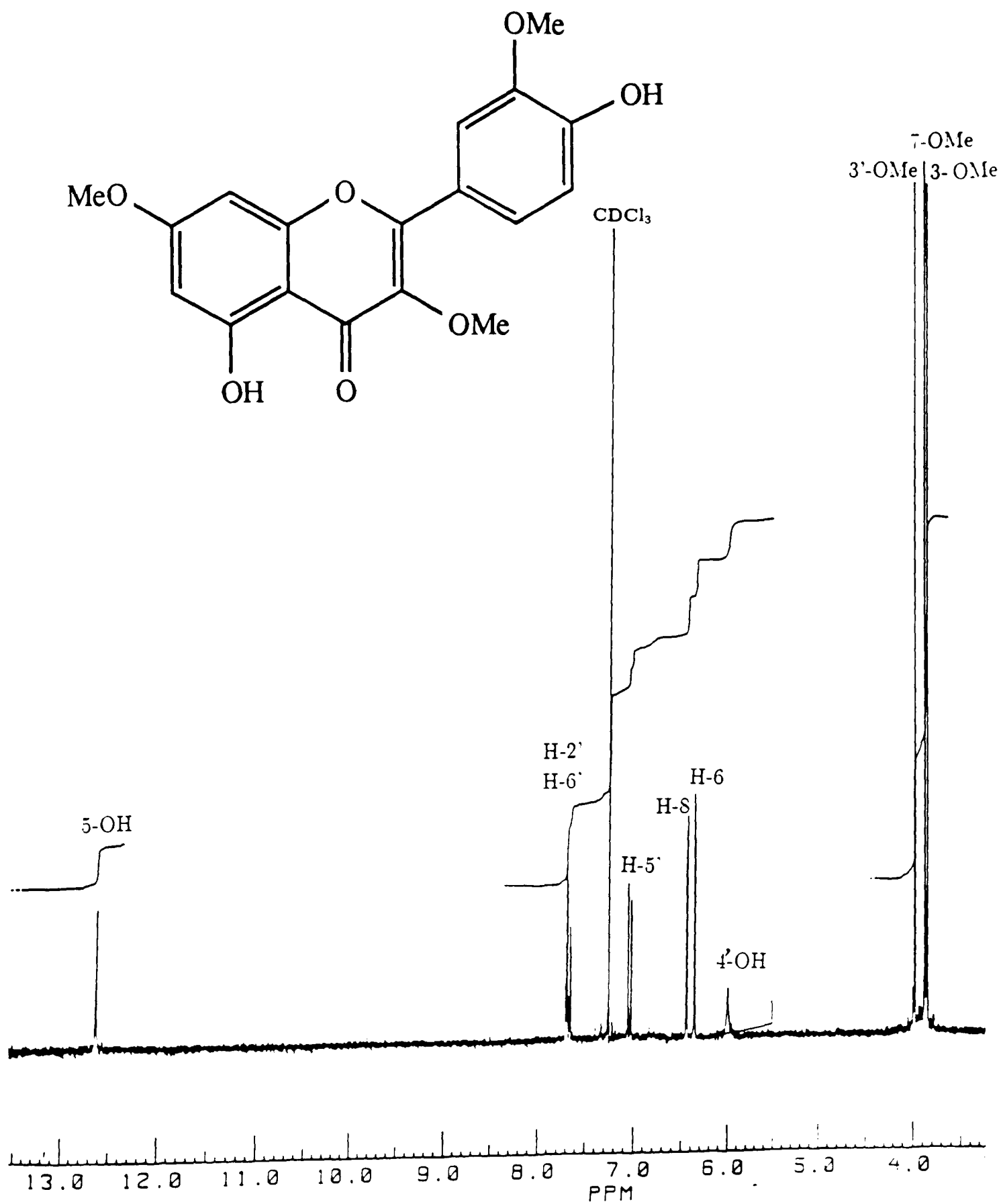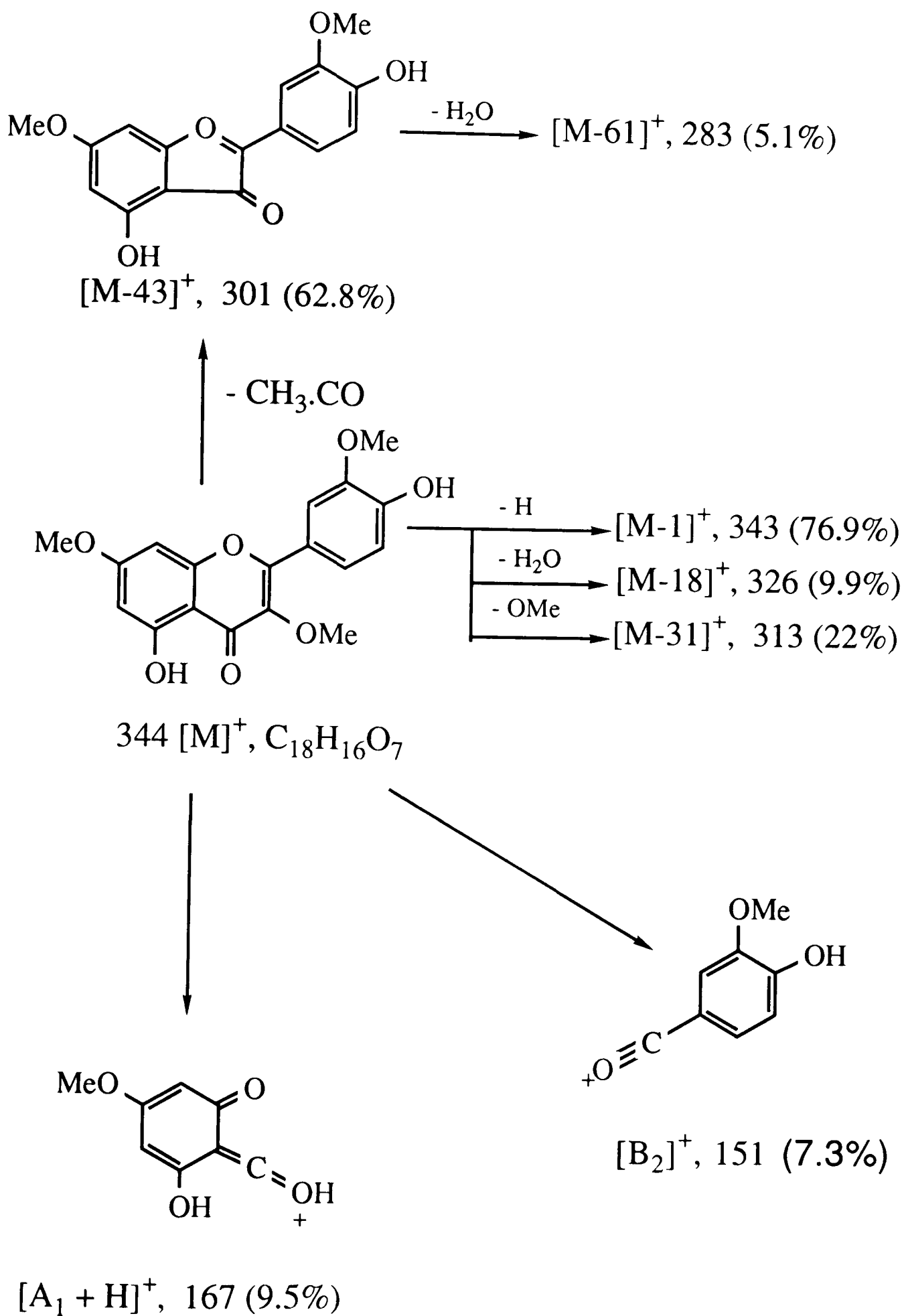
Scheme 5.1. Possible mass fragmentation pattern of SHM-8A

The assignments of these methoxyl proton resonances and their position were confirmed by NOESY NMR studies. In this study interaction between one methoxyl signal (δ 3.95) and the B ring proton signal at δ 7.80 (H-2') established the C-3' methoxyl position while interaction between another methoxyl signal (δ 3.84) and the A ring protons (H-6, H-8) support the C-7 methoxyl position. On the basis of these data, SHM-8A was characterised as the rare flavonol, 5,4'-dihydroxy-3,7,3'-trimethoxyflavone (161, pachypodol) (Ensemeyer and Langhammer, 1982).

5.2.1.2.3 Identification of SHM-11 as 5,3',4'-trihydroxy-3,6,7-trimethoxy-flavone (162, Chrysosplenol-D)

SHM-11 was obtained as orange needles in a yield of 0.0032%. The high resolution EIMS of this compound exhibited a molecular ion at m/z 360 (100%) ($C_{18}H_{16}O_8$) in accord with a flavonoid containing three hydroxyl and three methoxyl groups. The ^{1}H NMR spectrum (Table 5.2) showed a signal pattern typical of the 3',4'-dioxygenated flavonoid as described for SHM-8A. This spectrum further revealed one A ring proton H-6 or H-8 (δ 6.66) and three methoxyl resonances which were assigned on the basis of UV and HMBC studies.

In the UV spectrum of SHM-11 (Table 5.1), a bathochromic shift (14 nm) of band I region was caused by sodium acetate in the presence of boric acid. This was indicative of the 3',4'-*ortho* dihydroxyl functional groups (Mabry *et al.* 1970), a hypothesis supported by the EIMS data which showed the B_2 fragment at m/z 137 (25.8%). As the C-5 was carrying a free hydroxyl group (H-bonded signal in the ^{1}H NMR spectrum, δ 13.33), the three methoxyl groups must be

placed at C-3, C-7, and either C-6 or C-8. The C-8 position was eliminated by the EIMS data as described for SHM-15C (page 142).

Further evidence for unambiguous assignment of ^{1}H and ^{13}C chemical shift data (Table 5.2) came from an HMBC study (Table 5.3). The key features of this were the ^3J coupling of methoxyl proton resonances; δ_H 3.89 to δ_C 138.7, δ_H 3.99 to δ_C 132.8 and δ_H 3.87 to δ_C 159.3. This identifies the C-3, C-6 and C-7 methoxyl positions respectively. On the basis of these data, SHM-11 was identified as a rare flavonol **162** (chrysosplenol-D) (Wollenweber and Mann, 1983).

Reagent	SHM-8A	SHM-11
Methanol	272, 356	265 sh, 281
Sodium methoxy	272, 416	284, 410
Alumunium chloride	381, 292, 416 sh	284, 384, 428
AlCl$_3$+HCl	381, 392, 416 sh	281, 360
Sodium acetate	275, 392, 416	280, 360, 422
NaOAc+Boric acid	272, 356	274, 360

Table 5.1: **UV data of SHM-8A and SHM-11** (λ_{max} **(nm))**.

C	δ C	C mult.[b]	δ H	H pattern[c]	J (Hz)
2	156.9	s			
3	138.7	s			
4	179.7	s			
5	152.6	s			
6	132.8	s			
7	159.4	s			
8	91.3	d	6.66	s	
9	153.3	s			
10	106.9	s			
1'	122.1	s			
2'	116.8	d	7.82	d	2.2
3'	147.4	s			
4'	151.0	s			
5'	116.9	d	7.38	d	8.4
6'	121.7	d	7.82	dd	8.4, 2.2
3-OMe	59.9	q	3.89	s	
6-OMe	60.7	q	3.99	s	
7-OMe	56.5	q	3.87	s	
5-OH			13.33	br s	

Table 5.2: ^{1}H and ^{13}C NMR assignments for SHM-11 (162)[a]

[a] ^{1}H and ^{13}C NMR spectra were recorded at 400 and 100 MHz NMR respectively in CDCl$_3$

[b] ^{13}C NMR multiplicities were obtained from the J-mod. [13]C data and designated by the symbols: s=singlet, d=doublet and q=quartet.

[c] Patterns are designated by the symbols: s=singlet, d=doublet, dd=double doublet and br=broad.

164

H	¹³C		
	^1J	^2J	^3J
H-8	91.3	159.4, 152.6	132.8, 106.9
H-2'	116.8	147.4	156.9, 151.0, 121.7
H-5'	116.9	151.0	147.4,122.1
H-6'	121.7	116.9	156.9, 151.0
OMe-3			138.7
OMe-6			132.8
OMe-7			159.3

Table 5.3: HMBC correlations for SHM-11 (162)

5.2.1.3 5.2.1.3 Flavanone

5.2.1.3.1 Identification of SHM-8B as 5,7,4'-trihydroxyflavanone (106, Naringenin)

The white amorphous powder of SHM-8B was crystallised from methanol as needles in a yield of 0.0013%. The high resolution EIMS revealed a molecular ion at m/z 272 (100%) which analysed for $C_{15}H_{12}O_5$, identical to naringenin (106, Fig. 5.3). Identity as naringenin was based on the following data: A dioxy functional moiety was evidenced by the EIMS fragment m/z 120 (61.7%), B_3, (Scheme 5.2) and signals in the ¹H NMR spectrum (Table 5.4) at δ 6.80

SHM-8B 106

SHM-9 163

164
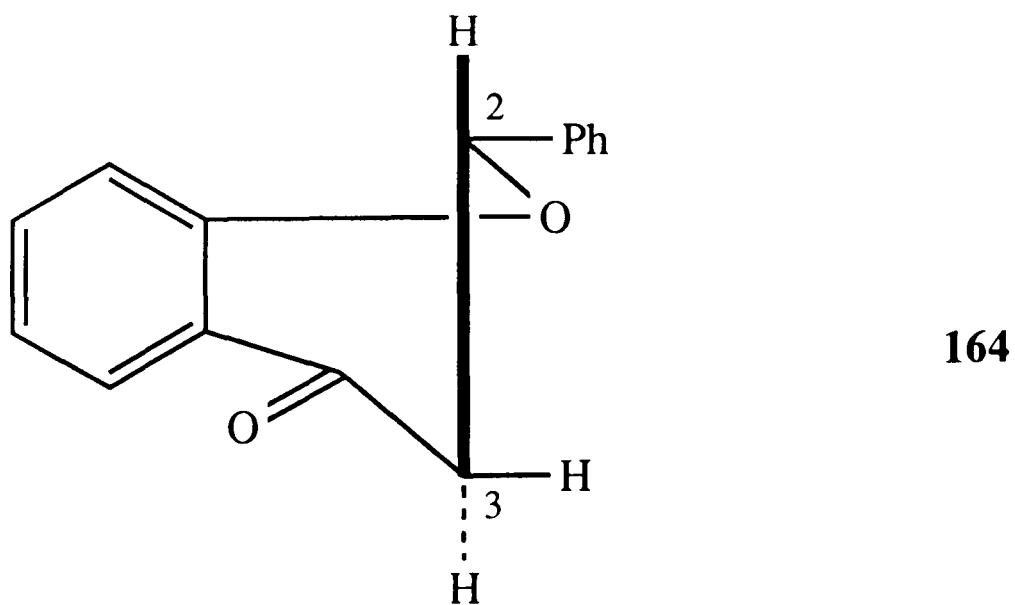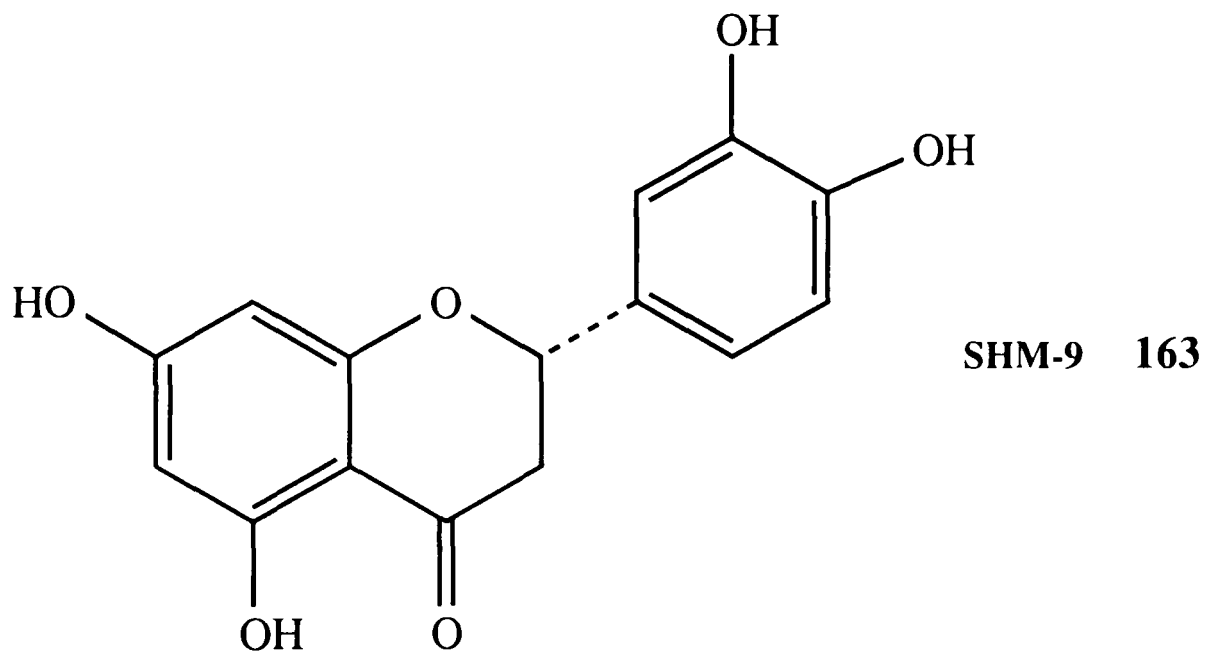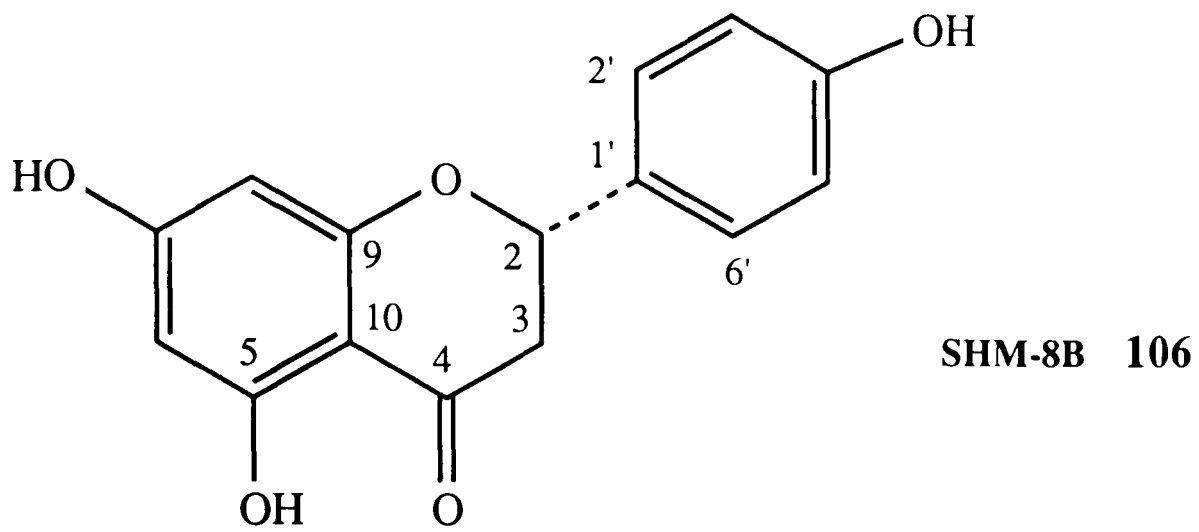
Fig. 5.3. Flavanones of *P. recinosa*

166
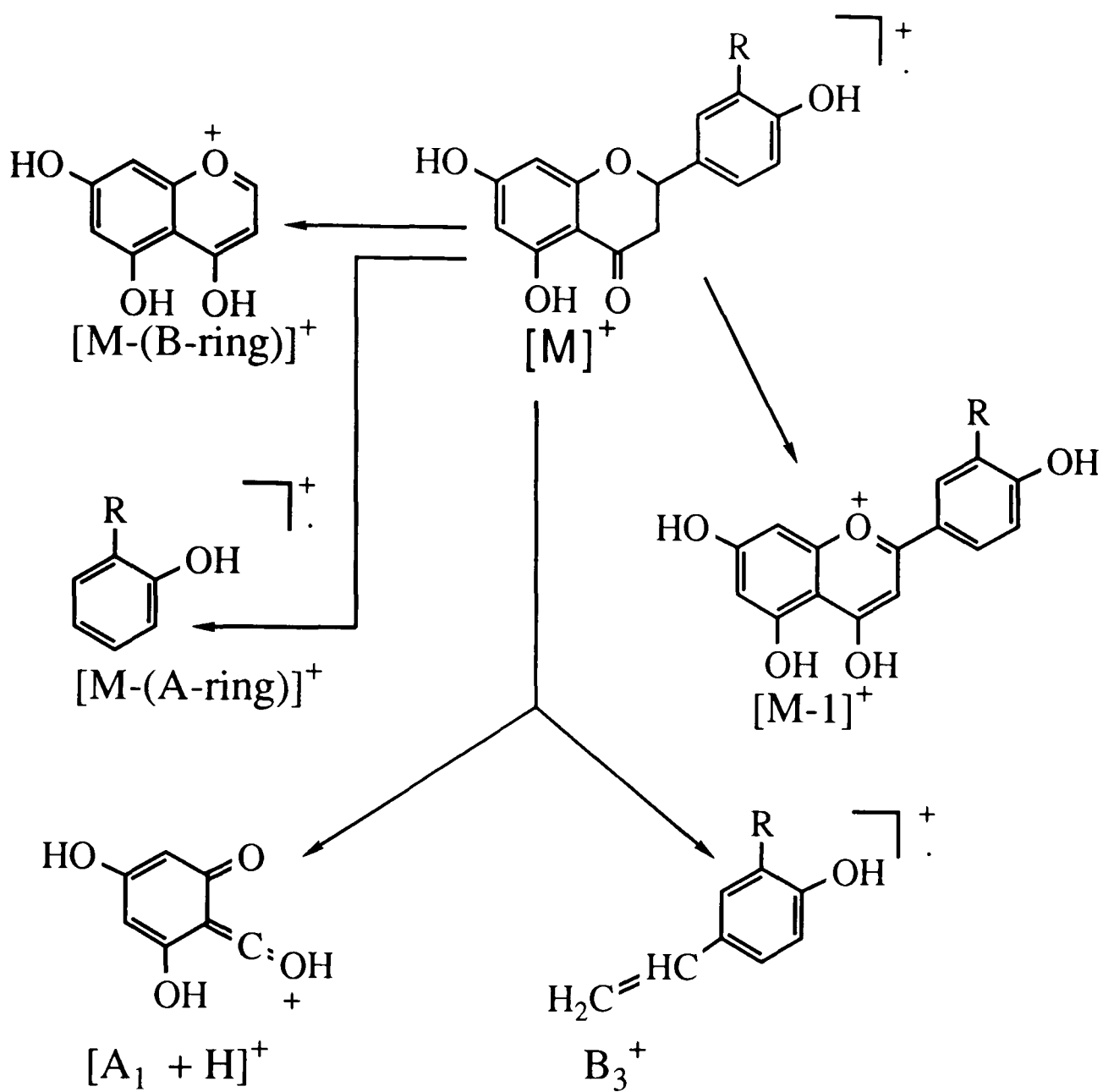
	R=H=SHM-8B	R=OH=SHM-9
$[M]^+$	272 (100)	288 (55)
$[M-1]^+$	---	287 (19.7)
$[M-(B\text{-ring})]^+$	179 (37.8)	179 (24)
$[M-(A\text{-ring})]^+$	94 (3.4)	110 (2.7)
$[A_1+H]^+$	153 (91.6)	153 (100)
B_3^+	120 (64.8)	120 (45.9)

Scheme 5.2. Possible mass fragmentation pattern of SHM-8B and SHM-9

167

(d, J=8.4 Hz; H-3', H-5') and δ 7.30 (d, J=8.4 Hz; H-2', H-6'). The ^{1}H NMR spectrum further revealed two *meta*-coupled (J=2.2 Hz) A ring protons at δ 5.86 (H-6) and 5.88 (H-8).

The coupling pattern of the C-ring signals is explained by the conformation of natural flavanones (structure **164**) where the bulky 2-phenyl substituent (**B ring**) is equatorial (Harborne *et al*, 1975). This conformation in the structure of SHM-8B was supported by the ^{1}H NMR (Table 5.4) which showed an axial-axial (12.9 Hz) and axial-equatorial (2.2 Hz) coupling pattern for the H-2 proton (δ 5.32). In this spectrum, a double doublets at δ 3.10 (J=17.2, 12.9) and 2.67 (J=17.2, 2.2 Hz) were assignable to the axial and equatorial C-3 protons respectively.

Since flavanones can readily be synthesised from chalcones (see Section 1.3.2.3), there is always a question as to whether these compounds are natural or simply artifacts resulting from overzealous treatment of chalcones. However, it has already established that almost all natural flavanones has 2S configuration and are hence laevorotary (Harborne *et al.* 1975). The negative specific rotation (-33°) observed for SHM-8B was in agreement with its assignment as in **106** (Balza *et al.*, 1985). Naringenin (**106**) is by far the most frequently encountered flavanone. It is common as a free phenol, occurs in a wide variety of glycosylated forms and as the base molecule for numerous C-alkylation derivatives.

5.2.1.3.2 Identification of SHM-9 as 5,7,3',4'-tetrahydroxyflavanone (163, eriodictyol)

The second flavanone, which showed a deep red colour with vanillin spray

H	SHM-8B	SHM-9
H-2	5.32 dd (12.9, 2.2)	5.47 dd (12.7, 2.9)
H-3a	3.10 dd (17.2, 12.9)	3.29 dd (17.1, 12.7)
H-3b	2.67 dd (17.2, 2.2)	2.89 dd (17.1, 2.9)
H-6	5.86 d (2.2)	6.35 d (2.0)
H-8	5.88 d (2.2)	6.45 d (2.0)
H-2'	7.30 d (8.4)	7.52 d (1.8)
H-3'	6.80 d (8.4)	
H-5'	6.80 d (8.4)	7.27 d (8.1)
H-6'	7.30 d (8.4)	7.01 dd (8.1, 1.8)
5-OH		12.81 br s

Table 5.4: ^{1}H NMR data of SHM-8B (250 MHz, CD$_3$O) and SHM-9 (400 MHz, pyridine-d$_5$)

^{1}H multiplicities are shown by symbols: s=singlet, d=doublet, dd=double doublet and br s=broad singlet. Figures in bracket represent coupling constants (J) in Hz.

was obtained in a yield of 0.0026%. The high resolution EIMS of this compound established a molecular formula C$_{15}$H$_{12}$O$_6$, one more oxygen than SHM-8B.

The ^{1}H NMR spectrum (Table 5.4) revealed signal patterns for the A and C-ring protons identical with that described for SHM-8B. In this spectrum, a *meta*-coupled (2.0 Hz) proton resonances at δ 6.35 and 6.45 could be assigned to H-6 and H-8 respectively. A big coupling constant (J=12.7 Hz) obseved for H-2

169

(δ 5.47) was again indicative of its axial orientation and of the equatorial bulky phenyl substituent (B-ring). A 1H double doublet signal centered at δ 3.29 must be assigned to the H-3 axial proton as its showed geminal (J=17.1 Hz) and axial-axial (J=12.7 Hz) couplings. In comparison, the H-3 equatorial proton appeared upfield (δ 2.89) and exhibited geminal (J=17.1 Hz) and small equatorial-axial coupling (J=2.9 Hz).

The ^{1}H NMR spectrum of this compound differed from that of naringenin by showing two doublets at δ 7.52 (1H, J=1.8 Hz, H-2') and 7.27 (1H, J=8.1 Hz, H-5') and a doublet of doublets at δ 7.01 (1H, J=8.1, 1.8 Hz). This was typical for the 3',4'-dihydroxylated B-ring which was further substantiated by a fragment in the EIMS for B$_3$ (Scheme 5.2). The negative specific rotation (-25°) indicated the stereochemistry of C-2 as described for naringenin. On the basis of this data, SHM-9 was identified as 5,7,3',4'-tetrahydroxyflavanone (**163**, eriodictyol) (Ahmed *et al.*, 1986).

5.2.2 Lignans of *Premna recinosa*

5.2.2.1 Identification of SHM-16A as (+)-8-hydroxy-pinoresinol (165)

The most non polar lignan was a gumy solid obtained in a yield of only 0.00026%. In the IR spectrum a broad band at 3400 cm^{-1} was indicative of a hydroxyl functional group in SHM-16A. The high resolution EIMS established a molecular formula $C_{20}H_{22}O_7$ suggesting a lignan containing two methoxyl groups (**165**, Fig. 5.5). The ^{1}H NMR spectrum, in the aromatic region (Table 5.5), showed two sets of an *ortho* and *ortho, meta*-coupled proton signals (for two

trisubstituted aromatic systems) and also two aromatic methoxyl groups at δ 3.93 and 3.91 indicating the presence of a partial structue **166** in the structure of SHM-16A. This was further substantiated by the ^{13}C NMR spectrum (Table 5.5) which showed signals in the aromatic region for two sets of two oxygen bearing, three methine, one quaternary and methoxyl carbon signals and also fragments at m/z 123 (12.0%) and 137 (95%) in the EIMS data (Scheme 5.3). This fragmentation pattern also ruled out the possibility of assigning two methoxyl groups in one ring. The methoxyl groups in this compound are presumed to be at 3 and 3' positions (not at 4 and 4') as these are the usual form for other lignans including from this species (SHM-16B and SHM-16E).

In addition to the previously mentioned carbon signals, the ^{13}C NMR spectrum (Table 5.5) revealed two oxygen-bearing aliphatic methylenes (δ 71.6, C-9' and 74.7, C-9) and two oxygen-bearing methines (δ 85.8, C-7' and 87.7, C-7), one quaternary carbinol (δ 91.6, C-8) and one methine carbon (δ 60.1, C-8'). Further assignment of proton resonances to these functional groups and the structure of SHM-16A as **165** was based on ^{1}H-^{1}H COSY NMR studies. This revealed (Fig. 5.4) coupling of a 1H multiplet at δ 3.12 (H-8') to a doublet at δ 4.87 (H-7') and also to methylene protons (δ 4.55, 3.86; H$_2$-9'). A 1H singlet at δ 4.86 (H-7) and an isolated methylene as δ 3.91, 4.07 (H$_2$-9) necessitated the assignment of a hydroxyl group at C-8. On the basis of these data SHM-16A was identified as 8-hydroxy-pinoresinol (**165**, Fig. 5.5).

The EIMS fragmentation pattern of SHM-16A (Scheme 5.3) was typical of the 7,9',7',9-bisepoxy type of lignan and proceeds *via* four major roots

C	δ C	C mult.[b]	H[c]	δ H	H pattern[d]	J value
1	132.4	s				
2	109.3	d	2	6.91	br s	
3	146.9	s				
4	146.0	s				
5	114.7	d	5	7.00	d	8.1
6	119.6	d	6	7.00	br d	8.1
7	87.7	d	7	4.86	s	
8	91.6	s				
9	74.7	t	9a	4.07	d	9.4
			9b	3.91	d	9.4
1'	127.0	s				
2'	109.0	d	2'	6.91	br s	
3'	146.7	s				
4'	145.4	s				
5'	111.2	d	5'	6.88	br d	8.1
6'	119.7	d	6'	6.96	d	8.1
7'	85.8	d	7'	4.87	d	5.0
8'	60.1	d	8'	3.12	m	
9'	71.6	t	9'a	4.55	dd	9.0, 8.6
			9'b	3.86	m	
3-OMe	56.0	q		3.93	s	
3'-OMe	55.9	q		3.91	s	
4-OH				5.67	br s	
4'-OH				5.62	br s	

Table 5.5: ^{1}H and ^{13}C NMR assignments for SHM-16A (165)[a]

[a] ^{1}H and ^{13}C NMR spectra were taken at 400 and 100 MHz NMR respectively in CDCl$_3$.

[b] ^{13}C NMR multiplicities were obtained from the J-Mod. [13]C data and designated by the symbols: s=singlet, d=doublet, t=triplet and q=quartet.

[c] a and b denote magnetically unequivalent protons where a appeared downfield to b.

[d] Patterns are designated by the symbols: s=singlet, d=doublet, dd=double doublets and m=multiplet.

Figure 5.4: COSY spectrum of SHM-16A (shielded region)

173
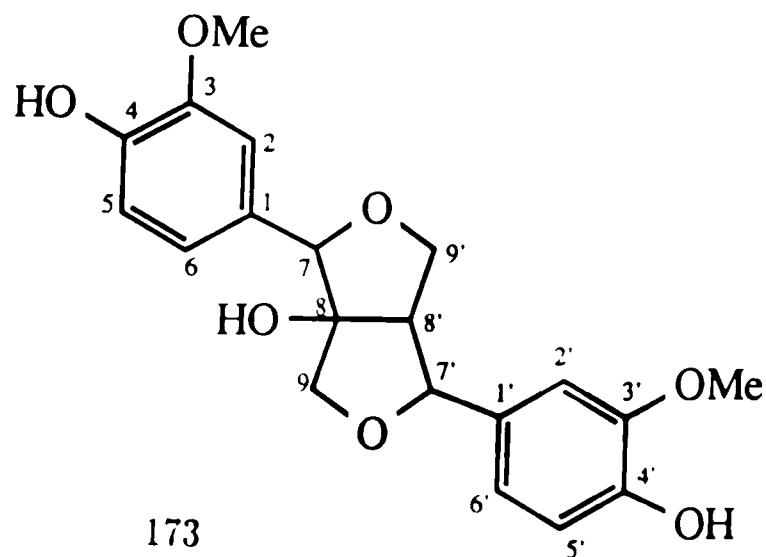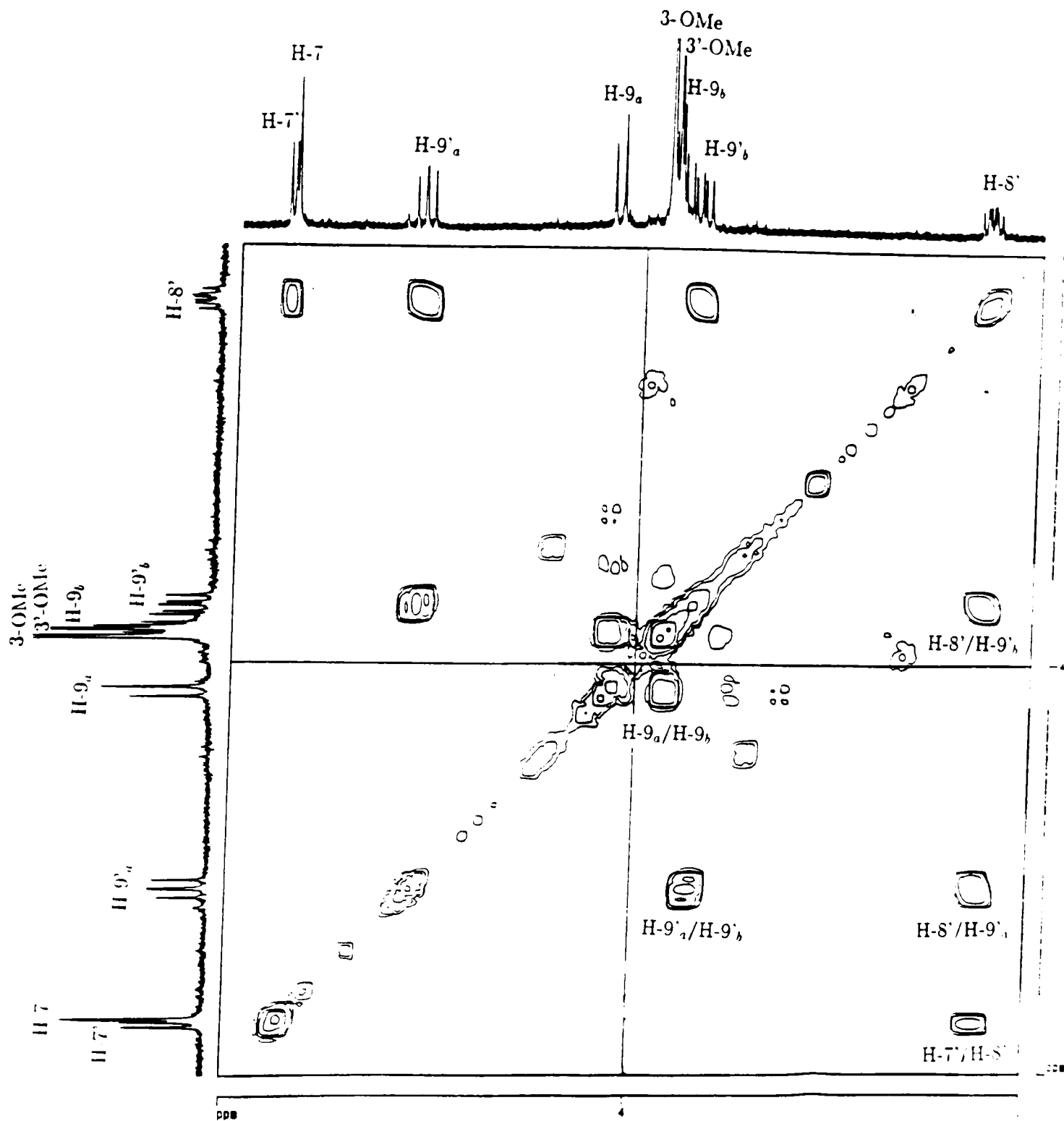
(Pelter, 1967). The base peak as an acylium cation at m/z 151 (Ar-C$\equiv$O$^+$) is formed *via* an aldehyde moiety at m/z 152 (Ar-CHO), while the cinnamyl alcohol (Ar-CH=CH-CH$_2$OH) derived directely from the molecular ion and in turn give rise to m/z 163 (Ar-CH=CH=CH$_2$) which may also be derived directly from the molecular ion. The benzylic ion at m/z 137, which is formed from the molecular ion, could also derive from an aryl ethoxy by a horizontal cleavage of the molecule followed by a loss of 28 MU. Finally, loss of Ar-CHO from the molecular ion gave m/z 222 which, in turn, lost a proton (m/z 221) and methylene group to give a prominant ion at m/z 207.

In theory, the structure of 8-hydroxy pinoresinol can be either of the four stereoisomers: diequatorial (**167**), one of the two axial-equatorial (**168, 169**) or diaxial (**170**) aryl groups (Fig. 5.5). Unfortunately, coupling constants as between H-7 and H-8 in such lignans are not indicative of stereochemistry (Birch *et al.*, 1967). Birch *et al.* (1967) and Atal *et al.* (1967) solved the stereochemistry of many 8-hydroxy-7,9',7',9-bisepoxy lignans from ^{1}H NMR chemical shift values. It has been shown by these authors that an axial aromatic group (C-7 or C-7') must lie face-on and extremely close to the axial hydrogen atom opposite (H-9 or H-9'). There is no possibility of rotation of the aryl moiety and H-9 (axial) and H-9' (axial) are held within the shielding-cone of a benzene ring and appear upfield in the ^{1}H NMR spectrum. In contrast, an equatorial aromatic ring (C-7 or C-7') is also inhibited in rotation, although less so than an axial group and the opposite hydrogen atom (H-9' axial and H-9' axial) both come to different degrees within the deshielding cone of the aromatic ring and would appear downfield in

the ^{1}H NMR spectrum. From a series of ^{1}H NMR (in CDCl$_3$) experiments on 8-hydroxy-7,9',7'9-bisepoxy lignans of known absolute chemistry, a correlation has been made between chemical shift (axial H-9 and H-9') and stereochemistry (C-7, C-7'). In diequatorial compounds (**167**), signals due to two methylene protons appear above δ 4.0 and none below δ 3.7. In equatorial-axial lignans (**168** or **169**), one proton appears at δ 4.1-4.4 and one at δ 3.3-3.5, whereas in the diaxial lignans (**170**) none of the protons appears above δ 4.0 and two appear below δ 3.7. The assignment of stereochemistry of many natural lignans in the past and at present is based on this principle (Anjaneyulu *et al.*, 1981; Taniguchi and Oshima, 1972). In the present study, the chemical shift values of the H-9 and H-9' methylenes (Table 5.5) agreed with the assignment of SHM-16A as a C-7 and C-7' diequatorial aryl structure **167** (Fig. 5.5).

SHM-16A appears to be a new natural product. It was first obtained by deacetylation and hydrolysis of 7-acetoxy-3-gluco-pinoresinol from *Olea europaea* (Chiba, *et al.*, 1979).

175

SHM-16A   165

= R = **166**

167

168   **169**   **170**
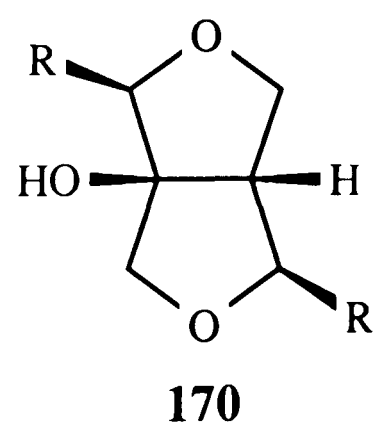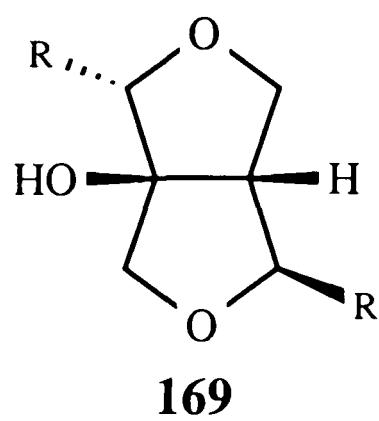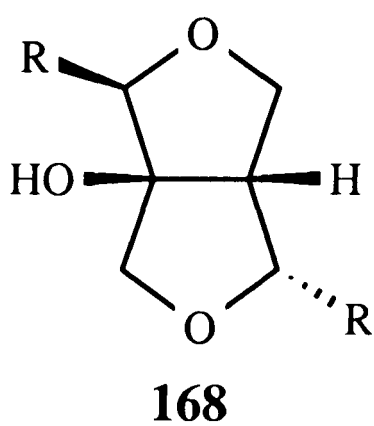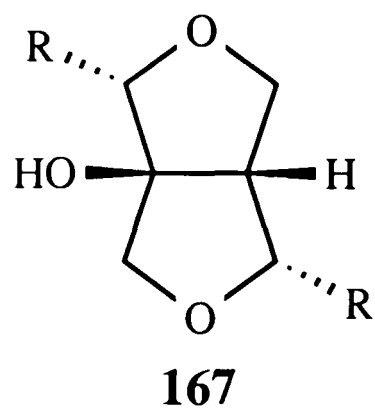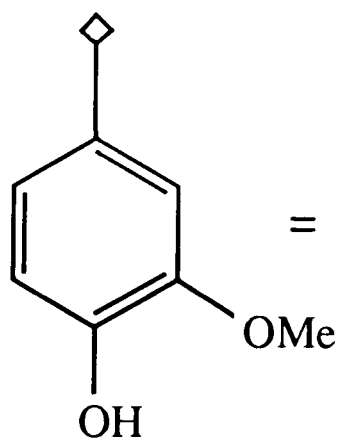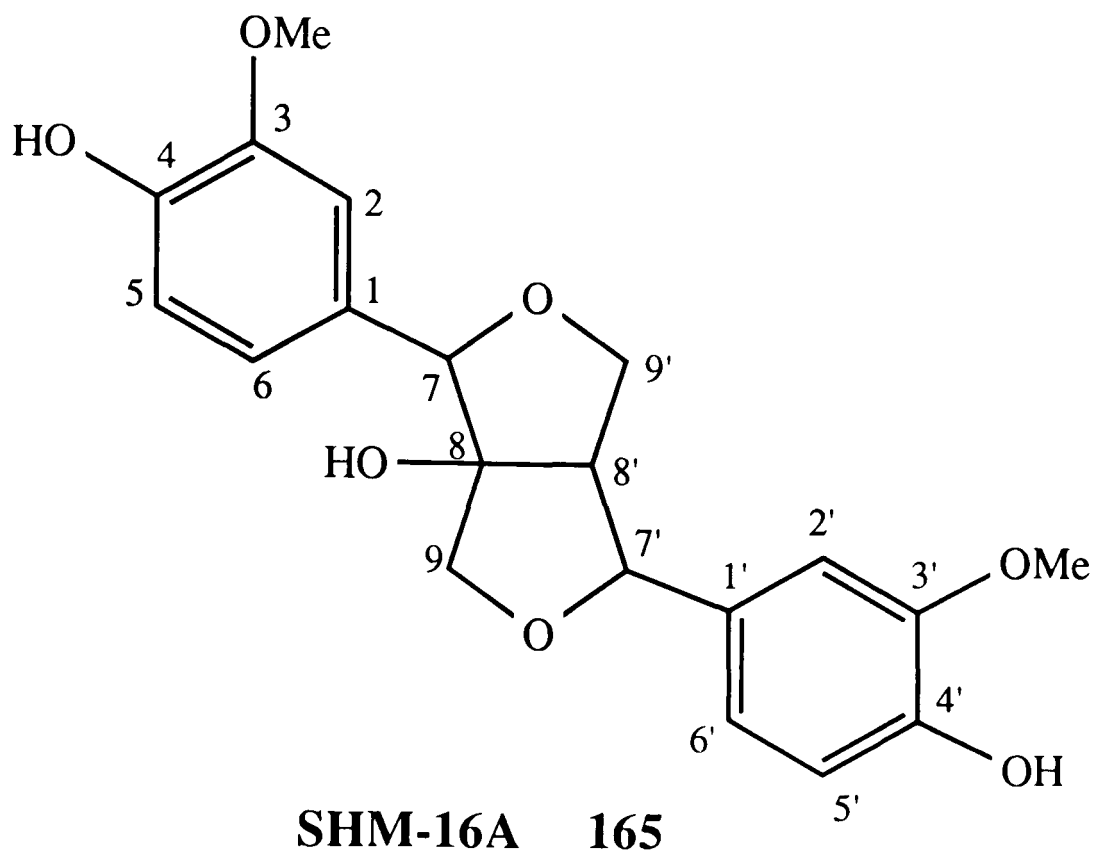
Fig. 5.5. Structure of SHM-16A and its stereoisomers

176

151 (100%)

131 (55.9%)

163 (39%)

152 (78.7%)

M⁺, 376 (66.1%)

180 (2.8%)

165 (50.4%)

207 (58.1%)

222 (28.2%)

137 (95.0%) ≡ **137 (95.0%)**

193 (22.8%)

124 (14.4%)

123 (12%)
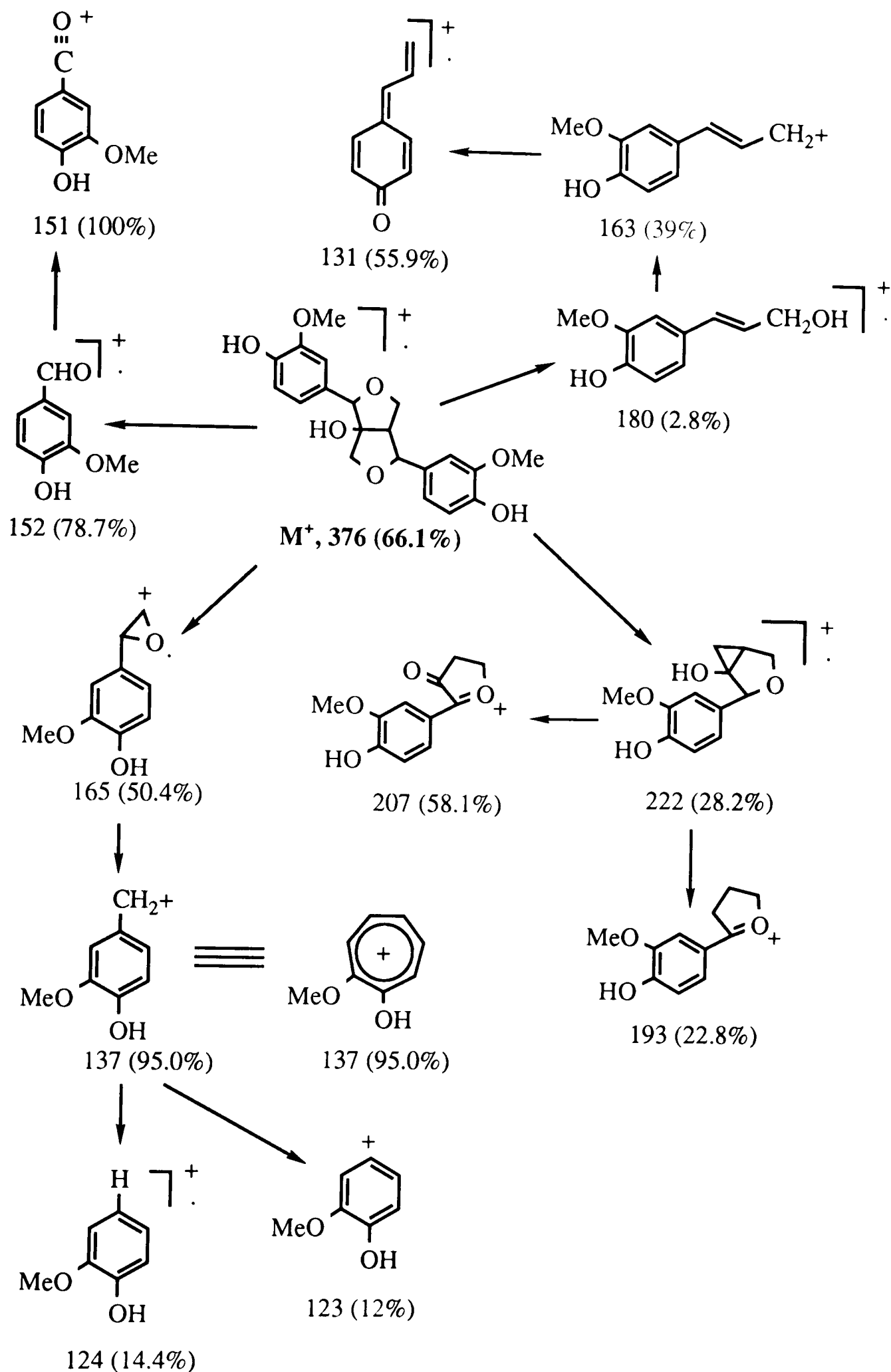
Scheme 5.3. Possible mass fragmentation pattern of SHM-16A

177

5.2.2.2 Identification of SHM-16B as (+)-Lariciresinol (171)

The high resolution EIMS of the second lignan (obtained in a yield of 0.0013%) established a molecular formula $C_{20}H_{24}O_6$ (**171**, Fig. 5.7). A broad band signal at 3400 cm^{-1} in the IR spectrum and conversion of the compound into a triacetate (**172**) were indicative of hydroxyl functional groups. Like SHM-16A, the ^1H NMR spectrum (Table 5.6) revealed two sets of an *ortho* and *ortho, meta*-coupling patterns for 1,3,4-trisubstituted aromatic ring systems and also two aromatic methoxyl groups. This was indicative of partial structure **166**; a hypothesis supported by the ^{13}C NMR data (Table 5.6). As shown for SHM-16A, a major fragment in the EIMS at m/z 137 (99.2%) and fragments at m/z 124 (10.3%) and 123 (7.1%) substantiated a partial structure **166** and also allowed the placement of the two methoxyl groups at differnt rings. Of the nine double bond equivalents required by the molecular formula, eight were due to the two aromatic rings, necessitating only one more ring system. Further assignment of this ring system and ^1H and ^{13}C NMR signals were based on ^1H-^1H COSY and HMBC studies.

In the ^1H-^1H COSY studies (Fig. 5.6), benzylic methylene protons at δ 2.54 and 2.91 (H_2-7) were coupled to a multiplet at δ 2.75 (H-8) which was further connected to other methylene proton signals at δ 4.05 and 3.75 (H_2-9) and a multiplet at δ 2.41 (H-8'). This latter 1H proton signal showed further coupling to one deshielded 1H proton at δ 4.78 (H-7') and to methylene protons at δ 3.91 and 3.78 (H_2-9').

The HMBC NMR studies (Table 5.7) were also in agreement with the

178

Figure 5.6: COSY spectrum (400 MHz, acetone-d₆) of SHM-16B (shielded region)
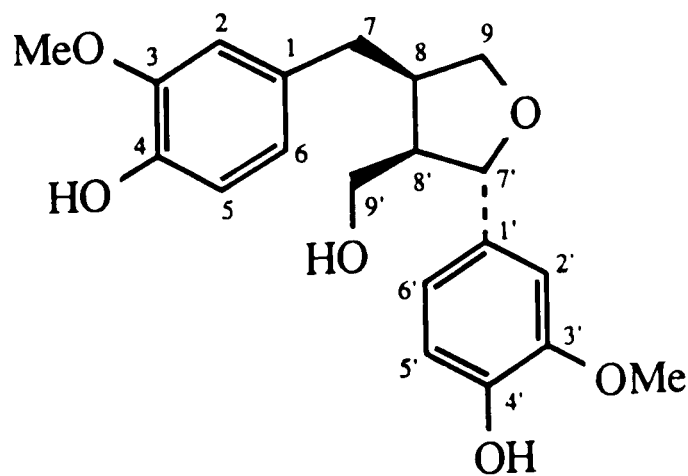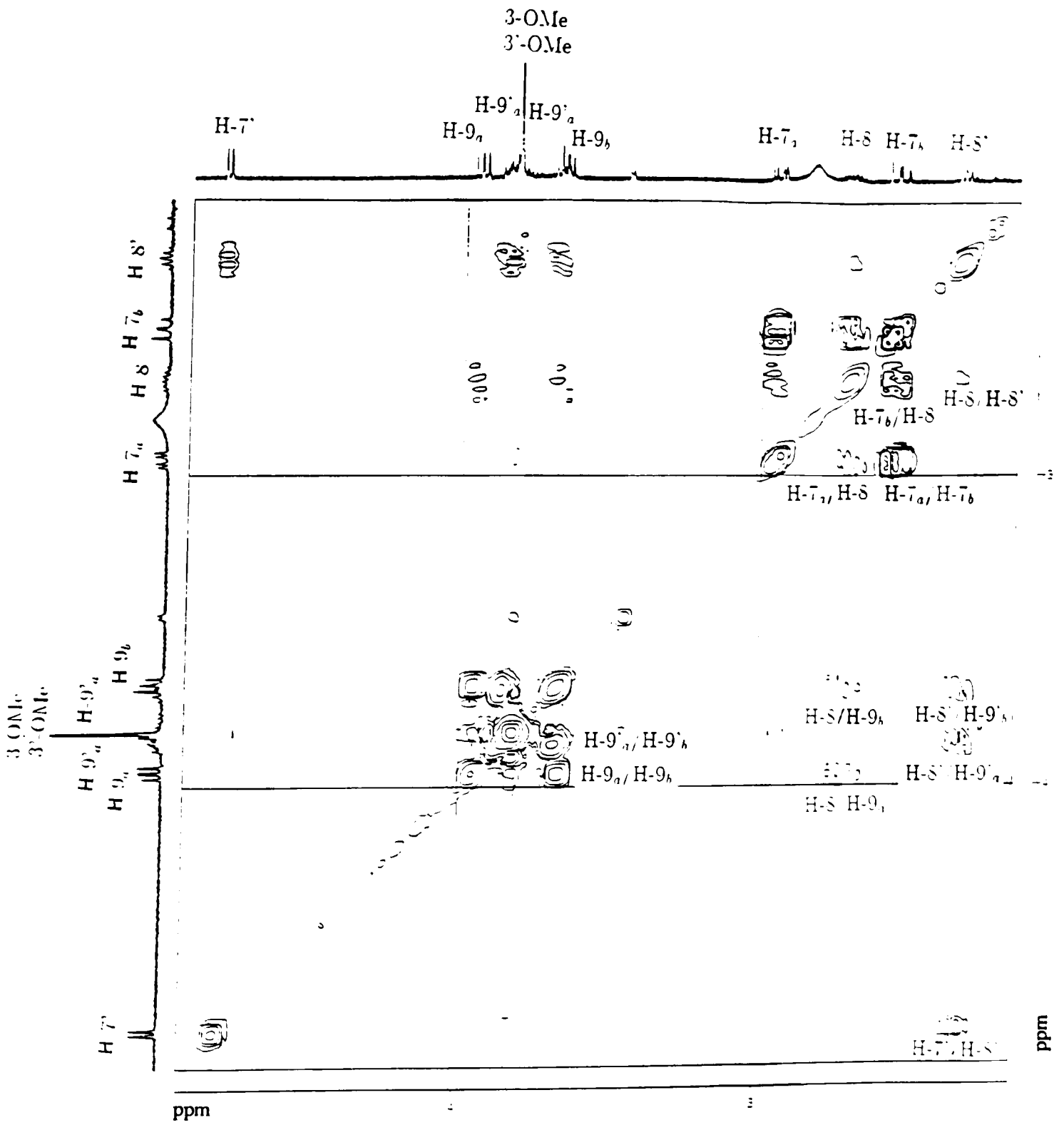
assignment of SHM-16B as **171**. In this study, a ^3J coupling of two aromatic protons (H-2', H-6') to an oxygen bearing aliphatic methine carbon at δ 82.8 which showed ^2J coupling to the multiplet signal (δ 2.41, H-8') and ^3J coupling to two methylene proton signals (H$_2$-9, H$_2$-9') identifies the C-7' position. A ^3J coupling of methoxyl protons to carbons coupled to a different set of proton patterns also supported the assignment of the two methoxyl groups in different rings. Except for the H-8 proton which appeared broad due to its multiplicities, all the expected connectivities were observed (Table 5.7). On the basis of these data SHM-16B was identified as (+)-lariciresinol (**171**).

Lariciresinol has been isolated from various sources as (+) (Fonseca *et al.* 1978; 1979), (-) (Badawi *et al.*, 1983) and (±) (Duh *et al.*, 1986) forms. The relative stereochemistry of (+)-lariciresinol is depicted in structure **171** (Kato *et al.*, 1990).

R = H = SHM-16B   **171**
R = Ac   **172**
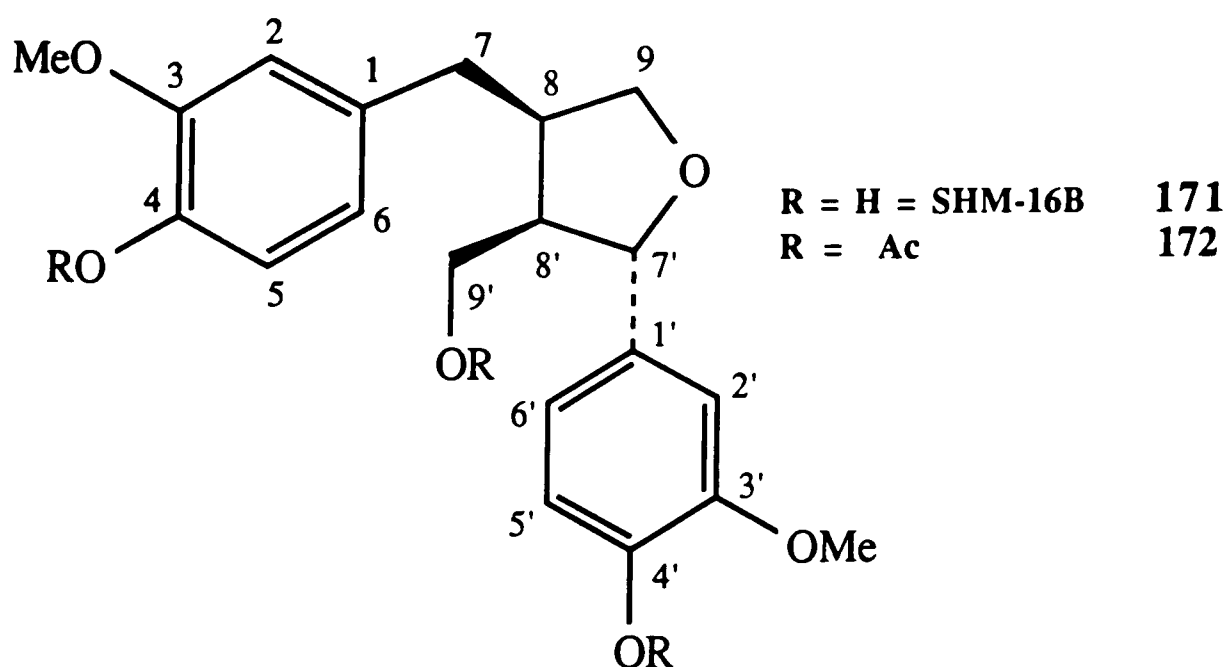
Fig. 5.7 Structure of SHM-16B

C	δ C	C mult.[b]	H[c]	δ H	H pattern[d]	J value
1	132.25	s				
2	111.2	d	2	6.69	d	2.1
3	146.5	s				
4	144.0	s				
5	114.4	d	5	6.83	d	8.5
6	121.2	d	6	6.69	dd	8.5, 2.1
7	33.3	t	7a	2.91	dd	13.3, 5.1
			7b	2.54	dd	13.3, 10.5
8	42.4	d	8	2.75	m	
9	72.9	t	9a	4.05	dd	8.6, 5.4
			9b	3.75	m	
1'	134.7	s				
2'	108.2	d	2'	6.86	d	1.3
3'	146.6	s				
4'	145.0	s				
5'	114.1	d	5'	6.87	d	6.8
6'	118.7	d	6'	6.78	dd	6.8, 1.3
7'	82.8	d	7'	4.78	d	6.6
8'	52.6	d	8'	2.41	p	7.0
9'	60.9	t	9'a	3.91	m	
			9'b	3.78	m	
3-OMe	55.9	q		3.88	s	
3'-OMe	55.9	q		3.87	s	
4-OH				5.61	br s	
4'-OH				5.53	br s	

Table 5.6: ^{1}H and ^{13}C NMR assignments for SHM-16B (171)[a]

[a] ^{1}H and ^{13}C NMR spectra were taken at 400 and 100 MHz NMR respectively in CDCl$_3$.

[b] ^{13}C NMR multiplicities were obtained from the J-Mod. ^{13}C data and designated by the symbols: s=singlet, d=doublet, t=triplet and q=quartet.

[c] a and b denote magnetically unequivalent protons where a appeared downfield to b.

[d] Patterns are designated by the symbols: s=singlet, d=doublet, dd=double doublets and m=multiplet.

H	δ C
H-2	146.5,144.0, 121.2
H-5	146.5
H-6	111.2
H-7	132.3, 121.2, 111.2, 72.9, 42.4
H-9	82.8, 52.6, 42.4, 33.3
H-2'	145.0, 118.7, 82.8
H-5'	46.6, 134.7
H-6'	145.0, 108.2, 82.8
H-7'	134.7, 118.7, 108.2, 60.9, 52.6
H-8'	134.7, 82.8, 72.9, 60.9, 42.4, 33.3
H-9'	82.8, 52.6, 33.3
3-OMe and 3'-OMe	146.6, 146.6

Table 5.7: **HMBC correlations for SHM-16B (171)**

5.2.2.3 Identification of SHM-16E as (-)-*seco*-isolariciresinol (173)

The high resolution EIMS of SHM-16E (yield 0.0009%) showed a molecular ion at m/z 362 (23.7), $C_{20}H_{26}O_6$ (**173**, Fig. 5.8). The partial structure **166** was again evident in the structure of SHM-16E as the EIMS showed a benzylic fragment at m/z 137 as base peak and also m/z 123 (4.9%) as described for SHM-16A. Unlike the previous two lignans, the ^{13}C spectrum of this com-

pound (Table 5.8) showed resonances for pairs of equivalent carbons suggesting a symmetrical molecule. This was substantiated by the ^{1}H NMR spectrum (Table 5.8) which showed only one set of *ortho* and *orto, meta*-coupling patterns for the 1,3,4-trisubstituted aromatic ring system. Conversion of this compound to a tetraacetate (174) and the estalished molecular formula, which necessitates no ring system other than the two aromatic rings, supported the assignment of this compound as 173.

The HMBC (Table 5.9) and ^{1}H-^{1}H COSY NMR spectra were also in agreement with the assignment of this compound as *seco*-isolariciresinol (173). In the latter specrum, H-8 (or H-8') (δ 1.87) was coupled to the methylene protons (H_2-9 or H_2-9') which showed coupling to each other.

seco-Isolariciresinol can have either of the 8R,8'R, 8S,8'S or 8R,8'S configuration. Kato *et al.* (1990) reported that similar compounds (175, 176) with negative specific rotation exhibit an 8R,8'R absolute configuration. SHM-16E is laevorotary and hence believed to have the stereochemistry as shown in structure 1173 (Fig. 5.8).

R = H = SHM-16E   **173**

R = Ac   **174**

$R_1 = R_2 = A$ **175**

$R_1 = R_2 = B$ **176**

A

B
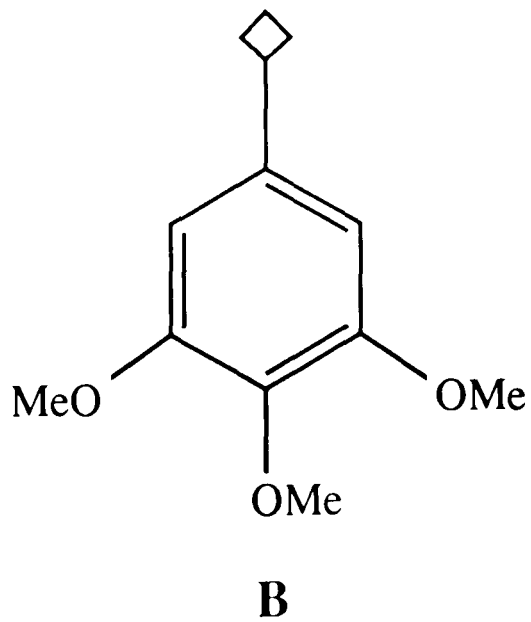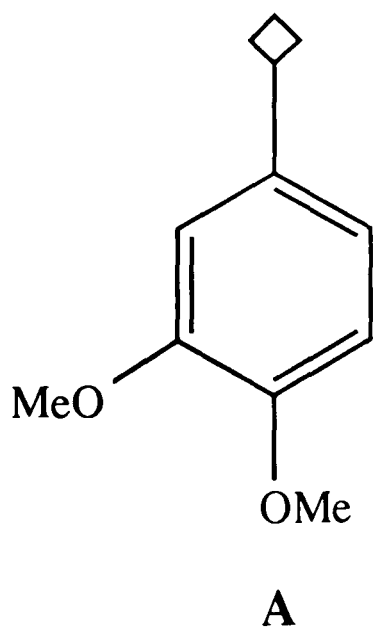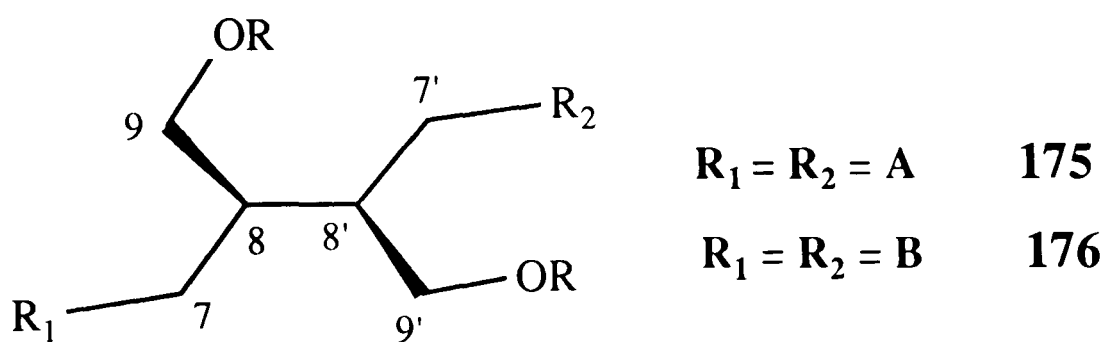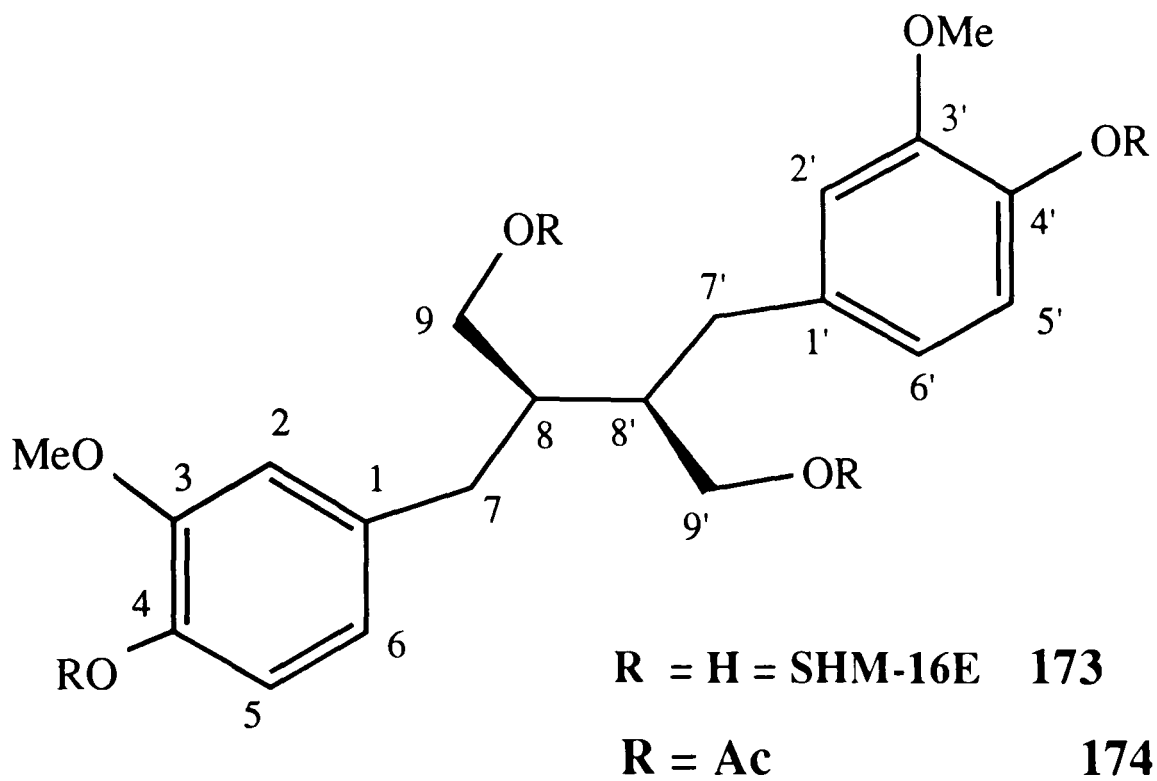
Fig. 5.8. Structure of SHM-16E

184

C	δ C	C mult.[b]	H[c]	δ H	H pattern[d]	J value
1,1'	132.4	s				
2,2'	111.4	d	2,2'	5.58	d	1.9
3,3'	146.4	s				
4,4'	143.8	s				
5,5'	121.6	d	5,5'	6.63	d	8.0
6,6'	114.1	d	6,6'	6.79	dd	8.0, 1.9
7,7'	35.9	t	7a.7'a,	2.75	m	
			7b,7'b	2.64	m	
8,8'	42.8	d	8,8'	1.87	m	
9,9'	60.9	t	9a,9b	3.83	m	
			9b,9'b	3.83	m	
3-OMe	55.8	q		3.80	s	
3'-OMe	55.8	q		3.80	s	

Table 5.8: ^{1}H and ^{13}C NMR assignments for SHM-16E (173)[a]

[a] ^{1}H and ^{13}C NMR spectra were taken at 400 and 100 MHz NMR respectively in CDCl$_3$.
[b] ^{13}C NMR multiplicities were obtained from the J-Mod. ^{13}C data and designated by the symbols: s=singlet, d=doublet, t=triplet and q=quartet.
[c] a and b denote magnetically unequivalent protons where a appeared downfield to b.
[d] Patterns are designated by the symbols: s=singlet, d=doublet, dd=double doublets and m=multiplet.

H	δ C
H-2 or H-2'	143.8, 121.6, 111.4, 35.9
H-5 or H-5'	146.4, 143.8, 132.4, 114.1
H-6 or H-6'	146.4, 143.8, 132.4, 114.1
H-7 or H-7'	132.4, 121.6, 111.4, 60.9, 43.8, 35.9
H-9 or H-9'	48.8
3-OMe or 3'-OMe	146.4

Table 5.9: **HMBC correlations for SHM-16E (173)**

5.3 Experimental

5.3.1 Isolation of compounds

Powdered leaves of *Premna recinosa* (750 g) were extracted by ethanol

as described for *Premna schimperi* (page 102). Removal of the solvent yielded 55

g of residue which was subsequentely fractionated using VLC (silica gel) eluting

with petroleum ether and EtOAc mixtures of increasing polarity. The 10% EtOAc

eluent was applied on a Sephadex LH-20 column (solvent, CHCl₃:MeOH 1:1) and

yielded **161** (SHM-8A, pachypodol) (25 mg) and impure **106** (SHM-8B, narin-

genin) which was purified by PTLC (silica gel, petroleum ether:CHCl₃:EtOAc,

4:6:4) to yield **106** (10 mg). The 20% EtOAc fraction afforded **167** (SHM-9,

eriodictyol) (20 mg). The 50-70% EtOAc fractions were bulked and subjected to

column chromatography (Sephadex LH-20, as above) to give pure **108** (SHM-10, quercetin) (10 mg) as the last fraction and a mixture of two flavonoids. PTLC of this mixture (silica gel, petroleum ether:CHCl$_3$:EtOAc, 4:6:6) yielded **162** (SHM-11, chrysosplenol-D) (25 mg) and **38** (SHM-12, luteolin) (8.7 mg). The heavier fraction obtained from the Sephadex column (fraction 1) was a mixture of three lignans which had similar R$_f$ values. Repetitive prep. TLC of this fraction (chloroform:methanol, 9:1) afforded 2 mg of SHM-16A (**165**, 8-hydroxy pinoresinol), 10 mg of SHM-16B (**171**, lariciresinol), and 7 mg of SHM-16E (**173**, *seco*-isolariciresinol).

5.3.2 Properties of compounds

5.3.2.1 Properties of SHM-12 (5,7,3',4'-tetrahydroxyflavone) (Luteolin, 38)

The spectroscopic data (UV, IR, ^{1}H NMR and EIMS) and TLC characteristics were identical with that described for SHM-35 (page 103).

5.3.2.2 Properties of SHM-10 (3,5,7,3',4'-pentahydroxyflavone) (Quercetin, 108)

The spectroscopic data (UV, IR, ^{1}H NMR and EIMS) and TLC characteristics were identical with that described for SHM-36-4 (page 104).

5.3.2.3 Properties of SHM-8A (5,4'-dihydroxy-3,7,3'-trimethoxyflavone) (Pachypodol, 161)

White needles, mp 172-173°. Found 344.0802, $C_{18}H_{16}O_7$, requires 344.0896; UV λ_{max}^{MeOH} nm = see Table 5.1; IR ν_{max}^{KCl} cm^{-1} = 3450 br ,3920, 1660, 1490, 1430, 1350, 1230, 1210, 1160; ^{1}H NMR (250 MHz, CDCl$_3$) δ = 12.61 (1H, s, 5-OH), 7.80 (1H, d, J=2.0 Hz, H-2'), 7.70 (1H, dd, J=8.3, 2 Hz, H-6'), 7.10 (1H, d, J=8.3 Hz, H-5'), 6.50 (1H, d, J=2.2 Hz, H-8), 6.40 (1H, d, J=2.2 Hz, H-6), 5.97 (1H, s 4'-OH) , 3.95 (3H, s, 3'-OMe), 3.84 (3H, s, 7-OMe), 3.82 (3H, s, 3-OMe); EIMS m/z (rel. int.) = 344 (100), 143 (76.9), 329 (65.3), 325 (11.2), 301 (62.8), 283 (5.1) 167 (9.5), 151 (7.3).

5.3.2.4 Properties of SHM-11 (5,3',4'-trihydroxy-3,6,7-trimethoxyflavone) (Chrysosplenol-D, 162)

Orange needles, mp 241-245°. Found 360.0856, $C_{18}H_{16}O_8$, requires 360.0845; UV λ_{max}^{MeOH} nm = see Table 5.1; IR ν_{max}^{KCl} cm^{-1} = 3450, 3920, 1660, 1600, 1490, 1430, 1350, 1230, 1210, 1160; ^{1}H and ^{13}C NMR δ = see Table 5.2; EIMS m/z (rel. int.) = 360 (100), 359 (18.9), 345 (75.8), 137 (25.8).

5.3.2.5 Properties of SHM-8B (5,7,4'-trihydroxyflavanone) (Naringenin, 106)

Needles, mp 248-250°, $[\alpha]_D$ -33° (c 0.1, MeOH). Found 272.0703, $C_{15}H_{12}O_5$, requires 272.0685; UV λ_{max}^{MeOH} nm = 226, 288, 321; IR ν_{max}^{KCl}cm^{-1} = 3200 br, 1630, 1600, 1310, 1250, 1160, 840; ^{1}H NMR δ= see Table 5.4; EIMS m/z (rel. int.) =

272 (100), 179 (37.8), 178 (11.6), 166 (36.2), 153 (91.6), 152 (25.8) 124 (13.2),

120 (64.8), 119 (10.7), 107 (18.5), 91 (10.4).

5.3.2.6 Properties of SHM-9C (5,7,3',4'-tetrahydroxyflavanone) (Eriodictyol, 163)

Needles, mp 247-250°, $[\alpha]_D$ -25° (c 0.1, MeOH). Found 288.0621, $C_{15}H_{12}O_6$, requires 288.0634; UV λ_{max}^{MeOH} nm = 226, 285, 321, 321 sh; IR ν_{max}^{KCl} cm^{-1}= 3350 br, 1600, 1445, 1300, 1160, 1090, 820; ^{1}H NMR δ = see Table 5.4; EIMS m/z (rel. int.) = 288 [M]$^+$ (55), 287 (19.7), 179 (24.6), 166 (38.4), 153 (100), 136 (45.91), 123 (14.5) 110 (2.7).

5.3.2.7 Properties of SHM-16A ((+)-8-hydroxy-pinoresinol, 165)

Yellow gum, $[\alpha]_D$ +10° (c 0.1, CHCl$_3$). Found 374.1390, $C_{20}H_{22}O_7$, requires 374.1365; UV λ_{max}^{EtOH} nm = 228, 278; IR ν_{max}^{KCl} cm^{-1} = 2400 br, 2920, 1700, 1560, 1510, 1210; ^{1}H and ^{13}C NMR δ = see Table 5.5; EIMS m/z (rel. int.) = 374 (66.1), 279 (20.0), 222 (28.2), 207 (58.1), 193 (22.8), 178 (14.9), 167 (10.2), 165 (50.7), 163 (39), 153 (87.8), 152 (78.7), 151 (100), 150 (13.8), 150 (16.1), 149 (59.3), 138 (21.5), 137 (95), 135 (14.1), 133 (25.4), 131 (55.9), 124 (14.4), 123 (12.0), 112 (15.5), 103 (20.3), 93 (26.4), 81 (11.9), 77 (23.5), 71 (15.8).

5.3.2.8 Properties of SHM-16B ((+)-Lariciresinol, 171)

Yellow gum, $[\alpha]_D$ +17° (c 0.1, CHCl$_3$). Found 360.1585, $C_{20}H_{24}O_6$, requires 360.1573; UV λ_{max}^{EtOH} nm = 225, 275; IR ν_{max}^{KCl} cm^{-1} = 3600-3170, 1593, 1518, 1466; ^{1}H and ^{13}C NMR δ = see Table 5.6; EIMS m/z (rel. int.) = 360

(100), 359 (9.0), 236 (10.3), 194 (24.6), 180 (21.4), 175 (13.5), 164 (11.5), 153 (35.5), 152 (11.2), 151 (39.1), 150 (15.6), 137 (99.2), 124 (10.3), 123 (7.1). SHM-16B acetate (172) = $[\alpha]_D$ +7° (c 0.1, CHCl$_3$); ^{1}H NMR (250 MHz, CDCl$_3$) δ = 2.05 (3H, s, 9'-acetates), 2.32 (6H, s, 4 and 4'-acetates), 2.55 (1H, m, H-8'), 2.56 (1H, m, H-8), 2.72 (1H, m, H-7), 2.87 (1H, dd, J=12.7, 6.6 Hz, H-7), 3.82 and 3.84 (3H each s, 3-OMe amd 3'-OMe), 3.74 and 4.40 (2H, m, H$_2$-9), 4.20 and 4.38 (2H, br dd, H$_2$-9'), 4.87 (1H, d, J=5.7 Hz, H-7') and 6.72-7.00 (6H aryl protons)

5.3.2.9   Properties of SHM-16E ((-)-*seco*-isolariciresinol, 173)

Yellow gum, $[\alpha]_D$ -15° (c 0.1, CHCl$_3$). Found 362.1719, C$_{20}$H$_{26}$O$_6$, requires 362.1729; UV λ_{max}^{EtOH} nm = 223, 275; IR ν_{max}^{KCl} cm^{-1} = 3680-3100, 1589, 1503, 1453, 1420; ^{1}H and ^{13}C NMR δ = see Table 5.8; EIMS m/z (rel. int.) = 362 (23.7), 194 (5), 189 (7.7), 163 (6.9), 150 (4.5), 139 (4.6), 138 (41.7), 137 (100), 131 (6.7), 123 (4.9), 122 (10.1), 94 (7.5). SHM-16E acetate (174) $[\alpha]_D$ -15° (c 0.1, CDCl$_3$); ^{1}H NMR (250 MHz, CHCl$_3$) δ = 1.67 (2H, m, H-8, H-8'), 2.06 (6H, s, 9 and 9'-acetates), 2.31 (6H, s, 4 and 4'-acetates), 2.86 (4H, m, H$_2$-7 and H$_2$-7'), 3.99 and 4.23 (4H, m, H$_2$-9 and H$_2$-9'), 6.63 (2H, dd, J=7.8, 1.8 Hz, H-6,H-6'), 6.63 (2H, d, J=1.8 Hz, H-2, H-2') and 6.92 (2H, d, J=7.8 Hz, H-5, H-5').

5.4   CONCLUSION ON PREMNA SPECIES

5.4.1   Phytochemical and Pharmacological Consideration of *Premna* species

5.4.1.1   Chemistry

The root of *Premna* species had been shown to be a rich source of diterpenes while leaves appeared to be devoid of these constituents (see Section 1.2). In the present study, roots of *Premna* species were not examined but leaves of *P. oligotricha* and *P. schimperi* were found to be a good source of labdane and clerodane diterpenoids. No diterpenes were isolated from the leaves of *P. recinosa*.

Flavones were the only class of flavonoids reported from the genus *Premna* (see Section 1.2). All three species of *Premna* examined under the present study were found to be good sources of flavones, flavanones and flavonols, the latter two for the first time in the genus. Cinnamate derivatives incorporated with other skeletons were well represented in the genus especially in *P. odorata* (see Section 1.2.2). Cinnamate derivatives were also common constituents of *P. schimperi*. In the case of *P. recinosa*, these cinnamates have dimerized to form lignans, for which this appears to be the first report on the genus.

Only one sesquiterpene was isolated (*P. oligotricha*) under the present study which brings the total number isolated from the genus to four. In general, the chemistry of *Premna* seems to be diverse and it is worthwhile to investigate the roots of species studied.

191

5.4.1.2 Pharmacology

The present study is the first systematic bioassay-guided isolation approach undertaken on *Premna* species. *P. oligotricha* and *P. schimperi* diterpenes and sesquiterpene demonstrated a good antimicrobial spectrum which explains their traditional use. Such compounds seem to be stored mainly in the oil glands of the leaves and could be involved in the defense of the plants. In this regard the insect antifeedant properties of diterpenes like compound **130** (Phadnis *et al.*, 1988) may be important.

Much work has been done during the past few years on the biolgical evaluation of flavonoids. Flavones like luteolin, a common constituent of *P. schimperi* and *P. recinosa*, are known for their papaverine-like action (Broucke, 1983). These compounds reduce the availability of Ca^{2+}, which is indispensable for smooth muscle contraction and hence have muscolotropic and analgesic activity (Ramaswamy *et al.*, 1988). The use of *P. recinosa* for stomach pain may be explained by such action as the ethanolic extract of the leaves inhibit response to acetyl choline, nicotine and histamine[1]. Recently, the antiviral activity of flavonols like pachypodol (Simoes *et al.*, 1990), a common constituent of *P. recinosa*, and antifungal properties of flavonols like quercetin (Weidenborner *et al.*, 1990) have been reported. The latter biological activity however is best known for flavanones (Weidenborner *et al.*, 1990). Naringenin and eriodictyol, constituents of *P. recinosa*, showed antifungal activity against *Aspergillus niger* and *Penicillium notatum* at concentrations higher than 200 μg per disc. Such

---

[1]concentations higher than 1.5 mg/ml of the extract reduce or totally abolish a guinea pig ileum response to these agonists

activity may account for the weak antifungal property of the crude extract (see Section 5.1) and may have a significant role in nature as defensive agents against pathogenic fungi.

Flavonoids and cinnamates of *Premna* species could play an active role in nature as scavengers of active oxygen species (Toda *et al*, 1991), and in plant-plant interactions (Marsh, 1990). Compounds like *p*-hydroxybenzoic acid could contribute to the antibacterial properties of the plant extract and/or enhance the effect of major antibacterial principles. The cytotoxic property of compounds isolated under the present study were not fully studied but lignans of *P. recinosa* are known for their cytotoxicity (Badwi *et al.*, 1983).

Part II

STUDIES ON THE LOCAL ANAESTHETIC AND/OR MUSCLE RELAXANT PROPERTY OF PLANT EXTRACTS

Chapter 6

STUDIES ON THE MUSCLE

RELAXANT PROPERTY OF

Portulaca oleracea

6.1 Distribution and Botanical Description of

Portulaca oleracea

Portulaca oleracea L. (Portulacaceae) belongs to a genus of succulent herbs, found throughout the warmer parts of the world. Several species occur in Africa, of which *P. oleracea* and *P. quadrifida* are best known.

P. oleracea is distributed world wide (from sea level to 2700m) in temperate and tropical countries. It is known to grow wild throughout Africa, particularly in East Africa where it sometimes beccoms a troublesome weed. The plant is cultivated in the more arid tropics and it is used as an ornamental.

P. oleracea is known in different countries by the local names: purslane, pigweed, pusky, and pusley (English), jiabara, mekhena, and marare (Ethiopia), pourpier (French), mataga atsanu, chingogo, matakoatsanu, nkhotchwe, tsotsope, matakaoali, matakogawaili, and kokwa (malawi), Rigla (Sudan), ekalitete, onjoroleo, tebere, ssezzira, ayiyoyiyo, and o/jipa (Uganda), nyelenyele, cintekenteke, nyelele, masode, katete, and kalvnda (Zambia), and gatamatonga and siachamubili (Zimbabwe).

Botanically, the plant is described as follow (FAO, 1988): Sprawling annual herb, with fleshy reddish stem, growing errect or more commonly prostrate depending on the light conditions. Leaves opposite, wedge-shaped at base with rounded tips, tick, fleshy, stalkless, 0.5-2.8 cm long. Flowers yellow, 5 petals, 1-5 at end of branches surrounded by leaves, open only on sunny mornings. Fruit ovoid capsules containing numerous seeds. Seeds black, shiny, nearly oval, about 5 mm in lengh.

Two types of *P. oleracea* are distinguished: common wild varieties (var *oleracea*) and cultivated varieties (var *sativa*), which are more upright, e.g., green, golden, and large-leafed golden in Europe.

6.2   Traditional uses of *P. oleracea*

6.2.1   Uses of *P. oleracea* as food

The leaves of *P. oleracea* are rich in vitamin A, calcium, phosphorus, iron, vitamin C (highest in young leaves and decreases after flowering) and sodium

(FAO, 1988).

The leaves of *P. oleracea* are used as a pot herb by many Africans (FAO, 1988), Aboriginals in Australia (Jennie *et al.*, 1983) and Asians (Bilgir, 1984). In Mozambique, Malawi and Nigeria, the large-leafed type is cooked as a vegetable. In France young shoots are eaten in salads. Stems are pickled, and dried for use in time of scarcity. Ash from the leaves is high in sodium, and can be used as salt. Seeds can be ground to flour and used for cooking. The whole plant is occasionally used as forage, notably as pig food. It is also used as a green manure, but not too often as it can raise the sodium content of the soil.

The plant contains high amount of oxalic acid which can interfere with calcium uptake (Kusum, 1988, Singh, 1973 and Tabeekhia, 1980). So there may be little benefit to be gained from its high calcium content and it may be toxic due to this high level of oxalate.

6.2.2 Medicinal Uses of *P. oleracea*

Although toxicity of *P. oleracea* associated with its high oxalate content has been documented since the earliest times, the plant has been suggested to have reputed medicinal value in West Africa (Okwuasaba, 1987). In Nigeria the leaves of *P. oleracea* have been applied topically on swelling, whitlow, bruises, boils and abscesses. The juice of the leaves has been used as drops for ear-ache and toothache. The leaves, macerated in water, are considered to be a useful heart "tonic" and to possess diuretic properties. The seed has been used as a vermifuge and been included in prescriptions for the treatment of syphilis. Recently, it has

been shown that the boiled leaves produce a rapid relief of muscular ache and pains associated with spastic paraplegia (Okwuasaba et al, 1986).

6.3 Previous Pharmacological Reports on P. oleracea

The first pharmacological report on P. oleracea came in 1986 from Nigerian scientists who showed that the leaf and stem extract of this plant could paralyse muscle in vitro (Okwuasaba et al., 1986). It was later confirmed that the plant has a significant muscle relaxant properties in vivo, including in man (Parry et al., 1987a, 1987b). The mechanism of action of the crude water extract has been studied by the same authors (Okwuasaba et al., 1986, 1987a, 1987b) using frog sciatic nerve sartorius muscle, rat phrenic nerve hemidiaphragm and frog rectus abdominis muscle preparations. In general the water extract has been shown to have the following properties.

- The extract produces a biphasic effect consisting of an initial enhancement followed by a secondary long lasting depression of twitch tension to both direct (MS) and indirect (NS) stimulation of the rat phrenic nerve hemidiaphragm and frog sciatic nerve sartorius muscle preparation. Twitch depression was more pronounced for the NS preparations than the direct muscle stimulated preparations.

- Contracture induced by nicotinic agonists (acetylcholine, carbachol and nicotine) were inhibited by the extract which also depressed the maximum

response.

- Incubation with d-tubocurarine failed to inhibit and physostigmine failed to potentiate the initial enhancement to twitch contractions to NS and MS caused by the extract. In addition tetrodotoxin alone or in combination with d-tubocurarine did not inhibit this initial enhancement of twitch amplitude to MS.

- The addition of EDTA or the use of Ca^{2+} free physiological solution potentiated the secondary depression of twitch amplitude to MS and NS produced by the extract, while an increase in extracellular Ca^{2+} as well as the addition of SCN anion reversed and/or abolished extract-induced depression of twitch tension in both rat phrenic nerve hemidiaphragm and frog sciatic nerve sartorius muscle preparation.

- The extract produced a partial blockade of potassium and caffeine induced contractures on the frog rectus abdominis preparation.

- The initial extract induced twitch augmentation to MS of the rat phrenic hemidiaphragm preparation and extract, acetylcholine, and potassium induced contractures of the rectus abdominis muscle preparation could be attenuated by D-600.

- $I.v.$ administration of the extract to chicks caused a flaccid limb paralysis like that of d-tubocurarine.

Bringing all these results together, it has been concluded that the muscle relaxant properties of $P.$ $oleracea$ extract was not mediated via a pre synaptic

199

mechanism and/or stimulation of the nicotinic receptors. Interference with the mobilization of calcium with the consequent impairment of the excitation contraction coupling mechanism was taken as a likely mode of action of the extract. Since the effect of the extract was dependant on the concentration of extracellular Ca^{2+} ion and also affected by calcium antagonists like D-600, the observed pharmacological activity was explained largely in terms of the impairment of extracellular Ca^{2+} influx, "trigger" Ca^{2+}, necessary for the release of Ca^{2+} from SR.

The non-dialysable water extract was shown to be devoid of the muscle relaxant properties and the activity of the dialysable fraction was higher than the methanol extract. It was suggested that the active principle could be very polar and small in molecular weight.

To our knowledge, the active principle(s) responsible for the muscle relaxant properties of *P. oleracea* is not known. The primary objective of this study was then to isolate and identify the muscle relaxant principle(s).

6.4 RESULTS AND DISCUSSION

6.4.1 Effect of the ethanolic extract of the leaves of *P. oleracea* on chick biventer cervicis preparation

For the sake of simplicity, the chick biventer cervicis muscle preparation was selected as a model for the bioassay guided isolation of the active principle(s) from *P. oleracea*. The crude ethanol extract of the leaves produced muscle re-

laxation (Fig. 6.1) in the same manner as that reported for the water extract on the sciatic nerve sartorius muscle and phrenic nerve hemidiaphragm preparations (Okwuasaba et al., 1986). Lower concentrations (0.25-1 mg/ml)[1] of the ethanol extract caused a dose dependant twitch augmentation. 2 mg/ml of the extract caused twitch augmentation followed by a rapid abolition of twitch height. Higher doses ($\geq$ 4 mg/ml) caused contracture and a rapid abolition of twitch which was not preceded by twitch augmentation. In general the extract has a rapid on-set of action and its effect could be quickly recovered by washing. Only 1 to 2 minutes were required for a complete recovery of the tissue by washing after a 100% twitch depression by the extract. All concentrations which could depress twitch height could also cause 100% abolition of NS twitch height but the time to reach this effect depend on the concentration of the extraxt used. For this reason it was not possible to plot a resonable dose response curve for the extract and hence the lowest concentration in a cumulative dose required for the 100% twitch paralysis (**LCD-100%**, 2 mg/ml for the ethanol extract) was used as a measure for comparing the activity of various fractions.

The muscle relaxant property of the ethanol extract of *P. oleracea* on both NS and MS chick biventer cervicis preparation could be abolished by 4×10^{-3} M CaCl$_2$ (Fig. 6.2) in the same manner as was reported for the rat phrenic nerve hemidiaphragm muscle preparation (Okwuasaba et al., 1986). This concentration of CaCl$_2$ could itself cause 100% abolition of twitch height, the effect of which was in turn attenuated by a 100% muscle paralysing dose of the extract (4 mg/ml)

---

[1] results are obtained from experiments on six preparations
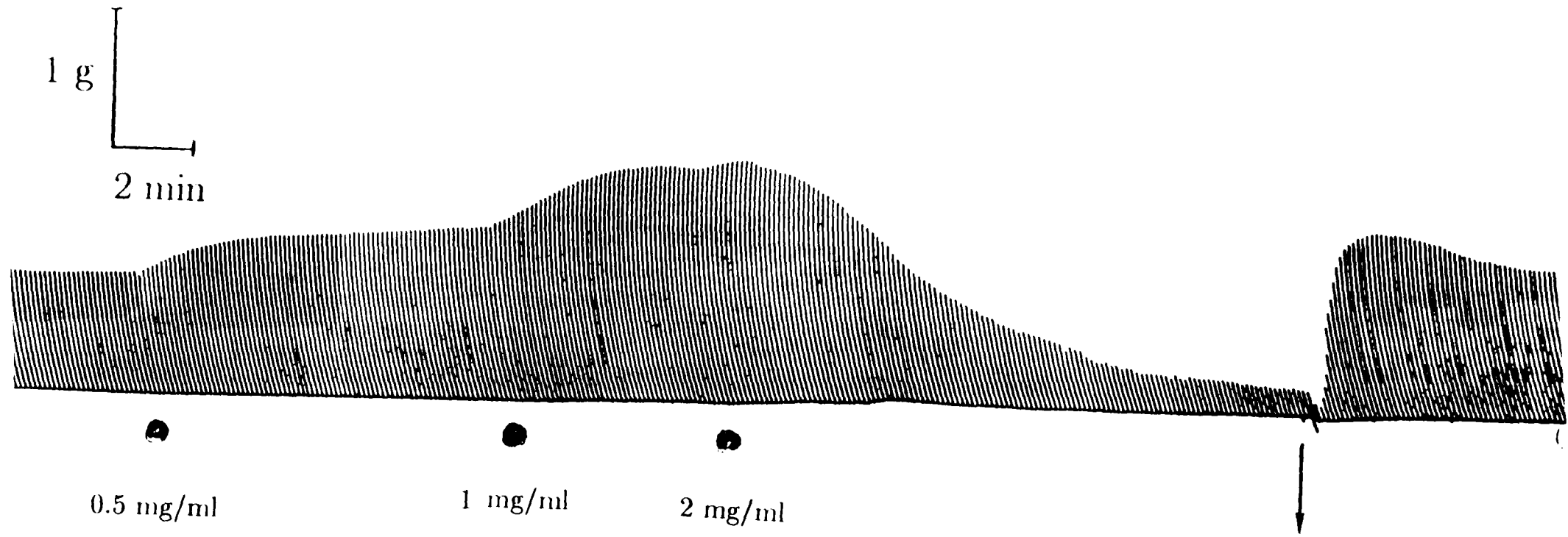
Fig. 6.1: The effect of ethanol extract of leaves of *P. oleracea* on NS chick biventer cervicis preparation. The extract was added in cumulative doses indicated by dots and recovery by washing is shown by a down ward arrow.
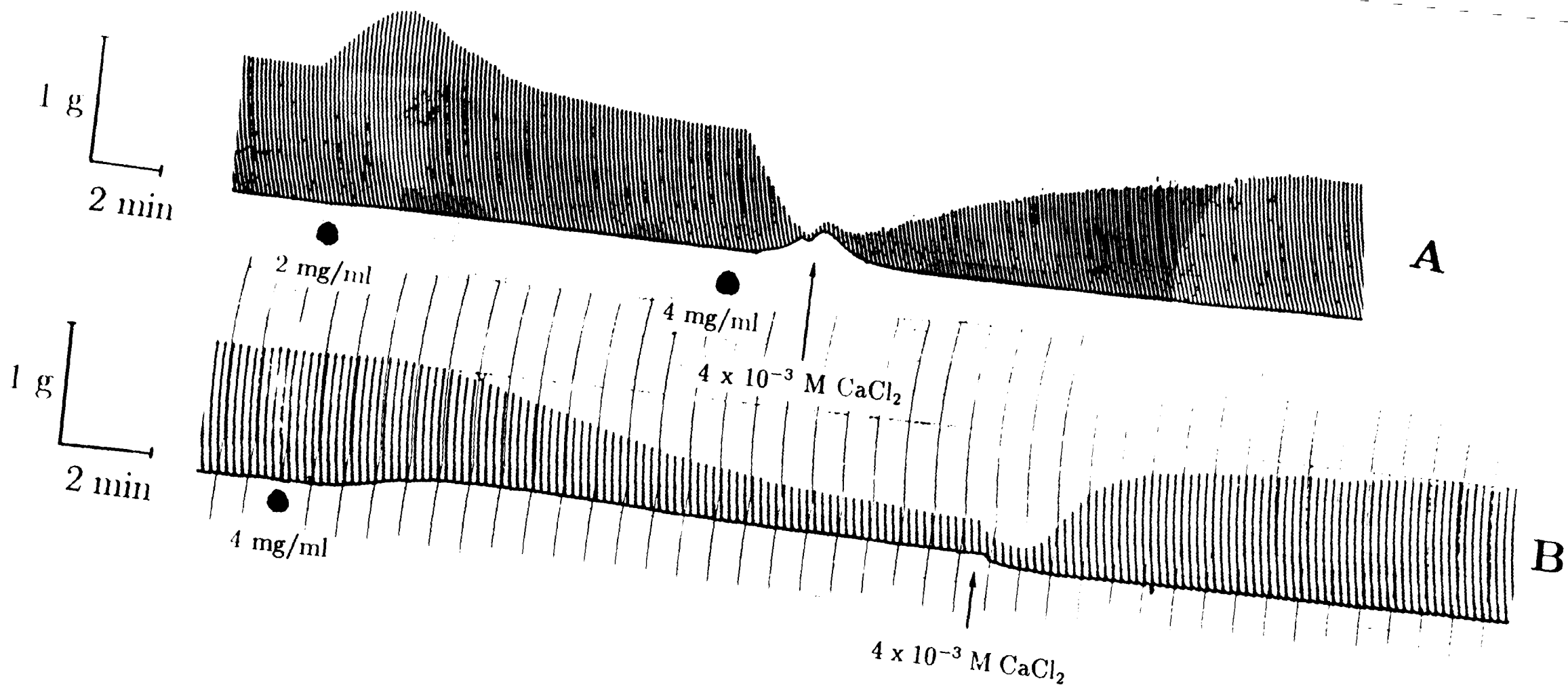
Fig. 6.2: Recovery of twitch depression caused by 4 mg/ml of the ethanol extract of *P. oleracea* by 4×10^{-3} M $CaCl_2$. (A) Twitch depression to NS preparation. The extract was added in cumulative doses shown by dots and $CaCl_2$ was added at the point shown by an arrow. (B) MS preparation.

1 g

2 min

4×10^{-3} M $CaCl_2$

4 mg/ml of the ethanol extract
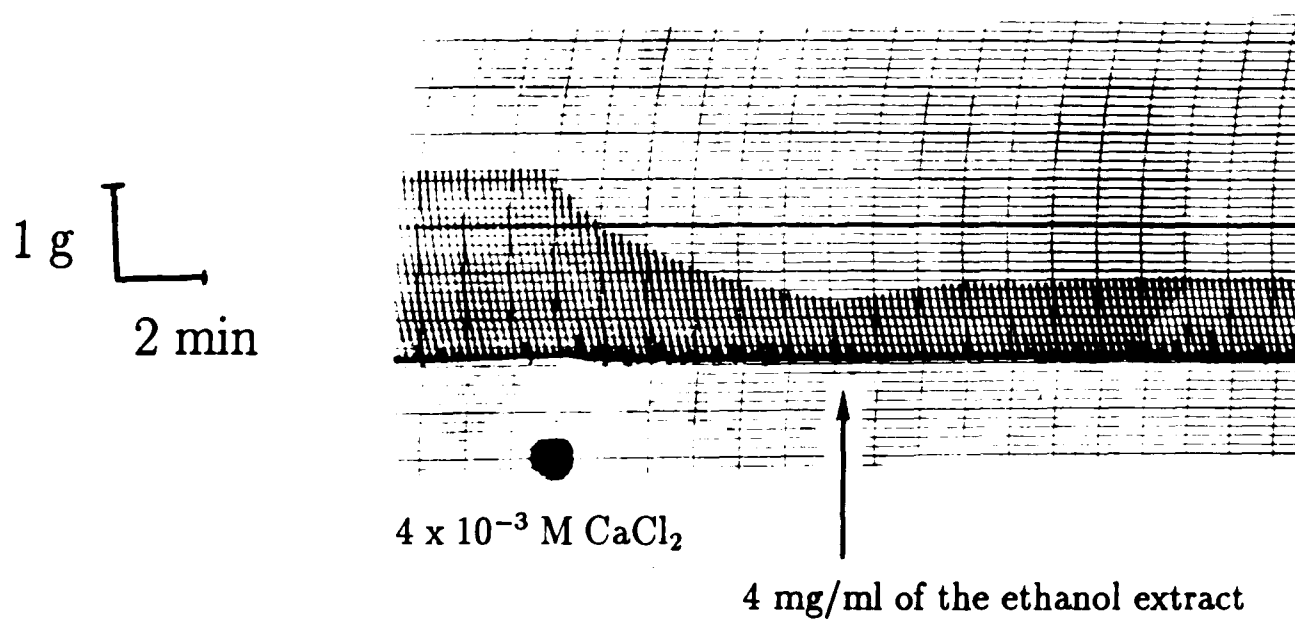
Figure 6.3: **Depression of Twitch (NS) by** $CaCl_2$

(Fig. 6.3). It could be inferrd therefore that whatever mechanism was involved, the effect of the extract was contradictory to that of excess Ca^{2+} ion in the physiological solution.

6.4.2 Fractionation of the crude extract

The crude extract of the leaves of *P. oleracea* was fractionated into various parts with solvents of increasing polarity (Scheme 6.1).

Evaluation of these fractions for muscle relaxant property using the chick biventer cervicis muscle preparation showed that the hexane and chloroform frac-

CRUDE ETHANOL EXTRACT, 23 g

Hexane/H₂O Partitioning

HEXANE, 7.555 g   WATER

CHCl₃/H₂O Partitioning

CHLOROFORM, 0.116 g   WATER

EtOAc/H₂O Partitioning

ETHYL ACETATE, 0.385 g   WATER

n-Butanol/H₂O Partitioning

n-BUTANOL, 2.593 g

WATER, 12.25 g
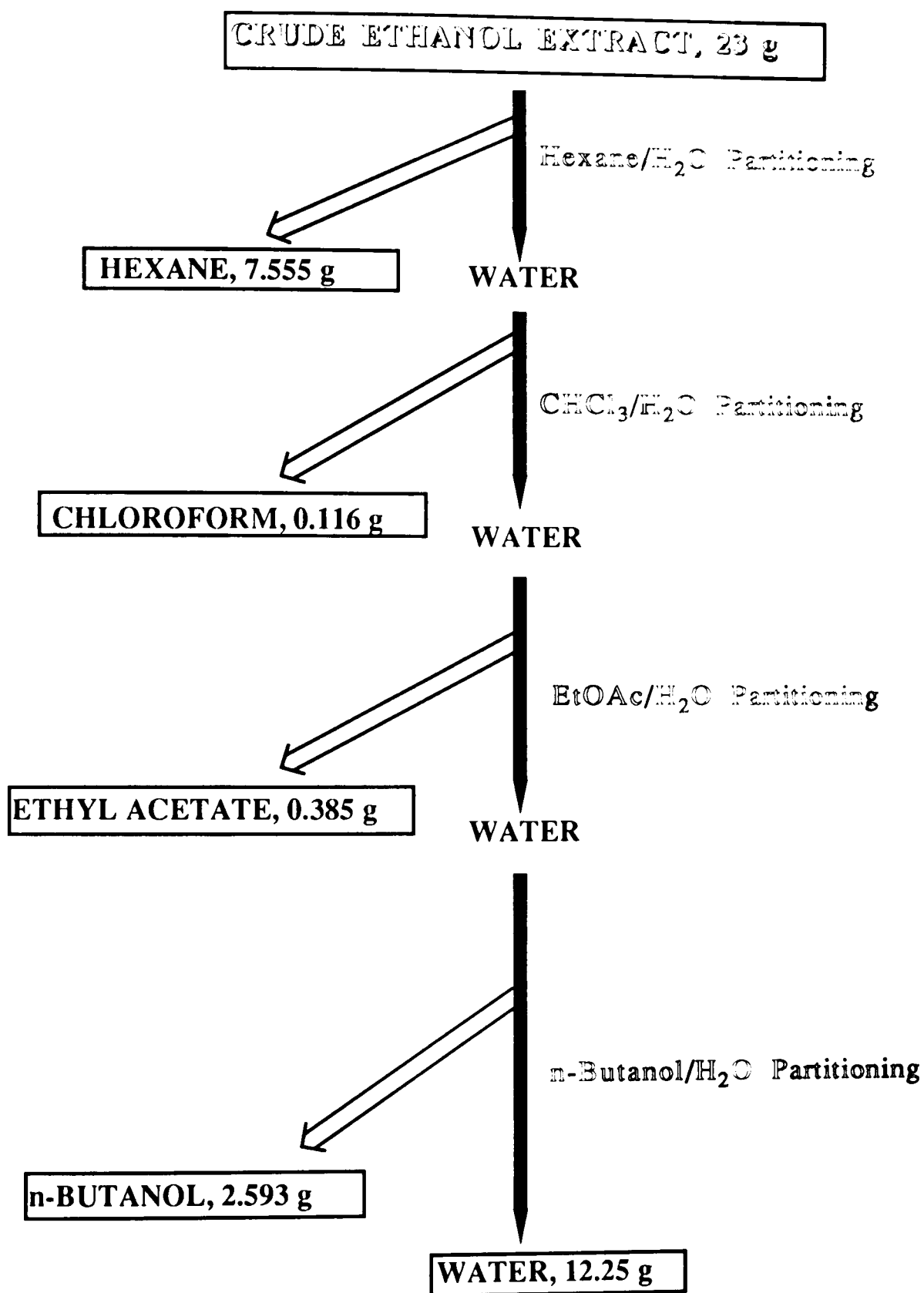
Scheme 6.1. Fractionation of crude ethanol extract of *P. oleracea*

tions did not contain the active principle(s). No activity was observed at 4 mg/ml solution of these two fractions; twice the LCD-100% of the crude extract. The ethyl acetate fraction had a comparable activity with that of the crude extract (LCD-100%, 2mg/ml). The water and butanol fractions were, however, the most active fractions with the LCD-100% $\leq$ 1 mg/ml and 1 mg/ml respectively.

This highly hydrophilic nature of the active principle(s) together with the quick onset of action and recovery profile (which is unlike that expected for organic compounds) suggested that possibly excess inorganic cations in the extract were responsible.

6.4.3 Level of inorganic ions in *P. oleracea* leaves extract and muscle paralysis

Occurence of high levels of Na^+ and K^+ ions in the leaves of *P. oleracea* has been documented (FAO, 1988). Altering the Na^+ ion concentration in the extracellular medium however did not produce significant effect on the conductivity of excitable tissues (Covino and Vassalo, 1976) and hence Na^+ ions in the extract was not expected to cause the observed pharmacological activity for the extract. Excess K^+ ions, however, has pronounced effect on the excitability of nerves and skeletal muscles and could quickly cause a depolarization block. For this reason, the crude extract and all active fractions (ethyl acetate, butanol and water) were analysed for their level of K^+ ion.

The level of potassium in the ethanol extract and various fractions were analysed directly using a flame photometer. The crude ethanol extract, ethyl

acetate butanol and water fractions were found to have 9.04, 12.2, 18, and 28% of potassium by weight respectively. Since the potency of these three fractions and the crude ethanol extract (water fraction $\geq$ butanol > ethyl acetate $\cong$ crude extract) was in the same order as the level of the potassium in the samples, the effect of potassium (as a drug) on the chick biventer cervicis preparation was also studied.

KCl was found to cause depression of twitch height in the same manner as shown for the ethanol extract (Fig. 6.4). This effect (LCD-100%, 320 μg/ml) was preceded by twitch augmentation and high doses ($\geq$ 400 μg/ml) also induced contracture. Moreover, the pharmacological activity and the level of potassium in KCl and the extracts were correlated. In both cases, 45 and 90 μg/ml of K$^+$ caused twitch augmentation, concentrations up to 180 μg/ml caused twitch augmentation followed by depression of twitch and higher doses induced contracture and abolished twitch height without being preceded by twitch augmentation. Interestingly, 100% depression of twitch height caused by KCl (600 μg/ml) could be reversed by 2 x 10^{-3} M CaCl$_2$ and *vice versa* in the same manner as described for the interaction of the extract and CaCl$_2$.

6.4.4 Bioassay of K$^+$ free extracts of *P. oleracea*

In order to rule out the possible contribution of organic compound(s) (or chelater) to the observed pharmacological activity, attempts were made to remove inorganic cations and evaluate the activity of K$^+$ free sample. The most active fraction obtained from the crude ethanol extract (water) was passed through

1 g

2 min

200 μg/ml

400 μg/ml
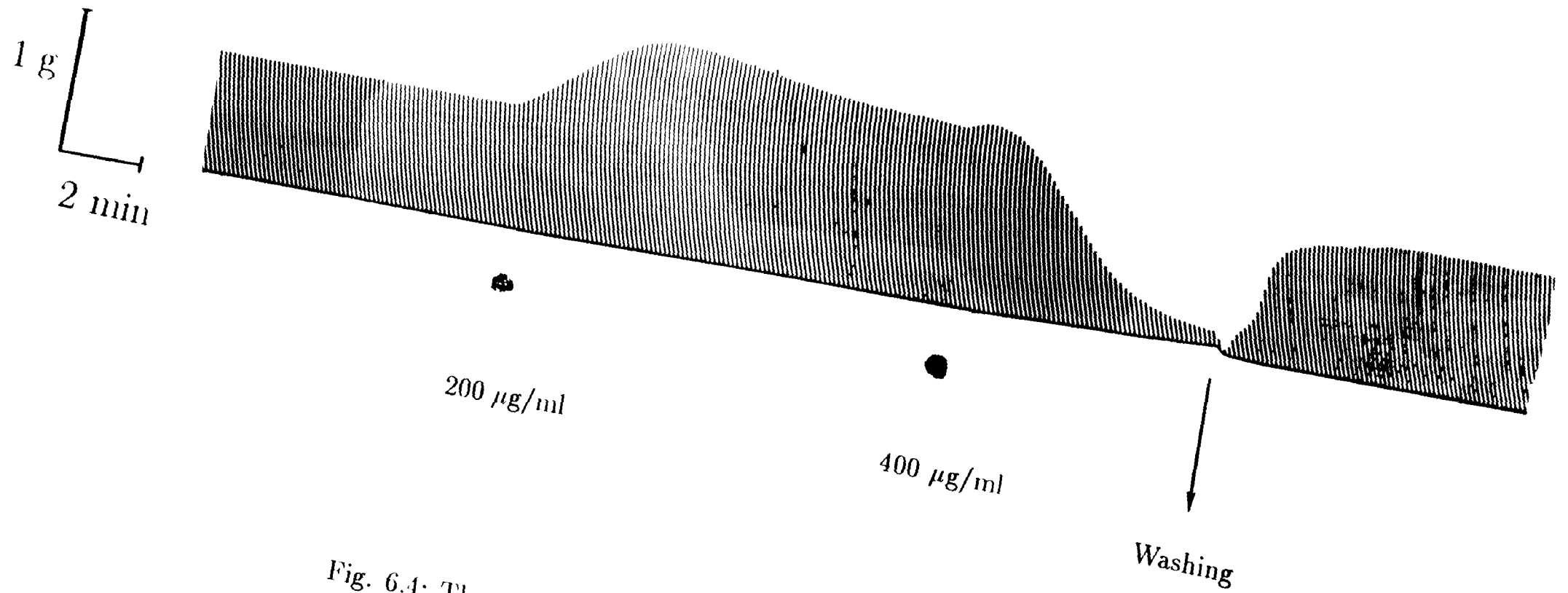
Washing

Fig. 6.4: The effect of 200 and 400 μg/ml (cumulative doses) of KCl on NS chick biventer cervicis preparation. Recovery of twitch by washing is shown by a downward arrow.

a long column of cation exchange resin (Dowex 50W-X8(H), activated by dilute HCl and eluted by water). The muscle relaxant effect of the water fraction (LCD-100%, ≤ 1 mg/ml) was completely lost after passing through this cation exchange resin. Up to 7.7 mg/ml of this fraction did not show either twitch augmentation or depression of the chick biventer cervicis muscle preparation (Fig. 6.5). The same was also observed for the direct water extract of the leaves. The presence of active organic compound contributing to the paralysis effect at the concentrations tested was therefore unlikely.

Excess and toxic level of oxalate in the leaves of *P. oleracea* occur paralally with inorganic cataions (Singh and Saxena, 1972). Recently, potassium oxalate was proved to be the active principle for the muscle relaxant property of banana juice (Benitez *et al* ., 1991) which acts in the same manner as the leaves extract of *P. oleracea*. The mechanism of potassium oxalate however is not yet established but Benitez *et al.* (1991) suggested a postjunctional phenomenon, primarily by reducing the level of Ca^{2+} ion through oxalate chelation. It can be argued that the excess oxalic acid in *P. oleracea* leaf extracts could chelate extracellular Ca^{2+} and hence affect the influx of "trigger" Ca^{2+} necessary for the release of Ca^{2+} from the SR. The failure of the extract to produce muscle paralysis after the removal of cations however showed that oxalic acid in the plant extract did not have any effect at the concentrations tested.

It seems that the muscle paralysis property of *P. oleracea* is due to its high level of K^+ which was also shown to be responsible for the diuretic property of the plant (Yasuye and Honda, 1944). All the *in vitro* pharmacological effects

1 g

2 min

1 mg/ml

Washing

A

7.7 mg/ml

B
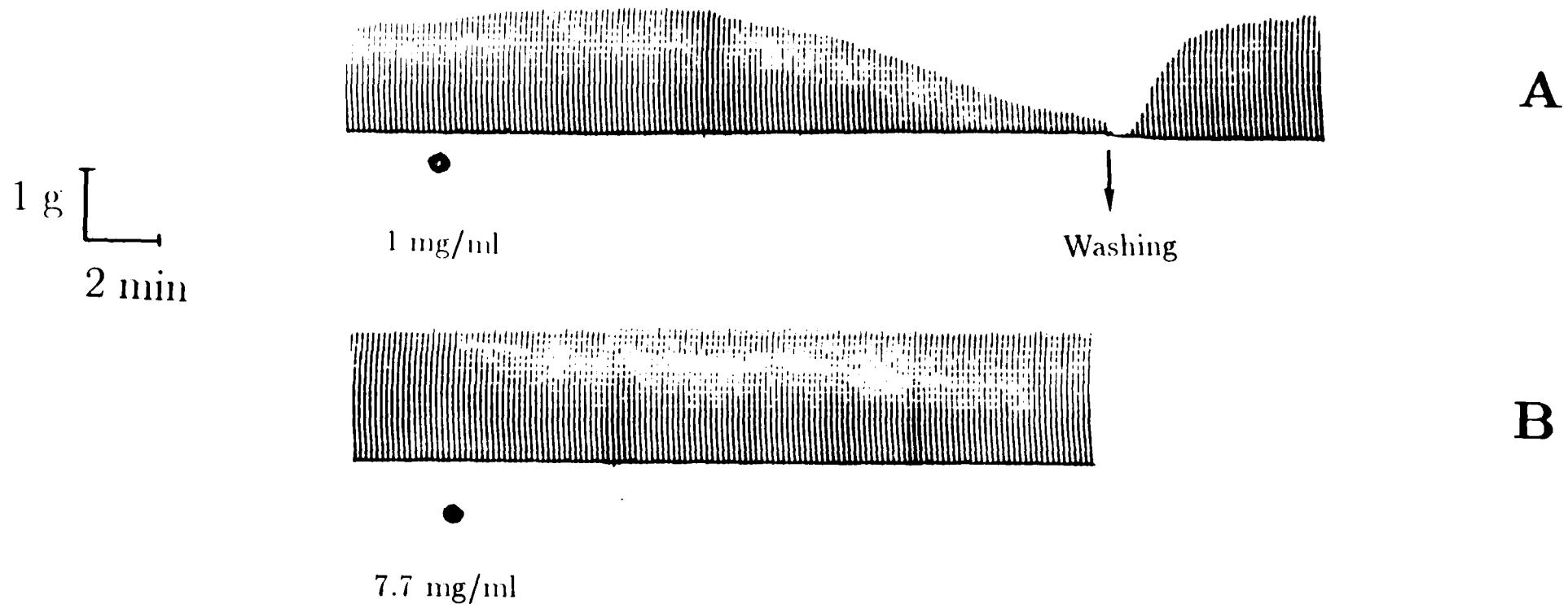
Fig. 6.5: Twitch depression of the NS chick biventer cervicis preparation by 1 mg/ml of the water fraction (**A**) and 7.7 mg/ml of the water fraction after passing through the cation exchange resin (**B**).

observed for *P. oleracea* in this study and also by previous authors could also be explained by the high level of K^+ in the extract. For example, Ca^{2+} stabilizes excitable tissues while K^+ sensitizes them at lower concentration and causes a depolarisation block at higher concentrations. The interaction of the extract with $CaCl_2$ or dependance on the level of Ca^{2+} ion in the physiological solution, blockade of the extract induced twitch augmentation and K^+ induced contracture by calcium antagonist (D-600) are then all expected. Since nerves are much more sensitive to conduction blockade by drugs than skeletal muscle, the higher sensitivity of NS muscle preparations to the extract than MS preparations could also be explained by the depolarization block caused by K^+. As described in Section 6.3, *i.v.* administration of the lethal dose of the leaves extract of *P. oleracea* causes flaccid limb paralysis in chick (Okwuasaba *et al*, 1987b). This has been explained by a post junctional phenomenon possibly due to active principle(s) acting like that of *d*-tubocurarine. Although muscle paralysis by K^+ is caused by a depolarization blockade, a high level of K^+ ions *in vivo* (in chick) first causes cardiac arrest before muscle paralysis and results in a flaccid limb paralysis (Bowman and Rand, 1980).

It is still not clear how K^+ ions could be absorbed through the skin when applied topically to relieve pain and cause muscle paralysis. Chelation with organic compounds like oxalate could however assist this process. This is the case awaiting further studies, but for the time being at least the *in vitro* pharmacological effect observed for *P. oleracea* appears to be due to the high potassium content of the plant.

211

6.5 EXPERIMENTAL

6.5.1 Preparation of the extract

Fresh aerial parts of *P. oleracea* were supplied by The Scottish Agricultural College, Auchincruive, and kept frozen until use. 1.3 kg of leaves of this frozen sample was ground in a blender and continually extracted by percolation with ethanol. Removal of the solvent under reduced pressure afforded 23 g of residue. The crude extract was then suspended in water and fractionated as shown in Scheme 1.

6.5.2 Chick biventer cervicis preparation

The chick biventer cervicis preparation was set up according to a standard procedure (Perry *et al.*, 1970). 7-10 days old chicks were killed with ether and the two biventer cervicis muscles were dissected out. A pair of these tissues were set up in a 10 ml organ bath containing Krebs-Henseleite solution of the following composition (mM): NaCl (118.4), KCl (4.7), $CaCl_2$ (2.5), $NaHCO_3$ (25), $MgSO_4$ (1.2), KH_2PO_4 (1.2) and glucose (11). The perfusion mixture was continually gassed with 95% O_2 and 5% CO_2 mixtures and the temperature was maintained at 32° C. Recording of twitch contraction was made by means of a Grass force-displacement transducer (FT03 C) tracing its course on a paper attached to either a Grass Poligraph Recorder (Model 79B) or Oscillograph 400 MD/Z moving at a speed of 5 mm per minute. The nerve was stimulated by a rectangular wave pulse of 0.2 ms duration and frequency of 1 Hz, delivered with

a Grass S88 stimulator *via* a Grass SIU5 stimulus isolation unit pulse generator, using a supramaximal voltage of 20 V. Direct muscle stimulation was performed in the presence of 2×10^{-5} M *d*-tubocurarine using a pulse of 1 ms duration, frequency of 1Hz and a voltage of 40 V. The tissue was stretched until the maximum twitch height was obtained and left to equilibrate for 30 minutes before the commencement of the experiment.

A stock solution of all extracts was prepared by dissolving 500 mg of the samples in 5 ml of physiological solution. The resulting solution was acidic (pH $\cong$ 3) and this was neutralised (pH = 7.4) by the addition of dilute NaOH. Drugs were added in a cumulative dose regime and all concentrations shown here are final bath concentrations. For each drug/extract, results are obtained from experiments on six preparations.

6.5.3 Analysis of K^+ in the extract

Extra care has to be taken to avoid contamination of samples with inorganic salts. All glassware was treated with 1% HNO_3 prior to washing and de-ionised distilled water was used both for washing and preparation of samples.

A standard K^+ solution with concentrations ranging from 0-4 $\mu g/ml$ was prepared. After calibrating each solution with 0.5% NaCl and 10^{-2} M HCl, absorbance at 766.5 nm was measured by aspirating the solution into an acetylene flame using a Philips PU 9100 atomic absorption spectrometer. A standard curve (concentration against absorbance) was then plotted from which the level of K^+ in the extract could be analysed.

A duplicate solution of each plant extract (1 mg/ml) was prepared in distilled water. Absorbance at 766.5 nm was measured as described for standard K^+ and mean results were correlated with K^+ concentration from the standard curve. The level of K^+ analysed in the solution was then converted to a percent dry weight of the extracts.

Chapter 7

STUDIES ON THE LOCAL

ANAESTHETIC PROPERTIES

OF *PENTAS SCHIMPERIANA*

7.1 INTRODUCTION

7.1.1 Distribution and botanical description

Pentas schimperiana Rich. is a spreading shrub belonging to the family Rubiaceae. The species is found in the mountainous regions of Ethiopia, Kenya, Malawi, Tanzania, Uganda and Zaire (Cufodontis, 1972). Botanically the species is described as follows (Court, 1976): shrub or woody herb (0.3-)1.3-2.7(-5) m tall, with wrinkled blackish or purplish-black woody stems, at first densely rusty pubescent (at least when dry), later glabrescent. Leaf-blades ovate, ovate-lanceolate or ovate-oblong, 6-21 cm long, 1.8-8 cm wide, acute to acuminate at

the apex, cuneate to round at the base, adpressed rusty hairy above and on the characteristically reticulate (but not prominent) venation beneath: petiole 0-1.5 cm long from a variable base 3-8 mm long, 4-8 mm wide; these bases conate and forming persistent cups at the nodes on old stems. Inflorescences branched, 2.5-1.5 cm wide; peduncles up to 1.5 cm long, velvetly pubescent. Calex-tube hairy outside, either 1/3-1/2 the lengh of the corolla-tube or approximately equalling it. Corolla white, often tinged pink, or entirely pinkish, glabrous or pubescent; in long-styled flowers, tube funnel-shaped 0.5-1.3 cm long, dilated at the apex for 2 mm; in short-styled flowers the tube is cylenderical, 0.5-1.4 cm long; lobes 3-7 mm long, 0.75-2.5 mm wide, the tips thickened and inflexed, style exerted for 0.5-5 mm long in long-styled flowers. Fruit 4-6 mm long and wide, the persistant calyx-lobe often reflexed, loculicidially into 2 locci.

7.1.2 Medicinal values of *Pentas schimperiana* and objective of the present srudy

In the central region of Ethiopia where the plant is locally called "WOY-NAGIFT", some medicinal uses have been documented (Abate and Taddesse, 1976). The flower is used for eye diseases (as an ointment) and the leaves (juice or water extract) for treating ear-ache administered as drops. Related species such as *P. longituba* and *P. purpurea* are used for treating fever and rheumatic pain (Watt and Breyer-Brandwijk, 1962). *Pentas* species are also known as drastic purgatives in some countries (Watt and Breyer-Brandwijk, 1962).

Since traditional herbal drugs involved in the treatment of eye diseases

have sometimes proved to have antibacterial activity (see Chapter 3), preliminary antimicrobial screening was undertaken on this plant. However, no significant antibacterial activity was observed for the ethanol extract of the aerial parts. Alternatively, the medicinal value of this plant might be the result of anaesthetic or analgesic actions. The primary objective of this project was to assess the possible local anaesthetic effect of the extract of *P. schimperiana*.

7.2 RESULTS AND DISCUSSION

7.2.1 Effect of the ethanol extract on nerve conduction

The *in vitro* local anaesthetic property of the extract of *P. schimperi-ana* was studied using a frog (*Rana pipiens*) sciatic nerve preparation (Schwartz, 1971). A typical externally recorded compound action potential obtained from the frog sciatic nerve preparation is shown in Fig. 7.1. A decrease in the height of these action potentials following exposure of the nerves to the extract (Fig. 7.1) indicates a blockade of conduction in indvidual nerve fibres. In general, the ethanol extract of *Pentas schimperiana* was found to depress the CAP of the frog sciatic nerve in a dose dependant manner (Fig. 7.2). The ED_{50} of the extract and lignocaine hydrochloride were found to be 22.5 mg/ml and 0.5 mg/ml respectively (Fig. 7.3).

A bioassay guided fractionation of the ethanol extract was carried out in order to isolate the active principle. Partitioning of the crude ethanol extract of *Pentas schimperiana* into chloroform/water showed that the aqueous fraction

217

2.5 mV

2.05 ms

A

B

C
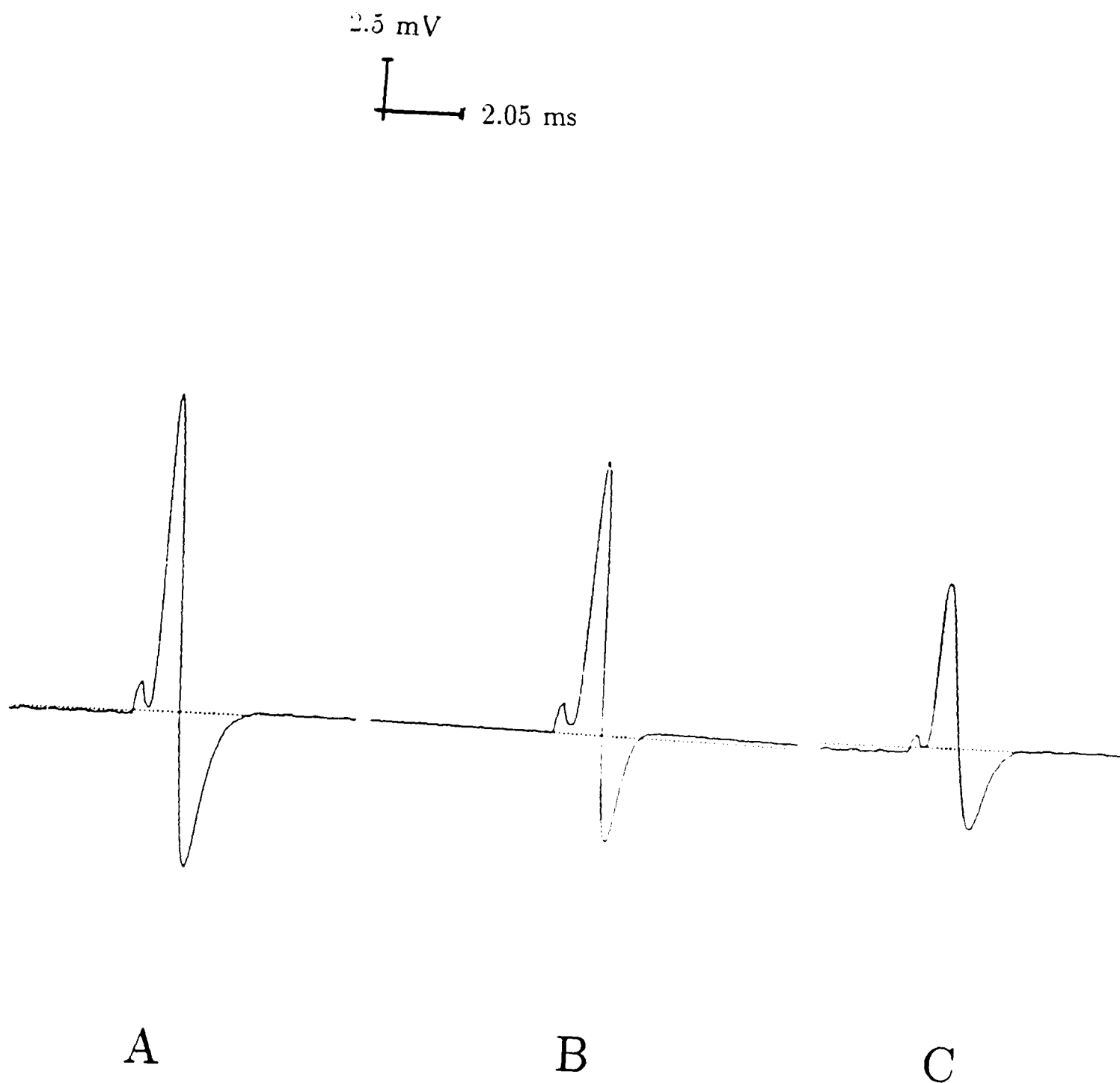
Fig. 7.1: Actual plots of action potentials. CAPs recorded at 0 (**A**), 1 (**B**) and 3 (**C**) minutes after the introduction of 20 mg/ml of the ethanol extract of *P. schimperiana*.
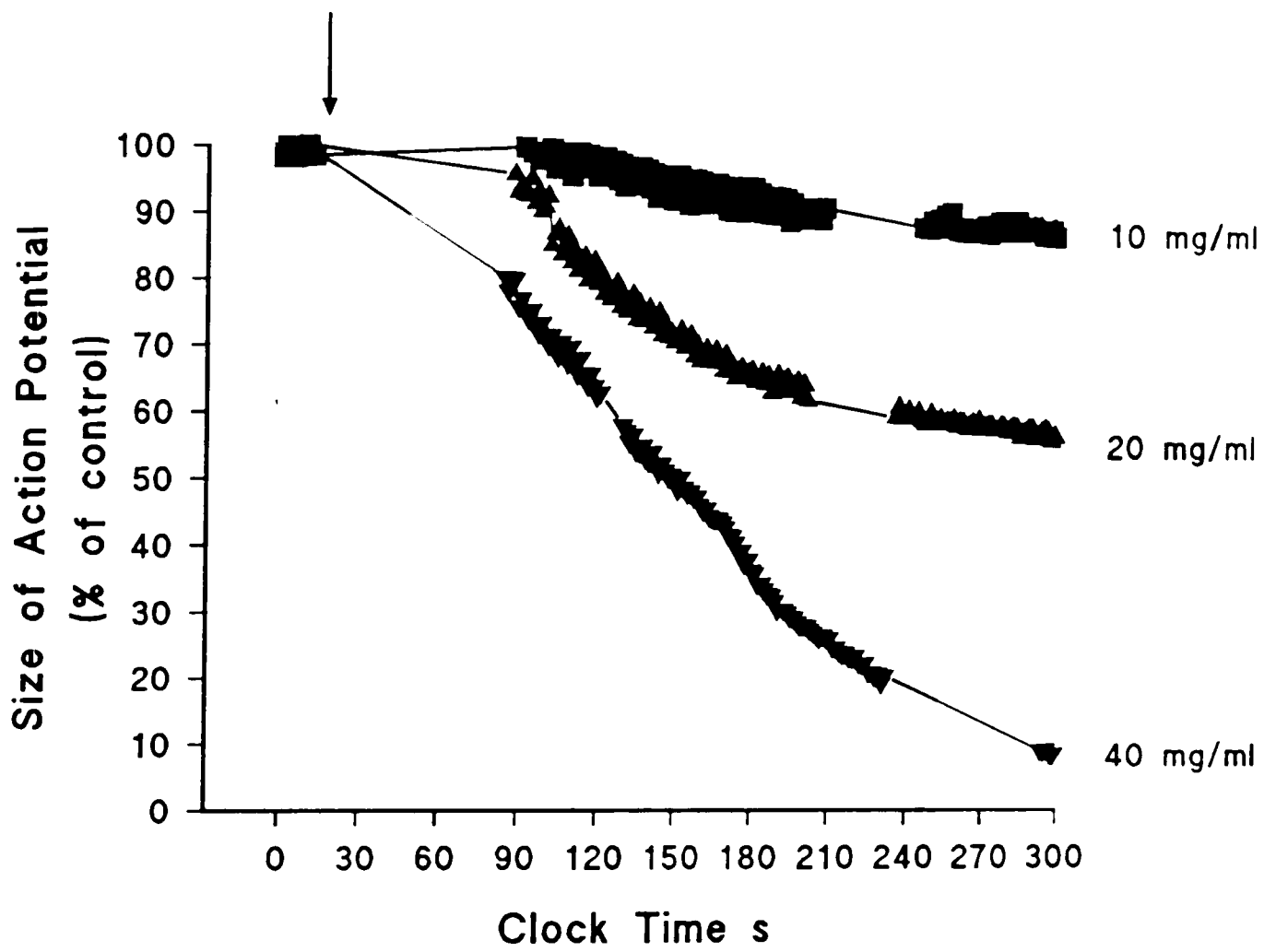
Fig. 7.2: The effect of ethanol extract of *P. schimperiana* on rate of conduction block. Peak value of CAPs recorded from the representative experiments. Each concentration of the extract was added after the 10th CAP indicated by the arrow. Recording was started soon after drug perfusion was stopped.
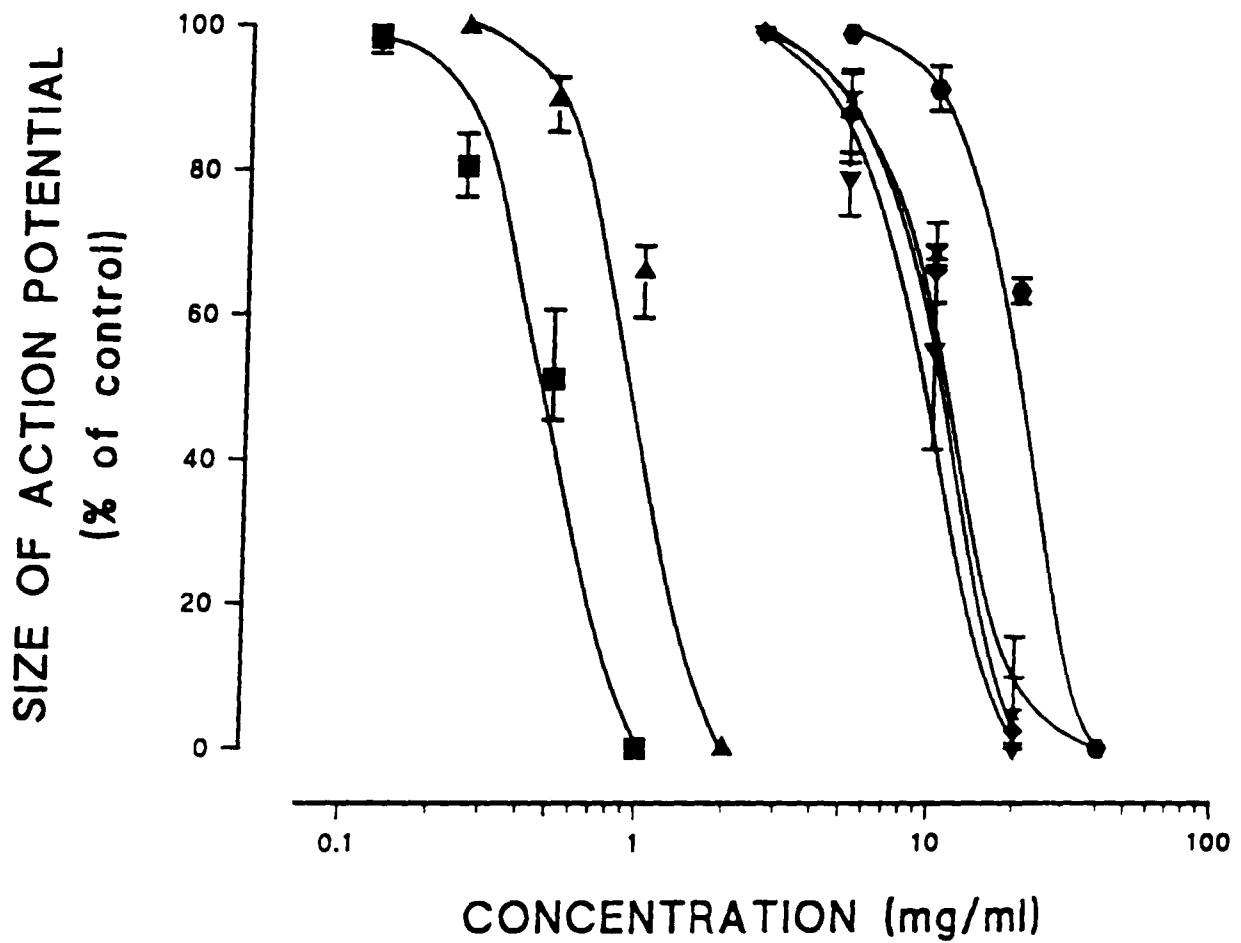
Fig. 7.3: The effect of Lignocaine, KCl, and various plant extracts on nerve conduction. Mean value (n=4) of CAPs were recorded 250 minutes after the introduction of plant extracts and drugs.

was active. The ethyl acetate extract of this active fraction was also found active but did not lead to any organic compound when subjected to further purification by column chromatography (silica gel 60). It was necessary then to analyse the inorganic constituents of active fractions and crude extract.

Moderate alteration of Na^+ concentration has no effect on excitable tissues (see Section 6.4.3). However, the interaction of K^+ and Ca^{++} with local anaesthetics and its effect on this preparation are well documented (Bondani and Karler 1970; Covino and Vassallo, 1976).

Earlier *in vitro* and *in vivo* (including man) studies have shown that some ions, particularly K^+, could enhance the activity of local anaesthetics and hence reduce the dose required for a particular effect (Covino and Vassallo, 1976).

7.2.2   Effect of K^+ and Ca^{++} ions on nerve conduction

Inorganic ion analysis of the *Pentas schimperiana* extracts showed that the ethanol and water extracts contained 0.02 and 0.4% Ca^{++} (w/w) respectively. Ca^{++} ions at the concentrations present in each dose did not have any effect on the CAP of the frog sciatic nerve when added to the Ringer solution. KCl however, depressed nerve conduction in a dose dependant manner at concentrations higher than 0.5 mg/ml or 6.76 mM (excluding KCl in the Ringer solution)(Fig. 7.3). The concentration of K^+ ion which produce significant nerve conduction blockade was found to be present in the crude extract (Fig. 7.4). K^+ analysis using the ashing method showed that 1.6% of the dried plant material was K^+. This was not an exceptionally high figure as the level of K^+ in plants can vary from 0.1

221

- KCl
- *Pentas schimperiana* (EtOH extract)
- *Pentas schimperiana* (H₂O extract)
- *Premna schimperi*

Mean ± S.E. (n=4)
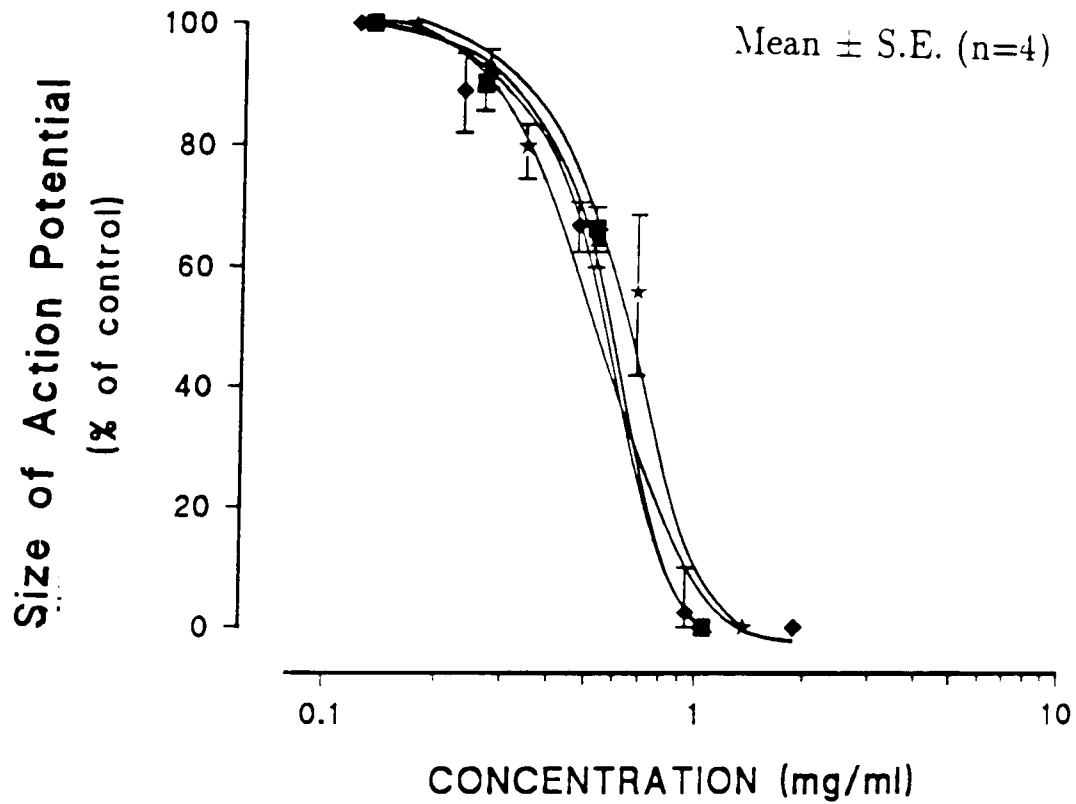
Fig. 7.4: Correlation between K$^+$ concentration in various extracts and conduction block. Mean value (n=4) of CAPs were recorded 250 minutes after the introduction of plant extracts and KCl. The size of CAPs were then correlated with the level of K$^+$ ions available at the concentration of the extracts (or KCl) used.

up to 5% (Scott et al., 1971). The level of K^+ in the dried leaves of *Premna schimperi*, for example, was comparable with that of *Pentas schimperiana* (Table 7.1). The concentration of K^+ in the ethanol extract of *Premna schimperi*, however, was found to be only 0.07% w/w (cf. 3.65% for *Pentas schimerina*- see Table 7.1) and the extract produce no conduction blockade even at concentrations higher than 160 mg extract/ml. This K^+ ions in *Pentas schimperiana* are thus believed to be in a more extractable form to account the observed activity.

SAMPLE	% K^+ (w/w) in the sample		
	Dry Sample	Ethanol extract	Water extract
Pentas schimperiana	1.60	3.65	6.80
Premna schimperi	1.69	0.07	4.69

Table 7.1: **Level of K^+ in dry sample and extracts of** *Pentas schimperiana* **and** *Premna schimperi*

While it is uncommon to extract excess inorganic ions by organic solvents, the water extract is invariably rich in potassium. The water extract of *Lagarosiphon major*, a plant which contains less K^+ in the dry weight than *Pentas schimperiana*, also showed comparable activity (Fig. 7.3). As compared with the ethanol extracts, the water extracts of *Pentas shimperiana* and *Premna schimperi* contained excess K^+ (Table 7.1) and could depress CAP (ED_{50} 10-13 mg/ml, Fig. 7.3) more than the ethanol extract. This activity was again correlated with the level of K^+ in the water extracts (Fig. 7.4).

Lignocaine is a local anaesthetic of short duration (Luduena, 1969) and only 25-30 minutes was required for a complete recovery of the nerve from 50-60% blockade (Table 7.2). Even from a 100% blockade by the various plant extracts, the time required for the CAP to return to its control amplitude was much shorter (2-4 minutes, Table 7.2). This is a feature also observed for K^+ (Table 7.2) and gives additional evidence that K^+ is the major factor for the observed nerve conduction blockade by the extracts.

The water and ethanol extracts of *Pentas schimperiana* were also found to be active on the sheathed frog sciatic nerve preparation. It is important also to note that the ethanol extract of *Pentas schimperiana* is acidic (pH of 20 mg/ml solution was 3.1) and depresses nerve conduction (ED_{50} 12 mg/ml) about twice as much as an extract maintained at pH 7.4 (Fig. 7.5). A 1 mg/ml solution of KCl which produces 50-60 % blockade of nerve conduction could cause a 100% blockade when the pH was lowered to 3.1 and thus the better activity of the extract (pH not adjusted) was not due to other factors.

It is difficult to generalize what would happen in *in vivo* or when people use the juice or the water extract of *Pentas schimperiana* to relieve pain. The biological activity observed in this experiment was attributed to the physical property of the extract rather than a genuine local anaesthetic activity. K^+ in *Pentas schimperiana* also seems to be highly extractable and could cause significant activity on nerves *in vivo* if it is absorbed from the site of application.

This result and studies on *Portulaca oleracea* (Chapter 6) clearly demonstrated the role of K^+ as a pharmacological agent. Such action could be valuable

♦ pH adjusted to 7.4

★ pH not adjusted ($\cong$ 3.1)

Mean ± S.D. (n=5)
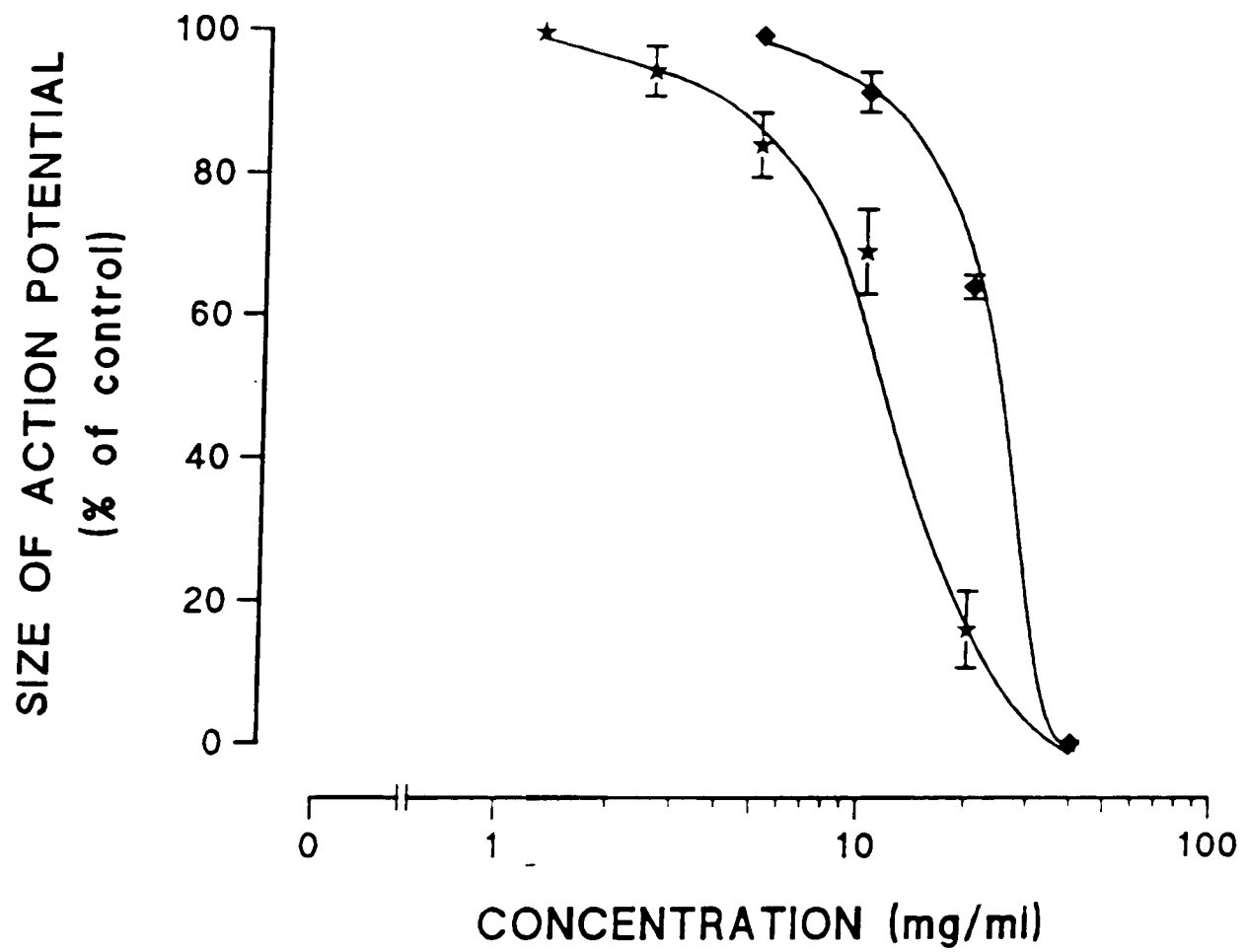
Fig. 7.5: The effect of pH on conduction block. Conduction block by the ethanol extract of *P. schimperiana* at pH adjusted to 7.4 and pH not adjusted ($\cong$ 3.1).

in relieving pain when the extracts are introduced locally. As described in Chapter 6, chelation with organic compounds could assist the absorption of K^+ in to a biological system and may account for the effectiveness of these plants as pain relieving agents. More importantly the experiment demonstrates that care must be taken when one examines the effect of water extracts, particularly on excitable tissues like nerves and heart tissue.

DRUG	TIME (minutes)
Pentas schimperiana	
(Ethanol extract)	2.8375 ±0.19
(Water extract)	2.8575 ±0.19
Premna schimperi	
(Water extract)	3.7825 ±0.19
Lagarosiphon major	
(Water extract)	3.2050 ±0.13
Lignocaine hydrochloride	27.4500 ±1.13
KCl	2.7475 ±0.20

Table 7.2: **Duration of action of various plant extracts, KCl and lignocaine hydrochloride.** Following the exposure of the nerve to the drugs (50-60 blocking dose of extracts and KCl) for 250 seconds, the drugs were removed and the time required for the CAP to return to its control amplitude was recorded.

N=4, Data with standard error

7.3 EXPERIMENTAL

7.3.1 Plant material and reference drug

The leaves of *Pentas schimperiana* were collected in September 1989 from Menagesha Forest, Menagesha Administrative Region (*ca.* 2800 m), Shoa, Ethiopia. A voucher specimen (SHM-15) was deposited at the National Herbarium of Ethiopia, Addis Ababa University. The leaves of *Lagarosiphon major* was obtained from the Commission of the European Communities, Community Bureau of Reference (B.C.R.), Reference material No. 60. Lignocaine hydrochloride (BP) was used as a standard local anaesthetic agent.

7.3.2 Preparation of extract

The cold ethanol extract of all plant materials (aerial parts of *Pentas schimperiana* and the leaves of *Premna schimperi* and *Lagarosiphon major*) were obtained by soaking 100 gm of the samples in two litres of absolute alcohol for two weeks. The solvent was then removed under reduced pressure using rotary evaporation. For water extraction, 50 gm of each sample was soaked in 500 ml of distilled water for five days. In order to avoid contamination of samples with potassium salts, all glassware was treated with 1% nitric acid and washed with distilled water before use. All doses of extracts were prepared in 10 ml of frog Ringer solution from a stock solution of 80 mg/ml.

Since the response of frog sciatic nerve preparation to local anaesthetic vary depending on the acidity or alkalinity of the medium (Ritchie *et al.*, 1965),

the pH of the test solution (extract in Ringer solution) was adjusted to 7.4 prior to the experiment.

7.3.3 Fractionation of the crude extract

The crude ethanol extract was partitioned into chloroform/water. Bioassay of these fractions showed that the aqueous fraction was active. Further partitioning of this active fraction into ethyl acetate/water showed that both fractions were active; activity being concentrated in the water fraction. A subsequent bioassay-guided fractionation (column chromatography, silica gel 60) did not gave any organic compound and led to the assumption that the observed activity was probably due to an excess of inorganic ions in the extract.

7.3.4 Analysis of Na^+ and Ca^{++} in plant specimens and extracts

Each plant specimen (1 g) was weighed into 30 ml silica crucibles. The samples were then placed in an oven at $120^\circ C$ and left overnight for drying. The dried samples were ashed by placing the crucibles in an oven at $450^\circ C$. 6M HCl (2 ml) was added to each ashed sample and left to dryness. The level of K^+ in these samples and plant extracts were then analysed using a standard procedure (see Chapter 6, page 213).

The Ca^{++} levels in the extracts were determined from the water solution as described for K^+ but, in the latter case, absorbance was read at 422.7 nm.

7.3.5   Local anaesthetic assay

The effect of extracts on nerve conduction was studied using a frog (*Rana pipiens*) sciatic nerve preparetion (Schwartz, 1971). The two sciatic nerves from each frog were dissected from their origin in the spinal cord down to the knee. Each nerve was partially desheathed by splitting the nerve in half by dissecting away the peroneal nerve which runs as a distinct bundle beside the sciatic nerve. The 2-3 cm length of nerve was then placed into a perspex recording chamber consisting of three pools of diameter 15 mm and 8 mm deep spaced 3 mm apart, filled with the frog Ringer solution.

The nerve was stretched across the centre pool with its ends dipping into each of the end pools. At the junction between pools the nerve was laid upon vaseline barriers and covered with the second layer of vaseline, to keep the solution in each pool apart. The centre pool was connected to the ground of the recording system.

The nerve was stimulated by applying 3-10v pulses lasting 50-100 μs, from a Grass S48 stimulator *via* an SIU5 stimulus isolation unit, between one of the end pools and the centre. The compound action potential (**CAP**) was recorded using a high gain (X1000-1500) AC coupled recording system (Neurolog NL105 + NL106), measuring the potential between the centre pool and the other end pool. The CAP recorded in this fashion was in the region of 8-18 mV in height and lasted 1-2 ms.

The frog Ringer solution was of the following composition: 120 mM NaCl, 2.5 mM KCl, 1.8 mM $CaCl_2$, 1 mM HEPES (N-[2-hydroxyethyl]-piperazine-

N'-[2-ethanesulfonic acid]) and the pH was adjusted at 7.4. The extracts and reference drug were applied to the centre pool by exchanging the solution using a two channel peristaltic pump controlling inflow and outflow. 10 ml of Ringer solution containing each extract dose was pumped through the pool to ensure complete exchange of solutions and this was accomplished within 1.25 minutes. The extracts were then washed out using 20 ml of Ringer solution.

CAPs were recorded and stored on disc for analysis, using an IBM PC AT personal computer, *via* a Data Translation DT2801A laboratory interface card. Stimulus pulses were applied at a rate of 1/sec, but to economise on the use of disc space, recording was interupted at some points 300 records being collected for every dose of extract tested.

Part III

PHYTOCHEMICAL

INVESTIGATION OF

LEONOTIS OCYMIFOLIA **var**

RAINERIANA

Chapter 8

PHYTOCHEMICAL

INVESTIGATION OF

LEONOTIS OCYMIFOLIA var

RAINERIANA

8.1   Introduction

8.1.1   Distribution and botanical description

Leonotis ocymifolia (Burm. f.) var *raineriana* (Visiani) Iwarsson is a
plant belonging to the family Labiatae. The plant is widely distributed in East-
ern (Cufodontis, 1972) and Southern Africa (Codd, 1985). In Ethiopia, voucher
specimens of the plant has been collected from almost every part of the coun-
try between the altitudinal range of 2500 and 2800m. Codd (1985) described

L. ocymifolia as follows: Shrub 1-5 m tall, branching from a thick woody base; internodes 20-80 mm long, in the inflorescence 45-325 mm long, sometimes with a few leafy nodes in between the verticils; nodes prominent; leaf scars prominent, sometimes with a marginal rim, broadly ovate or obovate, apex acute to rounded, base cordate, truncate or angustate, margin crenate, upper surface green, loosely pubescent to velvety, rarely almost smooth, lower surface silvery velvety, to pubescent or rarely almost smooth, except on nerves; when indumentum is sparse, the surface is covered by sessile, colourless glands; petiole 4-110 mm long. Inflorescence of 2 to 5 spherical to subspherical (horizontally flattened below) verticils; verticils (excluding corollas) 28-78 mm in diameter with verticil branches 5-20 mm long, dichasially branched at base; pedicels 0.5-7 mm long; bracts leaf-like, sometimes early deciduous, 8-85 x 2-25 mm; petiole 1-25 mm long; bracteoles 6-22 x 0.3-2.5 mm, linear, green with acuminate white apex. Calyx 14-13 mm long, 4-4.5 mm in diameter, usually curved forwards, slightly enlarging in fruit, bilabiate or without produced lips, 8(-11)-toothed or sometimes all teeth obsolete, shortly pubescent to velutinous; calyx teeth ridged, deltoid, with apiculate white apex, the dorsal one 2-14 mm long, the 3 or 5 lower teeth bend downwards, more or less united to a lower lip. Corolla 24-45 mm long, covered by orange-rufous hairs; tube 10-25 mm long, with one distinct ring of hairs inside, lower lip 6-10 mm long, the median lobe retuse, 2.5-4.5 mm long. Fresh pollen orange-coloured. Nutlets 2.4-4.3 x 1.2-2.1 mm. blackish brown, gloosy. *Leonotis ocymifolia* var *raineriana*; mature leaves typically longer than 50 mm, velvety to almost glabrous: stem sparsely branched with long internodes.

8.1.2 Chemistry of *Leonotis*

Only four species of *Leonotis* have been studied for their chemical constituents. Labdane type diterpenes with an oxygen bridge between C-8 and C-13, "grindelanes" (Table 8.1) appear to be the major constituents of these species. Except for **181**, all of these diterpenes exhibit oxidation at C-19 which often forms a lactone ring through C-6 (Table 8.1).

Several novel diterpenes have been isolated from *Leonotis nepetaefolia* (Fig. 8.1). Purushothaman *et al.* (1974) isolated diterpenes which have a 19→6 lactone (**184-185**) and also 19→20 lactone (**186**). This latter oxygenation pattern was also show in strucure **187** (Dahl and Norman, 1970) and acylated compounds **189-190** (Manchand, 1973; White and Manchand, 1972). Other non diterpene constituents of *Leonotis* species are shown in Table 8.2.

8.1.3 Medicinal values of *Leonotis*

Several species of *Leonotis* are known for their medicinal value and are sometimes regarded as narcotic and habit forming (Watt and Breyer-Brandwijk, 1962). *L. africana*, *L. dysophyla*, *L. leonurus*, *L. microphyla* and *L. nepetaefolia* are all known for their use as a remedy for ulcers, cramp, snake bite and as tonics and purgatives (Watt and Breyer-Brandwijk, 1962). Dreele *et. al.* (1975) reported the anticancer properties of extracts of *L. nepetaefolia*.

In Ethiopia *L. ocymifolia* var *raineriana* is known locally, "ras-kimer", and is cultivated for its medicinal uses. The underground part is applied topically on wounds and ulcers (Abate *et al.*, 1976). The leaves are macerated in water
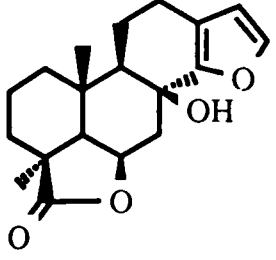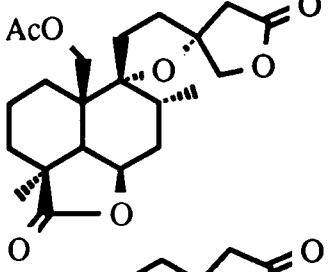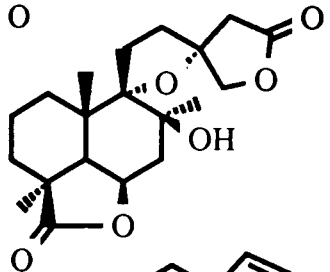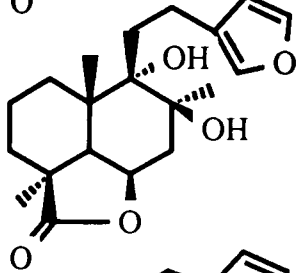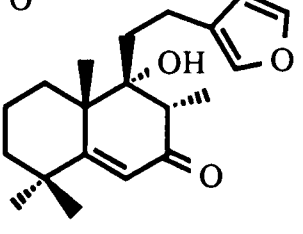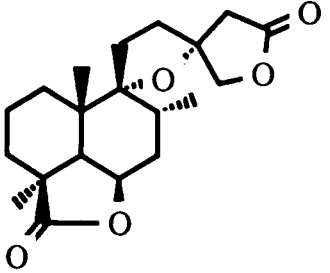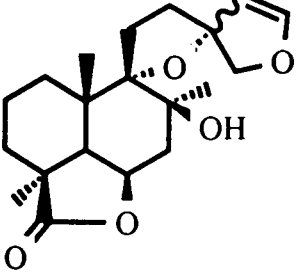
Stracture		Plant Name	Reference
	177	*L. dasophylla*	Kaplan *et al.*, 1970
	178	*L. leonotis*	Eagle *et al.*, 1977
	179	*L. leonorus*	Dekker *et al.*, 1987
	180		Kaplan and Rivett, 1968
	181		Kaplan and Rivett, 1968
	182		Kruger and Rivett, 1988
	183		Guglielmo *et al.*, 1979

Table 8.1. Grindelane diterpenes of *Leonotis* species

235

184   Purushothaman *et al*, 1974

185   Purushothaman *et al*, 1974

186   Purushothaman *et al*, 1974

187   Dahl and Norman, 1970

188   Manchand, 1973

189   White and Manchand, 1972

190   White and Manchand, 1972
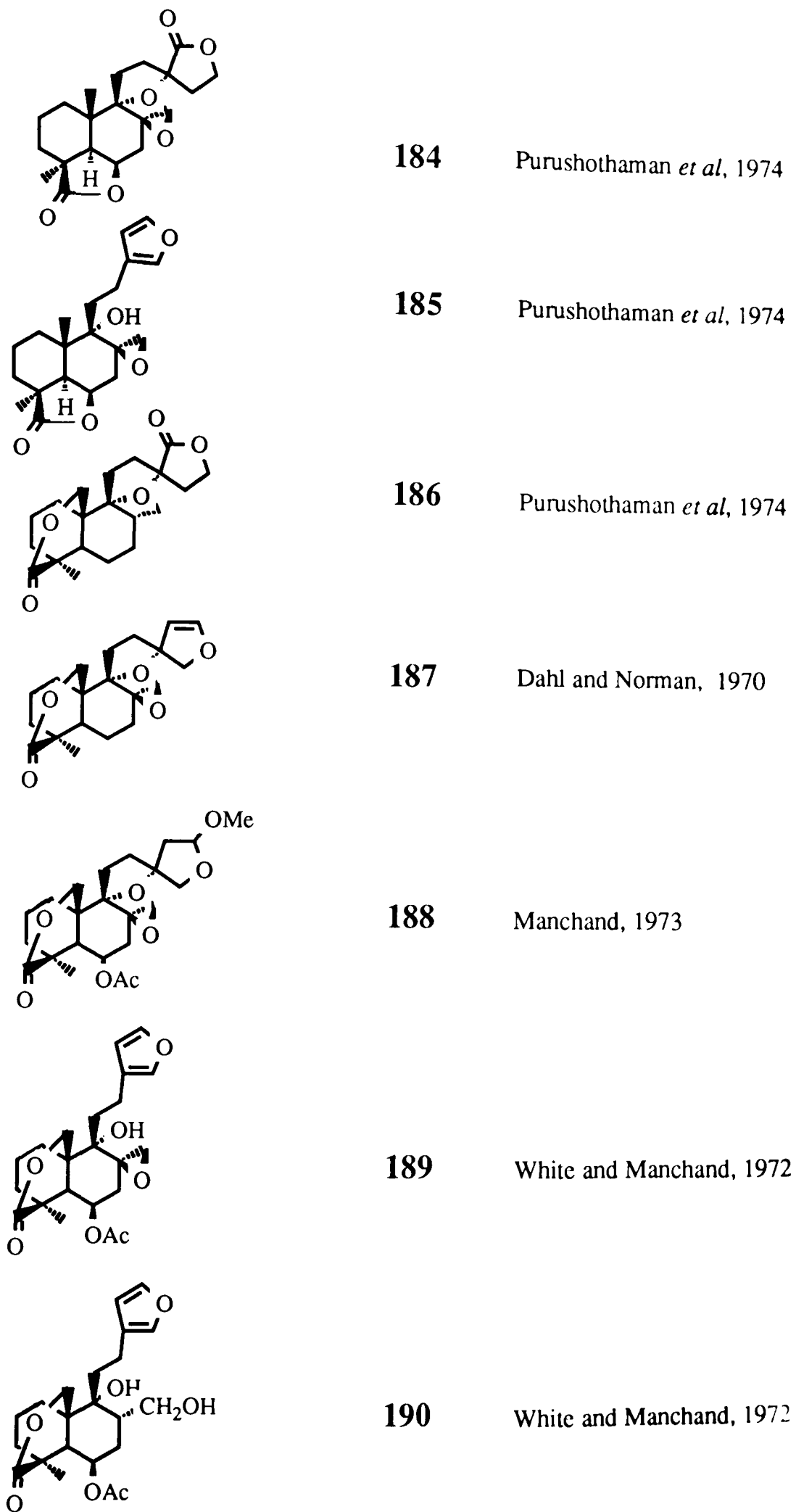
Fig. 8.1 Diterpenes isolated from the leaves of *L. nepetaefolia*

236
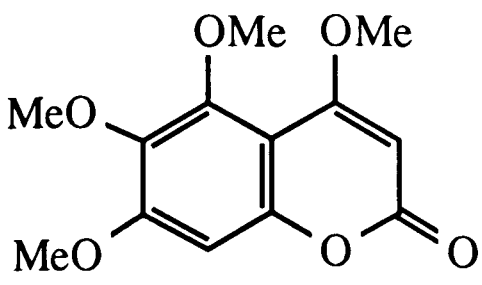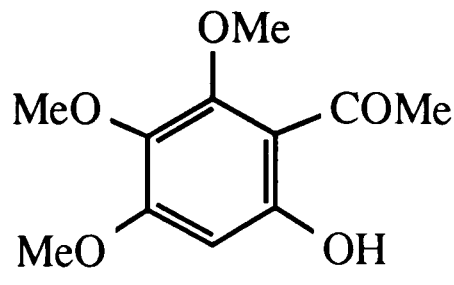
Compound	Plant Part	Reference

191   Leaves   Purushothaman et al., 1976

192

n-octacosanol   **193**
n-octacosanoic acid **194**
Campesterol   **195**   Root   Saradha and Bhima, 1989
β–sitosterol-β–D-glucopyranoside **196**
4,6,7-trimethoxy-5-Methylchromene-2-one **197**
Quercetin   **108**

Laballenic acid   **198**   Seed   Bagby et al., 1965

Table 8.2. Non diterpene constituents of *L. nepetaefolia*

and the extract taken orally to expel worms (ascaris).

The ethanolic extracts of the leaves and root of *L. ocymifolia* var *raine-riana* were found to be inactive when tested against a range of microorganmisms (see Section 3.1, page 52). The petroleum ether, ethyl acetate and aqueous extracts of the leaves were not also anthelminthic when tested against *Haemonchus contortus* (a 3rd stage larvae of a nematode infective to cattle)[1]. Up to 10 mg/ml of the extracts did not have any significant effect on the survival of the nematode *in vitro*. Further biological studies were not undertaken for this plant and this section describes only the phytochemical analysis of the leaves and root.

8.2   Results and Discussion

8.2.1   Constituents of the leaves of *L. ocymifolia* var *raineriana*

The cold ethanol extract was subjected to vacuum liquid chromatography over silica gel and eluted with solvents of increasing polarity. Four diterpenes were isolated from the 8:2 to 1:1 hexane:ethyl acetate eluents by a combination of column chromatography (Sephdex LH 20) and prep. TLC. Examination of the ethyl acetate VLC eluent by HPLC resulted in the isolation of caffeic acid and two compounds which appeared to be flavonoid glycosides. The latter compounds are not characterized as being acetylated under the normal procedure resulted in the opening of the sugar rings.

---

[1]Experiment was carried out at the Glasgow University, Veterinary School

8.2.1.1 Identification of SHM-76B as (13S)-20β-acetoxy-9,13α-epoxylabda-6(19)β,16(15)-diol dilactone (199)

The white powder of SHM-76B which crystalised as needles from methanol was obtained in a yield of 0.0006%. The UV spectrum measured in ethanol did not show any absorption above 200 nm. In the IR spectrum, bands at 1770 and 1780 cm^{-1} were indicative of γ lactones while bands at 1730 and 1240 cm^{-1} suggested ester carbonyl functionality (William and Fleming, 1989). The latter functional group was further corroborated by the ^{1}H NMR spectrum (Fig. 8.2) which showed a methyl singlet at δ 2.04 assignable to one acetoxy methyl group.

The high resolution EIMS (Scheme 8.1) gave a molecular ion which analysed for $C_{22}H_{30}O_7$, requirening eight double-bond equivalents. In the ^{13}C NMR spectrum (Table 8.3) resonances attributable to three carbonyls (δ 182.3, 174.6 and 170.1), two quaternary carbinols (δ 90.9 and 85.2), two oxymethylene (δ 78.9 and 65.9) and an oxymethine (δ 75.5) supported the assignment of two lactone rings, acetoxy and C-9–C-13 ether functional groups, as required in **199** (Fig. 8.3).

In the ^{1}H NMR spectrum (Fig. 8.2), the C-14 and C-16 methylene protons occured as AB quartets centered at δ 2.36 and 2.90 (J=17.3 Hz) and δ 4.10 and 4.22 (J=8.9 Hz) respectively. The C-20 methylene protons also appeared as an AB quartet centered at δ 4.19 and 4.33 (J=12.5 Hz) but one of these protons (δ 4.33, H-20a, Fig. 8.3) further showed W-bond coupling (J=2 Hz) due to the H-1 axial proton. Further assignment of ^{1}H resonances were based on the COSY NMR studies. In these studies, the C-17 methyl doublet (δ 0.89, J=6.4 Hz) was

Figure 8.2: ^{1}H NMR (400 MHz, CDCl$_3$) spectrum of SHM-76B
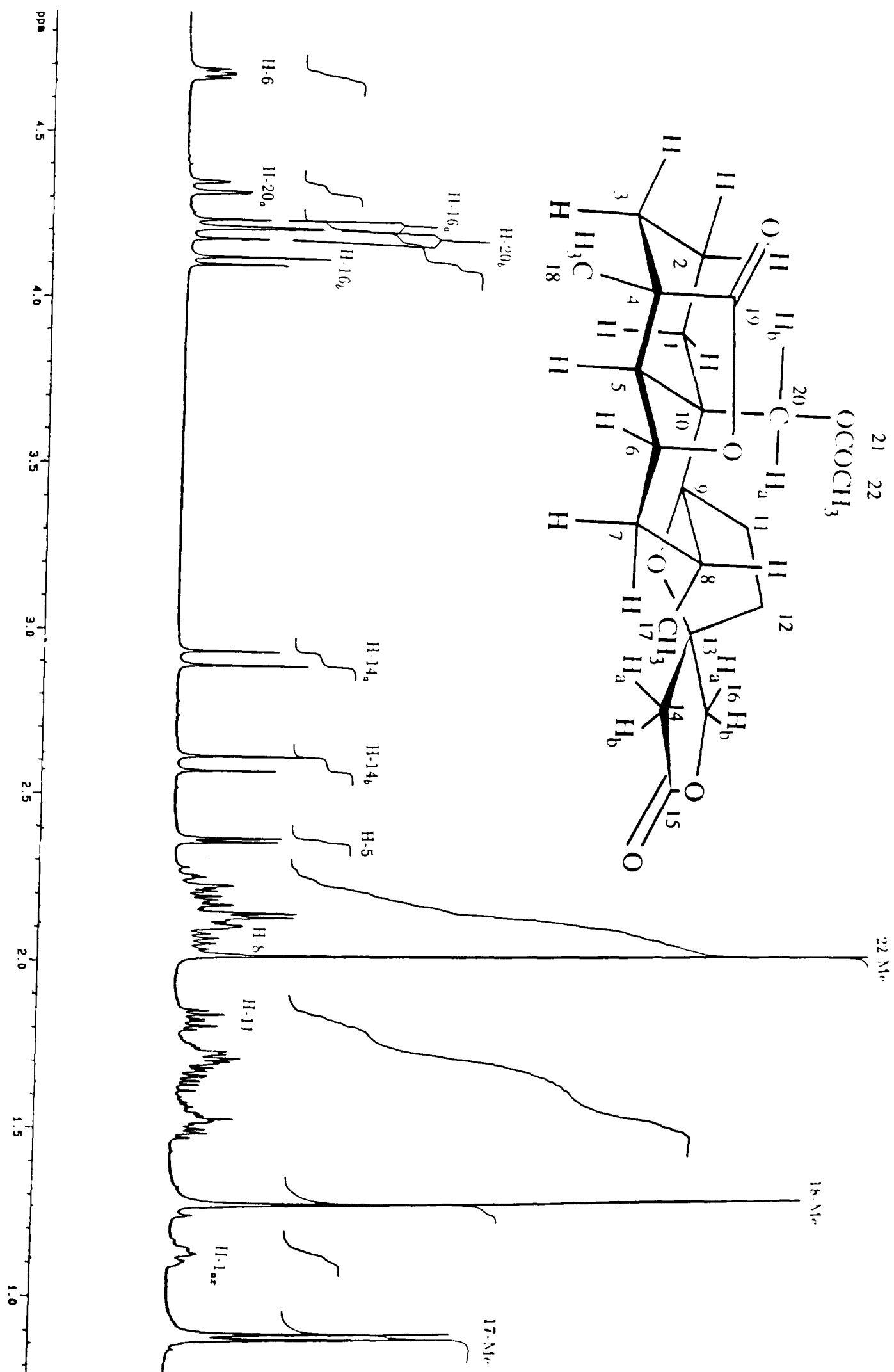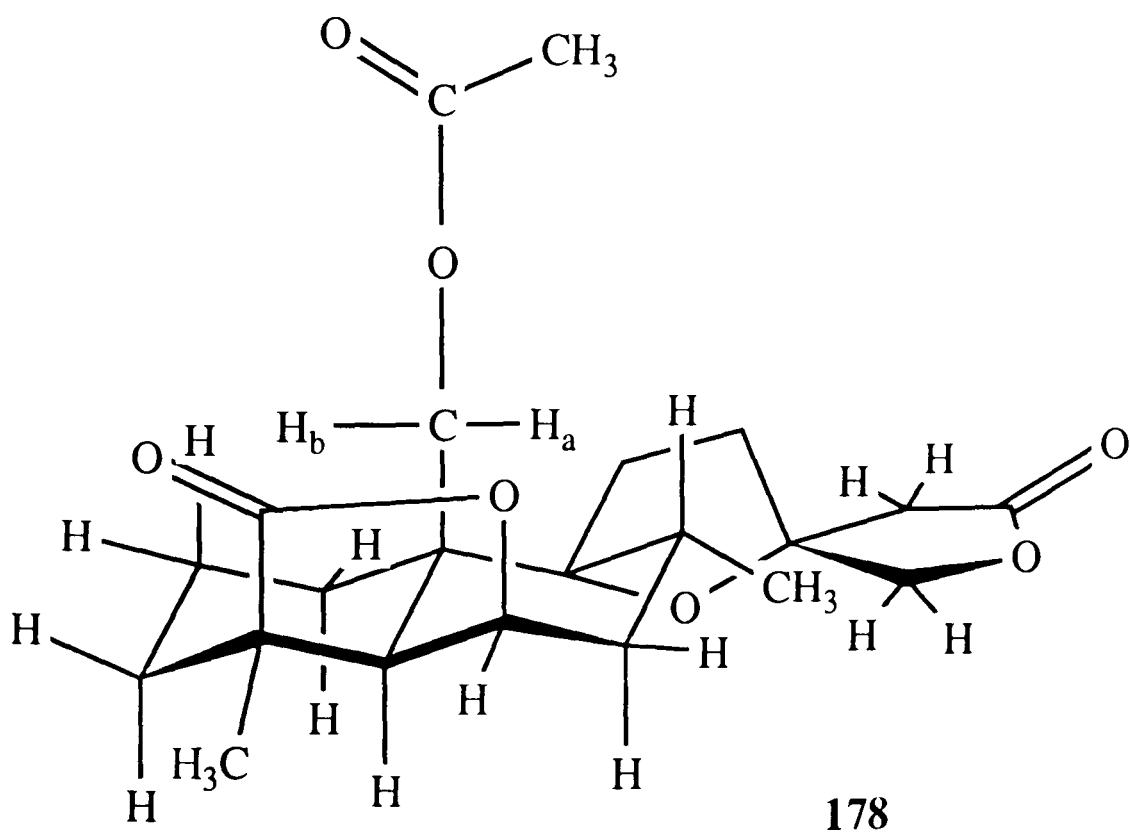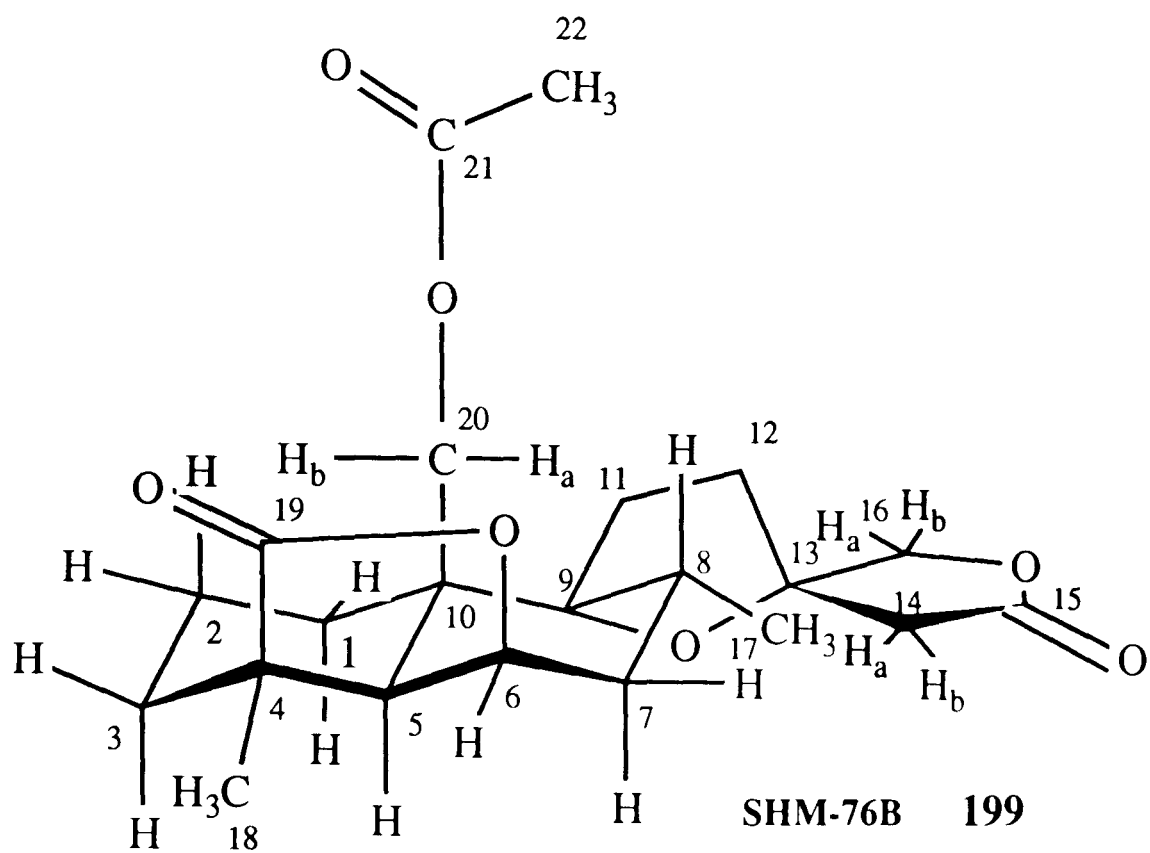
Fig. 8.3. Structure of SHM-76B and its isomer

coupled to a multiplet centered at δ 2.08, which thus identifies H-8. The oxyme-thine H-6 doublet of doublets at δ 4.67 exhibited a coupling pattern (J=6.4, 4.4 Hz) indicative of its equatorial position and showed coupling to a doublet (J=4.4 Hz) at δ 2.36. This latter proton must be H-5 and its coupling constant (axial-equatorial coupling) was indicative of its α orientation. Another key observation in the COSY NMR studies was coupling of one of the H-20 methylene protons (H-20a) to an isolated broad double doublet signal at δ 1.15. This must be as-signed to H-1 axial proton which showed long range (W) coupling to the C-20 methylene proton.

The HMBC NMR study (Fig. 8.4) was in agreement with the assignment of structure 199 and ^{13}C resonances (Table 8.3). In this study, ^3J coupling of proton signals at δ 2.36 (H-5) and δ 1.28 (H$_3$-18) to δ_C 182.3; δ_H 4.10 and 4.22 (H$_2$-16) to δ_C 174.6 (also ^3J coupling from the H$_2$-14) and δ_H 4.19 and 4.33 (H$_2$-20) to δ_C 170.1 (also ^2J coupling from the acetoxy methyl singlet, δ 2.02) identify the C-19, C-15 and acetoxy carbonyls respectively. The two quaternary oxygen bearing carbons (C-9 and C-13) could also be differentiated as C-9 showed ^3J coupling to the H$_2$-20 and H$_3$-17 protons while C-13 showed the expected ^2J coupling to H$_2$-14 and H$_2$-16 protons. Except for C-2 and C-11 all the ^{13}C resonances could be assigned directly from the HMBC studies.

The HMBC data together with that of the COSY spectrum further al-lowed the assignment of complicated proton resonances. The COSY studies re-vealed interaction between an isolated 1H proton pattern (ddd) at δ 1.82 and a multiplet at δ 2.23. Both of these protons were shown to have coupling with the

Figure 8.4: HMBC spectrum (400 MHz, CDCl₃) of SHM-76B
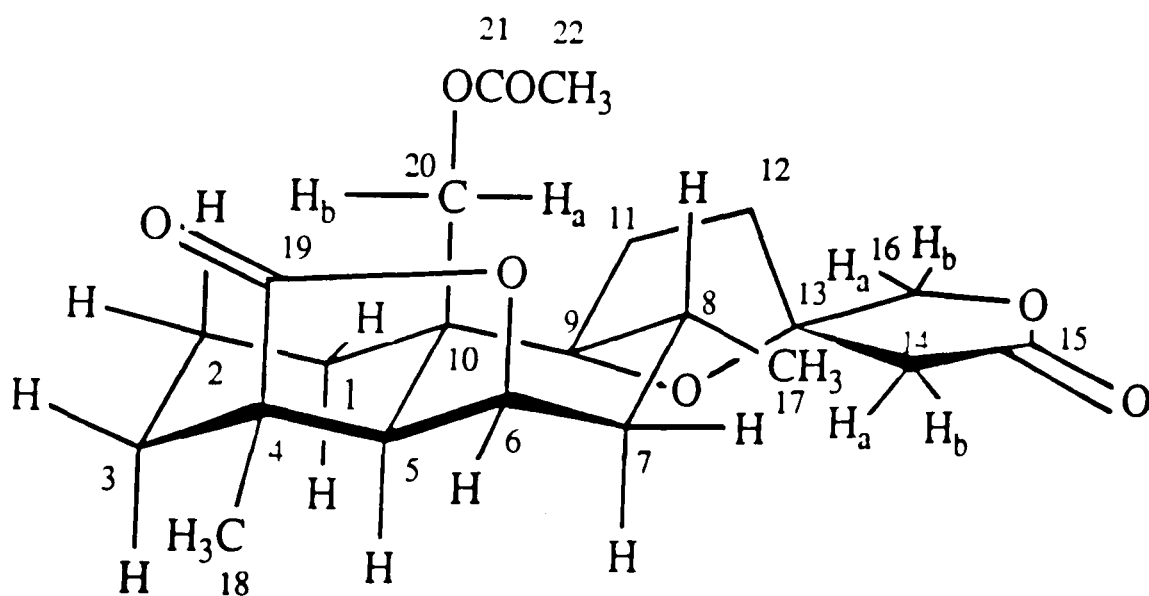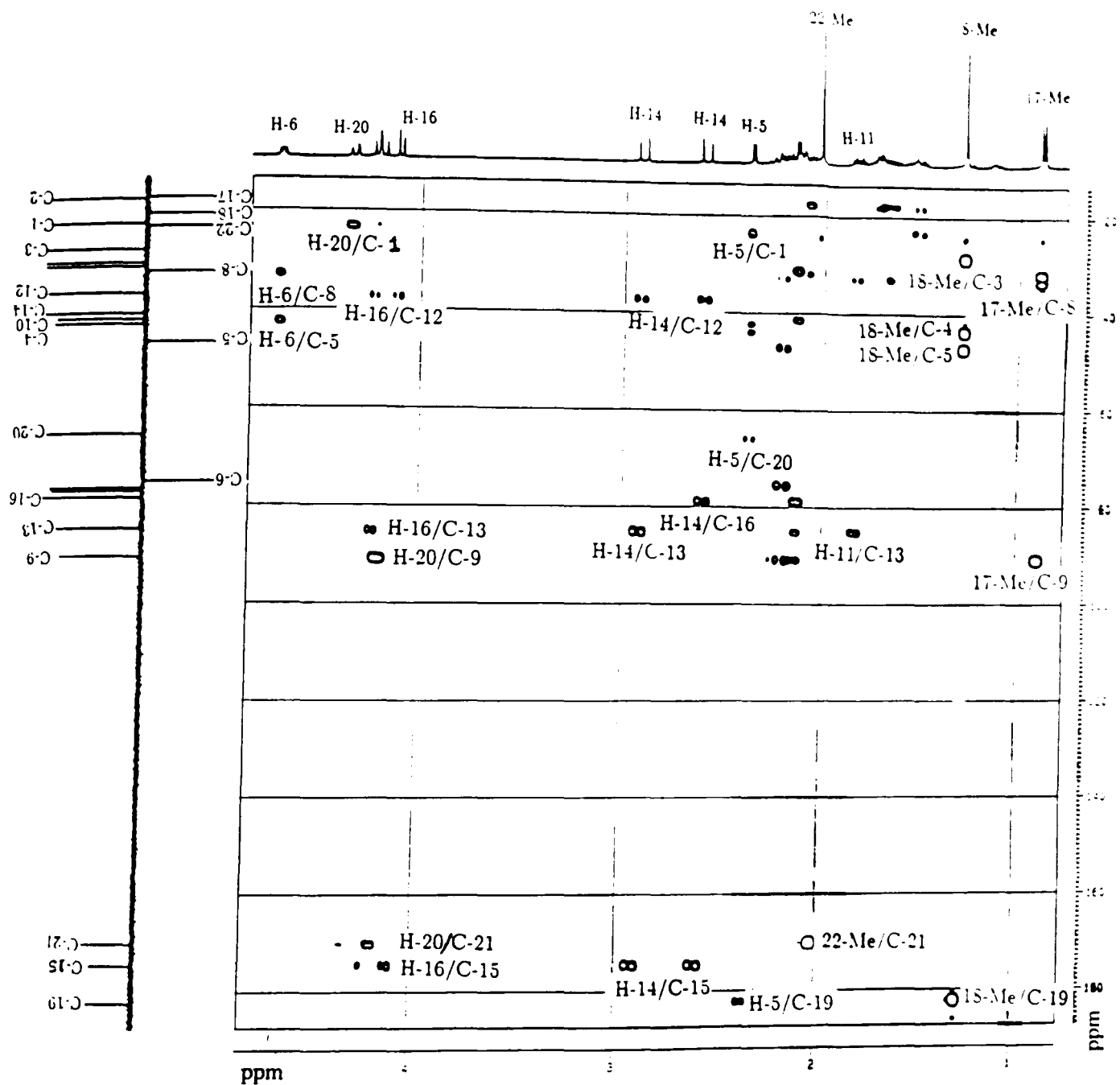
quaternary oxygen bearing carbon assigned to C-9 (δ 90.9) and the C-8 methine carbon (δ 32.9) in the HMBC spectrum (Fig. 8.4). This identifies the H_2-11 protons. Another multiplet at δ 1.65 was assigned as the H-7 axial proton as it showed coupling to H-6 in the COSY spectrum and showed ^2J coupling to C-8 (δ 32.9) in the HMBC spectrum. Further coupling of the latter proton pattern (H-7 axial) to a multiplet at δ 2.17 in the COSY spectrum also identifies the H-7 equatorial proton. Finally, a multiplet (2H) at δ 2.15 was similarly identified as H-12 as it showed ^3J coupling to C-9, C-14 and C-16 and also ^2J coupling to C-11 and C-13.

The relative stereochemistry of SHM-76B as shown in **199** was established from the NOESY NMR studies (Fig 8.5). Interactions between H-6 and H-5 and H-18 indicated that these groups are at the same face of the molecule. Similarly interactions between H-8 and H-20a signals supported their close proximity, as anticipated in structure **199**. The stereochemistry at the C-13 chiral carbon centre of grindelane diterpenes has not been assigned unambiguously. In the present study the assignment of SHM-76B as structure **199**, (not **178**) was clearly established from the NOESY spectrum (Fig. 8.5). Interaction between Me-17 and H-14a and H-14b supported the 13S stereochemistry shown in **199**. This was further substantiated by the observation of strong interaction between H-16a and H-1 axial proton which are very close in space in the structure **199** (not **178**) (Fig. 8.3). **199** was previously obtained from *L. leonitis* and assigned to a 13R compound **178** (Eagle *et al.*, 1978). Its identity as **199** was later established

by means of an X-ray diffraction study (Kruger and Rivett. 1978).

Carbon	SHM-76A	SHM-76B	SHM-76C
1	28.2	23.3	34.7
2	18.1	18.2	20.6
3	28.9	28.5	39.8
4	46.1	43.6	41.1
5	46.1	48.1	47.2
6	76.1	75.5	68.4
7	29.2	32.0	34.1
8	31.8	32.9	31.2
9	92.2	90.9	90.1
10	39.1	42.7	40.5
11	31.8	31.2	29.4
12	37.1	37.4	37.8
13	88.2	85.2	86.6
14	43.2	41.5	42.8
15	174.7	174.6	174.3
16	78.8	78.9	78.1
17	17.6	17.8	17.2
18	23.5	21.2	20.6
19	183.6	182.3	175.7
20	23.2	65.9	75.7
21	–	170.1	170.7
22	–	23.7	22.5

Table 8.3: ^{13}C data (100 MHz, CDCl$_3$) of SHM-76A, SHM-76B and SHM-76C.

Figure 8.5: **NOESY** spectrum (400 MHz, CDCl₃) of SHM-76B
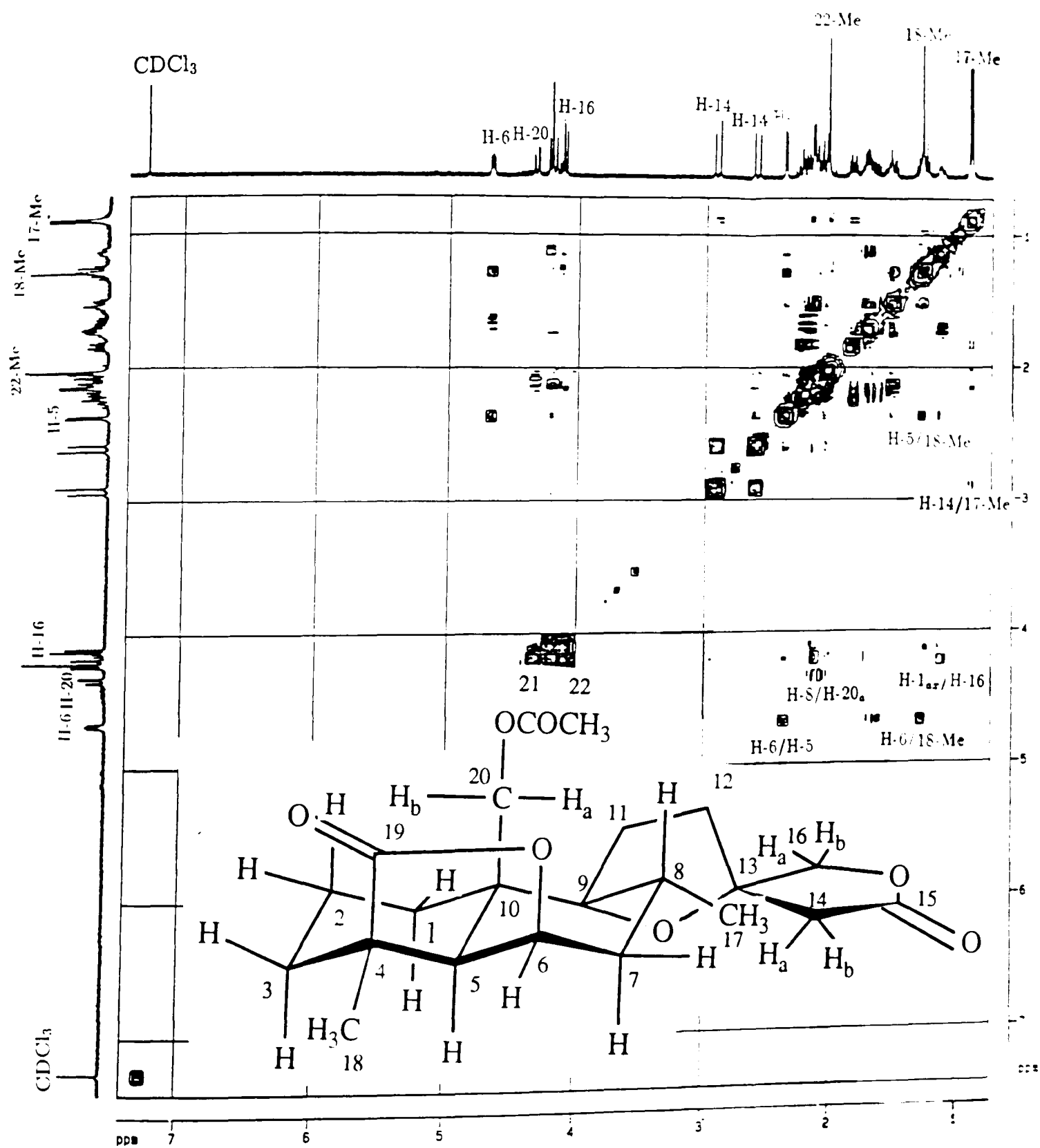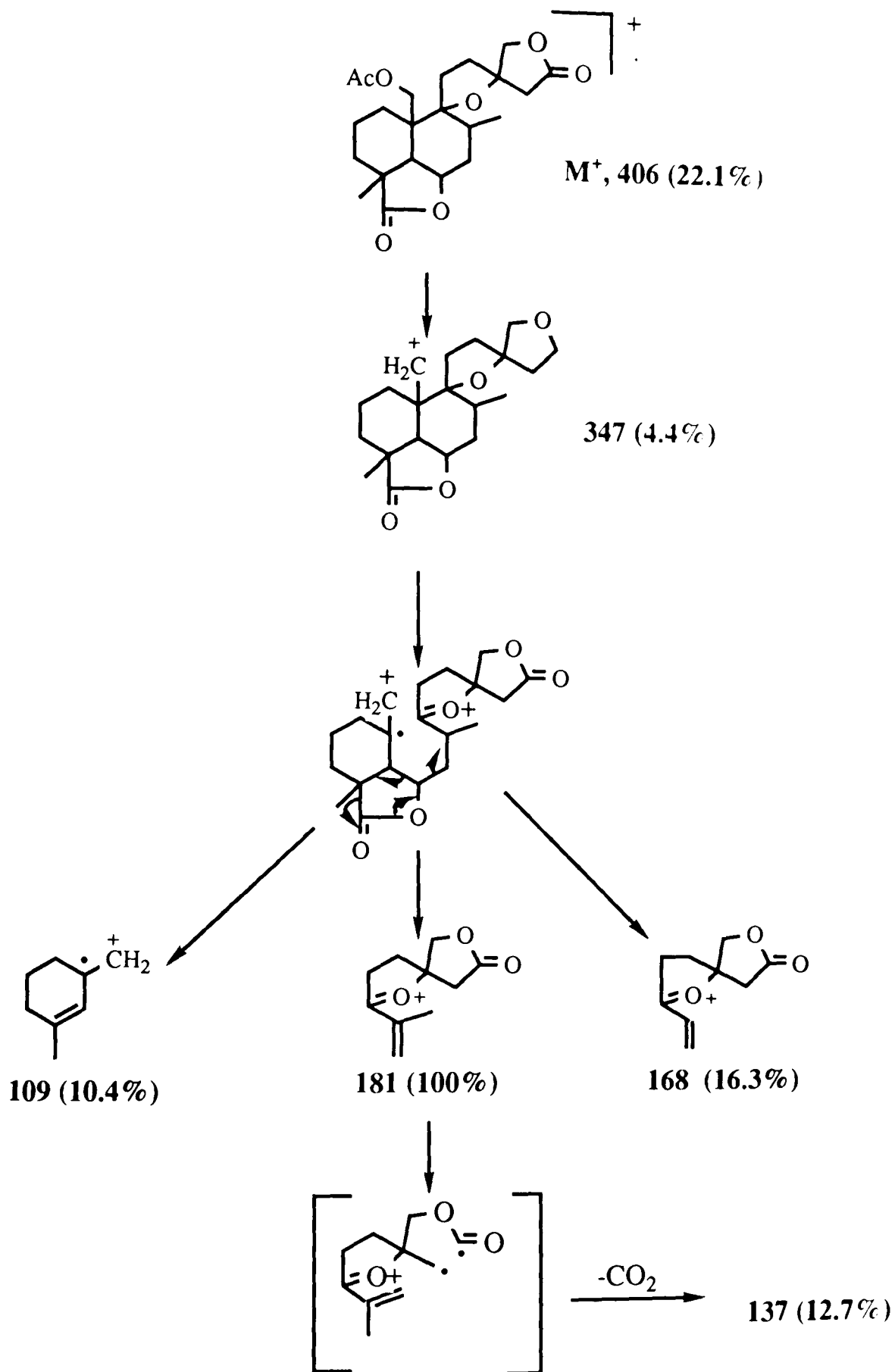
Scheme 8.1. Possible mass fragmentation pattern of SHM-76B

247

8.2.1.2 Identification of SHM-76A as ent-(13S)-9,13α-epoxylabda-6(19)β,16(15 diol dilactone (200)

SHM-76A was the major constituent of the ethanol extract. It was obtained in the yield of 0.05% and did not show UV absorption above 200 nm. The IR spectrum revealed bands at 1780 and 1760 cm^{-1} indicative of γ lactone functional groups as described for SHM-76B. The IR spectrum of this compound however differed from that of SHM-76B by lacking characteristic bands for ester functional group.

High resolution EIMS revealed the molecular ion at m/z 348 $C_{20}H_{28}O_5$, identical to that required for **200**. The ^{1}H NMR spectrum (Fig. 8.6) showed two AB quartet signals centred at δ 2.56 and 2.96 (J=17.2 Hz) and δ 4.12 and 4.24 (J=8.9 Hz) assignable to the H_2-14 and H_2-16 methylene protons respectively. A poorly resolved triplet at δ 4.68 (J=4.8) and a doublet at δ 2.07 (J=4.5 Hz) were indicative of the equatorial H-6 and axial H-5 protons respectively as described for SHM-76B. Like SHM-76B, the ^{1}H NMR spectrum of SHM-76A also showed the H_3-17 and H_3-18 methyl groups at δ 0.87 (d, J=6.3 Hz) and 1.28 respectively. The only differences in these two spectra were the lack of acetoxy methyl resonance in SHM-76A and the replacement of the C-20 methylene proton resonances of SHM-76B by a methyl singlet at δ 1.02 in SHM-76A.

The C-9–C-13 epoxy functional group was also supported by the ^{13}C NMR data (Table 8.3) which revealed the two oxygen bearing quaternary carbons at δ 92.17 (C-9) and 86.58 (C-13). Except for the absence of the acetoxy carbon signals and the replacement of the C-20 carbinol carbon by methyl carbon

Figure 8.6: ^{1}H NMR (400 MHz, CDCl$_3$) spectrum of SHM-76A

SHM-76A **200**

182
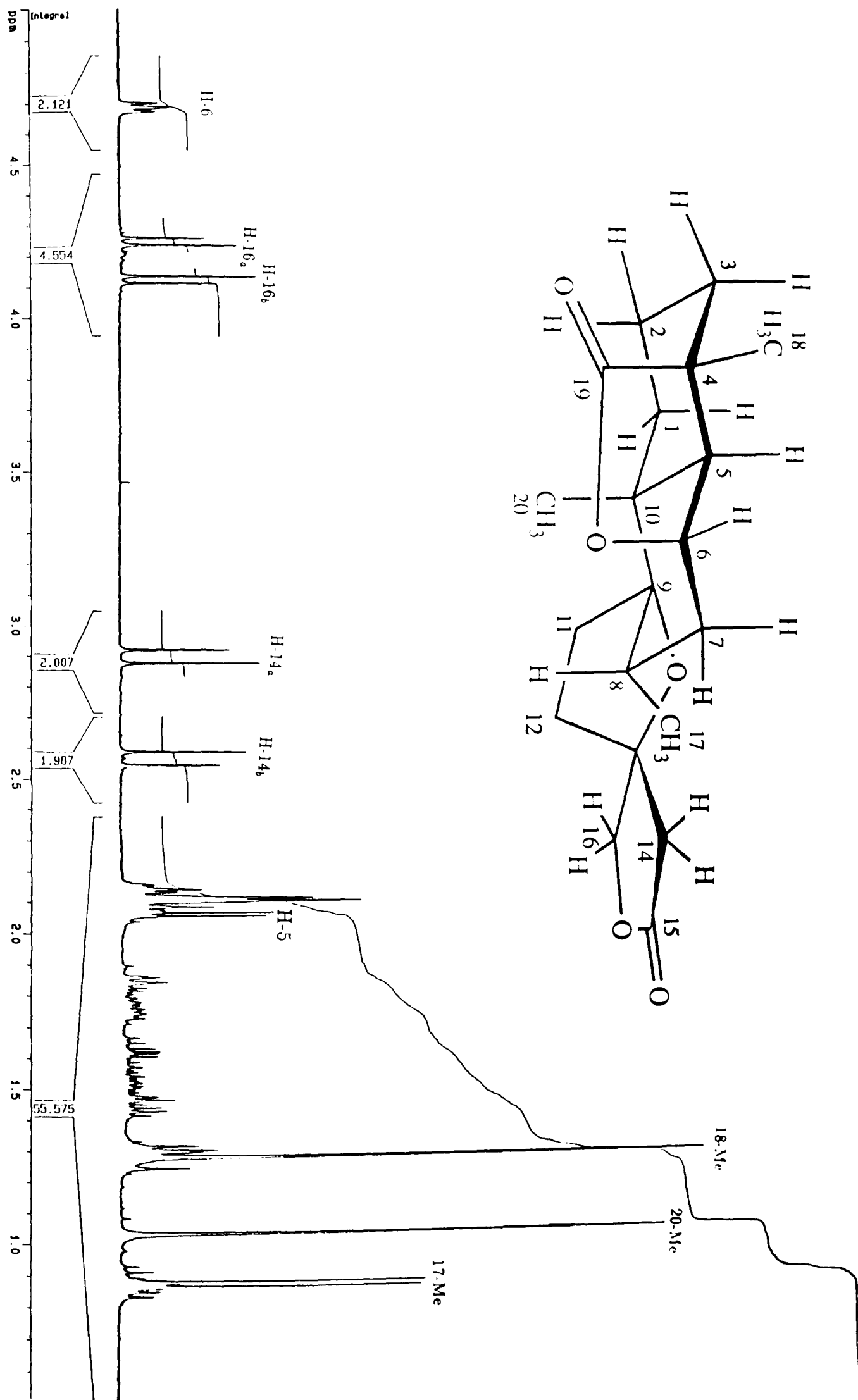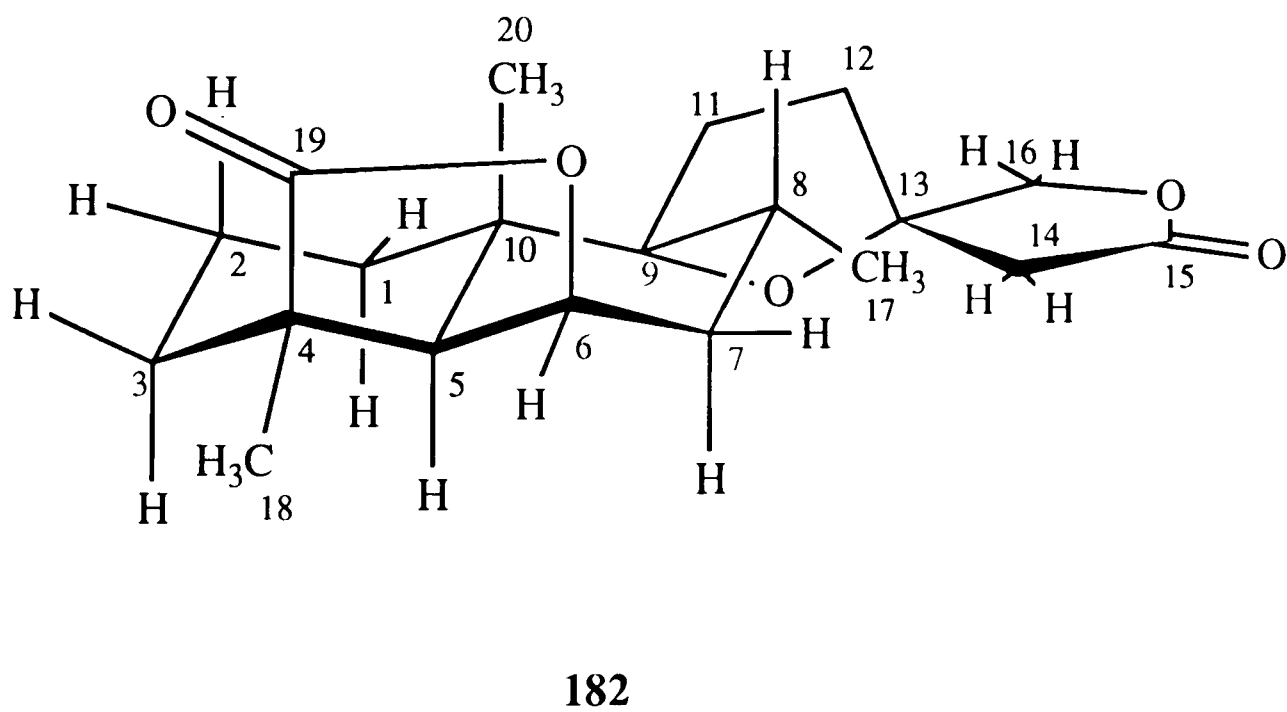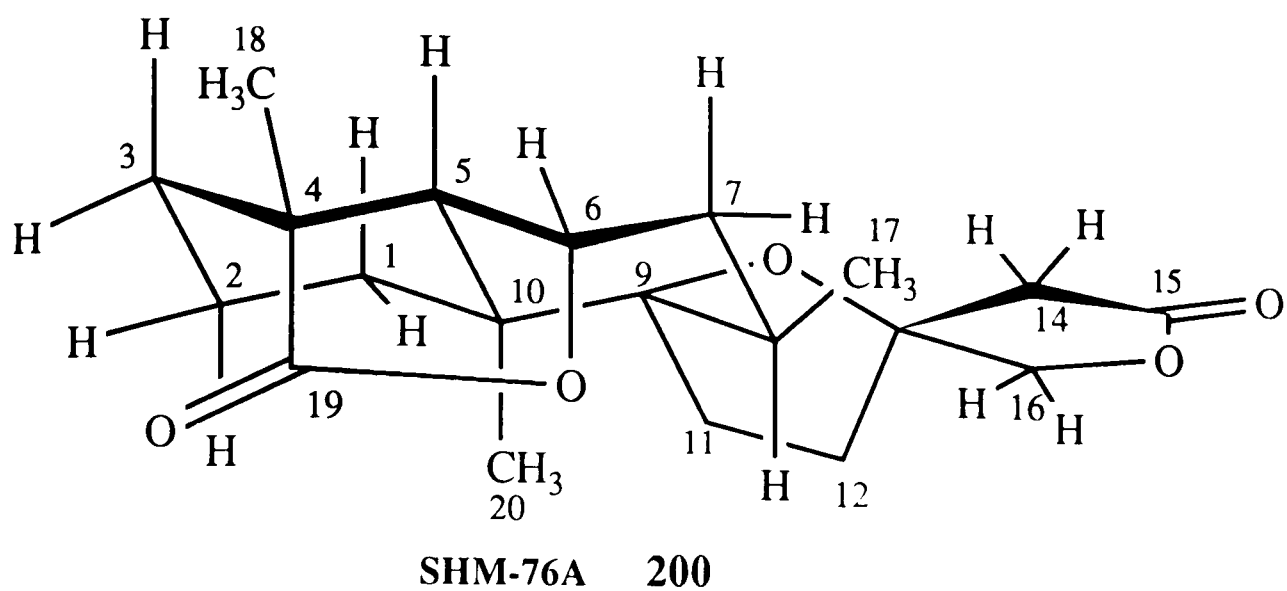
Fig. 8.7. Structure of SHM-76A and its mirror image

(δ 23.19), all features of the ^{13}C data were comparable with those of SHM-76B (Table 8.3). The stereochemistry of SHM-76A as 200 or 182 was finally established from the NOESY NMR studies which showed similar patterns as those of SHM-76B. The absolute stereochemistry of the dextrorotary compound, 182 (isolated from *L. leonurus*) has been established recently (Kruger and Rivett, 1988). SHM-76A was found to be laevorotary (-27°) and must be the mirror image of 182 (200, Fig. 8.7).

8.2.1.3 Identification of SHM-76C as (13R)-6β-acetoxy-9,13α-epoxylabda-19(20)β,16(15)-diol dilactone (201)

SHM-76C was obtained as white needles in a yield of 0.0018% and did not show any UV absorption above 200 nm. The IR spectrum revealed signals attributed to an ester (1730 and 1240 cm^{-1}) and two γ lactone carbonyl functional groups. In the ^{1}H NMR spectrum (Fig. 8.8) three methyl signals were observed; a doublet at δ 0.87 (J=6.64 Hz), and singlets at δ 1.14 and δ 2.03, assignable to the 17-Me, 18-Me and acetoxy methyl groups respectively. Two AB quartets centred at δ 2.51 and 2.92 (J=17.04 Hz) and δ 4.23 and 4.39 (J=9.24 Hz) were in agreement with the 15→16 lactone ring system already discussed for SHM-76B. This ring system and the C-9–C-13 ether functional groups were further substantiated by the ^{13}C NMR spectrum which showed similar resonances to these of SHM-76B (Table 8.3).

The ^{1}H NMR spectrum in the region δ 4-4.6 also revealed a similar pattern to that of SHM-76B. This was due to H$_2$-20 protons which appeared as

Figure 8.8: ^{1}H NMR (400 MHz, CDCl$_3$) spectrum of SHM-76C
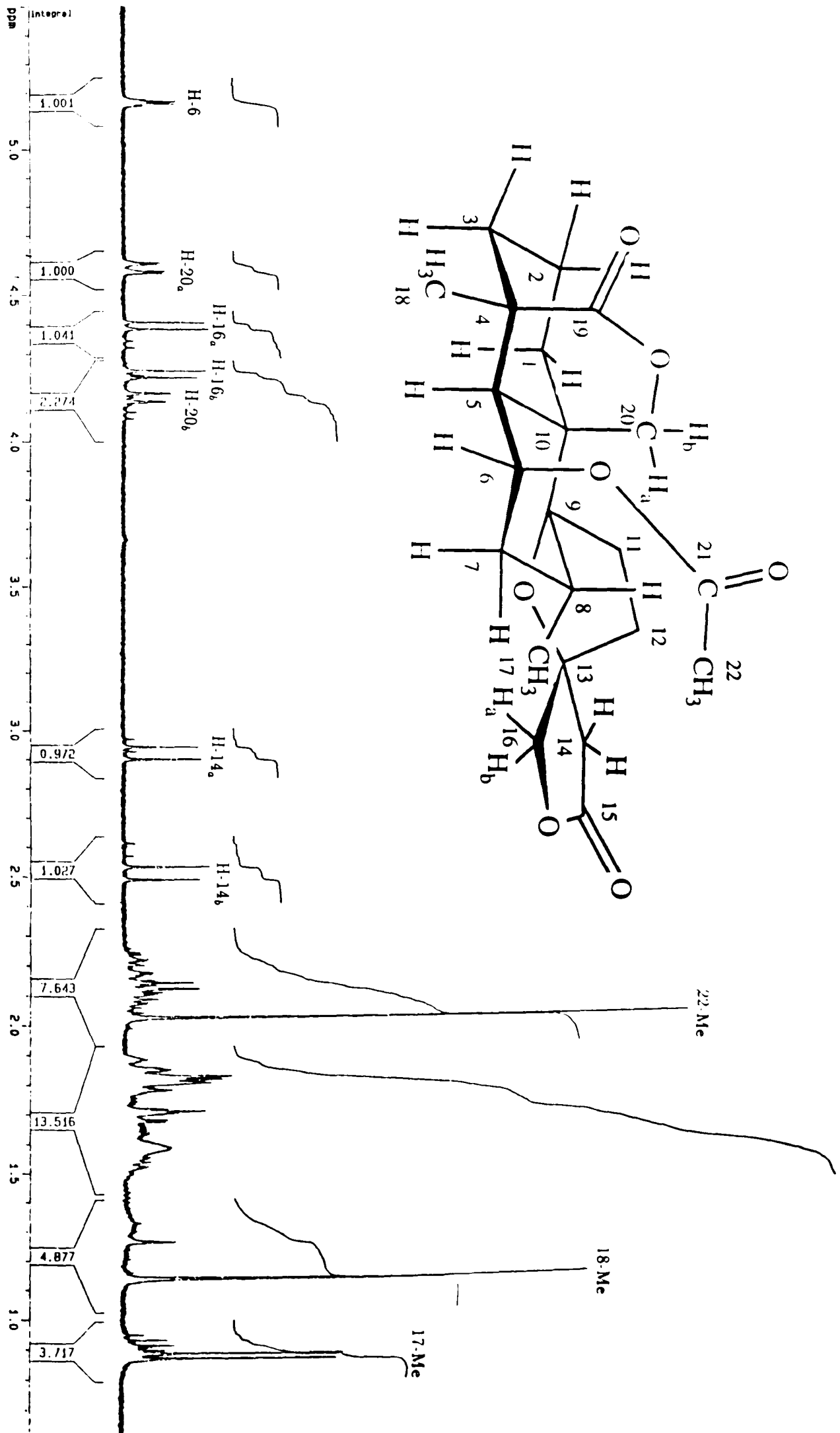
an AB quartets centered at δ 4.15 and 4.58 (J=11.52 Hz), one of the protons of which (δ 4.58, H-20a) showed long range (W) coupling (J=2.8 Hz) with the H-1 axial proton. The ^{13}C resonance of the C-20 carbinol carbon was however shifted downfield (δ 75.7) in comparison to SHM-76B (δ 68.9). This indicated that C-20 was part of the lactone ring system in this compound. Replacement of an overlapping triplet at δ 4.67 (H-6) in the ^{1}H NMR spectrum of SHM-76B (Fig. 8.3) by a quartet at δ 5.16 (J=3.04 Hz) in SHM-76C (Fig. 8.8) also supported the presence of a C-6 acetoxy group in **201** (Fig. 8.9).

The base peak in the MS of 9,13-epoxy labdanes normally occurs due to fission at C-6/C-7 and C-9/C-10 (see Scheme 8.1). (Eagle *et al.*, 1978). The occurrence of the molecular ion as the base peak at m/z 346 (100) for this compound indicated that the acetate group is expelled quickly to make a stable ion.

The HMBC NMR spectrum (Table 8.2) was in agreement with the assignment of SHM-76C as **201** and also assisted in the assignment of ^{13}C resonances. Important observations in this HMBC were a ^3J coupling of H_2-20 methylene protons to the C-19 carbonyl carbon (δ 183.6) which supported the 19→20 lactone ring in **201** rather than the 19→6 as in SHM-76B.

The stereochemistry of SHM-76C was established from ^{1}H NMR and NOESY studies. A small coupling constant (J=3.04 Hz) observed for the H-6 proton signal (δ 5.16) was indicative of its equatorial position. NOESY enhancement between H-6 and Me-18 (Fig. 8.10) supported the Me-18 equatorial orientation while enhancement between the acetoxy and H-20a proton was indicative
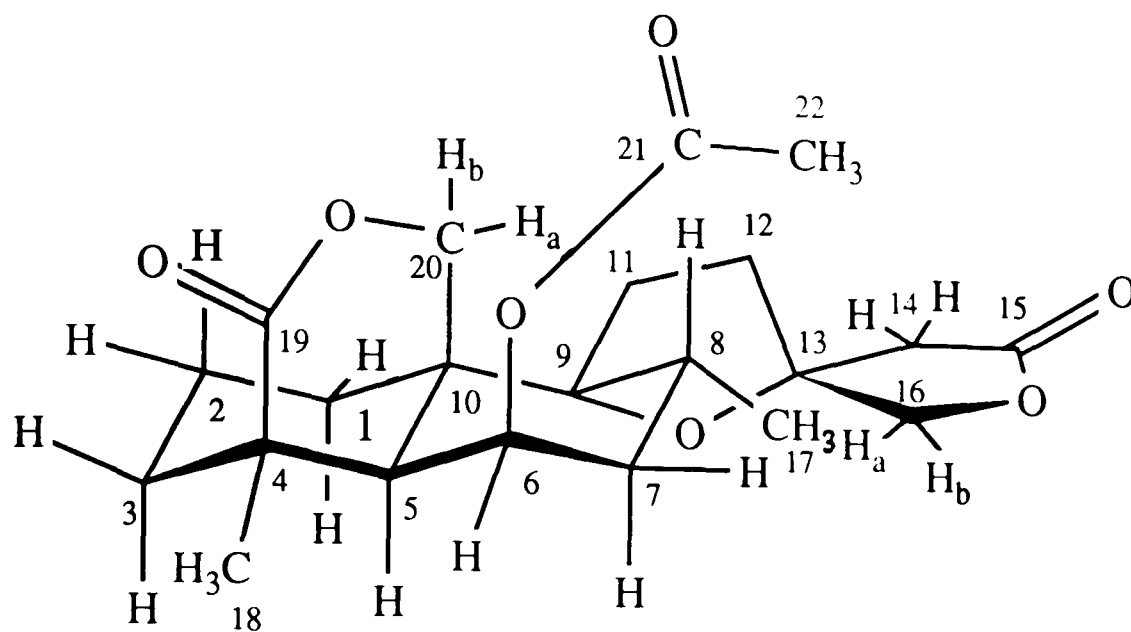
SHM-76C   **201**
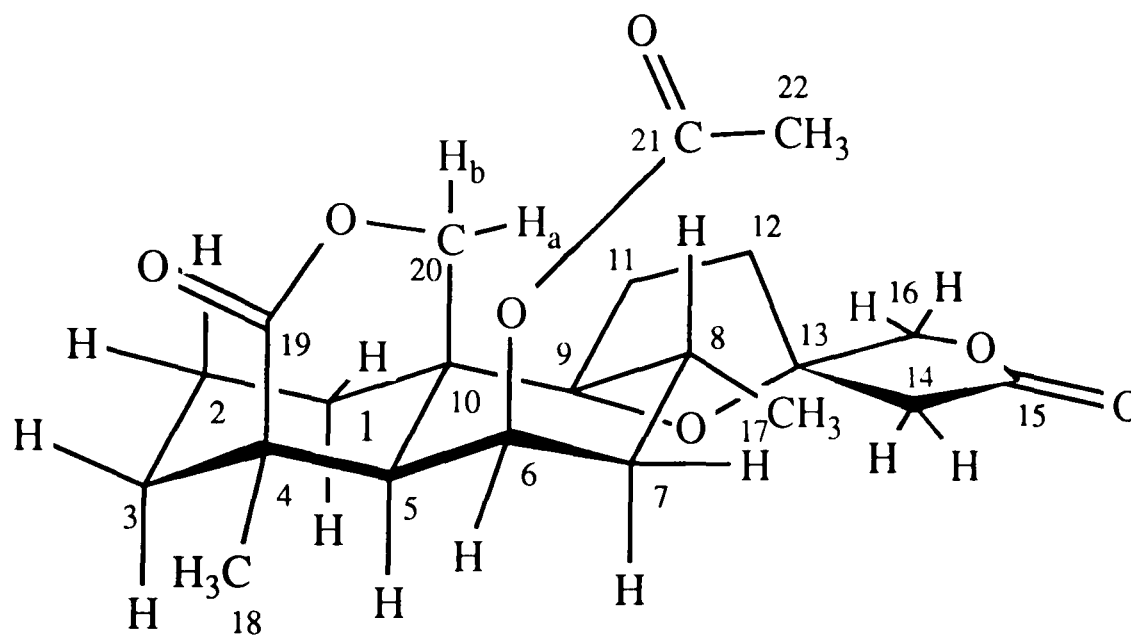
202

Fig. 8.9. Structure of SHM-76C

254

Figure 8.10: **NOESY** spectrum of SHM-76C
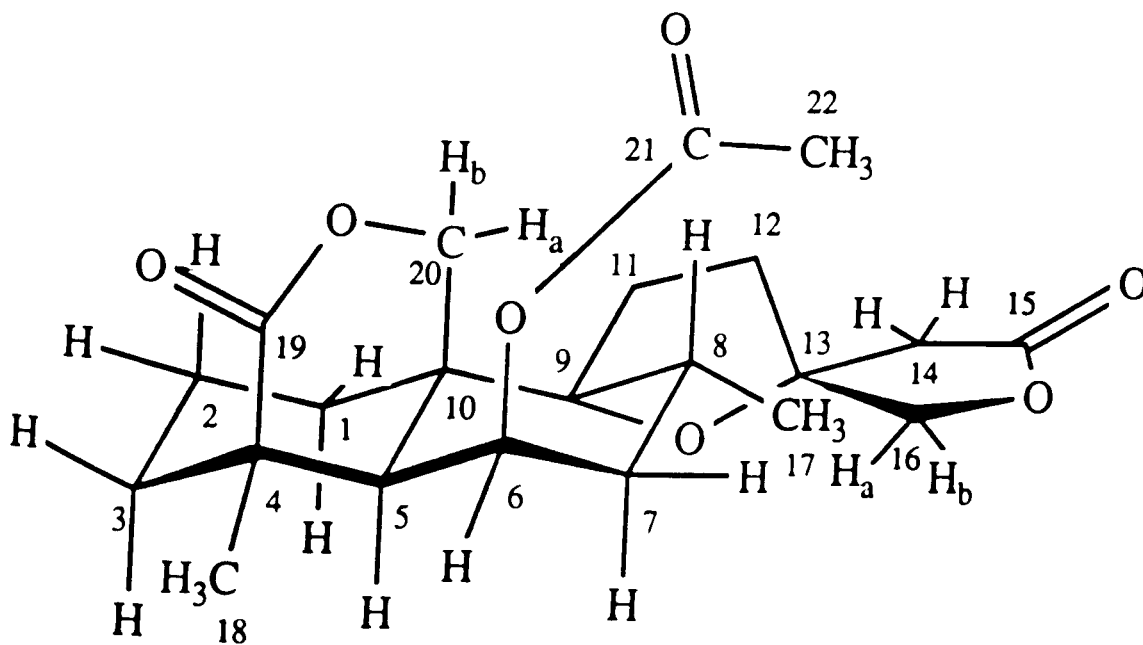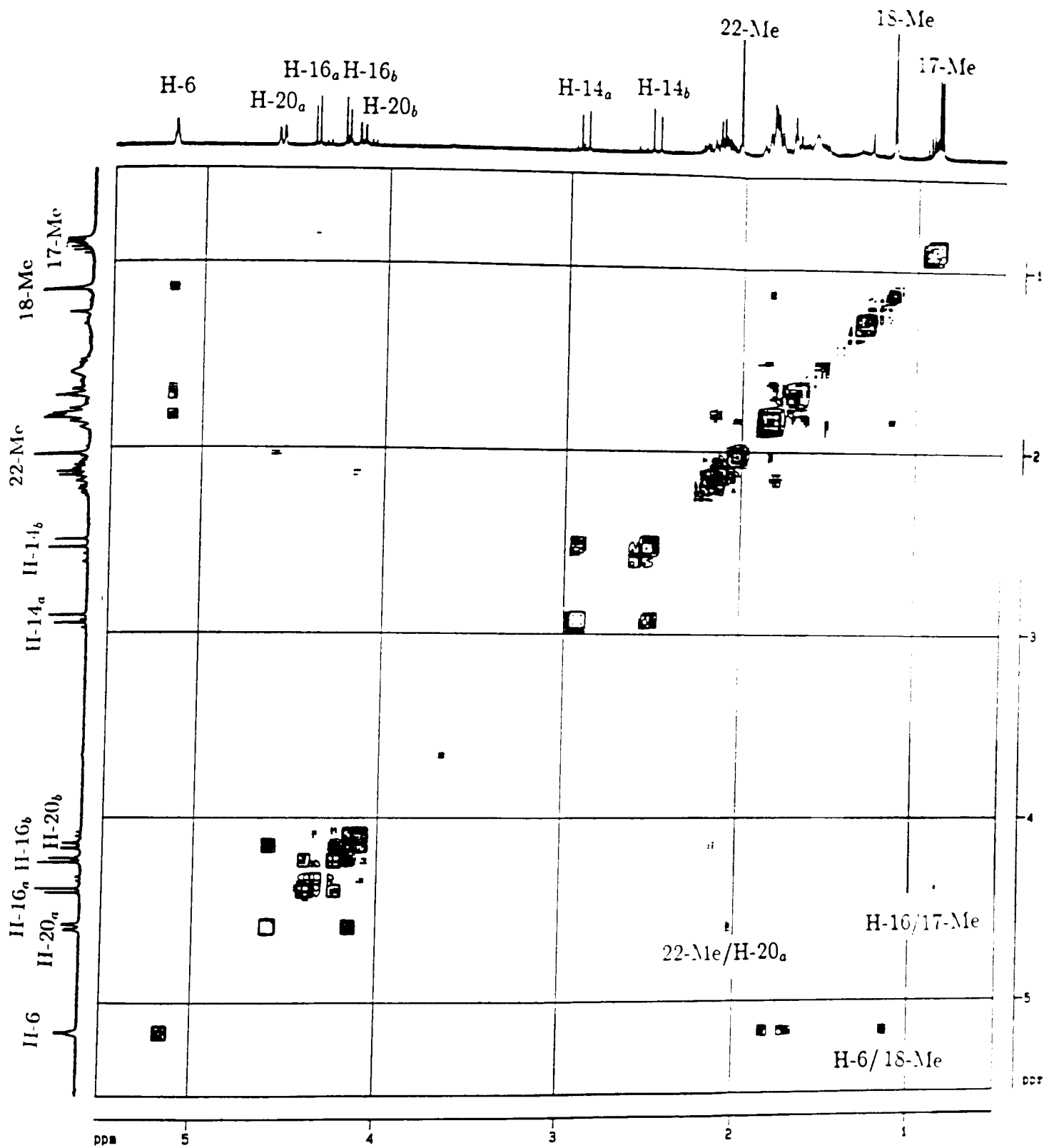
of their axial orientation. The stereochemistry of this compound at the C-13 chiral centre was found to be different from that of SHM-76B and SHM-76A. Interaction of the H_3-17 methyl doublet with H-16a resonances rather than the H-14 proton (as in SHM-76B) supported the 13 stereochemistry in structure **201** (Fig. 8.12).

SHM-76C appears to be a new natural product. The C-13 epimers (**201**, **202**) of this compound were synthesised by saponification of compound **186** followed by acetylation (Eagle *et al.*, 1978).

^{1}H	^{13}C	
	^3J	^2J
H_2-14	37.8, 78.1	86.2, 90.1, 174.3
H_2-16	86.6, 37.8, 174.3	86.6
H_2-20	34.7, 48.1, 175.7	
Me-17	90.5	31.2
Me-18	48.1, 175.7	41.1

Table 8.4: **HMBC correlations for SHM-76C (201)**

8.2.1.4   Identification of SHM-69 as 20β-acetoxy-9α,13ζ-dihydroxy-15(16)-epoxy-labd-14-en-6,19β-O-lactone (203)

The colourless gum SHM-69 was obtained in a yield of 0.001% and has UV absorption at 274 nm and specific rotation $[\alpha]_D$ +1°. The IR spectrum revealed bands at 1740 and 1240 cm^{-1} indicative of an ester functional group as described for SHM-76B and SHM-76C. The IR spectrum differed from those two compounds by showimg strong absorption at 3450 and 1600 cm^{-1} indicating hydroxy and olefinic functional groups respectively. Since only one γ lactone carbonyl absorption (1770 cm^{-1}) was observed, SHM-69 must has a different structure at the 6-carbon side chain of the labdane skeleton.

High resolution EIMS revealed the molecular ion at m/z 408, $C_{22}H_{32}O_7$, in agreement to that required for **203** (Fig. 8.12). The ^{1}H NMR spectrum (Fig. 8.11) revealed two clear AB quartets centred at δ 4.08 and 4.43 (J=10.44 Hz) and δ 4.22 and 4.35 (J=12.28 Hz) which were assignable to the H_2-16 and H_2-20 acetoxy bearing methylene functional groups. One of the H-20 protons (δ 4.35, H-20a) also exhibited further long range coupling (W-coupling, 2 Hz) to the H-1 axial proton, as anticipated in structure **203**. The presence of an acetoxy functional group in SHM-69 was further substantiated by the ^{1}H NMR spectrum (Fig. 8.12) which revealed a deshielded methyl singlet at δ 2.07. A 1H doublet of doublets at δ 4.67 (J=7, 4.9 Hz) and 1H doublet at δ 2.43 (J=4 Hz) were also in agreement with the assignment of equatorial H-6 and axial H-5 in **203**. Unlike the previous diterpenes discussed, the ^{1}H NMR spectrum of SHM-69 did not show H_2-14 methylene AB quartets (δ 2.5-3). These were replaced by two
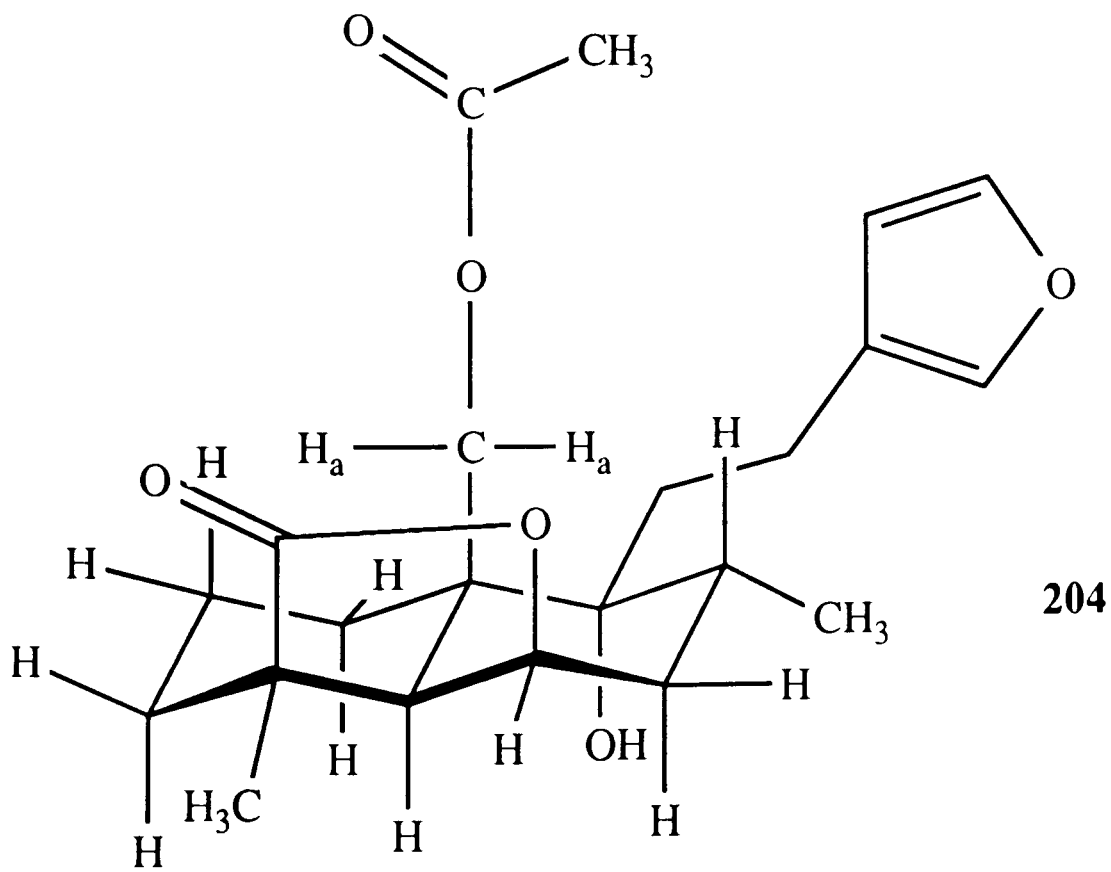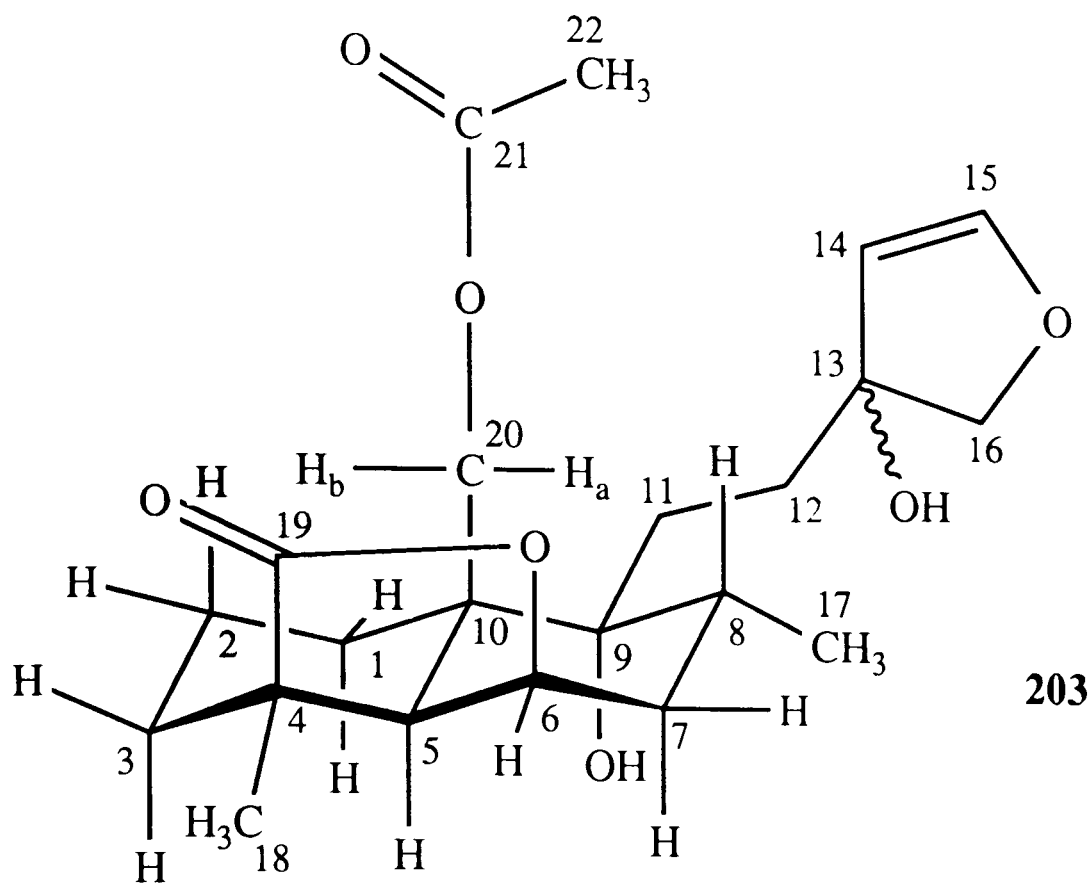
Fig. 8.11. Structure of SHM-69

Figure 8.12: ^{1}H NMR (400 MHz, CDCl$_3$) spectrum of SHM-69
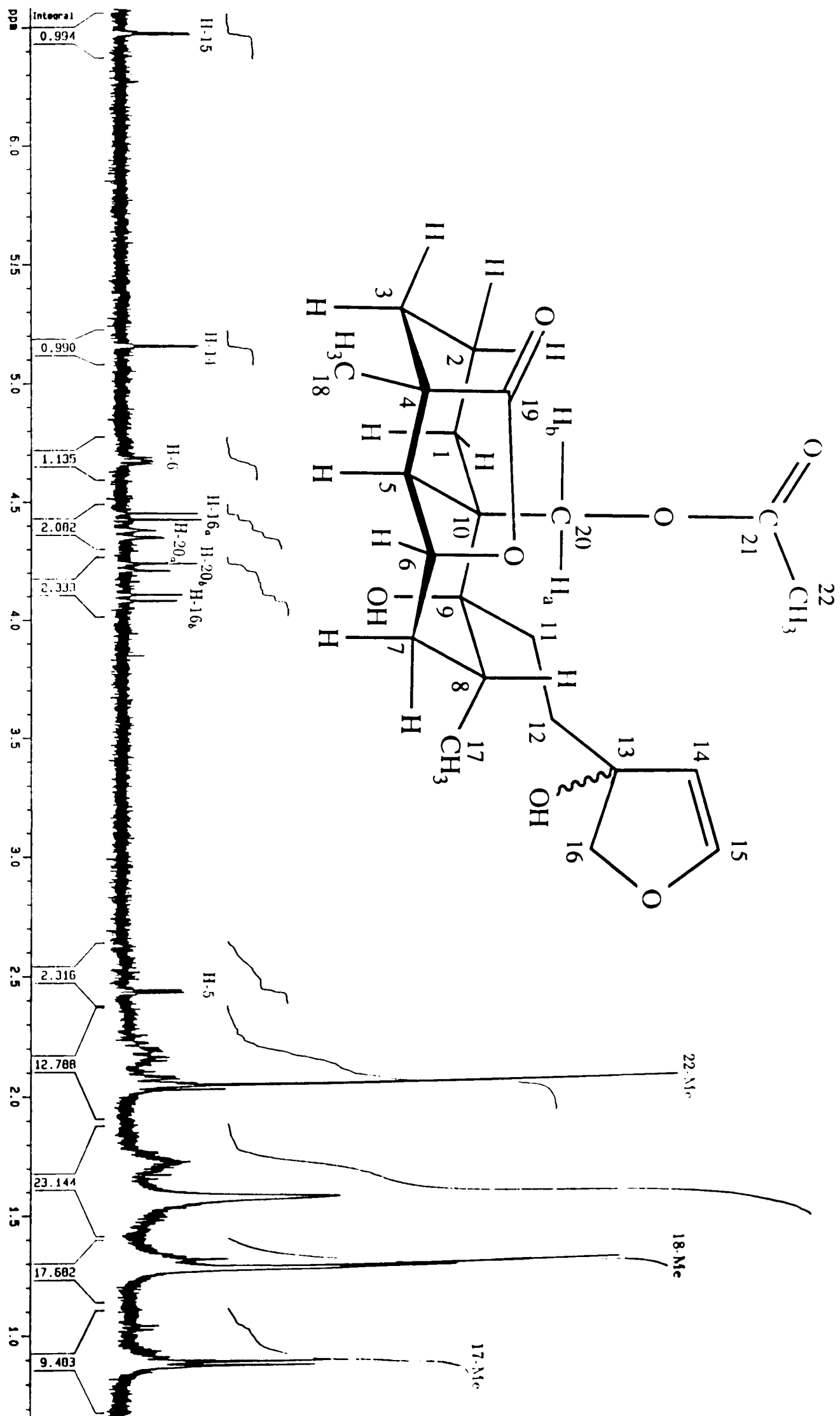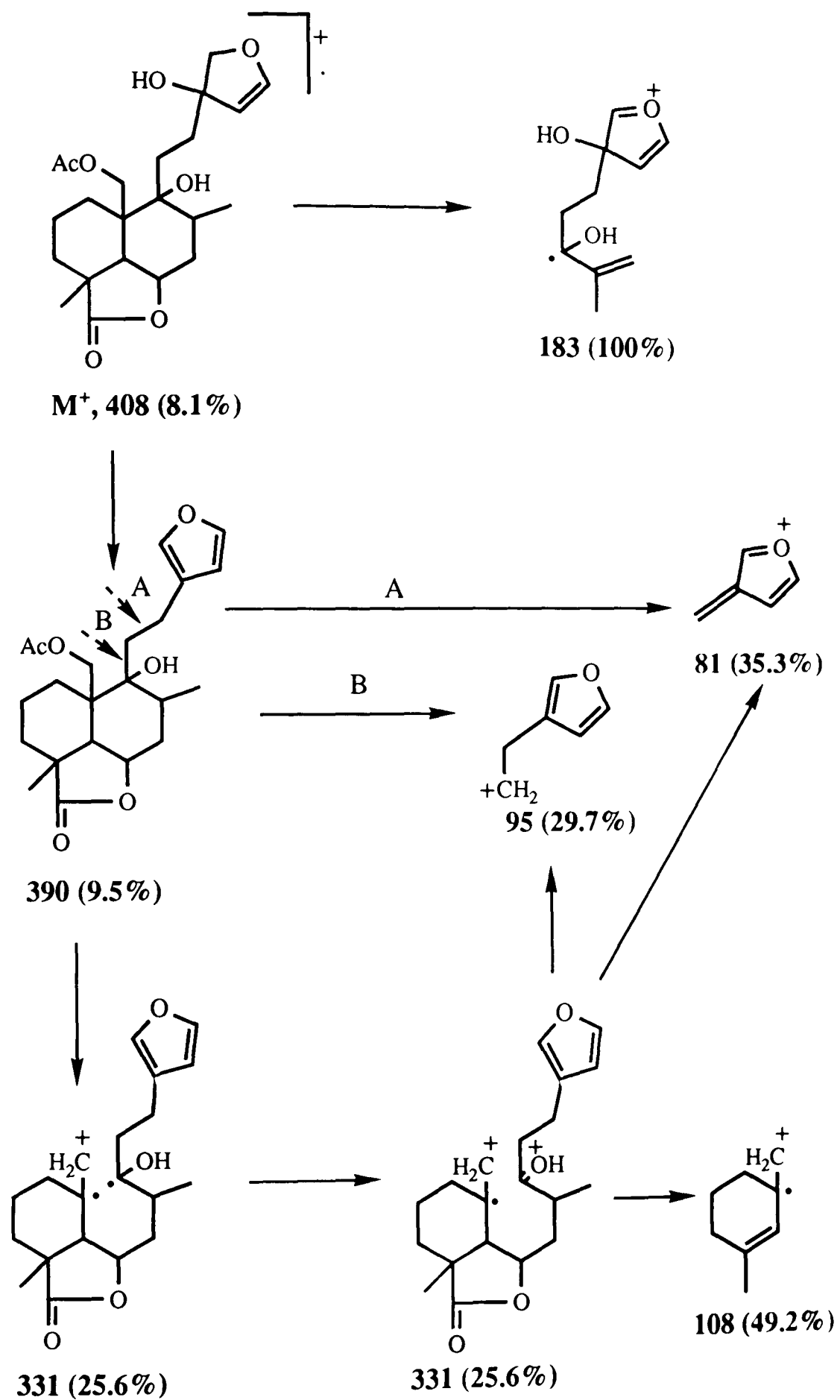
Scheme 8.2. Possible mass fragmentation pattern of SHM-69

olefinic proton signals at δ 6.47 and 5.16 which exhibited small coupling (J=2.68 Hz) indicative of a five member ring system in **203**. A methyl doublet at δ 0.87 (J=6.24 Hz) and 3H singlet at δ 1.22 were assignable to the Me-17 and Me-18.

SHM-69 was an unstable compound which changes to **204** (Fig. 8.11) on warming in chloroform. The transformation is characterised by dissappearance of ^{1}H NMR signals due to a vinyl ether (H-14, H-15 and H-16; see Fig. 8.11) and the appearance of a mono substituted furan (**204**) which show characteristic signals at δ 7.38 (1H, t, J=2.58), 7.23 (br s) and 6.27 (br s). The transformation of SHM-69 to **204** was further supported by the EIMS data (Scheme 8.2) which showed a fragment at m/z 390 (loss of 18 MU (water) from M$^+$) even before the expulsion of the acetoxy group. Major fragments at m/z 81 and 95 were also indicative of the furan ring system (Scheme 8.2).

SHM-69 appears to be a novel compound. The low optical activity recorded for this compound is attributed to it being a mixture of both C-13 epimers.

8.2.1.5   Identification of SHM-73C as caffeic acid (88)

SHM-73C was obtained in the yield of 0.001% and identified as caffeic acid on the basis of spectral data (UV, IR, ^{1}H NMR) and TLC and HPLC characteristics which were identical to these described for SHM-42A (page 77).

8.2.2 Constituents of the root of L. ocymifolia var raineri-ana

Examination of the cold ethanol extract of the roots of L. ocymifolia var raineriana resulted in the isolation of two known compounds.

8.2.2.1 Identification of SHM-79-4 as 3-methoxy-4-hydroxy-(trans)-cinnamaldehyde (205)

The brown oil SHM-79-4, obtained in the yield of 0.001% had a strong pleasant odour. The IR spectrum revealed a broad band between 3600 and 3000 cm^{-1} and a band at 1660 cm^{-1} indicating a hydroxy and an α,β-unsaturated carbonyl system respectively (William and Fleming, 1989).

High resolution EIMS revealed a molecular ion at m/z 178, $C_{10}H_{10}O_3$, identical to that required for 205 (Fig. 8.13). The ^1H NMR spectrum (Fig. 8.14) revealed, in the aromatic region, two doublets (1H each) at δ 7.08 (J=2.0) Hz) and 6.97 (J=8.1 Hz) and a doublet of doublets (1H) at δ 7.13 (J=8.1, 2.0); typical of the 1,3,4-trisubstituted aromatic ring system. The ^1H NMR further revealed a deshielded doublet at δ 7.48 which exhibited a trans coupling pattern (J=15.9 Hz) and was assignable to C-3', β to the the α,β unsaturated carbonyl system. H-2' appeared upfield (δ 6.00) due to its α position to the carbonyl and exhibited a dd coupling-pattern; trans coupling (J=15.9 Hz) to H-3' and another coupling (J=7.1 Hz) due to the aldehyde proton which was shown by its characteristic resonance at δ 9.65 (J=7.1 Hz). Other features of the ^1H NMR spectrum were an aromatic methoxyl group which appeared as a sharp 3H singlet at δ 3.96 and
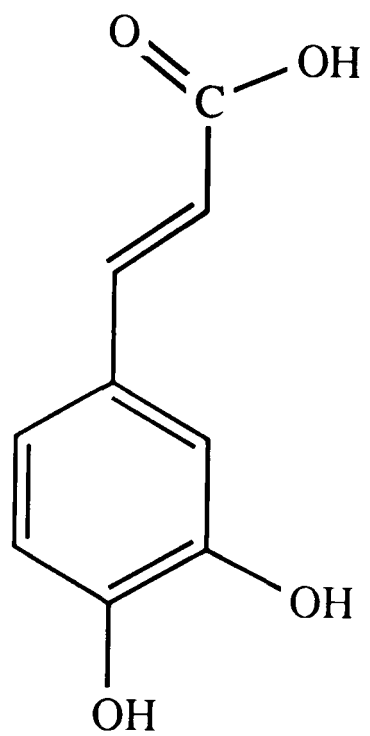
88
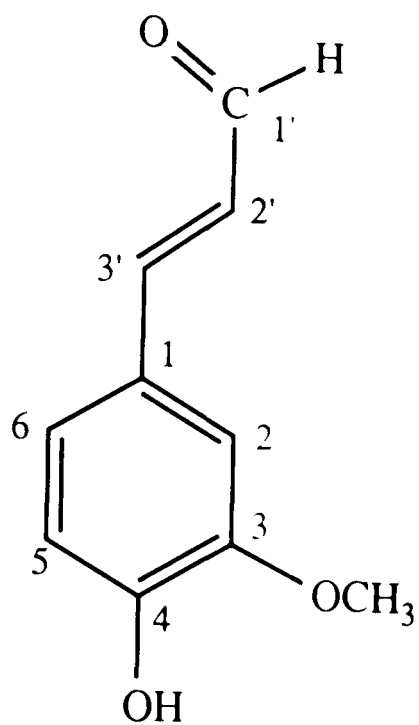
205
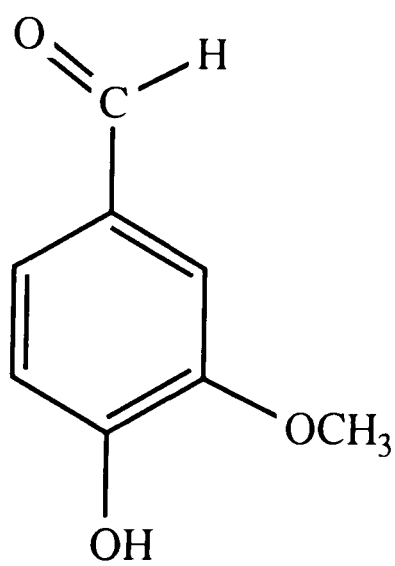
206

Fig. 8.14. Cinnamate and benzoate derivatives of *L. ocymifolia*
var *raineriana*

Figure 8.14: ^{1}H NMR (400 MHz, CDCl$_3$) spectrum of SHM-79-4

264
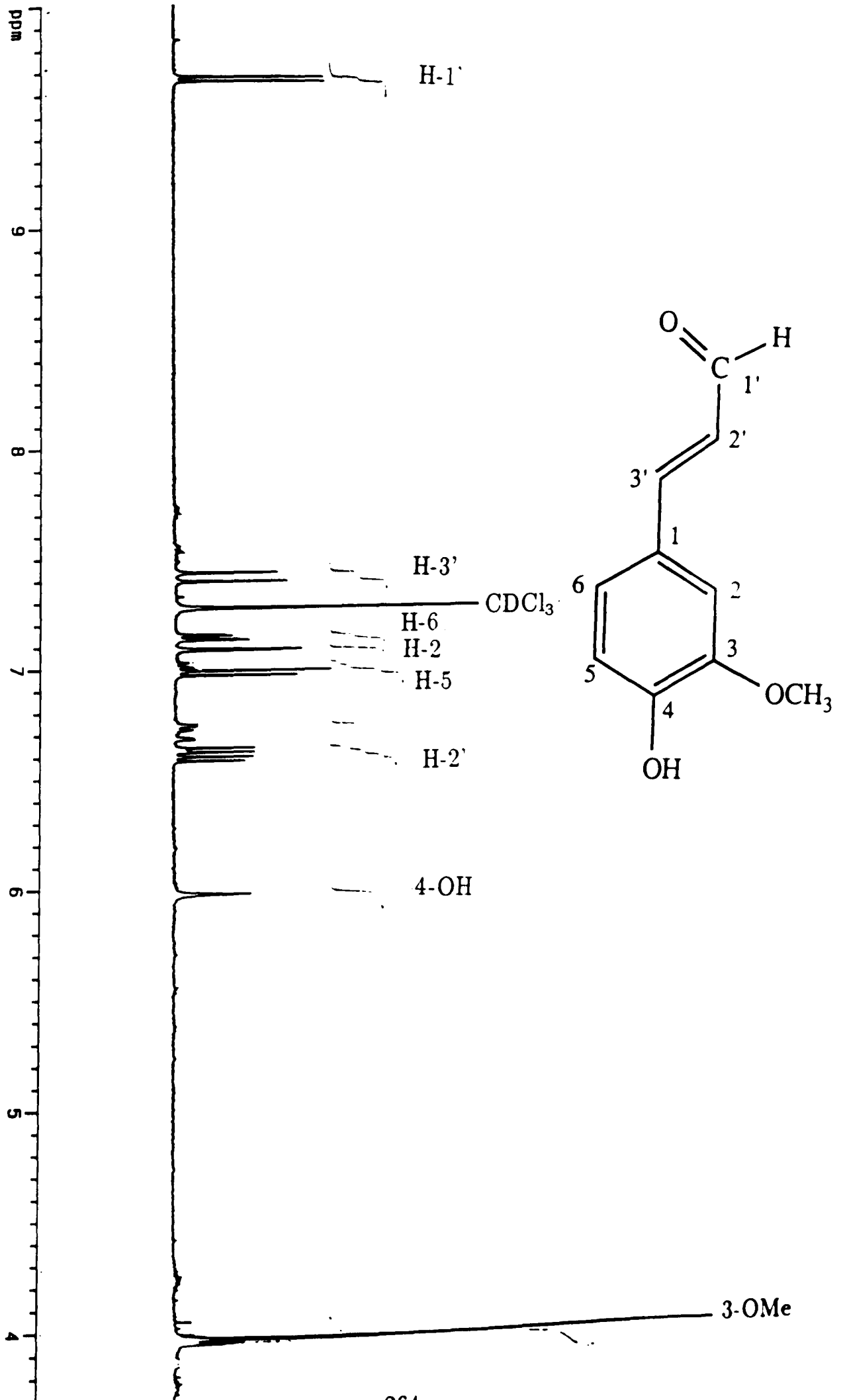
an aromatic OH (1H) which occured as a broad singlet at δ 5.99. Assignment of the methoxyl group at C-3 (not at C-4) was supported by the NOESY study which revealed a strong interaction between H-2 (δ 7.08) and the methoxyl protons.

8.2.2.2 Identification of SHM-79-3 as 3-methoxy-4-hydroxybezaldehyde (206)

The second constituent of the root also had a strong pleasant odour and was obtained as an oil in a yield of 0.0012%. The UV spectrum showed three absorption maxima between 200 and 350 nm. A band between 3600 and 3000 cm^{-1} and a band at 1670 cm^{-1} in the IR spectrum were indicative of a hydroxy and an α,β-unsaturated carbonyl systems respectively (William and Fleming, 1989). GCMS of the TMS derivative established a molecular formula as $C_8H_8O_3$.

The ^{1}H NMR spectrum in the aromatic region revealed two doublets at δ 7.43 (J=1.5 Hz) and 7.05 (J=8.5 Hz) and a doublet of doublets at δ 7.42 (J=8.45, 1.5 Hz) in agreement to the 1,3,4-trisubstituted aromatic ring system required in 206 (Fig. 8.13). The ^{1}H NMR spectrum further revealed a deshielded 1H singlet at δ 9.84 which was assignable to the aldehyde functional group conjugated to the aromatic system. Other features of the ^{1}H NMR spectrum were an aromatic methoxyl singlet at δ 3.98 and a broad phenolic hydroxyl singlet (1H) at δ 6.21. As with SHM-79-4, NOESY interaction between the methoxyl signal and a *meta*-coupled proton signal (δ 7.43, H-2) supported a 4-hydroxyl, 3-methoxyl positions in 206.

8.3 Experimental

8.3.1 Plant material

Leaves and root of *L. ocymifolia* var *raineriana* were collected from Addis Ababa City, Ethiopia, from beside the Ginfile river (ca 2450 m). A voucher specimen was authenticated by Dr Mesfin Taddesse and deposited at the National Herbarium of Ethiopia, Addis Ababa University.

8.3.2 Analysis of *L. ocymifolia* var *raineriana* leaves

Dried leaves of *L. ocymifolia* var *raineriana* were (500 g) placed in a glass percolator and continually extracted with ethanol for five days. Removal of the solvent under reduced pressure yielded 10 gm of extract residue which was subsequently fractionated by VLC over silica gel G (Merk 7749) with solvents of increasing polarity; i.e. hexane and hexane containing increasing amount of ethyl acetate. The 8:2 hexane:ethyl acetate fractions were bulked and subjected to a short Sephadex LH 20 column (solvent, chloroform:methanol, 1:1). The chlorophyll free column eluate was subjected to prep. TLC (solvent-hexane:chloroform:ethyl acetate, 4:6:4) to give 4 mg of SHM-69 (**203**) and 50 mg of SHM-76A (**200**).

The 7:3 hexane:ethyl acetate VLC eluate after the removal of chlorophyll (Sephadex LH 20 column, solvent-chloroform:methanol, 1:1) gave a fraction containing one major compound which showed a pink colour in vanillin spray. This compound was purified by prep. TLC (silica gel, solvent-hexane:chloroform:ethyl acetate, 2:4:6) to give 30 mg of SHM-76B (**199**). Similar treatment of the 1:1

hexane:ethyl acetate VLC eluent gave 9 mg of SHM-76C (201).

The ethyl acetate VLC eluent was subjected to HPLC under the same conditions described for *P. schimperi* on page 102 using solvent system B. Three major constituents; SHM-73A (2 mg, retention time 15.12 minutes, solvent system A), SHM-73B (7 mg, retention time 18.18 minutes, solvent system A) and SHM-73C (5 mg, retention time 7.2 minutes, solvent system A) were isolated. SHM-73A and SHM-73B which appeared to be flavonoid glycosides were not characterized in these studies as acetylation under normal procedures resulted in the opening of the sugar rings.

8.3.3 Properties of compounds

8.3.3.1 Properties of SHM-76A (*ent*-(13S)-9,13α-epoxylabda-6(19)β,16(15)-diol dilactone) (200)

Needles, mp 236°C [α]$_D$ -27° (c. 0.1, CHCl$_3$). Found 348.1964, C$_{20}$H$_{28}$O$_5$, requires 348.1937. IR ν_{max}^{KBr} cm^{-1} = 2970, 1780, 1760, 1470, 1200, 1170, 1090, 1070, 1030; ^{1}H NMR (400 MHz, CDCl$_3$) δ = 4.68 (1H, t, J=4.8 Hz, H-6), 4.24 and 4.12 (2H, AB quartet, J=8.9 Hz, H-16), 2.96 and 2.56 (2H, AB quartet, J=17.2 Hz, H-14), 2.07 (1H, d, J=4.5, H-5), 1.28 (3H, s, Me-18), 1.02 (3H, s, Me-20) and 0.87 (3H, d, J=6.3 Hz, Me-17); ^{13}C NMR δ = see Table 8.1; EIMS m/z (rel. int.) = 348 (19.3), 182 (12.4), 181 (100), 168 (14.8), 167 (12.1), 139 (16.3), 109 (18.8) and 69 (9.4).

8.3.3.2 Properties of SHM-76B ((13S)-20β-acetoxy-9,13α-epoxylabda-6(19)β,16(15)-diol dilactone) (199)

Needles, mp 240°C, $[\alpha]_D$ -9° (c. 0.1, CHCl$_3$). Found 406.2003, C$_{22}$H$_{30}$O$_7$, requires 406.1992. IR ν_{max}^{KBr} cm^{-1} = 2920, 1780, 1770, 1730, 1390, 1365, 1240, 1235, 1200, 1170, 1030; ^{1}H NMR (400 MHz, CDCl$_3$) δ = 4.67 (1H, dd, J=6.4, 4.4 Hz, H-6), 4.33 (1H, dd, J=12.5, 2.0 Hz, H-20a), 4.22 and 4.10 (2H, AB quartet, J=8.9 Hz, H-16), 4.19 (1H, d, J=12.5 Hz, H-20b), 2.90 and 2.36 (2H, AB quartet, J=17.3 Hz, H-14), 2.36 (1H, d, J=4.4 Hz, H-5), 2.23 and 1.82 (2H, m, H-11), 2.17 (1H, m, H-7$_{ax}$), 2.15 (2H, m, H-12), 2.08 (1H, m, H-8), 2.04 (3H, s, 22-Me), 1.65 (1H, m, H-7$_{eq}$), 1.28 (3H, s, Me-18), 1.15 (1H, br dd, H-2 axial) and 0.89 (3H, d, J=6.4 Hz, Me-17); ^{13}C NMR δ = see Table 8.1; EIMS m/z (rel. int.) = 406 (22.1), 347 (4.4), 247 (16), 183 (49.8), 182 (22.1), 181 (100), 168 (16.3) 137 (12.7), 135 (15.0), 109 (10.4), 107 (14.1), 97 (14.0), 93 (10.1), 91 (11.7) and 69 (16.3).

8.3.3.3 Properties of SHM-76C ((13R)-6β-acetoxy-9,13α-epoxylabda-19(20)β,16(15)-diol dilactone) (201)

Needles, mp 240°C, $[\alpha]_D$ +8° (c. 0.1, CHCl$_3$). M$^+$ not found but M$^+$-acetate found 346.1776 C$_{20}$H$_{26}$O$_5$, requires 346.1780. IR ν_{max}^{KBr} cm^{-1} = 2920, 1780, 1730, 1715, 1460, 1370, 1240, 1160, 1140, 1020; ^{1}H NMR (400 MHz, CDCl$_3$) δ = 5.16 (1H, q, J=3.04 Hz, H-6), 4.58 (1H, dd, J=11.5, 2.8 Hz, H-20a), 4.39 and 4.23 (2H, AB quartet, J=9.24 Hz, H-16), 4.15 (1H, d, J=11.5 Hz, H-20b), 2.92 and 2.51 (2H, AB quartet, J=17.04 Hz, H-14), 2.03 (3H, s, Me-18) and 0.87 (3H, d, J=6.64 Hz, Me-17); ^{13}C NMR δ = see Table 8.1; EIMS m/z (rel. int.) = 346

(100), 318 (5.9), 302 (14.0), 194 (29.4), 182 (4.6), 181 (27.2), 168 (6.8), 161 (4.8),

133 (5.2), 119 (4.6), 109 (7.2), 107 (5.4), 105 (6.1), 91 (7.9) and 79 (5.7).

8.3.3.4 Properties of SHM-69 (20β-acetoxy-9α,13ξ-dihydroxy-15(16)-epoxy-labd-14-en-6,19β-O-lactone) (203)

Gum, $[\alpha]_D$ +1° (c. 0.1, CHCl$_3$). Found 408.2141, C$_{22}$H$_{32}$O$_7$, requires

408.2148. UV λ_{max}^{EtOH} nm = 274; IR ν_{max}^{KBr} cm^{-1} = 3450 br, 2910, 1770, 1740,

1600, 1460, 1220, 1030; ^{1}H NMR (400 MHz, CDCl$_3$) δ = 6.47 (1H, d, J=2.68 Hz,

H-15), 5.16 (1H, d, J=2.68 Hz, H-14), 4.67 (1H, dd, J=7, 4.9 Hz, H-6), 4.43 and

4.08 (2H, AB quartet, J=10.44 Hz, H-16), 4.35 (1H, dd, J=12.3, 2.0 Hz, H20a),

4.22 (1H, d, J=12.3 Hz, H-20b), 2.43 (1H, d, J=4 Hz, H-5), 2.04 (3H, s, Me-22),

1.22 (3H, s, Me-18) and 0.87 (3H, d, J=6.24, Me-17); EIMS m/z (rel. int.) = 408

(8.1), 390 (9.5), 350 (14.0), 331 (25.6), 330 (98.1), 217 (9.7), 183 (100), 181 (18.2),

165 (13.7), 163 (25.9), 161 (13.6), 159 (9.1), 153 (14.1), 152 (10.9), 139 (10.7),

137 (17.7), 133 (15.6), 125 (17.9), 108 (49.2), 95 (28.7), 93 (23.2), 91 (20.2), 81

(35.3), 79 (18.6), 69 (15.2) and 67 (16.7).

8.3.3.5 Properties of SHM-73C (88, Caffeic acid)

The spectroscopic data (UV, IR, ^{1}H NMR), TLC and HPLC character-

istics were identical with that of SHM-42A (page 104).

8.3.4 Analysis of root of *L. ocymifolia* var *raineriana*

500 gm of the roots of *L. ocymifolia* var *raineriana* were extracted by cold

ethanol as described for *P. schimperi* (page 102). Removal of the solvent under

reduced pressure gave 40 gm of extract residue which was subsequentely defated by partitioning into 90% methanol (in water) and hexane. The methanol fraction was then subjected to a Sephadex LH 20 column and eluting with CHCl₃:MeOH (1:1). PTLC (solvent, petroleum ether:ethyl acetate, 6:4) of the heavier column fraction afforded 5 mg of SHM-79-4 (205) while similar treatment of the last column fraction afforded 6 mg of SHM-79-3 (206).

8.3.5 Properties of compounds

8.3.5.1 Properties of SHM-79-3 (3-methoxy-4-hydroxybezaldehyde) (206)

Yellow oil. UV λ_{max}^{EtOH} nm = 279, 327; IR ν_{max}^{KBr} cm^{-1} = 3600-3000, 2910, 2840, 1670, 1590, 1510, 1460, 1420, 1300, 1260, 1155, 1030, 860, 730 and 630; ^{1}H NMR (250 MHz, CDCl₃) δ = 9.84 (1H, s, H-1'), 7.43 (1H, d, J=1.48 Hz, H-2), 7.42 (1H, dd, J=8.45, 1.48 Hz, H-6), 7.05 (1H, d, J=8.45 Hz, H-5), 6.21 (1H, br s, OH-4), and 3.98 (3H, s, OMe-3).

8.3.5.1.1 GCMS analysis of SHM-79-3 (206)

Bis(trimethylsilyl)-acetamide (30 μl) was added to SHM-79-3 (50 μg) and the solution was kept at 60°C for 30 minutes. After removing the solvent an ethyl acetate (1 ml) solution of the sample was injected into an HP5988A GCMS system using a 15 m column (100% dimethyl polysiloxane). EIMS m/z (rel. int.) of a single peak (SHM-79-3 TMS) at 5.5 minutes = 224 (26.8), 209 (38.3), 194 (100), 193 (47.1), 165 (11.6), 163 (10.3), 75 (10.4), 73 (41.7), 59 (24.0), 45 (32.9),

43 (22.5).

8.3.5.2 Properties of SHM-79-4 (3-methoxy-4-hydroxy-(*trans*)-cinnam-aldehyde (205)

Yellow oil. Found 178.0630, $C_{10}H_{10}O_3$, requires 178.0630; UV λ_{max}^{EtOH} nm = 219, 238 sh, 309 sh, 339; IR IR ν_{max}^{KBr} cm^{-1} = 3600-3000, 2920, 2810, 1660, 1600, 1510, 1460, 1285, 1130, 810; ^{1}H NMR (400 MHz, CDCl$_3$) δ = 9.65 (1H, d, J=7.13 Hz, H-1'), 7.48 (1H, d, J=1585 Hz, H-3'), 7.13 (1H, dd, J=8.13, 1.95 Hz, H-6), 7.08 (1H, d, J=1.95 Hz, H-2), 6.97 (1H, d, J=8.13 Hz, H-5), 6.00 (1H, dd, J=15.85, 7.13 Hz, H-2'), 5.99 (1H, br s, OH-4) and 3.96 (3H, s, OMe-3); EIMS m/z (rel. int.) = 178 (62.0), 161 (11.0), 147 (15.9).

GENERAL CONCLUSION

GENERAL CONCLUSION

Almost all of the plants investigated during this study have been (and are being) used by man to treat some sort of illnesses. A systematic biological/pharmacological and phytochemical study of these plants has resulted in the isolation of several novel and known compounds some of which show considerable biological activities. Based on the study, the following conclusions are made:

- **There is a link between the traditional uses of the plants studied and the observed biological activity.** The finding of a compound with a potent antimicrobial action against *Staphyllococcus aureus* in *Premna schimperi* and the traditional use of that plant for treating wound infections is a typical example. The results in general show once again the use of higher plants as a potential source of new drugs. More importantly it supports the idea of plant selection for drug discovery based on their traditional uses.

- While some of the bioactive compounds are structurally complex, some are simple and these are often ignored due to their common abundence and simplicity. The pharmacological activity of potassium loaded extracts of *Portulaca oleracea* and *Pentas schimperiana* are good examples. **Such examples of simple bioactive compounds can be uncovered easily if**

one adopts a systematic bioassay-guided isolation approach but would be missed if the approach adopted was that of simply iso-lating compounds.

APPENDIX

APPENDIX

Structural determination and analysis of SHM-4 (139)

A unique data set was measured at $approx$ 295 K to 2 θ_{max} 50° [Enraf-Nonius CAD-4 diffractometer, monochromatic Mo-Kα radiation ($^H\lambda$ 0.71073 Å), $2\theta\theta$ scan model]. 1808 Independent reflextions were obtained, 1478 with $I \succ 3\delta(I)$ being considered 'observed' and used in the full-matrix least-squares refinement without absorption correction, after solution of the structure by direct methods. Anisotropic thermal parametres were refined with U_{iso} coventional residuals R, R' on $|F|$ were 0.033, 0.034 [statistical weights derivative of δ^2 $(I)=\delta^2(I_{diff}) + 0.0004$ $\delta^4(I_{diff})$]. Neutral atom complex scattering factors were employed (Ibers and Hamilton, 1974), the chirality being assumed from the chemistry; computation used the XTAL 3.0 programme system implimented by Hall (1990). Pertinent results are given in Fig 4.6 (page 131) and Table A.1-A.3.

Atom	x	y	z
C(1)	0.4765(2)	0.3217(3)	0.5928(3)
C(2)	0.5686(3)	0.2942(4)	0.5140(3)
C(3)	0.6561(3)	0.2597(3)	0.5923(3)
C(4)	0.6877(2)	0.3427(2)	0.6884(3)
C(5)	0.5927(2)	0.3739(2)	0.7644(3)
C(6)	0.6141(2)	0.4509(3)	0.8721(3)
C(7)	0.5205(2)	0.4899(3)	0.9402(3)
C(8)	0.4301(2)	0.4171(2)	0.9183(3)
O(8)	0.3492(1)	0.4765(2)	0.9761(2)
C(9)	0.4090(2)	0.4137(2)	0.7805(2)
C(10)	0.4978(2)	0.407792)	0.6900(2)
C(11)	0.3148(2)	0.4260(2)	0.7434(3)
C(12)	0.2283(2)	0.4274(2)	0.8306(3)
O(12)	0.2564(1)	0.4148(2)	0.9545(2)
C(13)	0.1522(2)	0.3399(2)	0.806493)
C(14)	0.0647(2)	0.3848(3)	0.7819(3)
C(15)	0.0752(2)	0.5013(3)	0.7873(3)
O(15)	0.0139(2)	0.5703(2)	0.7711(2)
O	0.1724(2)	0.5257(2)	0.8161(2)
C(16)	0.1823(3)	0.2252(3)	0.8118(5)
C(17)	0.4401(3)	0.3084(3)	0.9830(3)
C(18)	0.7637(3)	0.2886(4)	0.7762(4)
C(19)	0.7422(3)	0.4364(3)	0.6264(5)
C(20)	0.5068(3)	0.5190(3)	0.6284(4)

Table A.1: Non-hydrogen atom fractional co-ordinates for SHM-4 (139)

atom	Distance
C(1)-C(2)	1.532(5)
C(1)-C(10)	1.529(4)
C(2)-C(3)	1.503(5)
C(3)-C(4)	1.526(5)
C(4)-C(5)	1.558(4)
C(4)-C(18)	1.542(5)
C(4)-C(19)	1.530(5)
C(5)-C(6)	1.536(4)
C(5)-C(10)	1.555(4)
C(6)-C(7)	1.527(4)
C(7)-C(8)	1.526(4)
C(8)-O(8)	1.448(3)
C(8)-C(9)	1.517(4)
C(8)-C(17)	1.531(4)
O(8)-O(12)	1.473(3)
C(9)-C(10)	1.536(4)
C(9)-C(11)	1.325(4)
C(10)-C(20)	1.543(4)
C(11)-C(12)	1.488(4)
C(12)-O(12)	1.400(3)
C(12)-C(13)	1.511(4)
C(12)-O	1.442(3)
C(13)-C(14)	1.318(4)
C(13)-C(16)	1.486(5)
C(14)-C(15)	1.461(5)
C(15)-O(15)	1.199(4)
C(15)-O	1.364(4)

Table A.2: Non-hydrogen bond lengths ($\mathring{A}$) for SHM-4 (139)

Atoms	Angle
C(2)-C(1)-C(10)	113.0(3)
C(1)-C(2)-C(3)	111.7(3)
C(2)-C(3)-C(4)	113.8(3)
C(3)-C(4)-C(5)	107.8(2)
C(3)-C(4)-C(18)	107.7(3)
C(3)-C(4)-C(19)	110.5(3)
C(5)-C(4)-C(19)	115.1(3)
C(18)-C(4)-C(19)	107.1(3)
C(4)-C(5)-C(6)	114.0(2)
C(4)-C(5)-C(10)	117.0(2)
C(6)-C(5)-C(10)	112.0(2)
C(5)-C(6)-C(7)	114.4(2)
C(6)-C(7)-C(8)	112.2(3)
C(7)-C(8)-O(8)	102.4(2)
C(7)-C(8)-C(9)	108.4(2)
C(7)-C(8)-C(17)	112.8(2)
O(8)-C(8)-C(9)	107.5(2)
O(8)-C(8)-C(17)	108.7(2)
C(9)-C(8)-C(17)	116.1(2)
C(8)-O(8)-O(12)	106.6(2)
C(8)-C(9)-C(10)	119.0(2)
C(8)-C(9)-C(11)	118.0(2)
C(10)-C(9)-C(11)	122.6(2)
C(1)-C(10)-C(5)	108.4(2)
C(1)-C(10)-C(9)	109.3(2)
C(1)-C(10)-C(20)	110.4(2)
C(5)-C(10)-C(9)	107.9(2)
C(5)-C(10)-C(20)	113.8(2)
C(9)-C(10)-C(20)	107.0(2)
C(9)-C(11)-C(12)	122.7(3)
C(11)-C(12)-O(12)	113.5(2)

Table A.3: Non-hydrogen bond angles (°) for SHM-4 (139)

Table A.3 cont.

Atoms	Angle
C(11)-C(12)-C(13)	113.5(2)
C(11)-C(12)-O	109.7(2)
O(12)-C(12)-C(13)	105.3(2)
O(12)-C(12)-O	109.7(2)
C(13)-C(12)-O	104.5(2)
C(13)-C(12)-O	104.5(2)
O(8)-O(12)-C(12)	108.5(2)
C(12)-C(13)-C(14)	108.6(3)
C(12)-C(13)-C(16)	120.6(3)
C(14)-C(13)-C(16)	130.8(3)
C(13)-C(14)-C(15)	109.3(3)
C(14)-C(15)-O(15)	130.1(3)
C(14)-C(15)-O	108.8(3)
O(15)-C(15)-O	121.2(3)
C(12)-O-C(15)	108.9(2)

PUBLICATIONS

PUBLICATIONS

[1] Habtemariam, S., Gray, A.I., Halbert, G.W. and Waterman, P.G. (1990). A novel antibacterial diterpene from *Premna schimperi*. *Planta Medica* **56** 187.

[2] Habtemariam, S., Gray, A.I. and Waterman, P.G.(1991). Antibacterial diterpenes from the aerial parts of *Premna oligotricha*. *Planta Medica*, **58**, 109.

[3] Habtemariam, S., Gray, A.I., Lavaud, C., Massiot, G., Skelton, B.W., Waterman, P.G. and White, A.H. (1991). *ent*-12-oxolabda-8,13(16)-dien-15-oic acid and *ent*-8β,12α-epidioxy-12β-hydroxylabda-9(11),13-dien-15-oic acid γ-lactone: Two new diterpenes from the aereal parts of *Premna oligotricha*. *J. Chem. Soc. Perkin Trans.* I, 893.

[4] Habtemariam, S., Gray, A.I. and Waterman, P.G. (1991). Flavonoids from three Ethiopian species of *Premna*. *Z. Naturforsch.*, **47B**, 144 .

[5] Habtemariam, S., Gray, A.I., and Waterman, P.G. (1992). A new antbacterial sesquiterpene from *Premna oligotricha*. *J. Nat. Prod.*, sent for publication.

[6] Habtemariam, S., Gray, A.I., and Waterman, P.G. (1992). Diterpenes from the leaves of *Leonotis ocymifolia* var *raineriana*. *Phytochemistry.*, sent for

publication.

REFERENCES

References

[1] Abate, G., Gebre-Igziabher, T. and Taddesse, M. (1976) A study of medicinal plants of Ethiopia. Part 1A. The identity of some of the plants. Department of Biology, Science Faculty, Addis Ababa University, A.A.

[2] Abebe, W. (1986). *J. Ethnopharm.* **18**, 147

[3] Abelson, P.H. (1990). *Science*, **247**, 513

[4] Ahmad, A., Khan, K.A., Ahmad, V.U. and Quazi, S. (1986). *Planta Medica* **51**, 285

[5] Ahmed, A.A., Norris, J.A. and Mabry, T.J. (1986). *Phytochemistry* **25**, 1501

[6] Aesen, A.J., Hlubucek, J.R. and Enzell, C.R. (1975). *Acta Chemica Scandinavia* **B 29**, 589

[7] Almagboul, A.Z., Bashir, A. K., Farouk, A., and Salih, A.K. (1985) *Fitotherapia* 331

[8] Anjaneyulu, A.S.R., Ramaiah, P.A., Row, L., Venkateswarlu, R. and Ward, P.R. (1981). *Tetrahedron* **37**, 3641

[9] Atal, A.J., Dhar, K.L. and Pelter, A. (1967). *J. Chem. Soc.* C 2228

[10] Badawi, M.M., Honda, S.S., Kinghorn, A.D., Cordell, G.A. and Farnsworth, N.R. (1983). *J. Pharm. Sci.* **72**, 1285

[11] Bagby, M.O., Smith, C.R. and Wolff, I.A. (1965). *J. Org. Chem.* **30**, 4227

[12] Balza, F., Jamieson, L. and Towers, G. H. (1985). *J. Nat. Prod.* **46**, 471

[13] Basu, N.K. and Dandiya, P.C. (1943). *J. Am. Pharm.. Assoc. Sci. Edu.* **36**, 389

[14] Bax, Ad., and Subramaniam, S. (1984). *J. Magn. Reson.* **13**, 471

[15] Bax, Ad. and Summers, M.F. (1986). *J. Am. Chem. Soc.* **108**, 2093

[16] Benitez, M.A., Naurro, E., Feria, M., Trujillo, J., and Boada, J. (1991). *Toxicon.* **29**, 511-515.

[17] Bilgir, B. (1984). *Chemical abstract* **100**, 101835q.

[18] Birch, A.J., Macdonald, P.L. and Pelter, A. (1967). *J. Chem. Soc.* C 1968

[19] Biswanth, D., Sinha, N.K., Pandy, V.B. and Ray, A.B. (1985). *Planta Medica* **50**, 281

[20] Bladon, P. and Sleigh, T. (1965). *J. Chem. Soc.* **1291**, 6991

[21] Bohlmann, F., Zdero, C. and Huneck, S. (1985). *Phytochemistry* **24**, 1027

[22] Bondani, A. and Karler, R. (1970). *J. Cell. Physiol.* **75**,199.

[23] Bowden, B.F., Cambie, R.C. and Parnell, J.C. (1975). *Aust. J. Chem.* **28**, 91

[24] Bowman, W.C. and Rand, M.J. (1980). Textbook of pharmacology, 2nd edition, Blackwell scientific publications. London. pp 22.43

[25] Broucke, C.O.V.D. (1983). *Phytotherapia* 171

282

[26] Buckingham, J. (1982-87). Dictionary of chemical compounds. 5th Ed. and Supplements. Chapman and Hall, London

[27] Caputo, R., Mangoni, C., Monaco, P. and Previtera, L. (1974). *Phytochemistry* **13**, 471

[28] Chiba, M., Okabe, K., Hisada, S., Shima, K., Takemoto, T. and Nishibe, S. (1979). *Chem. Pharm. Bull.* **27**, 2868

[29] Codd, L.E. (1985). Lamiacea. Flora of Southern Africa. D.A. Leistner (ed). Vol. 28, part 4, pp 33

[30] Cooksen, D.J. and Smith, B.E. (1981). *Org. Magn. Reson.* **16**, 111

[31] Court, V.B. (1976). Flora of Tropical East Africa. Whitefriars Press LTD. London. pp 187

[32] Covino, B.G. and Vassallo, H.G. (1976). Local anesthetics. Mechanism of action and clinical use. Grune and Stratton, N.Y. pp 13

[33] Cufodontis, G.(1972) Enumeratio Plantarum Aethiopia Spermatophyta. Jardin Batanique National De Belgique.

[34] Dahal, A.R. and Norman, A.D. (1970). *J. Am. Chem. Soc.* **92**, 5527

[35] Dekker, T.G., Fourie, T.G., Matthee, E., Snyckers, F.O., Boeyens, J.C.A. and Denner, L.S. (1987). *S. Afr. J. Chem.* **40**, 228

[36] Demissew, S. (1988). Revision of the plant family Verbenaceae for the flora of Ethiopia. Manuscript for inclusion in volume 4. The National Herbarium of Ethiopia, Addis Ababa University.

[37] Derome, A.E. (1989). *Nat. Prod. Rep.*, 111

[38] Diak, J. (1977). *Planta Medica* **32**, 181

[39] Dreele, R.B.V., Pettit, G.R., Ode, R.H., Perdue, R.E., White, J.D. and Manchand, P.S. (1975). *J. Am. Chem. Soc.* **97**, 6236

[40] Duh, C-Y, Phoebe, J.C., Pezzuto, J.M., Kinghorn, A.D. and Farnsworth, N.R. (1986). *J. Nat. Prod* **49**, 706

[41] Eagle, G.A., Kaplan, E.R., Naidu, K. and Rivett, D.E.A. (1978). *J. Chem. Soc. Perkin I*, 994

[42] Ensemeyer, M. and Langhammer, L. (1982). *Planta Medica* **46**, 254

[43] FAO food and nutrition paper 42. Traditional food plants. (1988). FAO. pp 411

[44] Fonseca, S.F., Campello, J.P., Barata, L.C.S. and Ruveda, E.A. (1978). *Phytochemistry* **17**, 499

[45] Fonseca, S.F., Nielsen, L.T. and Ruved, E.A. (1979). *Phytochemistry* **18**, 1703

[46] Frimer, A.A., Bartlett, P.D., Boschung, A.F. and Jewett, J.C. (1977). *J. Amer. Chem. Soc.* **99**, 7977

284

[47] Gonzalez, A.G., Francisco, C.G., Freire, R., Hernandez, R., Salazar, J.A. and Suarez, E. (1976). *Tetrahedron Lett.* 2725.

[48] Groutas, W.C., Theodorakis, M.C., Tomkins, W.A.F., Herro, G. and Gayanor, T. (1984). *J. Med. Chem.* **27**, 548

[49] Hall, S.R. and Stewart, J.M. (1990). The XTAL user's manual, version 3.0. University of Western Australia and Maryland.

[50] Hamberg, M. and Samuelsson, B. (1973). *Proc. Natl. Acad. Sci. N.Y.* **70**, 899

[51] Harborne, J.B. (1988). The Flavonoids. Advances since 1980. Chapman and Hall, N.Y. pp 399

[52] Harborne, J.B., Mabray, T.J. and Mabry, H. (1975). The flavonoids. Chapman and Hall, London

[53] Harborne, J.B. and Williams, C.A. (1972). *Phytochemistry* **11**, 1741

[54] Hartman, P.A. (1968). Miniturized microbiology methods. Academy Press, N.Y. pp 101

[55] Haasnoot, G.A.G., Van de Van, F.J.M. and Hilbers, C.W. (1984). *J. Magn. Reson.* **56**, 343

[56] Higgs, M.D. and Faulkner, D.J. (1978). *J. Org. Chem.* **43**, 3454

[57] Ibers, J.A. and Hamilton, W.C. (1947). International table of X-ray chrystallography, Vol 4, Kynoch, Press, Birmingham.

[58] Jenner, J., Meier, B.H., Bachman, P. and Ernst, R.R. (1979). *J. Am. Chem. Soc.* **101**, 6441

[59] Jennie, B.C., Cheryl, R., Jenny, M., Anna, L., Vic, C. and Stewart, T.A. (1983). *Food Technol. Aust.* **35**, 293-6.

[60] Kaplan, E.R., Naidu, K. and Rivett, D.E.A. (1970). *J. Chem. Soc. (C)*, 1656.

[61] Kato, T., Tanemura, M., Kanno, S., Suzuki, T. and Kitahara, Y. (1971). *Bioorganic Chemistry* **1**, 84

[62] Kato, M.J., Yoshida, M. and Goltlieb, O.R. (1990). *Phytochemistry* **29**, 1799

[63] Kalpan, E.R. and Rivett, D.E.A. (1968). *J. Chem. Soc. (C)*, 262

[64] Korolkovas, A., Burcklalter, J.H. (1976). Essentials of medicinal chemistry. John Wiley and Sons, N.Y. pp 541

[65] Krogsgaard-Larsen, P. and Christensen, S.B. (1984). Natural products and drug development. Munksgaard, Copenhagen, Tokyo. pp 17, 94

[66] Kruger, G.J. and Rivett, D.E.A. (1978). *S. Afr. J. Chem.*, 59.

[67] Kruger, G.J. and Rivett, D.E.A. (1988). *S. Afr. J. Chem.* **41**, 124

[68] Kusum, B. (1988). *Res. Ind.* **33**, 249

[69] Lanonigro, G., Lanzetta, R., Parrilli, M., Adinofi, M. and Mangoni, L.G. (1979). *Chim. Ital.* **109**, 145

[70] Lopes, L.M.X., Bolzani, V.S. and Trevisan, L.M.W. (1987) *Phytochemistry* **26**, 2781

[71] Luduena, F.P. (1969). Duration of local anesthetics. *Ann. Rev. Pharmacol.* **9**, 503.

[72] Mabry, T.J., Markham, K.R. and Thomas, M.B. (1970). The systematic identification of flavonoids. Springer. N.Y.

[73] Manchand, P.S. (1973) *Tetrahedron Lett.* **21**, 1907

[74] Marderosian, A.D. and Liberti, L. (1988). Natural product medicine, George F. Stickley Co., Philadelphia. pp 1

[75] Marsh, J. (1990). Bioactive compounds from plants. Ciba foundation symposium 154. John Wiley & Sons. N.Y. pp 126.

[76] Menaker, L. (1980). The biologic basis of dental caries. Harper and Row Hagerstown. N.Y, pp 293

[77] Meng, Q., Piantinia, U. and Hesse, M. (1989). *J. Nat. Prod.* **52**, 581

[78] Meng, Q., Zhu, N. and Chen, N. (1988). *Phytochemistry* **27**, 1151

[79] Merkel, P.B. and Kearns, D.R. (1972). *J. Am. Chem. Soc.* **94**, 7244

[80] Mossa, J.S., Al-Yahaya, M.A. and Al-Meshal, I.A. (1987). Medicinal plants of Saudi Arabia. vol. 1, King Saud University Libraries, Riyadh. pp 128

[81] Munehiro, N. and Tunao, H. (1975). *Chemical Abstract* **82**, 152220c

[82] Nagadjuie, B., Ayafor, J.F. and Sondengam, B.C. (1991). *Tetrahedron* **147**, 3555

[83] Norman, R.O.C. (1978). Principles of organic synthesis. 2nd Ed. John Wiley and Sons, N.Y., pp 619

[84] Odebiyi, O.O. and Sofowara, E.A. (1979). *Planta Medica* **36**, 204

[85] Okwuasaba, F., Ejike, C., and Parry, O. (1986). *J. Ethnopharm.* **17**, 139.

[86] Okwuasaba, F., Ejike, C., and Parry, O.(1987a). *J. Ethnopharm.* **21**, 55.

[87] Okwuasaba, F., Ejike, C., and Parry, O.(1987b). *J. Ethnopharm.* **21**, 91

[88] Otsuka, H., Kubo, N., Yamasaki, K. and Padolina, W. (1989a). *Phytochemistry* **28**, 513

[89] Otsuka, H., Kubo, N., Yamaski, K. and Padolina, W.G. (1989b). *Phytochemistry* **28**, 3063

[90] Panichpol, K. and Waterman, P.G. (1978). *Phytochemistry* **17**, 1363

[91] Parry, O., Okwuasaba, F., and Ejike, C. (1987a). *J. Ethnopharm.* **21**, 99.

[92] Parry, O., Okwuasaba, F., and Ejike, C. (1987b). *J. Ethnopharm.* **19**, 247.

[93] Patt, S.L. and Shoolery, J.N. (1982). *J. Mag. Res.* **46**, 535

[94] Patai, S. (1983). The chemistry of peroxides. John Wiley & Sons, N.Y., pp 201

[95] Paudler, W.W. (1987). Nuclear magnetic resonance. John Wiley & Sons. pp 249

[96] Pelletier, S.W., Choksi, H.P. and Desai, H.K. (1986). *J. Nat. Prod.* **49**, 892

[97] Pelter, A. (1967). *J. Chem. Soc.* C, 1376

[98] Perry W.L.M. and Staff of the department of pharmacology Edinburgh University (1970). Pharmacological experiments on isolated preparations. Churchill Livingstone, London. pp 56

[99] Phadnis, A.P., Patwardhan, S.A., Dhaneshwar, N.N., Tavale, S.S. and Row, T.N. (1988). *Phytochemistry*, **27**, 2899

[100] Purushothaman, K.K., Vasanth, S. and Connolly, J.D. (1974). *J. Chem. Soc. Perkin I*, 2661

[101] Purushothaman, K.K. and Vasanth, S. (1986). *Indian Drugs* **23**, 482

[102] Quisumbing, A. (1978). Medicinal plants of the Philippines. Katha, Philippines. pp 800

[103] Ramaaiah, S.T., Laxman, R.K. and Kamaraji, S.K. (1978). *J. Indian. Chem. Soc.* **55**, 102

[104] Ramawamy, S., Krishnamurthy, V., Mythirayee, I.C., Ramachandran, S. and Kameswaran, L. (1988). *Euro. J. Pharm.* **152**, 367

[105] Rao, P.V.S., Aruna, G.D., Raju, G.V.S., Trimurtulu, G. and Rao, C.B. (1987). *Indian J. Chem.* **26B**, 191

[106] Rao, C.B., Krishna, P.G. and Suseela, K. (1985). *Indian J. Chem.* **24B**, 403

[107] Rao, C.B. and Raju, G.V.S. (1981). *Curr. Sci.* **50**, 180

[108] Rao, C.B., Raju, G.V.S. and Krishna, P.G. (1982a). *Indian J. Chem.* **21B**, 267

[109] Rao, C.B., Raju, G.V.S. and Krishna (1982b). *Indian J. Chem.* **21B**, 294

[110] Rao, C.B, Suba, R.G.V. and Krishna, P.G. (1982c). *Indian J. Chem.* **21B**, 267

[111] Rao, C.B., Rao, J.N. and Vijayakumar, E.K.S. (1979). *Indian J. Chem.* **18B**, 513

[112] Rao, C.B., Suseela, K. and Raju, C.V.S. (1984). *Indian J. Chem* **23B**, 177

[113] Rao, C.B. and Vijayakumar, K.S. (1980). *Indian J. Chem* **19B**, 240

[114] Ritchie, JM., Ritchie, B. and Greengard, P. (1965). *J. Pharmacol. Exp. Ther.* **150**, 152, 160

[115] Roitman, T.N. and James, L.F. (1985). *Phytochemistry* **24**, 835

[116] Sadler, I.H. (1988). *Nat. Prod. Rep.* 102

[117] Sankaram, A.V.B., Bhaskaiah, K., Marthandamurthi, M. and Subrahmanyam, M. (1989). *Tetrahedron Lett.* **30**, 867

[118] Sankaram, A.V.B., Bhaskariah, K., Murthi, M.M. and Subrahmayam, M. (1988). *Tetrahedron Lett.* **29**, 4881

[119] Sankaram, A.V.B. and Rao, G.L.N. (1980). *Symp. Pap-IUPAC. Int. Symp. Chem. Nat. Prod.* 11th Ed.

[120] Saradha, V. and Bhima, R.R. (1988). *Indian Drugs* **26**, 127

[121] Schwartz, A. (1971) Methods in Pharmacology. Vol 1. Appleton-Century-Crofts. Educational Division, Meredith Corporation, N.Y. pp 1

[122] Schwarz, C.H. and Brown, B.A. (1954). *Antibiot. Chemotherapy* **4**, 333

[123] Scott, R.,O., Mitchell, R.L., Purves, D. and Voss, R.C. (1971). Spectro-chemical methods for the analysis of soils, plants and other agricultural materials. Consultative Committee for the Development of Spectrochemi-cal Work. Bulletin 2. pp 27

[124] Shuichi, I., Yoshikazu, S., Kyoyu, S. and Yoshimasa, H. (1976). *Chemical Abstract* **85**, 25376v

[125] Simoes, C.M.O., Girre, M.A.L., Gleye, J. and Fauvel, M.T.H. (1990). *J. Nat. Prod.* **53**, 989

[126] Singh, P.P. (1973). *Qul. Plant. Mater. Veg.* **22**, 335

[127] Singh, P.P. and Saxena, S.N. (1972). *Indian J. Nutr. Diet.* **9**, 269

[128] Song, W., Siuling, S., Xuejian, X., Quan-Long, P., Pannell, L.K. and Highet, R.J. (1991) *Planta Medica* **57**, 93

[129] Sprinson, D.B. (1961). *Adv. carbohyd. Chem.* **15**, 235

[130] Stang, P.J. and Trepton, W.L. (1981). *J. Med. Chem.* **24**, 468

[131] Stierle, D.B. and Faulkner, D.J. (1979). *J. Org. Chem.* **44**, 964

[132] Szmant, H.H. and Halpern, A. (1949). *J. Am. Chem. Soc.* **71**' 1133

[133] Tabeekhia, M.M. (1980). *Dtsch. Lebensm.-Rundsch* **76**, 2 80

[134] Taniguchi, E. and Oshima, Y. (1972). *Tetrahedron Lett.* 653

[135] Tavormina, P.A., Gibbs, M.H. and Huff, J.W. (1956). *J. Am. Chem. Soc.* **78**, 4498

[136] Toda, S., Kumura, M. and Ohnishi, M. (1991). *Planta Medica* **57**, 8

[137] Thiselton-Dyer, W.T. (1959). Flora of tropical Africa. Vol 5, part 2, The Oast House, England. pp 2

[138] Torssell, K.B.G. (1983). Natural product chemistry. A mechanistic and biosynthetic approach to secondary metabolism. John Wiley and Sons LTD, N.Y., pp 69

[139] Tyotsana, D., Sarma, P.N., Srimannarayana, G. and Rao, A.V.S. (1984) *Curr. Sci.* **53**, 573

[140] Watt, J. and Breyer-Brandwijk, M.G. (1962) The medicinal and poisonous plants of Southern and Eastern Africa. E. S. Livingstone LTD. 2nd edition. pp 516

[141] Weeks, J.L. and Rabani, J. (1966). *J. Phys. Chem.* **70**, 2100

[142] Weidenborner, M., Hindorf, H., Jha, H.C. and Tsotsonos, P. (1990). *Phytochemistry* **29**, 1103

[143] White, J.D. and Manchand, P.S. (1972). *J. Org. Chem.* **38**, 720

[144] William, D.H. and Fleming I (1989). Spectroscopic methods in organic chemistry. 5th Ed.

[145] Willis, J.C. and Shaw, H.H.A. (1973). A dictionary of flowering plants and ferns. 8th Ed., Cambridge University Press. pp 942

[146] Wollenweber, E. and Mann, K. (1983). *Planta Medica* **48**, 126

[147] Yasuye, M. and Honda, Y. (1944). *J. Pharm. Soc. Japan* **64**, 177